PNL-4712

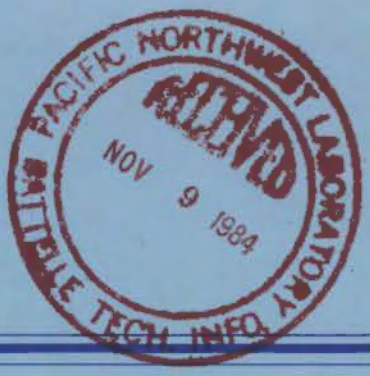

NUREG/CR-3841
PNL-4712

Steam Generator Group Project

Task 6 - Channel Head Decontamination

Prepared by R. P. Allen, R. L. Clark, W. D. Reece

Pacific Northwest Laboratory
Operated by
Battelle Memorial Institute

Prepared for
U.S. Nuclear Regulatory
Commission

For sale by the Superintendent of Documents, U.S. Government Printing Office
Washington, D.C. 20402

NUREG/CR-3841
PNL-4712
R5

Steam Generator Group Project

Task 6 - Channel Head Decontamination

Manuscript Completed: March 1983
Date Published: August 1984

Prepared by
R. P. Allen, R. L. Clark, W. D. Reece

Pacific Northwest Laboratory
Richland, WA 99352

Prepared for
Division of Engineering Technology
Office of Nuclear Regulatory Research
U.S. Nuclear Regulatory Commission
Washington, D.C. 20555
NRC FIN B2097

ABSTRACT

The Steam Generator Group Project utilizes a retired from service pressurized water reactor steam generator as a test bed and source of specimens for research. Program objectives emphasize validation of the ability to nondestructively characterize the condition of steam generator tubing in service. Remaining integrity of tubing with service induced defects is studied through burst and leak rate tests. Other program objectives seek to characterize overall generator condition, including secondary side structure, and provide realistic samples for development of primary side decontamination, secondary side cleaning, and nondestructive examination technology.

An important preparatory step to primary side research activities was reduction of the radiation field in the steam generator channel head. This task report describes the channel head decontamination activities. Though not a programmatic research objective it was judged beneficial to explore the use of dilute reagent chemical decontamination techniques. These techniques presented potential for reduced personnel exposure and reduced secondary radwaste generation, over currently used abrasive blasting techniques. Two techniques with extensive laboratory research and vendors prepared to offer commercial application were tested, one on either side of the channel head. As indicated in the report, both techniques accomplished similar decontamination objectives. Neither technique damaged the generator channel head or tubing materials, as applied. This report provides details of the decontamination operations. Application system and operating conditions are described. Areas of improvement are suggested. The report should be of benefit to utilities contemplating decontamination work, and provides basic data of interest to regulators.

TABLE OF CONTENTS

TABLE OF CONTENTS (Continued)

TABLE OF CONTENTS (Continued)

LIST OF TABLES

LIST OF TABLES (Continued)

LIST OF FIGURES

LIST OF FIGURES (Continued)

LIST OF FIGURES (Continued)

LIST OF FIGURES (Continued)

LIST OF FIGURES (Continued)

LIST OF FIGURES (Continued)

LIST OF FIGURES (Continued)

LIST OF FIGURES (Continued)

LIST OF FIGURES (Continued)

ACKNOWLEDGEMENTS

Appreciation is extended to the members of the BNW Corrosion Research & Engineering Section who assisted with the preparation and decontamination activities by providing technician assistance and shift coverage. Special thanks also are due the following:

- R. L. Clark and R. L. McDowell for the corrosion monitoring and specimen characterization work.
- L. K. Fetrow, S. Saenz and G. H. Hauver for their invaluable assistance in solving some of the problems encountered in the decontamination operations and for the development of special devices and installation methods that substantially reduced personnel exposure.
- G. H. Giddings for conscientiously and efficiently handling the many supply details required for the SGEF and task operations.
- L. W. Hankel, J. J. Reck and other members of the Radiation Monitoring Section for their dedicated service during the decontamination operations.
- G. R. Hoenes, W. D. Reece and other members of the Radiological Sciences Department for their comprehensive services throughout the course of the decontamination task.
- R. L. Lundgren for assistance with a number of problem areas that otherwise could have impacted the task schedule.
- K. H. Pool and R. L. McDowell for the laboratory support activities.
- N. L. Scharnhorst for decontamination of the manway cover bolts.
- E. B. Schwenk and R. L. Bickford for the development and implementation of the liquid waste transfer system.
- W. E. Skiens for development of the coating system used to preserve sections of the original tube sheet surface and to isolate the hot leg nozzle cover.
- J. E. Coleman and D. H. Parks for scanning electron microscopy and metallography support.
- H.E. Kissinger for X-ray diffraction analyses.

The assistance of the Virginia Electric and Power Company (VEPCO) in obtaining the use of the research generator removed from service at their Surry Nuclear Station Unit 2 is hereby acknowledged. VEPCO has also provided valuable assistance with historical information on the generator's operation inspection and maintenance.

1. INTRODUCTION

The Steam Generator Group Project represents a unique opportunity to thoroughly evaluate a service degraded steam generator under carefully controlled study conditions. However, like operations performed on operating units, many of the preparatory, examination and sampling activities require access to the tubes and tube sheet through the hot leg and cold leg channel head regions. The objective of the channel head decontamination task was to comply with ALARA concepts and facilitate these subsequent task activities by substantially reducing channel head exposure levels without adversely affecting other components and surfaces.

The specific technical requirements for the decontamination task were:

- Surface radiation levels of approximately 5 R/h shall be reduced by at least a factor of ten, as measured by shielded thermoluminescent dosimeters (TLD) placed directly on the channel head interior surface.

- Substances or processes employed shall be controllable to the extent that they are not damaging to primary side surfaces and components not associated with the channel head region.

- Removed contaminants shall be completely contained. Methods and substances shall be compatible with the space, equipment, services, and waste handling capabilities of the Steam Generator Examination Facility.

- A maximum radiation worker exposure limit of 2 rem/quarter shall be observed. Contractor shall comply with all health and safety requirements of the DOE-operated facility including ALARA principles.

Like the steam generator project as a whole, the decontamination task, in addition to performing a necessary function, represented a unique opportunity to test and demonstrate innovative equipment and decontamination processes without the outage time constraint and other concerns attendant to decontamination operations on installed steam generators. To capitalize on this opportunity and provide the Group Sponsors with comparison information, it was decided to solicit separate contractors for the hot leg and cold leg decontaminations. It also was hoped that potential bidders would be willing to share in the expense of the work both in recognition of the opportunity for further development and demonstration of a commercial process and for access to the supporting information to be developed as part of the decontamination task.

Based on this approach, a Request for Proposal (Battelle-F1668, Decontamination of Nuclear Steam Generator Channel Head Region) was distributed on 4/23/82 to 35 domestic and foreign firms and groups, including several respondents to a 3/22/82 notice in the Commerce Business Daily. The following proposals were received and evaluated:

- Allied Nuclear, Inc. - In situ electropolishing.
- Combustion Engineering, Inc. and Kraftwerk Union AG - Wet abrasive blasting with the option of a two-step chemical decontamination process.
- KUE Engineering Canada, Ltd. - Low-pressure wet abrasive blasting.
- London Nuclear Services, Inc. - CAN-DECON dilute chemical process.
- NUS Corporation and Halliburton Services - AP/Citrox chemical process with an electrolytic decontamination option.
- Quadrex Corporation with Babcock-Woodal Duckham, Ltd. (BWD) and the Central Electricity Generating Board (CEGB) - LOMI dilute chemical process with electropolishing as a backup.
- Framatome - Abrasive blasting using a remotely operated system (telexed response).

After extensive consideration of both technical and cost factors, London Nuclear Services, Inc. was selected to decontaminate the cold leg region and Quadrex Corporation to do the hot leg region. Although both approaches were dilute chemical decontamination methods, it was felt that the process and chemistry details were sufficiently different to provide valuable comparison information on effectiveness, corrosion effects and other areas of interest to regulatory groups and potential users. It also was felt that application of these methods by commercial vendors could provide a demonstrated alternative to current industry practice. Dilute chemical decontamination offered advantages over current abrasive techniques by generating potentially less secondary waste and offering possibly reduced operator exposure during the process.

The channel head dimensions and surface materials are shown in Figures 1-1 and 1-2, respectively. The divider plate and bottom of the tube sheet are Inconel 600, while the interior surface of the bowl is a weld overlay of 309 stainless steel (22-24% Cr, 12-15% Ni). As noted in Figure 1-1, the Inconel and stainless steel surface areas are equal. One difference between the Surry unit and an operating steam generator was that the Surry nozzle openings were sealed at the Surry site with a welded, galvanized carbon steel cover. This was exposed to the decontamination solutions for the cold leg operation, but, as will be discussed later, was covered with a protective silicone rubber coating for the hot leg decontamination. The only other materials exposed during the two decontaminations were the 304 stainless steel manway covers used by the decontamination contractors.

The initial radiation readings in the cold leg and hot leg regions are illustrated in Figures 1-3 and 1-4. These were made using TLDs in three configurations:

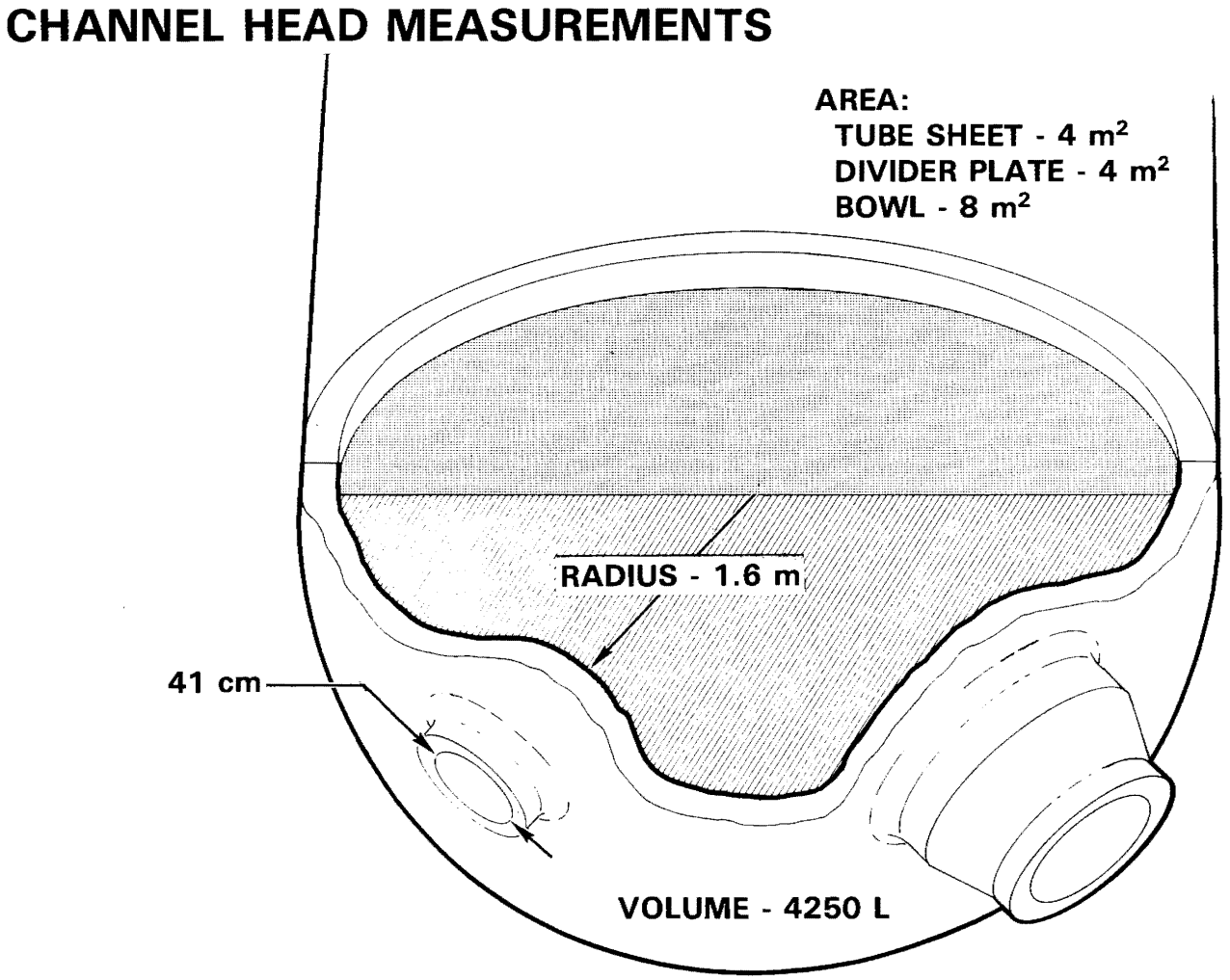
CHANNEL HEAD MEASUREMENTS
AREA:
TUBE SHEET - 4 m²
DIVIDER PLATE - 4 m²
BOWL - 8 m²
RADIUS - 1.6 m
41 cm
VOLUME - 4250 L

FIGURE 1-1.

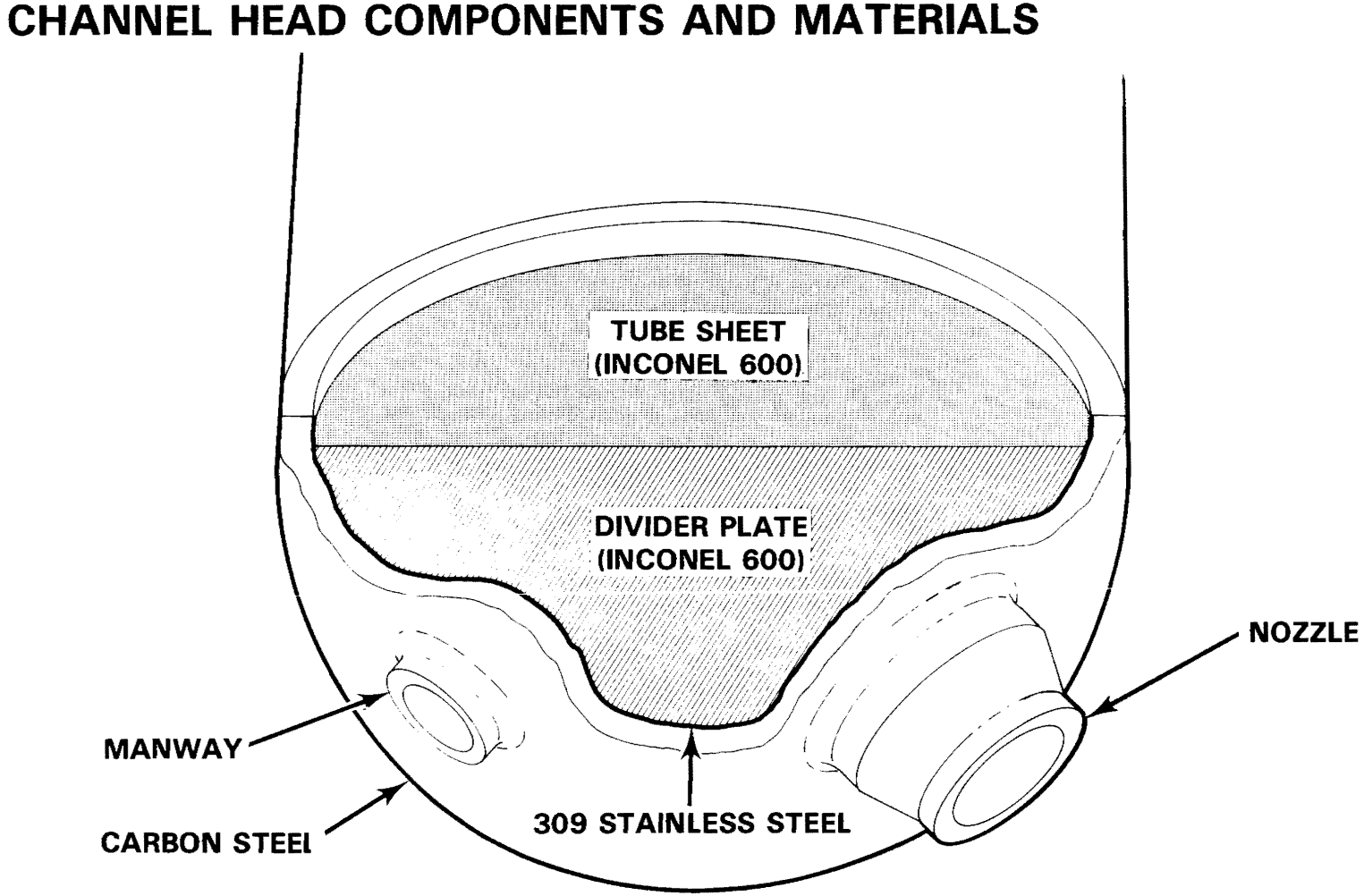
CHANNEL HEAD COMPONENTS AND MATERIALS
TUBE SHEET
(INCONEL 600)
DIVIDER PLATE
(INCONEL 600)
NOZZLE
MANWAY
CARBON STEEL
309 STAINLESS STEEL

FIGURE 1-2.

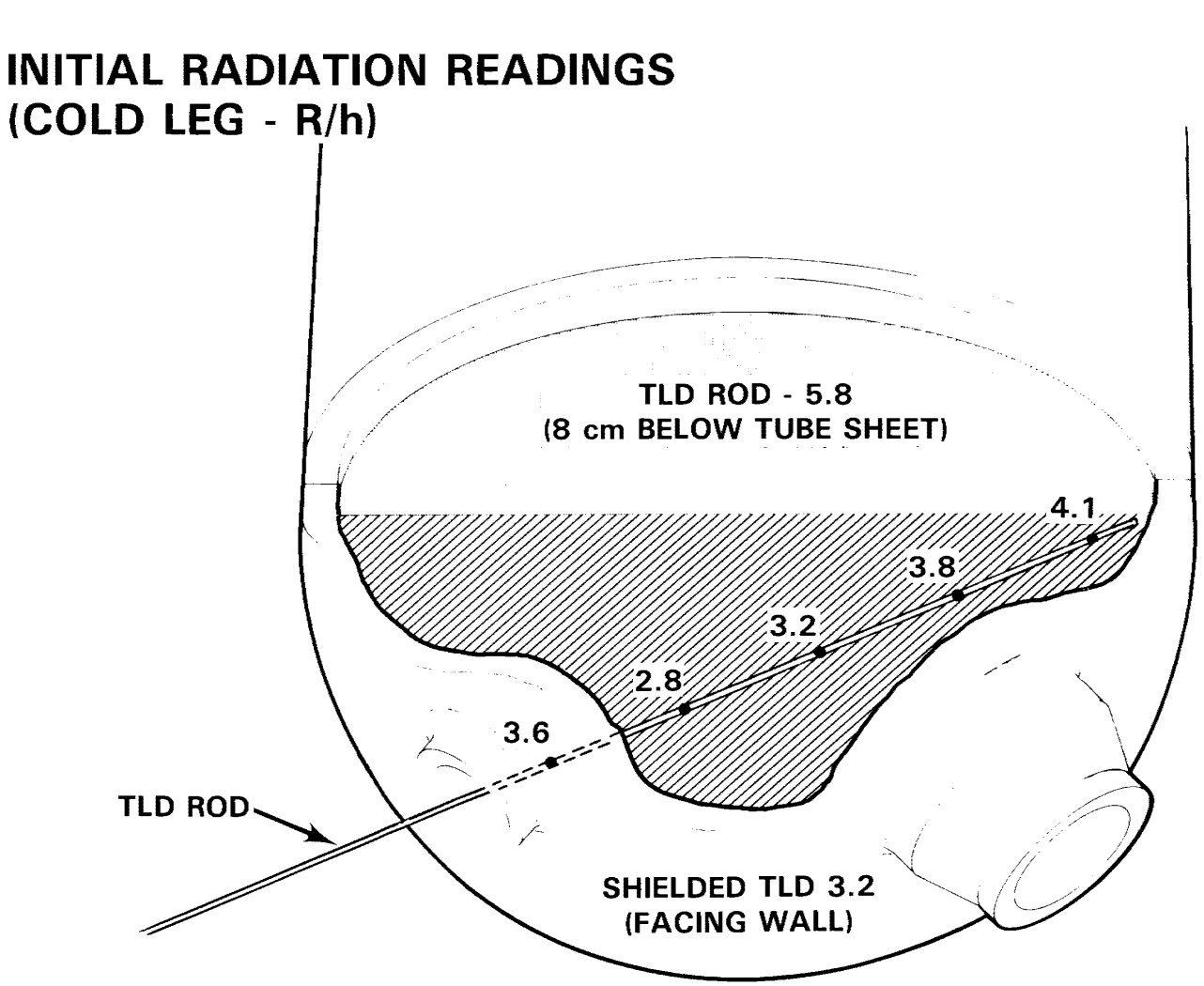
INITIAL RADIATION READINGS
(COLD LEG - R/h)
TLD ROD - 5.8
(8 cm BELOW TUBE SHEET)
4.1
3.8
3.2
2.8
3.6
TLD ROD
SHIELDED TLD 3.2
(FACING WALL)

FIGURE 1-3.

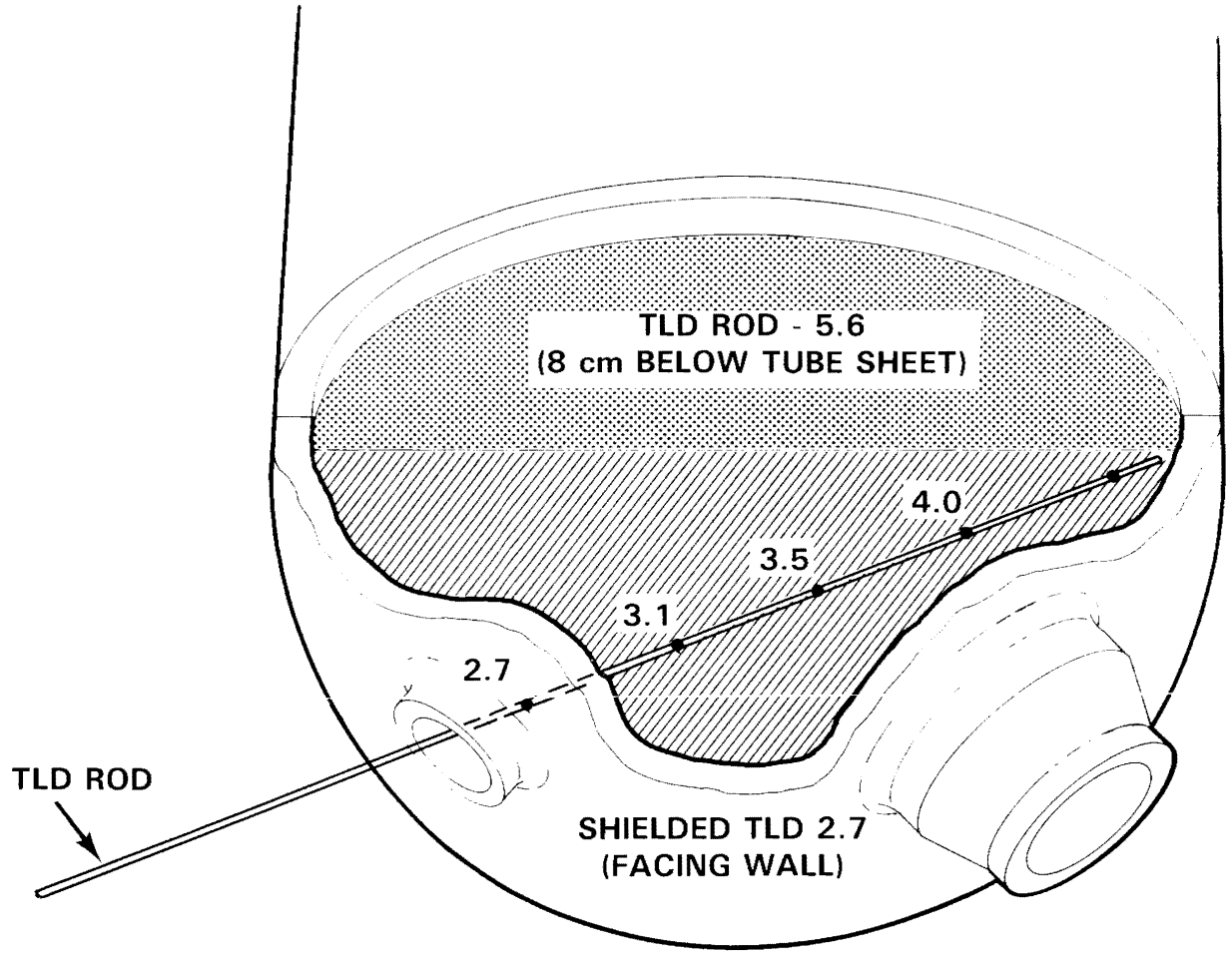
INITIAL RADIATION READINGS
(HOT LEG - R/h)
TLD ROD - 5.6
(8 cm BELOW TUBE SHEET)
4.0
3.5
3.1
2.7
TLD ROD
SHIELDED TLD 2.7
(FACING WALL)

FIGURE 1-4.

- In a rod suspended approximately 8 cm below the bottom of the tube sheet.

- In a rod passing through the manway and extending to the far corner junction of the bowl, divider plate and tube sheet as illustrated in Figures 1-3 and 1-4.

- Inset into the surface of a lead brick and placed against the surface of the bowl to measure the surface contamination levels.

The readings in the two halves were similar, ranging from ∿6 R/h just under the tube sheet to ∿3 R/h in the lower portions of the bowl and on the surface film.

As noted earlier, the objective of the decontamination work was to substantially reduce these radiation levels, as demonstrated by the achievement of at least a factor of ten decrease in the surface readings. This would not correspond to an equivalent decrease in the general levels inside the channel head because of the contribution from tube shine. For the decontamination of an operating steam generator, an effort would be made to decontaminate into the tubes some distance to reduce this contribution. In the case of the Surry operation, decontamination was constrained for reasons previously noted to the bottom of the tube sheet and no more than 3 cm into the tubes.

a report specially prepared for

BATTELLE PACIFIC NORTHWEST LABORATORIES

REPORT 722-1

CAN-DECON DECONTAMINATION OF THE RETIRED SURRY STEAM GENERATOR CHANNEL HEAD

February, 1983

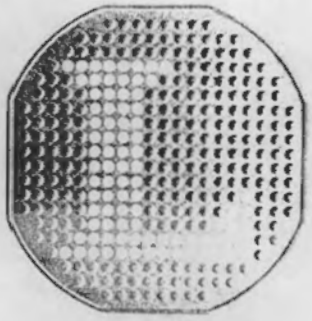

London Nuclear Services Inc.

3. COLD LEG DECONTAMINATION

The cold leg region of the Surry steam generator channel head was decontaminated during the September 4-10, 1982 time period by London Nuclear Services, Inc. using their CAN-DECON dilute chemical decontamination process. This section of the report contains the project report provided by London Nuclear Services, Inc. followed by a PNL addendum with supplemental details and figures.

8207468-5

FIGURE 2-17. Detector, Analyzer and Data Acquisition System for Co-60 Concentration Measurements

- Co-60 Activity - The concentrations of Co-60 in the decontamination solutions was measured throughout the decontamination operations using the Ge(Li) detector, analyzer and data acquisition system shown in Figure 2-17. A description of the evaluation procedures is included in Section 5.

- Corrosometer Data - Corrosion rate data (μm penetration) were obtained at approximate 2-h intervals for carbon steel, 304 stainless steel and 304L stainless steel for the cold leg decontamination, and for carbon steel, 304 stainless steel and Inconel 600 for the hot leg decontamination.

The data for these PNL evaluations is included in Section 6 and in Appendix B.

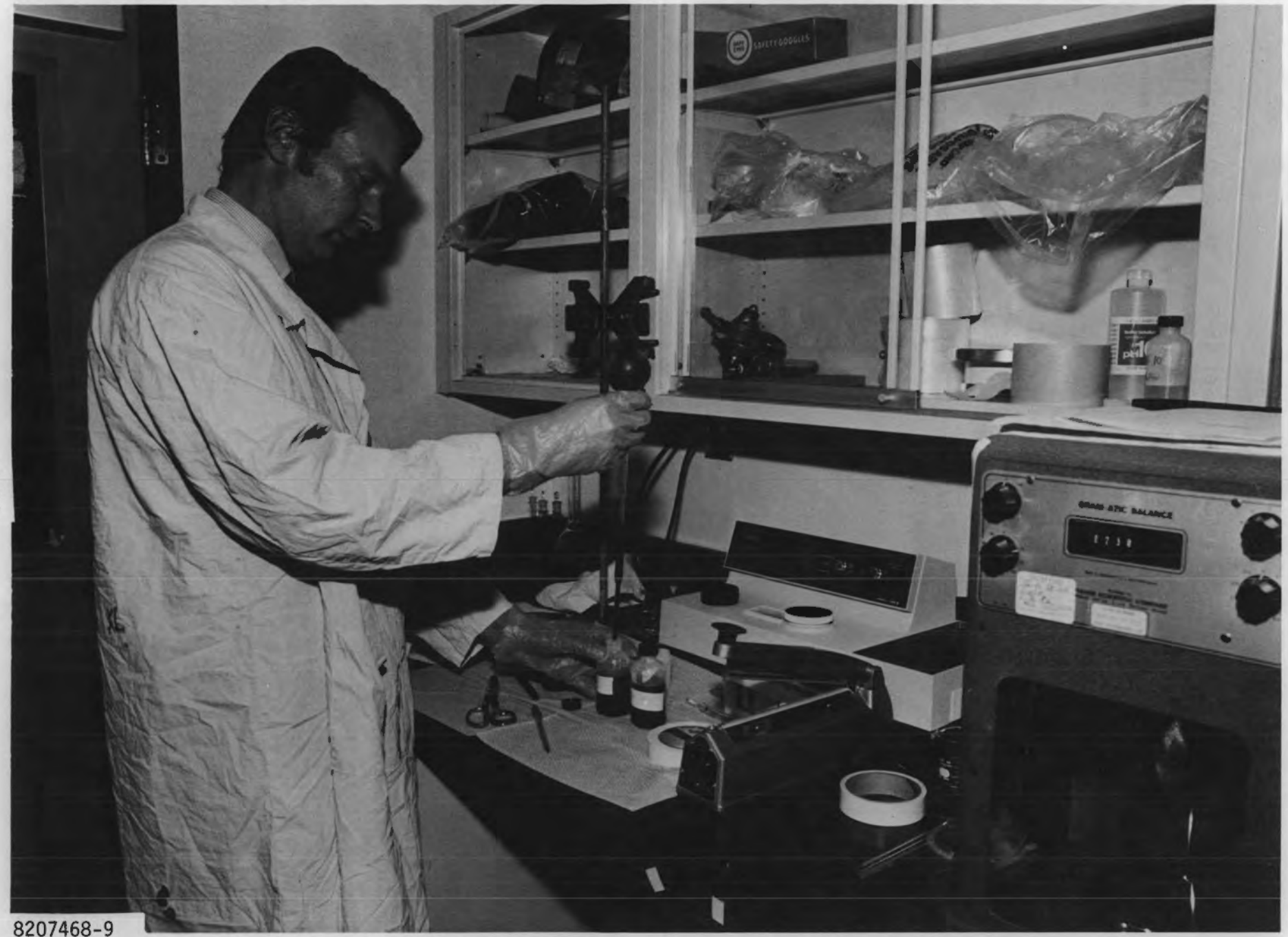

8207468-9

FIGURE 2-16. SGEF Laboratory During Hot Leg Decontamination Operations

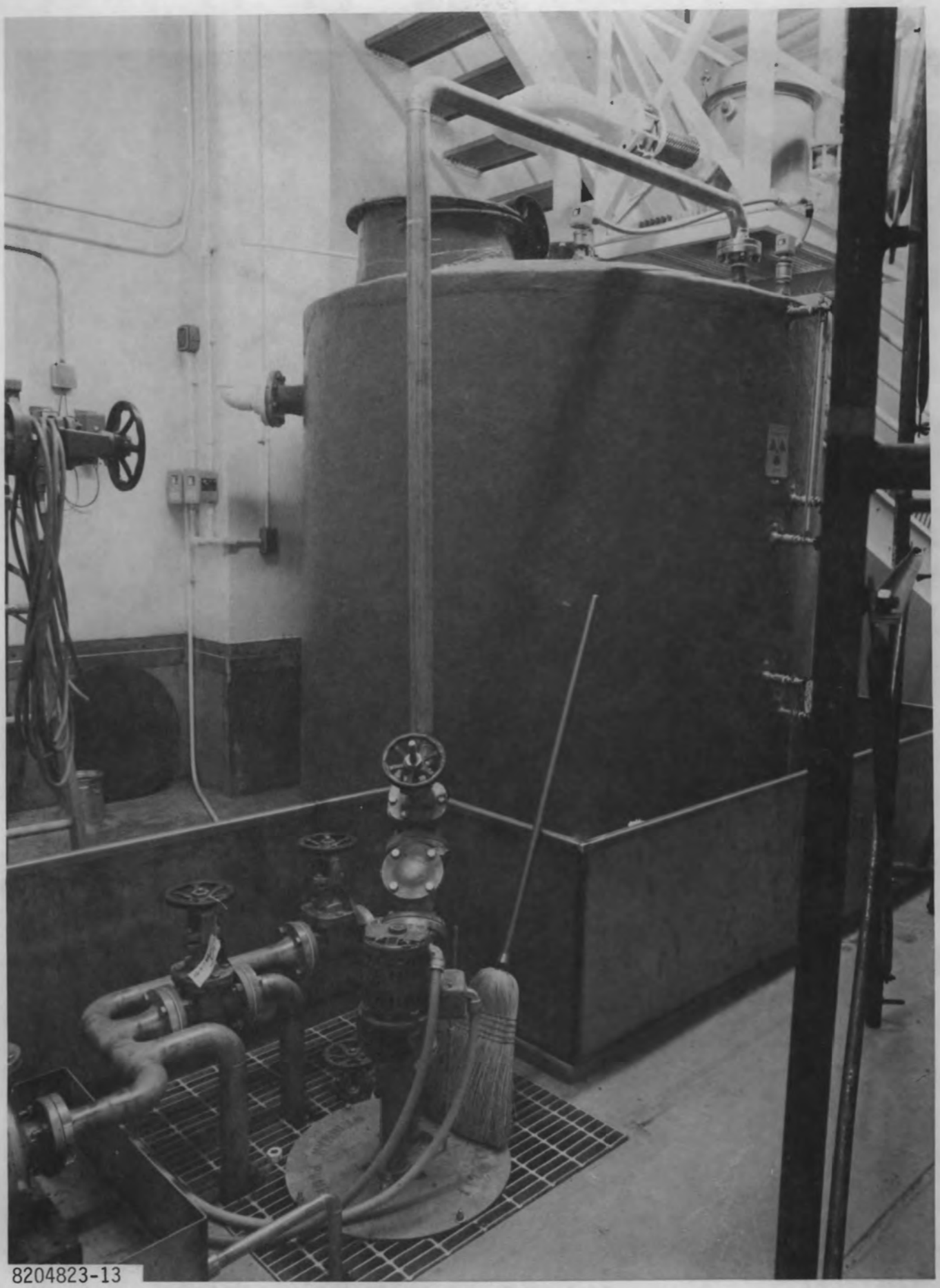

8204823-13

FIGURE 2-15. Basement Liquid Waste Holding Tank

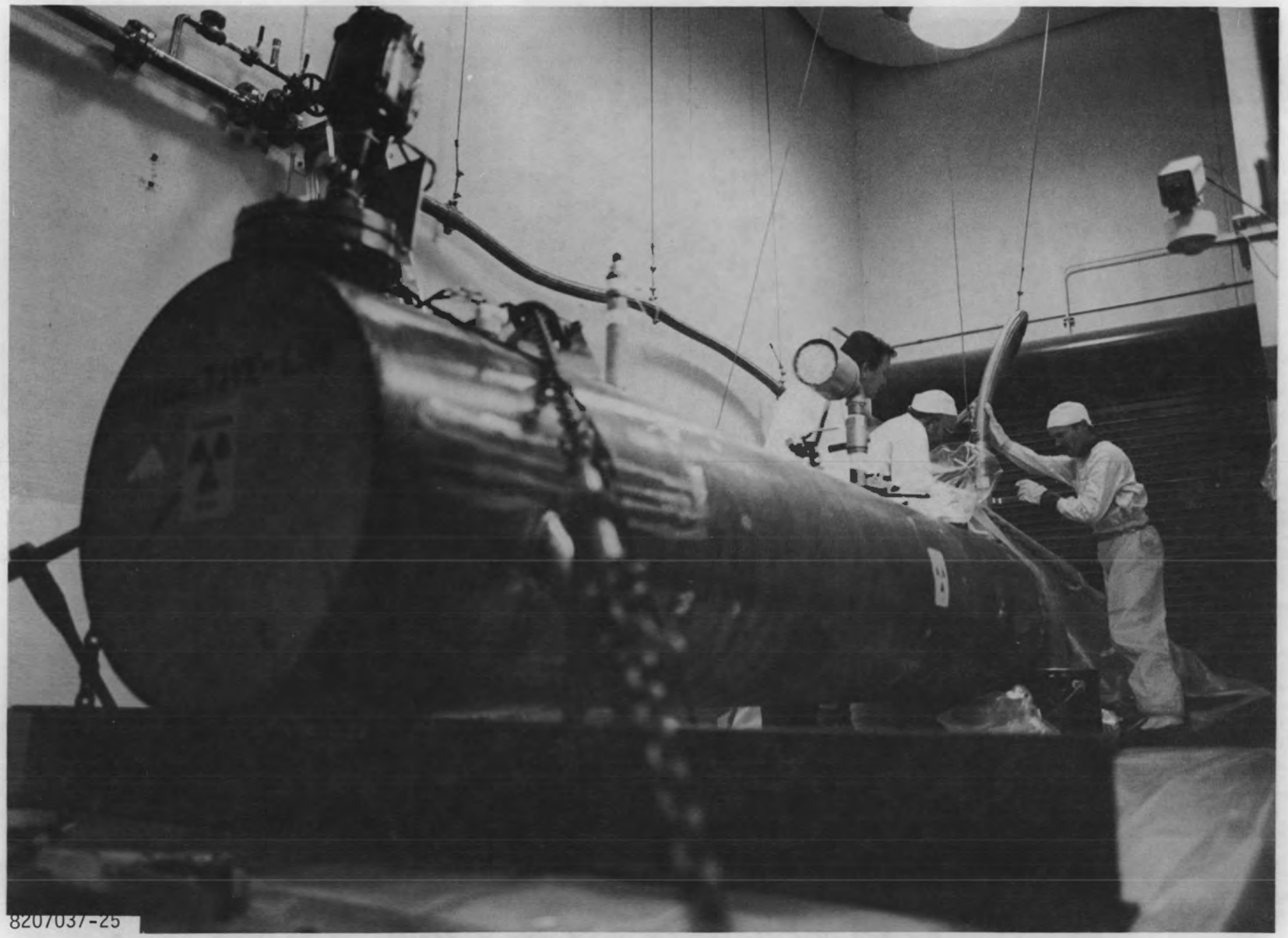

8207037-25

FIGURE 2-14. Liquid Waste Transfer Operation

8207037-40

FIGURE 2-13. Liquid Waste Transfer Tank

Liquid Waste Transfer/Disposal System (R. L. Bickford)

An existing 1900 ℓ tank was modified to serve as a liquid waste transport tank for the SGEF. Modifications were made on the tank so that it would sit horizontally on a truck trailer and could be filled through a 5 cm line from the SGEF basement holding tank. A drum pump was added so that waste could be pumped from the tank into the waste sump at the waste disposal facility. Other modifications included safety features such as two level indicators and an overflow line as well as a HEPA filter for venting air. When the modifications were completed on the transfer tank, safety personnel witnessed the leak tests and pressure tests.

During waste transfer operations, the transfer tank was mounted and fastened on a trailer bed (Figure 2-13). The trailer was backed into the SGEF truck lock where the transfer tank was filled with liquid waste pumped from the basement holding tank (Figures 2-14 and 2-15). The trailer was then moved to the waste disposal facility for the Hanford Site 300 Area where the liquid waste was pumped from the transfer tank into the waste sump. Chemical analyses of the liquid waste were taken before transit and results were given to personnel at the waste disposal facility. After being pumped dry, the transfer tank was moved back to the SGEF. When the 7600 ℓ SGEF basement holding tank is full, it takes four such trips to dispose of all the liquid waste.

Process Chemistry Support

The laboratory in the SGEF (Figures 2-6 and 2-16) was equipped with the instrumentation and supplies needed by London Nuclear Services and Quadrex/CEGB personnel to control the respective decontamination processes. Procedures and analyses conducted using periodic samples of the process solutions included:

- pH and conductivity
- Particulates
- EDTA
- Iron II^{+} and total iron
- Dissolved oxygen/hydrazine
- Proprietary conditioning/decontamination reagents.

A more detailed description of the analytical procedures and process monitoring schedules is provided in Sections 3 and 4.

In addition to the process chemistry work by the decontamination contractors, PNL provided around-the-clock analytical/evaluation support in the following areas:

- Dissolved metals - Atomic absorption spectroscopy was used to determine the concentration (in ppm) of Fe, Cr, Ni, Cu, Mn and Zn in the decontamination solutions during the decontamination operations.

8207891-53

FIGURE 2-12. Installed Nozzle Cover Coating and Hold-Down

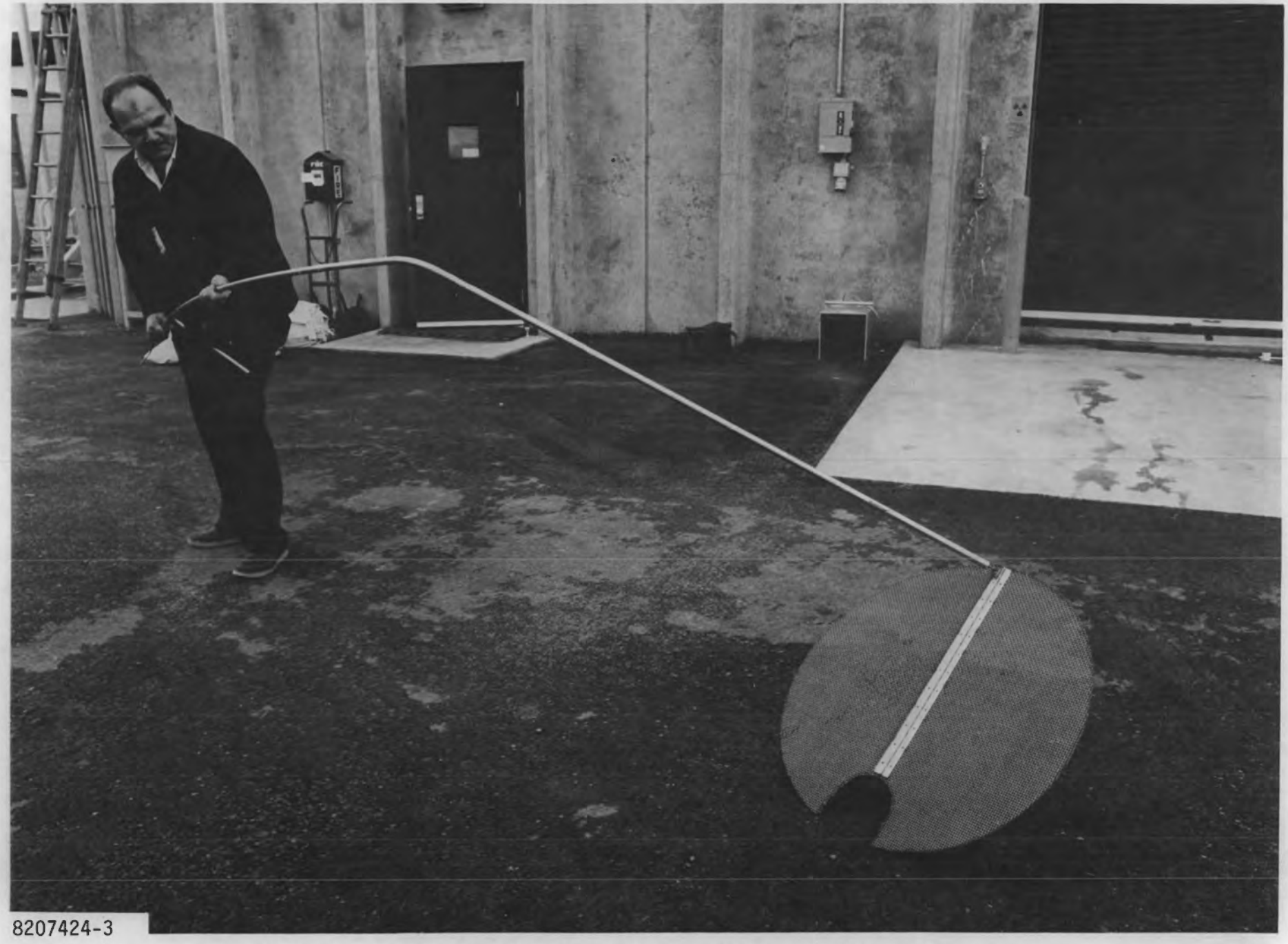

8207424-3

FIGURE 2-11. Nozzle Cover Coating Hold-Down and Remote Placement Fixture

Deionized Water Supply

The deionized water required for both the cold leg and hot leg decontamination processes was obtained from an 8 ℓ/min purification system located in a building adjacent to the SGEF. The water was accumulated in a 3800 ℓ tank just outside the SGEF and supplied as needed by a small pumping system.

Nozzle Cover Coating and Hold-Down

As noted previously, all of the materials in the channel head were either stainless steel or Inconel 600 with the exception of the galvanized carbon steel covers welded over the nozzle openings at the Surry site. This was not considered a problem for the cold leg decontamination process. However, for the hot leg decontamination operation, there was concern about possible adverse effects of the zinc on the decontamination reagents, excessive consumption of reagents via corrosion of the steel, complication of process control and evaluation work because of the additional iron in solution, and possible precipitation problems. The area of the nozzle cover was approximately 2.5% of the total area to be decontaminated, and estimates by CEGB personnel indicated that the amount of iron in solution from corrosion of the carbon steel could be of the same order of magnitude as that from dissolution of the oxide film. It was felt that this would complicate or possibly invalidate the corrosion measurements. In order to avoid these problems, the hot leg cover was coated on the inside with sprayable silicone rubber using a spray nozzle operated through a 10-cm-diameter drain hole in the cover. A stainless steel mesh was placed over the coating (using the remote placement arrangement shown in Figure 2-11) to prevent detachment of the coating and plugging of the pump or other system components. The installed coating and hold-down are shown in Figure 2-12.

Other Preparatory Activities

Other miscellaneous activities required to prepare for the decontamination operations included:

- A detailed photographic examination of the lower portion of the channel head to ensure the absence of an interconnecting drain hole that is present in some steam generator designs.

- Careful measurements to establish the position of the tube sheet to set the control point for the maximum level of the decontamination solutions.

- Welding a strong-back on the outside of the nozzle covers to prevent a catastrophic failure of the welds. The cover on the hot leg nozzle also was rewelded in response to a leak that developed in the weld on the cold leg cover, resulting in premature termination of the last part of the decontamination run.

- Construction of greenhouses around each manway to support the preparatory operations inside the channel head.

8205988-13

FIGURE 2-10. Heat Exchanger System

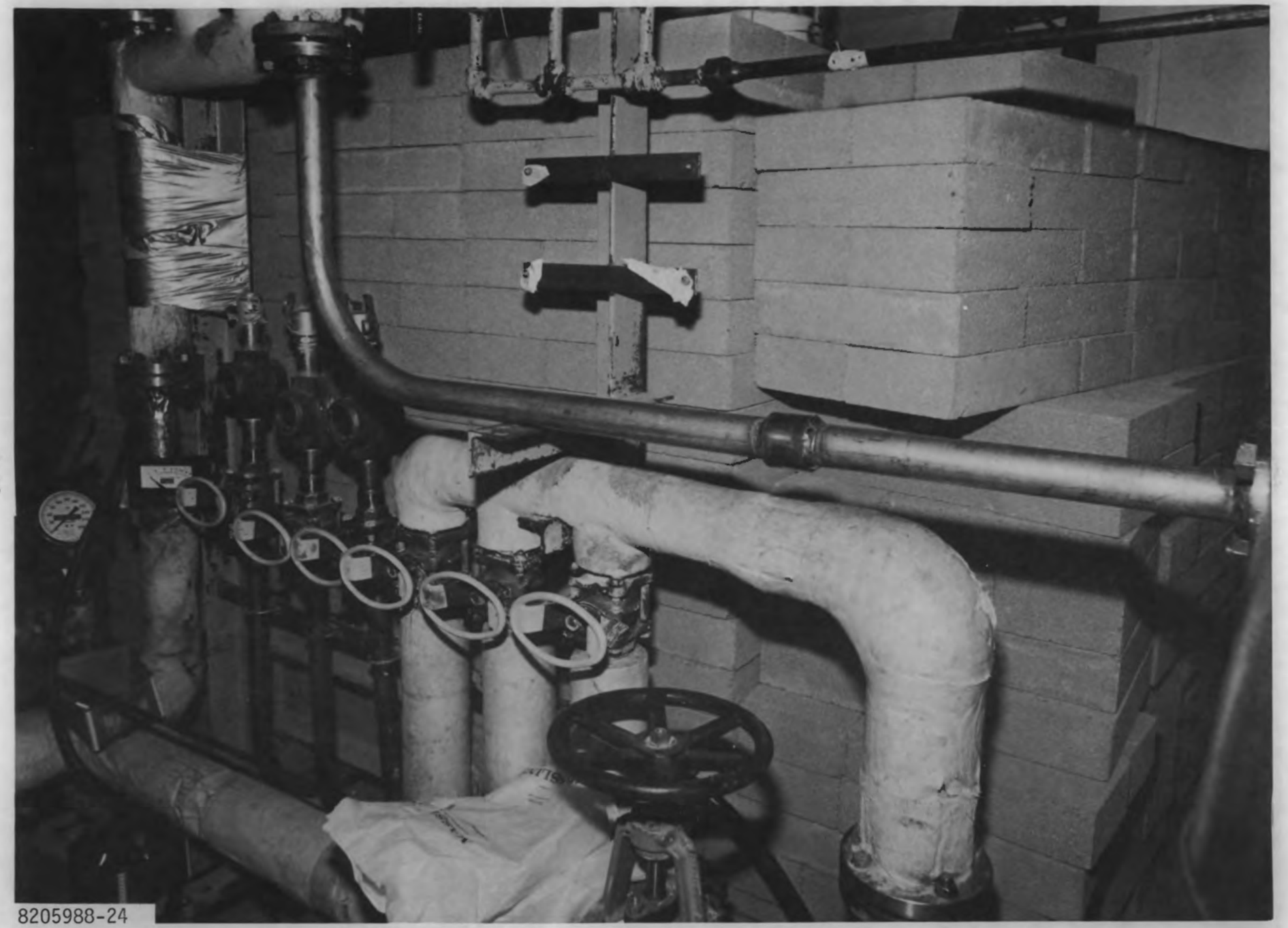

8205988-24

FIGURE 2-9. Shielded Ion Exchange Columns

8206784-86

FIGURE 2-8. Concrete Block Shielding Wall Outside the Steam Generator Examination Facility

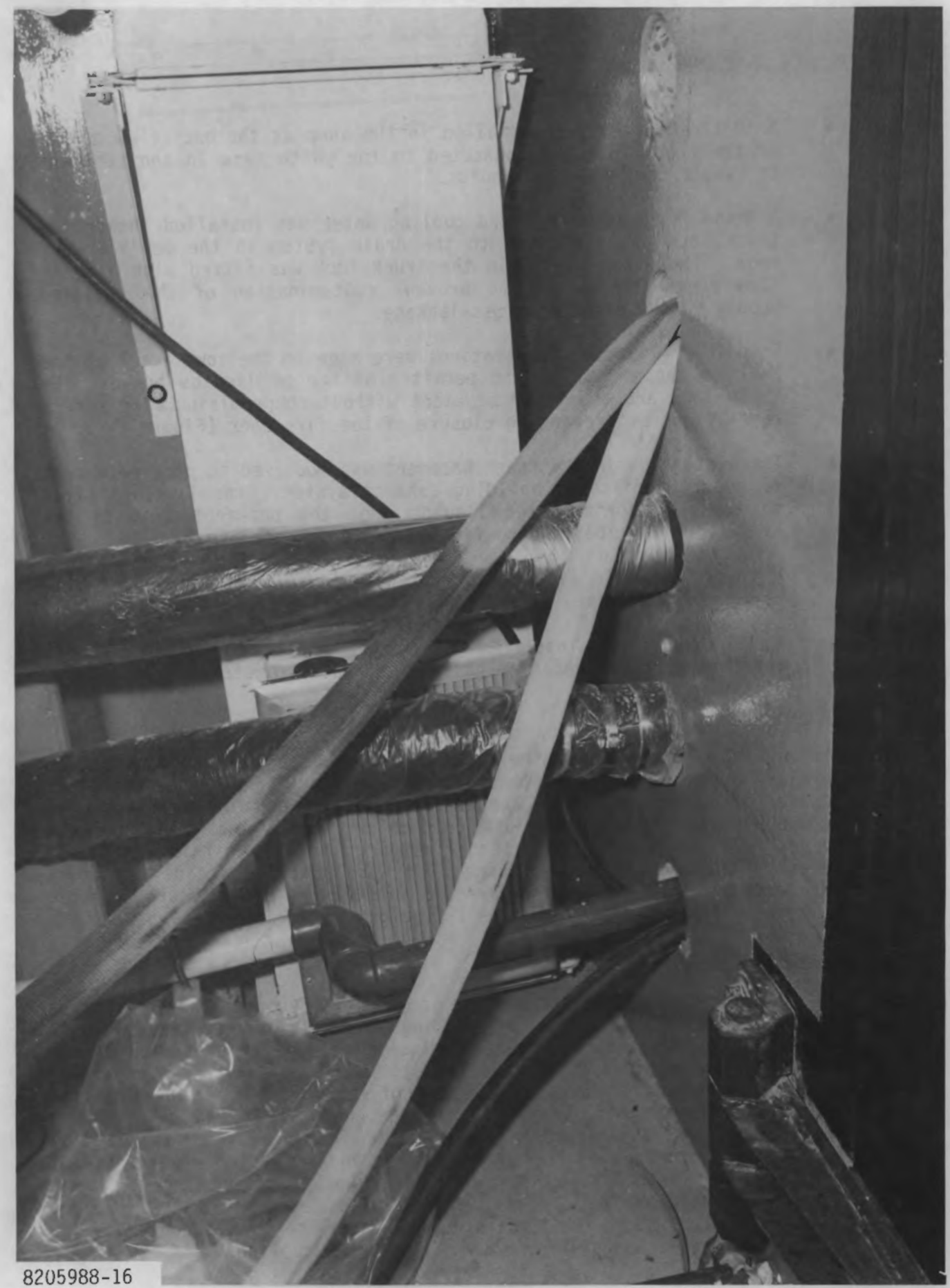

8205988-16

FIGURE 2-7. Wall Penetrations for Transfer of Liquids Between the Truck Lock and Tower Basement

- A 19 ℓ/min. pump was installed in the sump at the back (low point) of the truck lock and connected to the waste tank in the basement to handle contaminated liquids.

- A drain for noncontaminated cooling water was installed inside the truck lock and connected to the drain system in the men's locker room. The water supply in the truck lock was fitted with a back-flow prevention device to prevent contamination of the building supply in the event of cross-leakage.

- Five 10-cm-diameter penetrations were made in the tower wall at the back of the truck lock to permit transfer of liquids between the truck lock and the tower basement without compromising fire safety regulations by preventing closure of the fire door (Figure 2-7).

- The waste tank in the tower basement was modified to provide a vent to the HEPA-filtered building exhaust system. The line installed to transfer contaminated liquids from the basement tank to the truck lock was modified to fit the waste transfer tank.

- A truck-mountable liquid waste transfer tank was designed, fabricated and certified.

- A TV camera was installed in the truck lock to permit remote monitoring of the decontamination and waste transfer operations.

Radiation Safety

The activity removed from the cold leg surfaces by the London Nuclear Services decontamination process was collected by ion exchange equipment located in the truck lock. The concrete block shielding wall shown in Figure 2-8 was constructed just outside the truck lock wall and was successful in reducing the external readings to well within acceptable levels. The ion exchange columns also were shielded inside the truck lock with block as shown in Figure 2-9 to minimize the exposure to those working in the truck lock and the laboratory.

Heat Exchanger System

The reagent removal step of the cold leg decontamination process required a 114 ℓ/min. flow of cooling water for sufficient time to reduce the system temperature to the value needed for operation of the mixed bed ion exchange resin (Section 3). Radiological safety considerations prevented the direct disposal of the cooling water into the building drain system; therefore, an independent heat exchanger system was used to provide the cooling capacity while minimizing the potential for cross-contamination. The heat exchanger system (Figure 2-10) consisted of a shell/tube heat exchanger capable of cooling 230 ℓ/min water from 35°C to 29°C when supplied with 190 ℓ/min water at 18°C maximum, and a pump to circulate the water to the decontamination equipment heat exchangers for sample and system cooling.

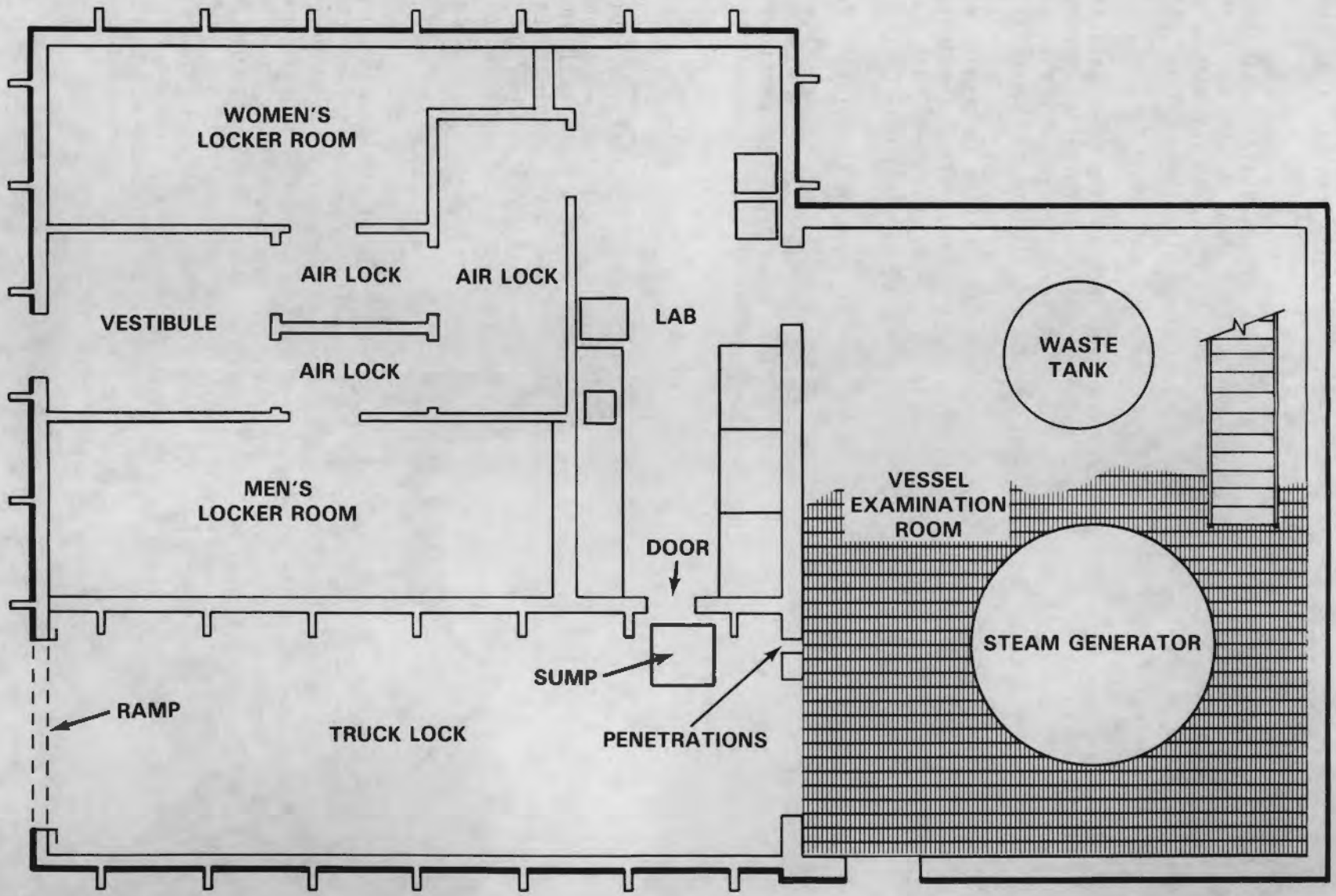

FIGURE 2-6. Floor Plan of the Steam Generator Examination Facility

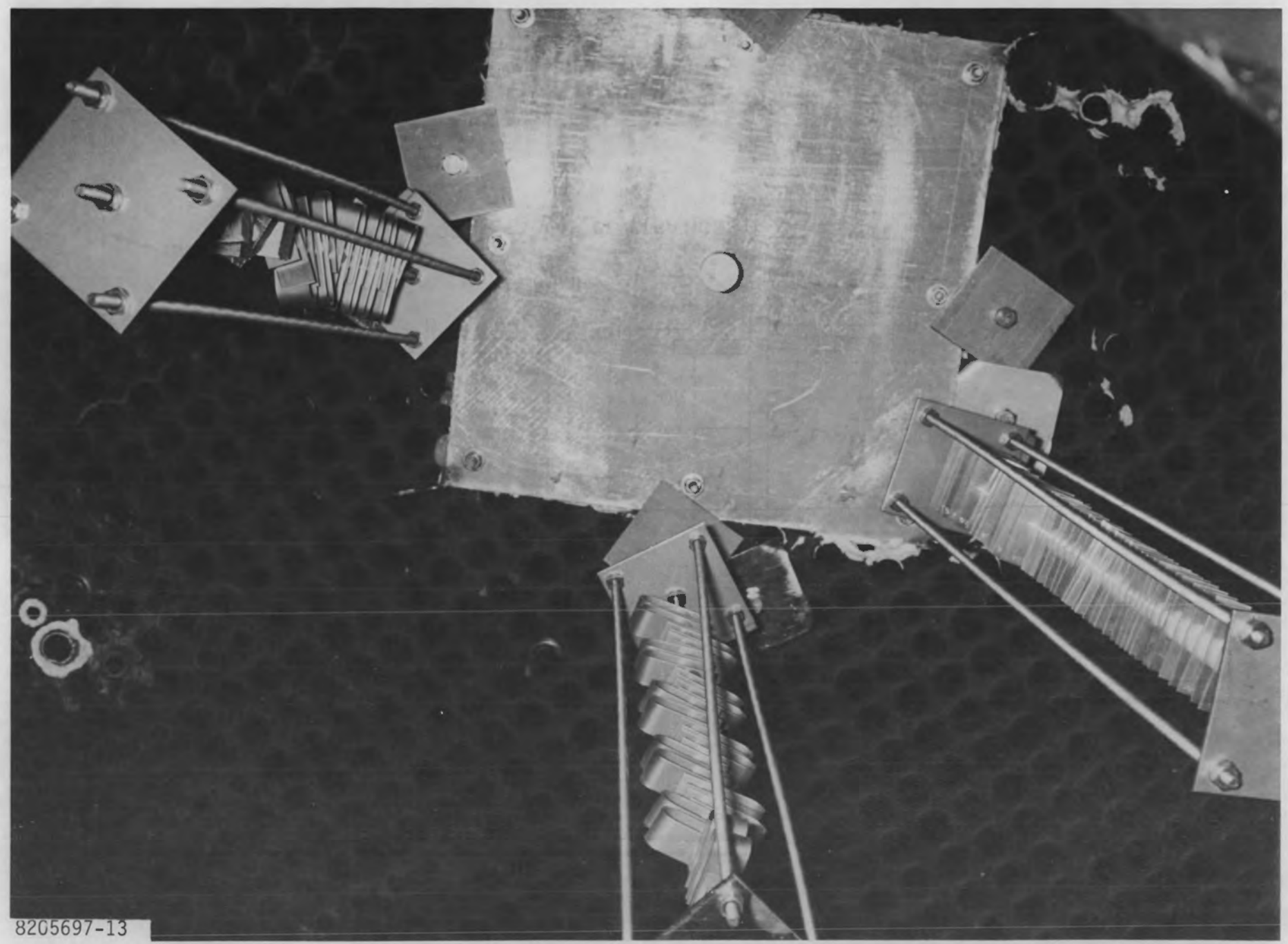

8205697-13

FIGURE 2-5. Installed Protective Plate and Corrosion Specimens for Cold Leg Decontamination

8205627-40

FIGURE 2-4. Special Fixturing Developed to Remotely Install the Protective Plate

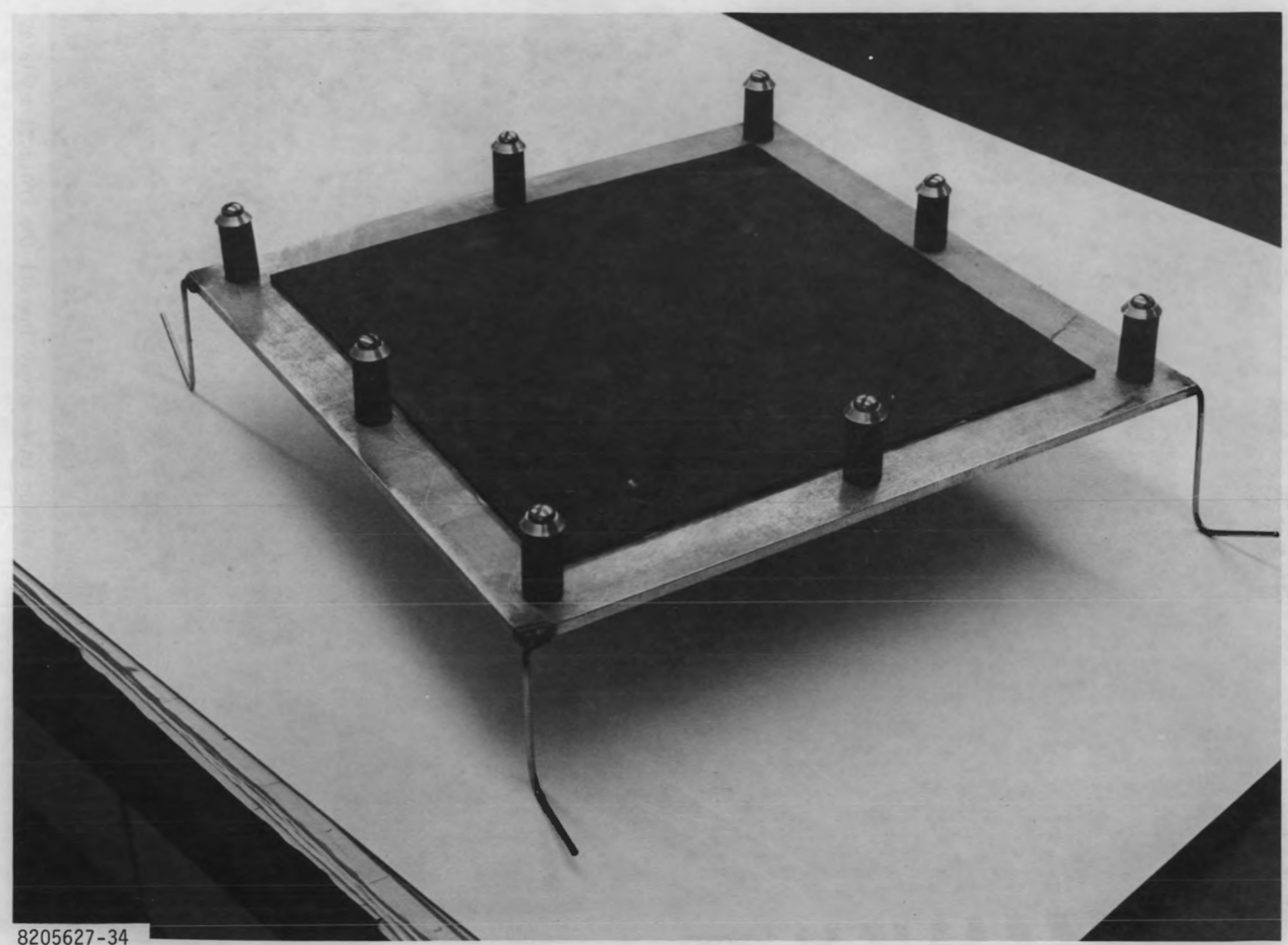

FIGURE 2-3. Protective Plate Used to Preserve a Section of the Contaminated Tube Sheet

Preparation/Installation of Protective Plates

In order to preserve a section of the contaminated tube sheet bottom surface on each side for future studies, a special protective plate covering an approximate 30 cm x 30 cm area was developed and installed prior to each of the decontamination operations. The plate (Figure 2-3) was stainless steel with 6-in. lead anchor fasteners designed to lock into selected tubes around its perimeter. A silicone rubber sealing compound was applied around the edge just before installation as an added protection against intrusion of the decontamination solutions. Radiation exposure during installation of the protective plate was minimized by developing the special fixturing illustrated in Figure 2-4. Installation of the plate was accomplished in less than 20 minutes working from outside the channel head through the manway.

Preparation/Placement of Corrosion Specimens

More than 50 corrosion specimens representing a range of materials and conditions were obtained and mounted in racks as described in detail in Section 6. These racks were suspended inside the channel head using hooks installed in conjunction with the protective plate (Figure 2-5). The corrosometer probes (Section 6) used to monitor corrosion behavior during the decontamination operations were mounted on the manway covers provided by the decontamination contractors.

Decontamination of Manway Cover Bolts

The steel bolts originally used to fasten the manway cover on the operating steam generator were of a special type that could not readily be obtained. Twenty-four of these bolts therefore were decontaminated to a nonsmearable condition by soaking and scrubbing using concentrated hydrochloric acid and a thread cleaning device and then used to fasten the new manway covers provided by the decontamination contractors.

Facility Modifications

A number of minor modifications to the Steam Generator Examination Facility (Figure 2-6) were required to accommodate the placement of the contractor process equipment and to enhance the radiological and industrial safety of the decontamination operations. These included:

- Installation of a door between the laboratory and the truck lock to serve as an emergency escape route for personnel working in the truck lock and to permit operation, from inside the laboratory, of the pump used to transfer waste into the truck lock.

- Modification of the truck lock to provide secondary containment for the cold leg decontamination equipment and the liquid waste transfer operations. An 8-cm high ramp was constructed at the entrance of the truck lock and the floor and walls were sealed to a height of 1.5 m with successive coatings of Carboline 305 and Butvar.

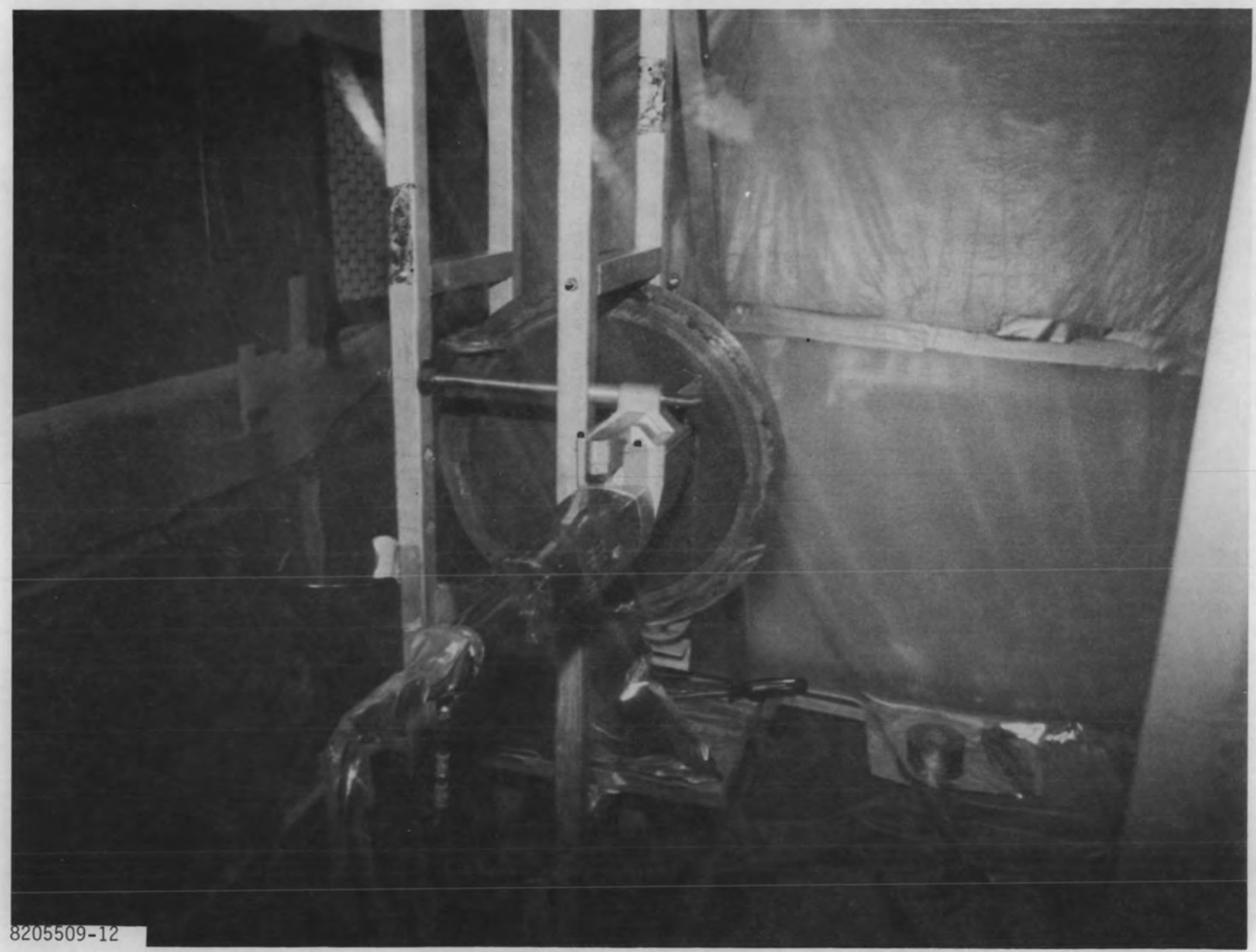

8205509-12

FIGURE 2-2. Sectioning the Manway Inserts to Obtain Evaluation and Decontamination Specimens

8204823-44

FIGURE 2-1. Core Drilling to Obtain Samples of the Interior Channel Head Surfaces

2. PREPARATORY AND SUPPORTING ACTIVITIES

Although the decontamination contractors were to provide the necessary equipment and conduct the decontamination operations, there were a number of project supported activities required to prepare the Steam Generator Examination Facility (SGEF), obtain pre- and post-decontamination data, prepare corrosion and decontamination effectiveness samples, and provide analytical, waste management and other support during the actual operation. The following is a summary of the more important preparatory and support activities. Some of these are described in greater detail in the subsequent sections.

Channel Head Pictures

The interior surfaces of the channel head were comprehensively photographed before and at the conclusion of each decontamination stage. Selected color photographs illustrating the surface changes are included in the results section for each decontamination process (Figures 3-15 to 3-17 and 4-10 to 4-12). A complete listing of available picture sequences is included in Appendix A. Video tapes also were prepared for the hot leg and cold leg operations.

Radiological Measurements

The radiation levels at various locations inside the channel head were comprehensively measured using TLD techniques before and at the conclusion of each decontamination stage as described in detail in Section 5.

Removal of Core and Tube Specimens

Samples of the hot leg and cold leg stainless steel surfaces were obtained prior to decontamination by core drilling through the outer carbon steel shell as illustrated in Figure 2-1. This was a very difficult operation because of the hardness of the weld overlay stainless steel. Similar samples were taken after the decontamination operations. A 25-cm section of the tubing (Row 1, Column 94, between support plates 6 and 7) was removed and used to prepare ring specimens for the corrosion and decontamination effectiveness studies. This was to assess effects of the decontamination processes on tube ID (primary side) and OD (secondary side) films.

Sectioning of Manway Inserts

The hot leg and cold leg manway inserts, which had respective radiation levels of 2.0 R/h and 3.6 R/h, were remotely sectioned into strips using the self-feeding, reciprocating saw arrangement shown in Figure 2-2. The coupons prepared from these strips were used to evaluate decontamination effectiveness for 304 stainless steel.

SUMMARY

The dilute chemical decontamination process, CAN-DECON, was applied to the cold-leg channel head of the retired Surry steam generator at Battelle PNL.

The CAN-DECON process, applied in five steps, removed 2.1 curies of activity and produced 24 cubic feet of ion exchange resin waste. The average decontamination factor (DF) observed in the channel head was 6.3. The tubes were not included in the decontamination, at the request of Battelle. A considerable portion of the remaining field is attributed to shine from the tubes. Readings on-contact with the lower channel head interior, shielded from the tube shine, gave DFs of about 30, indicating that almost complete removal of the oxide film was achieved with the CAN-DECON process.

The results indicate that the CAN-DECON dilute chemical decontamination process can effectively remove PWR oxide deposits and can effectively reduce fields in steam generator channel heads. The final fields in this demonstration fell to about 0.5 R/h.

TABLE OF CONTENTS

1. INTRODUCTION

Under Battelle Pacific Northwest Laboratories' Subcontract No. B-F166-8-A-P-1, London Nuclear was contracted to decontaminate one-half of the channel head of the Retired Surry Steam Generator. The steam generator was housed in the Steam Generator Examination Facility; a building designed to support study and non-destructive testing of the steam generator.

The decontamination was performed between September 4, 1982, and September 10, 1982. The decontamination utilized the London Nuclear CAN-DECON Dilute Chemical Decontamination Process.

This report presents the process operations, chemistry, and results of the decontamination, including metallic and radionuclide removals, corrosion rates, decontamination factors, estimated radiation exposure, and radiation fields.

2. PROCESS OPERATIONS

The major decontamination activities performed at Battelle are summarized in Table 2.1. The steam generator channel head was decontaminated using a five-step process. The process alternated between reducing and oxidizing steps at reagent concentrations between .05 and .10 wt %.

Attached Figure 2.1 shows the simplified flow path for the CAN-DECON process. LND 101A and LND 104 reagents were dissolved in demineralized water and circulated from the channel head through ion exchange columns and back to the channel head. A process heater was used to maintain tempertures at 200°F. Two cation columns were used to remove corrosion products and radionuclides. A mixed-bed column was used to remove the CAN-DECON reagent. A more detailed description of the operating procedures is contained in Attachment 1, Section 3, "Standard Operation."

There were some operating problems during the decontamination. Due to the fact that only one side of the channel head was to be decontaminated by London Nuclear, it was necessary to operate the system at atmospheric pressure. This limited the operating temperature to 200°F. The CAN-DECON process is more effective at 250°F. The circulation pump seal failed during the decontamination. After numerous attempts were made to repair the seal, it was decided to use Battelle's waste transfer pump to complete the decontamination. A later inspection revealed that an improper shaft had been supplied with the circulation pump. Near the end of Step 5 of the decontamination, the nozzle cover plate on the steam generator developed a sizeable leak. This plate had been poorly welded over the primary nozzle stub when the steam generator was transferred from Surry to PNL. This failure caused early termination of the decontamination.

Upon completion of the decontamination, the mixed-bed and cation columns were slurried into 55-gallon collection drums for final disposal. The waste was contained in 12 drums, (660-gallon capacity) of which 180 gallons was contaminated resin and approximately 360 gallons was slurry water. The water was decanted from the drums and transferred to the waste storage tank. The resin was buried by Battelle.

The channel head was inspected after final draining. The fields observed were partially attributed to the shine from the tubes, and partially to a thin, blackish deposit unevenly distributed around the head. This deposit was washed into a collection vessel, using a simple water spray. Final radiation fields were then measured.

FIGURE 2.1

CAN-DECON FLOW PATH

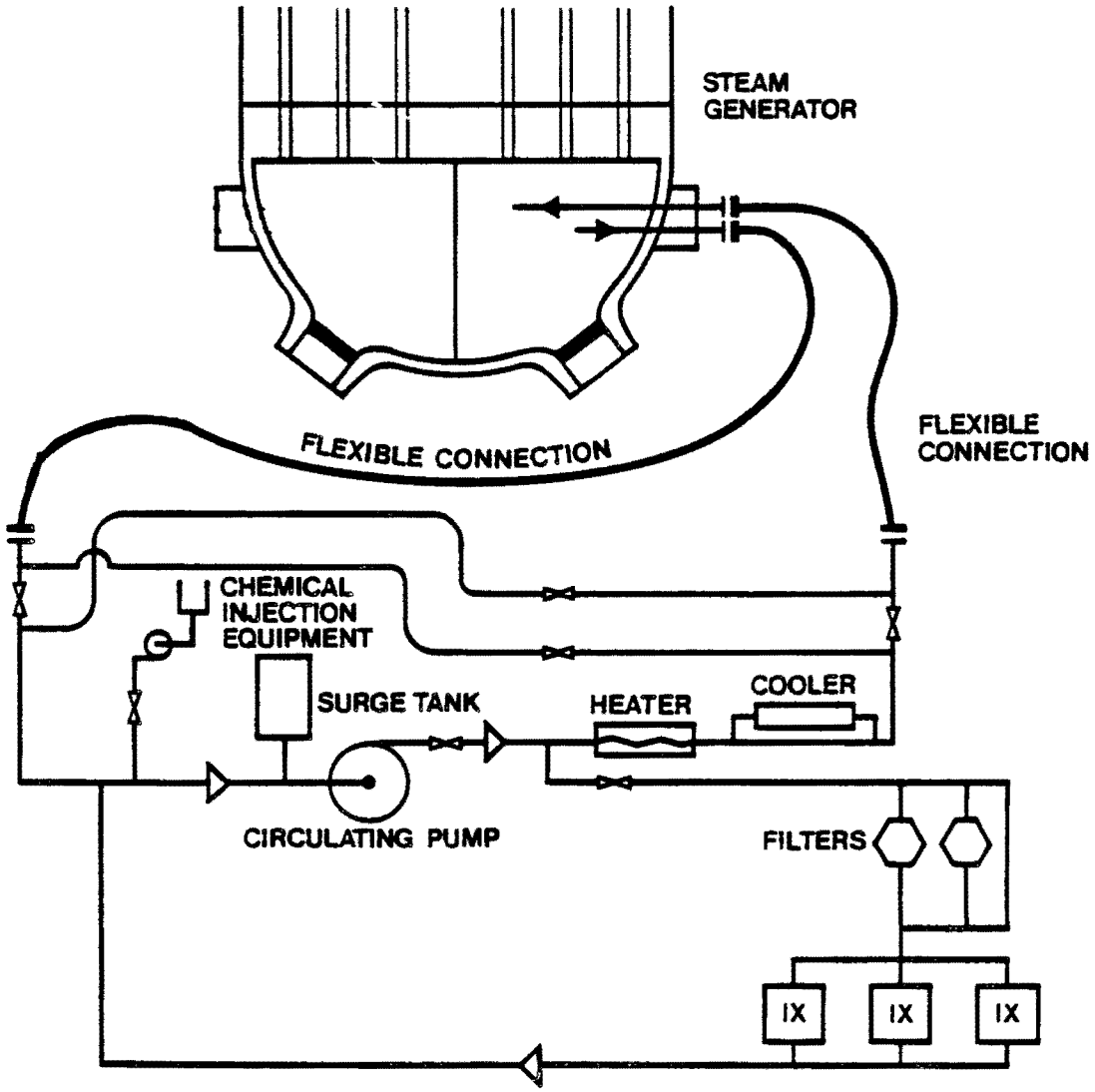

TABLE 2.1

DECONTAMINATION ACTIVITIES

DATE	TIME	ACTIVITY
8/23/82	13:00	London Nuclear Representative Arrived at Job Site
8/30/82	10:30	Arrival of London Nuclear Staff at Job Site
	15:00	Indoctrination and Training Completed
9/2/82	20:00	Instrument Calibration & Equipment Installation Completed
9/4/82	9:30	System Started Up
9/5/82	2:20	LND 101A Reagent Added/Cation Column On-Line
	15:35	Mixed-Bed on Line to Remove LND-101A
	18:00	Mixed-Bed off Line
	19:15	LND-104 Reagent Added
9/6/82	09:00	Mixed-Bed on Line to Remove LND-104
	12:30	Mixed-Bed off Line
	17:00	LND-101A Reagent Added/Cation Column on Line
9/7/82	3:00	Mixed-Bed on Line to Remove LND-101A
	6:00	System Shut Down
	13:00	System Opened for Inspection
	15:00	Determined that 4th & 5th Steps Desirable
9/8/82	20:50	System Started Up
9/9/82	1:00	LND-104 Reagent Added
	10:00	Mixed-Bed Valved in to Remove LND-104
	11:30	LND-101A Added/Cation Column on Line
	15:30	Mixed-Bed Valved in to Remove LND-101A
	17:00	Decontamination Terminated
9/10/82	15:00	Resin Slurry Completed

3. CHEMISTRY AND CORROSION

This section summarizes aspects of chemistry, corrosion, and radiation monitoring associated with the decontamination.

Chemistry

A summary of the pH, conductivity, reagent concentration, dissolved iron, and dissolved Co-60 data, during all steps of the decontamination, is included as Table 3.1. As shown in Table 3.2, a total of 2.08 Ci of Co-60 was removed from the system by ion exchange columns. In addition to dissolved Co-60, trace amounts of other radionuclides, such as Cr-51, Cs-131, etc., were also detected periodically. However, their minute concentration had no significant contribution to the overall amount of dissolved activity removed. Given in Table 3.3 is a list of dissolved metals removed from the system. Slightly more than 2.4 kg of dissolved metals (iron and chromium) were removed with a majority (97%) being iron. This is equivalent to a removal of 4.8 kg of oxide film. Analysis of particulates during the operation indicated only traces of activity and metals present as non-dissolved species.

Corrosion

Corrosion rates for 304 stainless steel and Inconel 600 were measured during decontamination. Four coupons of each material were weighed and installed in the coupon holder of the decontamination skid. After completion of the decontamination, these coupons were removed and re-weighed. They were found to have gained marginally in weight (average weight gained of 0.03% and 0.008% for the 304 SS and Inconel 600 coupons respectively). This phenomenon is attributed to the presence of an extremely thin film of deposit of unknown nature on the surface of all exposed coupons. Brushing of these coupons failed to remove the film. Visual inspection of the exposed coupons revealed no obvious sign of corrosion. As a result, it is concluded that no corrosion occurred on either the stainless steel or Inconel coupons employed. Furthermore, data generated on a real-time basis by an on-line corrosometer with a 304 SS probe during the decontamination supported this judgment. Table 3.4 presents the corrosion coupon results.

TABLE 3.1

SUMMARY OF OPERATING CONDITIONS DURING EACH
STEP OF THE STEAM GENERATOR CHANNEL HEAD DECONTAMINATION

Step	pH	Cond. (umho/cm)	Reagent Conc. (wt%)	Dissolved Iron (ppm)	Dissolved Co-60 (uCi/ml) $x10^{-3}$
1. Reducing					
Before Reagent Addition	9.1	57	0	0.3	5.0
During Reagent Regeneration	2.8	725	0.07	18.7	4.8
After Reagent Removal	5.0	11	0	2.4	0.47
2. Oxidizing					
Before Reagent Addition	5.0	11	0	*	2.7
During Reagent Circulation	10.9	1220	0.1	4.3	1.3
After Reagent Removal	5.4	22	0	5.0	*
3. Reducing					
Before Reagent Addition	9.9	74	0	0.1	1.2
During Reagent Regeneration	2.5	1333	0.1	17.5	140
After Reagent Removal	6.4	25	0	1.1	0.52
4. Oxidizing					
Before Reagent Addition	4.0	95	0	9.2	4.1
During Reagent Circulation	10.6	909	0.05	1.3	2.9
After Reagent Removal	9.4	33	0	0.2	0.76
5. Reducing					
Before Reagent Addition	3.2	392	0	0.2	0.3
During Reagent Regeneration	2.8	892	0.07	15.6	8.9
After Reagent Removal	4.1	44	0	1.5	0.34

* Not Measured

TABLE 3.2

DISSOLVED Co-60 REMOVED (Ci)

Step 1	
Reducing	0.166
Step 2	
Oxidizing	-
Step 3	
Reducing	1.608
Step 4	
Oxidizing	-
Step 5	
Reducing	0.301
TOTAL	2.075

TABLE 3.3

DISSOLVED METALS REMOVED (g)

	Fe	Cr	Total
Step 1	970	-	970
Step 2	-	43	43
Step 3	910	-	910
Step 4	-	25	24
Step 5	470	-	470
Total (rounded)	2350	68	2420
Equivalent Oxide			4840

TABLE 3.4
WEIGHT CHANGE IN CORROSION COUPONS

Corrosion Coupon Designation	Initial Weight (g)	Final Weight (g)	Weight Change (g)
H-1	5.3370	5.3392	+ .0022
2	5.3461	5.3473	+ .0012
3	5.3385	5.3398	+ .0013
4	5.3427	5.3439	+ .0012
	Average wt. Change = + .001475 g		
A-1	11.1772	11.1780	+ .0008
2	11.0877	11.0888	+ .0011
3	11.0454	11.0462	+ .0008
4	11.0777	11.0785	+ .0008
	Average wt. Change = + .000875 g		

Note:

H - 304 SS
A - Inconel 600

4. DECONTAMINATION FACTORS AND RADIATION EXPOSURE

Radiation readings were taken, by Battelle staff, using a TLD rod at various locations in the steam generator channel head. Figure 4.1 shows initial and final radiation readings.

Table 4.1 summarizes the radiation data collected. The DF (decontamination factor) varied from 4.5 to 80.0. The average DF of 6.3 was calculated by averaging points 3 to 6. The low DF for Point 1 was accredited to shine from the tubes. Point No. 7 was taken facing the vessel and did not reflect the actual fields in the vessel. However, point No. 7 does indicate that tube shine may be the major contributor to radiation fields in the vessel.

Note that these final readings were taken after the decontamination of the hot-leg channel head. The contribution from the hot-leg had limited the DF to about 2.8; that is, the average cold-leg channel head fields behaved as follows:

Before any decon	3.35 R/h
After cold-leg decon	1.2 R/h
After hot-leg decon	0.53 R/h
Final DF	6.3 R/h

Shielded dosimeters on the stainless steel surfaces gave DFs of about 30 (as reported by Battelle staff).

Active stainless steel coupons and Inconel tubes were placed in the steam generator vessel, giving DFs of 5.7 to 8.5 for stainless sheet and 4.1 to 4.3 for Inconel.

Total radiation exposure to London Nuclear personnel was 1.4 man-rem.

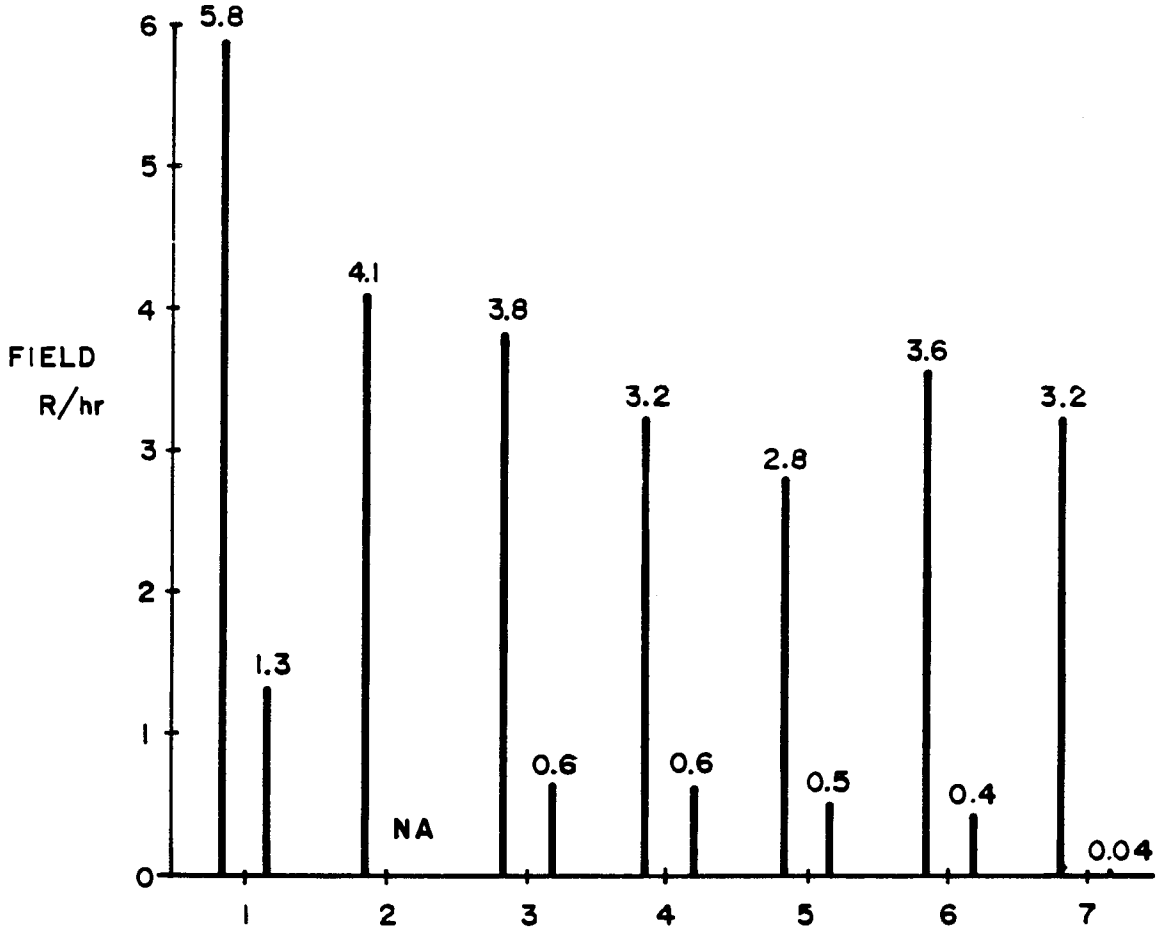

BEFORE AND AFTER FIELD READINGS*
ON TLD ROD POSITIONS

* FROM BATTELLE TLD ROD,
AFTER INSERTION IN CHANNEL HEAD
NA — NOT AVAILABLE

	LONDON NUCLEAR
DECONTAMINATION RESULTS	FIG. 4.1

TABLE 4.1

DECONTAMINATION RESULTS

	Field, R/h		
	Before	After	D.F.
1. TLD Rod 8 cm Below Tube Sheet	5.8	1.3	4.5
2. TLD Rod 274 cm from Bottom of Shell	4.1	-	-
3. TLD Rod 213 cm from Bottom of Shell	3.8	0.6	6.3
4. TLD Rod 152 cm from Bottom of Shell	3.2	0.6	5.3
5. TLD Rod 91 cm from Bottom of Shell	2.8	0.5	5.6
6. TLD Rod 30 cm from Bottom of Shell	3.6	0.4	9.0
7. Shielded TLD at Tube Sheet Facing Wall	3.2	0.04	80.0

$$\text{Average DF} = \frac{\text{Average Pts. 3-6 Before}}{\text{Average Pts. 3-6 After}} = \frac{3.35}{0.53} = 6.3$$

Shielded Dosimeters on Stainless Steel Surfaces	-	-	30.0*

* Results reported by Battelle Staff

5. CONCLUSION

The decontamination of the Surry Steam Generator demonstrated that PWR deposits can be effectively removed by the CAN-DECON process.

An average decontamination factor of 6.3 was achieved. The decontamination resulted in the transfer of 2.08 curies of activity from the steam generator onto 24 cubic feet of ion exchange resin. The resin was dewatered, solidified, and buried by Battelle.

Upon completion of all decontamination activities, a visual inspection of the steam generator revealed it to be clean and free of any deposits. This, combined with low radiation levels found on the vessel surface (Point No. 7 Figure 4.1), infers that the residual fields are produced from tube shine. It is felt that the CAN-DECON application to the steam generator was successful in removing PWR deposits and a subsequent application to the tubes would improve fields in the steam generator channel head.

ATTACHMENT 1

Battelle Pacific Northwest Laboratories

CAN-DECON Decontamination of the
Retired Surry Steam Generator Channel Head

- Procedures -

1. INTRODUCTION

This document summarizes the operational requirements for the decontamination of the steam generator head. It contains three sections which detail (1) the necessary preparations for equipment and services (2) process operations for the various steps required for the decontamination and (3) process chemistry for effective decontamination monitoring.

2. EQUIPMENT INSTALLATION AND SYSTEM PREPARATIONS

2.1 Equipment Installation

The decontamination equipment will arrive at site in a number of sections which require assembly, as well as connection to the channel head, before decontamination. These sections are:

- one ion exchange skid (skid 1)
- two ancillary equipment skids (skid 2 & skid 3)
- one piping header for skid 1
- three interskid connecting spool pieces
- miscellaneous equipment and instrumentation (disconnected for ease of shipping or due to fragile nature)
- two man-way covers for the channel heads

The following outlines the installation sequence:

(a) Add the ion exchange resin to the ion exchange columns as follows:

CU101 1.7 cu. ft. cation, 6.3 cu. ft. anion
CU102 7.5 cu. ft. cation, 0.5 cu. ft. anion
CU103 1.6 cu. ft. cation, 6.4 cu. ft. anion

(b) Install the man-way cover on the Steam Generator Channel Head to be decontaminated.

(c) Locate the pump skid (No. 3) in the basement near the Steam Generator Channel Head as per Figure 1.

(d) Locate the main skid (No. 2) and the IX skid (No. 1) on the main floor in the truck lock as per Figure 1.

(e) Construct temporary shielding around the IX skid (No. 1) using concrete blocks.

(f) Install the piping header along the front of skid 1.

(g) Install the interskid connecting spool pieces.

(h) Connect the following process services to the skids:

- demineralized water supply (interface S-5)*
- cooling water supply and return (interfaces S-3 and S-4)*
- drain lines (interfaces S-6 and S-6A)*

(i) Install and calibrate instrumentation as necessary.

(j) Connect the nitrogen bottle and regulator to the surge tank. (Interface S-7)*

(k) Complete the electrical connections to skid 2 (Interfaces S-8, S-8A, and S-9)*

(l) Connect the slurry hose to CU-102 and route to the collection header (interface S-11).* See Figure 2. (Note that the hose should be temporarily supported to prevent kinking and have sufficient slack so as to be easily moved to the other two slurry connections.

(m) Attach a 3" x 50' hose to connect skid No. 2 at the surge tank and to the man-way cover. (Interface S-2 and S-2A)*

(n) Attach a 3" x 50' hose to connect the man-way cover to skid No. 3 at the pump suction. (Interface S-12 and S-12A)*

(o) Attach a 3" x 50' hose to connect the outlet of skid No. 3 to the inlet of skid No. 1. (Interface S-1 and S-1A)*

(p) Connect a ½" tubing line from the vent line on skid No. 3 to the vent line on skid No. 2. (Interface S-10 and S-10A)*

System Preparation

The following tasks are to be completed by Battelle staff before the decontamination starts:

(a) Supply the miscellaneous equipment listed in Appendix I.

(b) Radiation level readings are to be taken as necessary.

(c) Prepare the chemistry laboratory with support from London Nuclear staff.

*Note: Interfaces detailed in Table 1.

(d) Connect the rad-waste drain connection to the collection header.

(e) Supply 2,000 gallons of demineralized water to the job site.

(f) Supply cooling water for sample and process cooling.

FIGURE 1

EQUIPMENT LOCATION

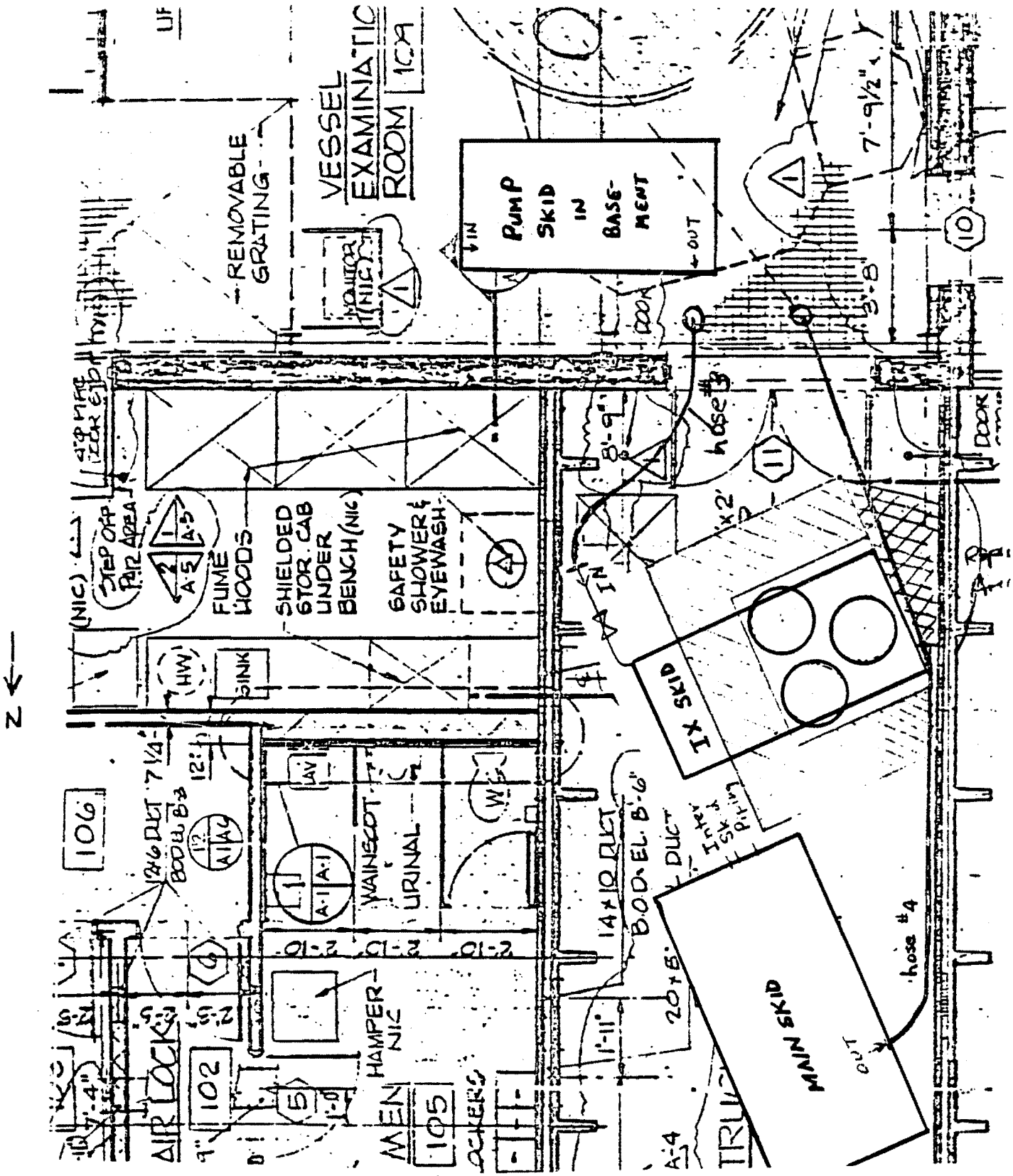

TABLE 1

INTERFACE CONNECTIONS

ITEM NO.	INTERFACE	CONNECTION
S-1 & S-1A	Outlet Skid 3 to Inlet Skid 1	3" X 50' hose; 3", 300 lb. R.F. Flg.
S-2 & S-2A	Surge Tank to Channel Head	3" x 50' hose; 3", 300 lb. R.F. Flg.
S-3 & S-4	Cooling Water Supply & Return (Process Cooler)	1½", 150 lb. R.F. Flg.
S-3A & S-4A	Cooling Water Supply & Return (Sample Cooler)	Mating 3/4" Union For Hose Connection
S-5	Demineralized Water Inlet	1½", 300 lb. R.F. Flg.
S-6	Rad-waste Drain	Mating 3/4" Union for Hose Connection
S-6A	Drain Line Connection Skid 3	1", 150 lb. R.F. Flg, Connect to 1" hose and Run to Waste Tank
S-7	Nitrogen Cylinder to System	½" Swagelock Fitting for Tygon Hose
S-8	150 Kw Heater Power Supply	480V/150A/3-phase (*See Note 1)
S-8A	Circulating Pump Power Supply	480V/150A/3-phase (*See Note 1)
S-9	Instrumentation & Control Power Supply	110V/20A/1-phase
S-10 & S-10A	Vent Line Connection Skid 3 to Skid 2	½" Swagelock Fitting; Run ½" tygon Tube to Collection Tank
S-11	Resin Slurry to 55-gallon Drums	1¼" Cam-lock or equivalent
S-12 & S-12A	Channel Head to Skid 3	3" x 50' hose; 3", 300 lb. R.F. Flg.

* Note: Common Supply for Interfaces 8 and 8A

3. STANDARD OPERATION

This section details the operating procedures carried out for the decontamination and should be read in conjunction with Sketch 3722.

3.1 Initial Decontamination System Status

After the equipment is installed as outlined in section 2 herein, its equipment status and valve lineup will be adjusted as per Tables 3-1, and 3-2 respectively.

3.2. System Filling

3.2.1 Prerequisites

Prior to filling of the decontamination system, the following prerequisites apply:

(a) Decontamination system status as detailed in subsection 3.1.

(b) Demineralized water is available to RS1-V1 and CD1-V1.

(c) Steam Generator Channel Head is available with man-way cover connected.

(d) Power is available to the required decontamination equipment.

(e) The set point on relief valve ST2-RV1 has been set to 60 psig.

(f) Ion exchange columns are filled with resin.

(g) A drain facility is installed under the Channel head to adjust level if necessary.

3.2.2 Filling and Venting

With the equipment status as per subsection 3.2.1 initiate the following operations:

(a) Open the following valves: V104/107/108/125/126/128

(b) Commence filling by opening CD1-V1. Observe the channel head level indicatior. Adjust rate of fill by throttling CD1-V1. As the system fills, verify flow to vents, then close V125/V126.

(c) Monitor the decontamination system equipment for leakage as the system fills.

(d) When the channel head level indicator reads just below the tube sheet, close V128/V101/V102.

(e) Open the following valves: CU2-V1/V2/V3, CU3-V1/V2/V3, CS1-V1, CS2-V1, CV1-V1/V2/V3, DG1-V1, DG2-V1.

(f) Slowly throttle open RS1-V1 to maintain a reasonable filling rate.

(g) Stroke CU3-V4/V5/V6 and verify flow to drain then close the valve.

(h) Monitor the rad-waste drainage flow from collection tank DG-101. Once water starts flowing to drain, close CD1-V1 and CV1-V1/V2/V3.

(i) Open V113/V114 to fill the chemical injection discharge lines. Close the valves when the tank appears to be one-half full. Open V122 and verify flow to drain. Close V122.

(j) Open individually V121/V123 to verify flow to drain; then close.

(k) Close RS1-V1.

TABLE 3-1

MISCELLANEOUS DECONTAMINATION EQUIPMENT STATUS
REFERENCE STATE

Equipment	Description	Status
CU-105	Electric Heater	Off
RS-103/105	Slurry Line Connectors	Caps On
Nitrogen Bottle and Regulator	Surge Tank Charging System	Connected and Isolated
Resin Slurry Hose	Connection between IX Column Outlet and Collection Manifold	Connected to RS-104
CU-101/102/103	IX Column	Charged with Resin
P-101	Circulating Pump	Off
--	Man-Way Cover	Installed

TABLE 3-2

DECONTAMINATION EQUIPMENT VALVE STATUS
REFERENCE STATE
(continued)

VALVE	DESCRIPTION	STATUS
DG1-V1	Degasser vent	Closed
DG2-V1	Collection tank drain	Closed
ST1-V1	Surge tank vent	Closed
ST2-RV1	Surge tank relief	Set to 60 psig
CD1-V1	Demineralized water supply	Closed
SC1-V1	Sample cooling supply	Closed
V101	No. 3 Skid isolation	Open
V102	Circulation pump (P-101) suction	Open
V103	Circulation pump (P-101) Check	Open
V104	Circulation Pump (P-101) Bypass	Closed
V105	Circulation Pump (P-101) Discharge	Open
V106	Cooler (HX-101) Bypass	Open
V107	Cooler (HX-101) Inlet	Closed
V108	Cooler (HX-101) Outlet	Closed
V109	Auxillary Bypass	Open
V110	Auxillary Inlet	Closed
V111	Auxillary Outlet	Closed
V112	No. 3 Skid Outlet	Open
V113	Chemical injection (CI-101) Inlet	Closed
V114	Chemical injection (CI-101) Outlet	Closed
V115	Chemical Addition	Closed
V116	Pressure Switch (PS-101) isolation	Open
V117	Pressure switch (PS-102) isolation	Open
V118	Pressure Indicator (PI-103) Isolation	Open
V119	Cooling Water Supply to Filter (F-101)	Closed
V120	Cooling Water Return	Closed
V121	Upstream drain	Closed
V122	Chemical injection (CI-101) Drain	Closed
V123	Downstream drain	Closed
V124	Auxillary Drain	Closed

TABLE 3-2

DECONTAMINATION EQUIPMENT VALVE STATUS
REFERENCE STATE

VALVE	DESCRIPTION	STATUS
CU1-V1	Inlet flow control	Open
CU1-V2	IX column bypass	Open
CU1-V3	Pressure indicator (CU-200) isolation	Open
CU1-V4	Pressure indicator (CU-201) isolation	Open
CU1-V5	Pressure instrument header isolation	Open
CU2-V1	IX column (CU-101) inlet	Closed
CU2-V2	IX column (CU-102) inlet	Closed
CU2-V3	IX column (CU-103) inlet	Closed
CU3-V1	IX column (CU-101) outlet	Closed
CU3-V2	IX column (CU-102) outlet	Closed
CU3-V3	IX column (CU-103) outlet	Closed
CU3-V4	IX column (CU-103) drain	Closed
CU3-V5	IX column (CU-102) drain	Closed
CU3-V6	IX column (CU-101) drain	Closed
RS1-V1	Resin slurry inlet	Closed
RS2-V1	Resin slurry outlet (CU-101)	Closed
RS2-V2	Resin slurry outlet (CU-102)	Closed
RS2-V3	Resin slurry outlet (CU-103)	Closed
CV1-V1	IX column (CU-101) vent	Closed
CV1-V2	IX column (CU-102) vent	Closed
CV1-V3	IX column (CU-103) vent	Closed
CS1-V1	Upstream sampling isolation	Closed
CS2-V1	Downstream sampling isolation	Closed
CS3-V1	Sample cooler isolation	Closed

TABLE 3-2

DECONTAMINATION EQUIPMENT VALVE STATUS
REFERENCE STATE
(continued)

VALVE	DESCRIPTION	STATUS
V125	Cooling Water Vent	Closed
V126	Cooler Vent	Closed
V127	Channel Head Drain	Closed
V128	Channel Head Supply	Closed

3.2.3 Interlock Checks and System Leak Check

With the operations outlined in subsection 3.2.2 completed, initiate the following operation:

(a) Have instrument personnel set and check high pressure switch PS102 to 55 psi.

System Leak Check

(a) Check closed V101/V128 for isolatation of the man-way cover.

(b) Gradually increase the nitrogen cover gas pressure in steps to 50 psig by adjusting the nitrogen bottle pressure regulating valve.

(c) Check all exposed joints for leaks and drops in pressure.

(d) After the system has been checked for leaks and necessary adjustments are completed, crack open ST1-V1 and reduce the pressure to atmospheric. Close ST1-V1.

(e) Switch the electric heaters to on to verify that the indicator lights and heaters will not energize.

(f) Close CU2-V1/V2/V3, CU3-V1/V2/V3, CS1-V1, CS2-V1.

(g) Isolate HX101 by closing V107/V108.

3.2.4 Recirculation Pump Startup

(a) Open V101/V102/V128

(b) Close V104.

(c) Throttle V105 to approximately one-half open.

(d) Place the cleanup recirculation pump (P101) switch to start and hold for 3 to 5 seconds.

(e) Monitor the level in the channel head using the Tygon tubing sight glass.

(f) Adjust the circulation rate to 200 gpm on FI101 by adjusting V105.

(g) Vent, as necessary, by opening and closing V125/V126.

3.3 System Startup and Chemistry Preparations

With the operations described in subsection 3.2 completed, initiate the following operations.

3.3.1 Circulation Stabalization

(a) Check the channel head level to make sure it stays no more than 3" above the tube sheet.

(b) Check the flow through FI101 and adjust V105 to maintain 200 gpm.

(c) Open SC1-V1 and verify cooling water flow through the sample cooler.

(d) Initiate sampling procedures.

3.3.2 Raising Temperature to 200° F

With previous step operations completed and a stable circulation maintained, complete the following:

(a) Raise the temperature gradually to 200° F using heater CU-105.

(b) Check closed V113/V114. Open V122 to depressurize the chemical injection tank. Close V122.

(c) When the system temperature reaches 185° F, add 4 L. of 30 percent hydrazine to the chemical injection system via the chemical injection valve V115. Close V115.

(d) Immediately add the hydrazine to the decontamination system by opening V113/V114 and throttling V106.

(e) Continue operation until the system reaches 200° F and the dissolved oxygen concentration is less than 500 ppb (or as directed by chemists). Add additional hydrazine as necessary.

(f) Isolate the chemical injection tank by opening V106 fully and closing V113/V114.

3.4 Decontamination Steps

3.4.1 General

This section details the steps involved in completing the actual decontamination and has been subdivided into three steps:

1. First Reduction
2. First Oxidation
3. Second Reduction

Steps 1 and 3 consist of three parts:

- reagent injection
- reagent regeneration
- reagent removal

Step 2 consists of two steps:

- reagent injection
- reagent removal

Reagent injection involves the addition of LND-101A or LND-104 to the decontamination system. Reagent regeneration involves the use of a cation exchange column to maintain reagent concentration while removing radio nuclides. Process and chemistry monitoring and adjustment are also carried out during the regeneration step to maintain adequate control during the progress of the decontamination.

During the reagent removal step, system temperature is lowered and the cation exchange column is isolated. Mixed bed ion exchange resin is then used to remove the reagent. Chemistry and process parameters again are monitored to maintain adequate control during this step.

3.4.2 First Reduction Step

3.4.2A Reagent Injection

(a) Raise the system temperature to 200° F using Procedure 3.3.2.

(b) Place CU-102 on-line by opening CU2-V2/CU3-V2 and closing CU1-V2 until the flow on CU207 reads 40 gpm.

(c) Isolate the chemical injection tank CI101 by closing V114 and V113. Depressurize CI101 as per Procedure 3.3.2B

(d) Slowly open V115. Look into tank CI101 and observe the level. Drop the level to one-half by opening V122. Close V122.

(e) Add 12.5 lbs. LND-101A through the chemical hopper via V115. Close V115 once all reagent is added. Rinse off inlet port of V115 to remove any reagent.

(f) Open V113 and V114. Throttle V106.

3.4.2B Reagent Regeneration

(a) Repeat steps (d) through (g) of subsection 3.4.2A during decontamination to maintain reagent concentration as deemed necessary by chemical analysis.

(b) Continue sampling procedures.

(c) Monitor process parameters at regular intervals.

(d) Continue system operation in this manner until chemistry staff decides to terminate the decontamination.

3.4.2C Reagent Removal

(a) On completion of subsection 3.4.2B, switch process heater control switches to off.

(b) Once the decontamination system temperature drops below 200° F, isolate CU102 by closing CU3-V2 and CU2-V2.

(c) Open V107/V126 to vent cooler, then close V126.

(d) Lower the system temperature to 160° F by valving in the cooler HX-101. Open V108 and close V106.

(e) Open CU2-V1/CV1-V1 to vent. Close CV1-V1.

(f) Valve in CU101 by opening CU3-V1 and adjust CU1-V2 until the flow on CU207 reads 40 gpm.

(g) Continue system operation in this manner until chemistry staff decides to terminate the removal operation.

(h) Upon completion, valve out CU101 closing CU3-V1/CU2-V1.

3.4.3 First Oxidation Step

3.4.3A Reagent Injection

(a) Raise the system temperature to 200° F using Procedure 3.3.2.

(b) Isolate the chemical injection tank CI101 by closing V113/V114. Depressurize CI101 as per Procedure 3.3.2B.

(c) Slowly open V115. Look into tank CI101 and observe the level. Drop the level to one-half by opening V122. Close V122.

(d) Add 25.1 lbs. LND-104 through the chemical addition hopper via V115. Close V115 once all reagent is added. Rinse off the inlet port of V115 to remove any reagent.

(e) Open V113/V114. Throttle V106.

(f) Repeat steps (b) through (e) as necessary during decontamination to maintain reagent concentration.

3.4.3B Reagent Removal. Follow procedures 3.4.2C.

3.4.4 Second Reduction Step

3.4.4A Reagent Injection. Follow procedure 3.4.2A adding up to25.1 lbs. LND-101A.

3.4.4B Reagent Regeneration. Follow the same procedure as 3.4.2B.

3.4.4C Reagent Removal. Follow procedure 3.4.2C except use CU103 for reagent removal.

3.5 System Shutdown

Shut down the system by turning off the circulation pump and closing V101/V102/V128.

3.6 Resin Slurry

The purpose of this step is to transfer the contaminated resin from each of the ion exchange columns to the collection drums for disposal.

3.6.1 Prerequisites

(a) Connect up cooling water to interface S-5.

(b) Insure the resin receipt drums are connected to the resin slurry lines as per Figure 2.

3.6.2 Slurry Procedure

The following is the procedure for slurrying the resin from ion exchange column CU-102. Equivalent equipment designations for CU-101 and CU-103 are shown in brackets:

(a) Set up radiation monitoring equipment as required to ascertain levels before, during, and after slurry operation.

(b) Make all personnel involved aware of the hazards involved during the slurry process. Keep personnel not essential to the operation clear of the area.

(c) Close CU1-V2; check closed CU2-V1/V2/V3, CU3-V1/V2/V3, CU3-V1/V2/V3/V4/V5/V6, CV1-V1/V2/V3.

(d) Open RS1-V1.

(e) Open RS2-V2 (RS2-V1, RS2-V3) and watch the sight glass RS-101 (RS-100, RS-102) for resin flow to the disposal drums.

(f) Open ball valve on header to selected drum. Throttle valve as drum fills.

(g) Close valve when drum is completely full. Open valve to next drum.

(h) Continue slurry operation until flow is completely water.

(i) Close RS1-V1 and RS2-V2 (RS2-V1, V3).

(j) Once all the resin is disposed of in the collection drums, check the remaining fields on the ion exchange columns to make sure they are at acceptable levels.

3.7 System Draining

3.7.1 General

The final procedure is to drain the equipment. General procedure will be to drain the channel head first, then skids Nos. 1 and 2, and finally, drain No. 3 skid.

3.7.2 Procedure

(a) Check the decontamination system to make sure the pump is shut down and supplies of demineralized and cooling water are disconnected.

(b) Connect the 1¼" drain hose to the Steam Generator Channel Head. Make sure the drain line is connected to the waste tank.

(c) Open the drain valve V127 and allow the channel head to drain. Close V127 when complete.

(d) Open: CU1-V1/V2/V3, V121, V122, V123, V124, CU3-V4/V5/V6.

(e) Open the following valves: CU1-V2, CU1-V1, CU2-V1/V2/V3, CS1-V1, DG1-V1.

(f) When the water level is below the level of the tube sheet, open the following valves on skid 3: V101, V102, V105, V106, V107, V108, V125, V126, V109, V110, V111, V113, V114, V115, V119, V123, V128

(g) When draining is complete, purge lines as necessary with nitrogen through the surge tank.

4. PROCESS CHEMISTRY

4.1 GENERAL

This section details the various chemistry and corrosion monitoring procedures to be carried out before, during, and after the decontamination. In addition, Table 4.1 of this section provides a monitoring schedule based upon the operations outlined in Section I, System Operations. Water samples will be taken for process monitoring durng the decontamination.

4.2 pH AND CONDUCTIVITY

Laboratory pH and conductivity meters will be used to monitor these parameters. Measurements will be made on all water samples throughout the various oxidizing and reducing steps of the decontamination.

The pH cell will be calibrated with standard buffer solutions at pH 4, 7 and 10 at approximately 25°C (77°F). The conductivity probe and meter will be calibrated with standard KCl solutions. Below is a list of specific conductance for KCl solutions at 25°C (77°F)

Concentration (eq/L)	Specific Conductance (ohm^{-1}/cm)
0.1	0.012886
0.01	0.0014114
0.001	0.0014695

4.3 REDUCING STEP

4.3.1 Crud, Radionuclides, and Dissolved Metals Analyses

Selected water samples will be filtered in the laboratory using 0.45-micron filter papers. A standard volume between 500 and 1000 mL will be filtered through two back-to-back identical filter papers, the first to retain the crud and the second to be used as a blank. If significant crud is present, it will be analyzed for weight, specific and gross activity, and chemical composition.

The crud filtrates and all other water samples taken before and after the ion exchange column will be counted and analyzed for dissolved metals.

4.3.2 Reagent Analysis (Reducing step)

The reagent concentration will be monitored by analyzing for EDTA. This analysis will be performed on samples taken before the ion exchange column. The concentration of EDTA in CAN-DECON reagent solutions is determined by complexing the EDTA with iron III. If the total iron III concentration is known, from oxide dissolution and iron III titration, then the EDTA concentration can be determined.

One mole of EDTA complexes with one mole of iron III. If the EDTA in the reagent solution is fully complexed with iron III from oxide dissolution, then the solution is titrated with EDTA. If it is not, then additional iron III is added to fully complex the EDTA. The procedure requires that the iron III concentration from oxide dissolution be known. This is done by analyzing for iron II and total iron, the difference being the iron III concentration. Iron II is determined by complexing it with o-phenanthroline. Standard iron solutions are made to obtain a calibration curve in the range zero to 150 ppm. The solutions are analyzed using a spectrophotometer at a wave length of 518 nm.

Iron II Analysis

Reagent

- 0.5% o-phenanthroline (in CH_3OH)

Procedure

(a) Accurately pipette an aliquot (usually the sample solution containing 10 to 100 ug of iron into a 25-mL volumetric flask.

(b) Add a few millilitres of distilled water and 1 mL of 0.5% o-phenanthroline.

(c) Mix and make up to mark with distilled water, and determine the optical density.

(d) Make determination as soon as possible after making up the sample.

Total Iron Analysis

Total iron is determined by reducing iron III to iron II with hydroxylamine hydrochloride and analyzing for iron II.

Reagents

(a) 10 wt% hydroxylamine hydrochloride ($NH_2OH.HCl$)
(b) 2 M^2 sodium acetate
(c) 0.5% ophenanthroline (in CH_3OH)

Procedure

(a) Accurately pipette an aliquot of sample solution containing 10 to 100 ug of iron into a 25-mL volumetric flask (usually 1 mL of stripping solution).

(b) Add a few millilitres of distilled water and 2 mL of 10% hydroxylamine hydrochloride.

(c) Adjust the volume to approximately 10 mL with distilled water, and adjust the pH to between 3 and 6 by adding 2 mL of 2 M sodium acetate.

(d) Mix and let stand five to 10 minutes, then add 1 mL of ophenanthroline.

(e) Mix up to mark with distilled water, mix, and determine the optical density at 518 nm.

Notes

(a) If the original sample solution is coloured, read the sample against a blank consisting of the sample, plus reagents, less ophenanthroline.

(b) If sample solution is colourless, a blank may consist of water, plus reagents, plus ophenanthroline.

EDTA Analysis

Reagents

(a) 2 M sodium acetate solution
(b) 2% salicylic acid in methanol
(c) standard iron III solution (0.05%)
(d) standard EDTA solution (0.05%)

Procedure

(a) Analyze sample for iron III concentration.
(b) Take a 25 mL aliquot of sample.
(c) Add 1 mL salicylic acid solution.

If the resulting solution is colourless, follow item 1 below; if the solution is coloured (violet), follow item 2:

1. Titrate the sample with the standard iron III solution until a violet colour appears.

   One mole EDTA reacts with one mole iron III; EDTA concentration equals original iron III concentration plus iron III concentration in titer.

2. Titrate the sample with the standard EDTA solution until the colour changes from violet to colourless.

   Original EDTA concentration equals iron III concentration less EDTA concentration added.

4.4 OXIDIZING STEP

4.4.1 Dissolved Radionuclides and Dissolved Metals Analyses

All water samples taken will be filtered and filtrate subjected to a full -scan by a Ge-Li counter for dissolved radionuclides and analyzed by an Atomic Absorption Spectroscopy (AA) for dissolved chromium and iron concentrations. Selected samples will be analyzed for crud content.

4.4.2 Reagent Analysis

Reagent analysis requires filtration using a glass filter to remove interfering particulate matter. Filtrate from selected water samples will be analyzed using a UV visible spectrophotometer at 527 nm wavelength.

Procedure

Standard Solution Preparation

Add 4 gm of KMnO4 to one litre of distilled water. The resulting solution contains 4000 ppm of KMnO4. Appropriate dilutions are made with this stock solution to give the following standards = 500, 1000, 1500, 2000, and 2500 ppm. The absorbance of each standard is determined against a blank (distilled water) in a UV/visible spectrophotometer at wavelength of 527 nm.

4.5 DISSOLVED OXYGEN

Dissolved oxygen measurements will be taken at the appropriate system sampling point during the hydrazine addition step to ensure low oxygen levels during the decontamination. It is recommended that a colorimetric method, such as the Chemet dissolved oxygen test kit, be used for these determinations.

4.6 Corrision Coupons

4.6.1 Preparation by London Nuclear

Six (6) coupons of each of the two (2) materials, Inconel 600 and 304 stainless steel, will be cut to size, drilled, stamped, and pickled if necessary. All twelve (12) coupons will then be shipped to site.

4.6.2 Site Activities

Four (4) coupons of each material will be weighed installed on the coupon holder, and inserted in the decontamination system. After the decontamination, all eight (8) coupons will be weighed, counted, descaled if necessary, and reweighed. From these weights base metal corrosion rate for each individual material will be calculated.

TABLE 4.1

CHEMISTRY MONITORING SCHEDULE

Readings & Analyses	Pre-Decontamination Step	Decontamination					
		LND-101A Addition		LND-101A Removal	Oxidizing Step		LND-101A Addition		LND-101A Removal
		First 2h			Reagent Injection	Reagent Removal	First 2h		
pH & Conductivity	Analyses as required	15 min intervals	30 min or 1h intervals		1h intervals		15 min intervals	30 min or 1h intervals	
Temperature	1h intervals								
Dissolved O_2	Analyses as required after N_2H_4 injection								
Reagent		Analyses as required			Analyses as required		Analyses as required		
Dissolved Metals AA & Count	Analyses as required	15 min intervals	30 min or 1h intervals		1h intervals		15 min intervals	30 min or 1h intervals	

4.7 DECONTAMINATION COUPONS

A number of contamined specimens to be supplied by Battelle Pacific Northwest Laboratories will be included in the coupon holder to measure decontamination factors (DF).

Three to four contaminated specimens will be counted for specific and gross activity before being installed in the coupon holder. After the decontamination, all will be recounted. From the initial and final activies, a decontamination factor can be determined:

$$DF = \frac{\text{initial activity}}{\text{final activity}}$$

APPENDIX I

MISCELLANEOUS EQUIPMENT REQUIREMENTS

The following were made available for the decontamination:

(a) sufficient concrete blocks of dimensions 15.5 x 7.5 x 5.5 in to complete a temporary shielding wall of overall dimensions 7.0 ft. high x 7.0 ft. long x 2.0 ft. thick;

(b) a nitrogen cylinder complete with an adjustable pressure regulator of suitable range;

(c) a positive displacement test pump complete with an indicating gauge;

(d) lead blankets in sufficient quantities to shield pieces of the decontamination equipment;

(e) gamma radiation meter with extended probe for remote monitoring of ion exchange columns (0 to 50 R range).

PNL Addendum

The following subsections provide additional information and figures relating to the cold leg decontamination operation and results:

Decontamination Process - The CAN-DECON dilute chemical decontamination process, major features and chemistry are described and compared with other chemical decontamination processes in an overview paper by Smee (1982).

Equipment Installation - The London Nuclear Services (LNS) equipment consisted of a pump skid (Figure 3-1), an ion exchange skid (Figure 3-2), and an ancillary equipment skid (Figure 3-3) containing the heater and the chemical addition, sampling and control systems. The equipment was unloaded outside the SGEF using a Hydro-Crane (Figure 3-4), and moved inside with a forklift (Figure 3-5). The pump skid was installed in the tower basement and the remainder of the equipment was installed in the truck lock. The size of the equipment compared with the available space (Figure 3-6) complicated the positioning and installation process. Also, as noted previously, it was necessary to connect the equipment in the truck lock with the equipment and channel head in the tower basement via penetrations in the tower wall.

The manway cover and nozzle system used to contain and circulate the decontamination solution inside the channel head is shown in Figure 3-7. The system was sized and installed (Figure 3-8) so that the solution was introduced near the top of the divider plate and returned from about the midpoint of the bowl. The completed installation of the manway cover, pump skid and connecting hoses in the tower basement is shown in Figure 3-9.

Decontamination Operations - The decontamination operation went well from a chemistry standpoint. However, as noted in the LNS report, there were pump problems that possibly diminished the effectiveness of the process and a nozzle cover leak that forced early termination of the second decontamination cycle. There also were problems with control of the solution level in the channel head. Level control for the cold leg decontamination was maintained primarily through control of the liquid inventory in the closed system. The actual level was indicated by a sightglass running vertically past a mark designating the bottom of the tube sheet. The level was monitored by the operating staff either directly or via the remote TV camera from the operations control room (Figure 3-10). Despite these precautions, the liquid level did vary from the prescribed limits on three occasions. During initial filling with deionized water, the level exceeded the control limit before equilibrium was established among the various system components. Near the start of the first oxidation cycle the level dropped about 5 cm below the bottom of the tube sheet for about an hour. This resulted in an enhanced refluxing action that, based on subsequent measurements described in Section 5, apparently washed some contamination from the tubes into the channel head. Some of the water vapor also condensed on

FIGURE 3-1. Pump Skid

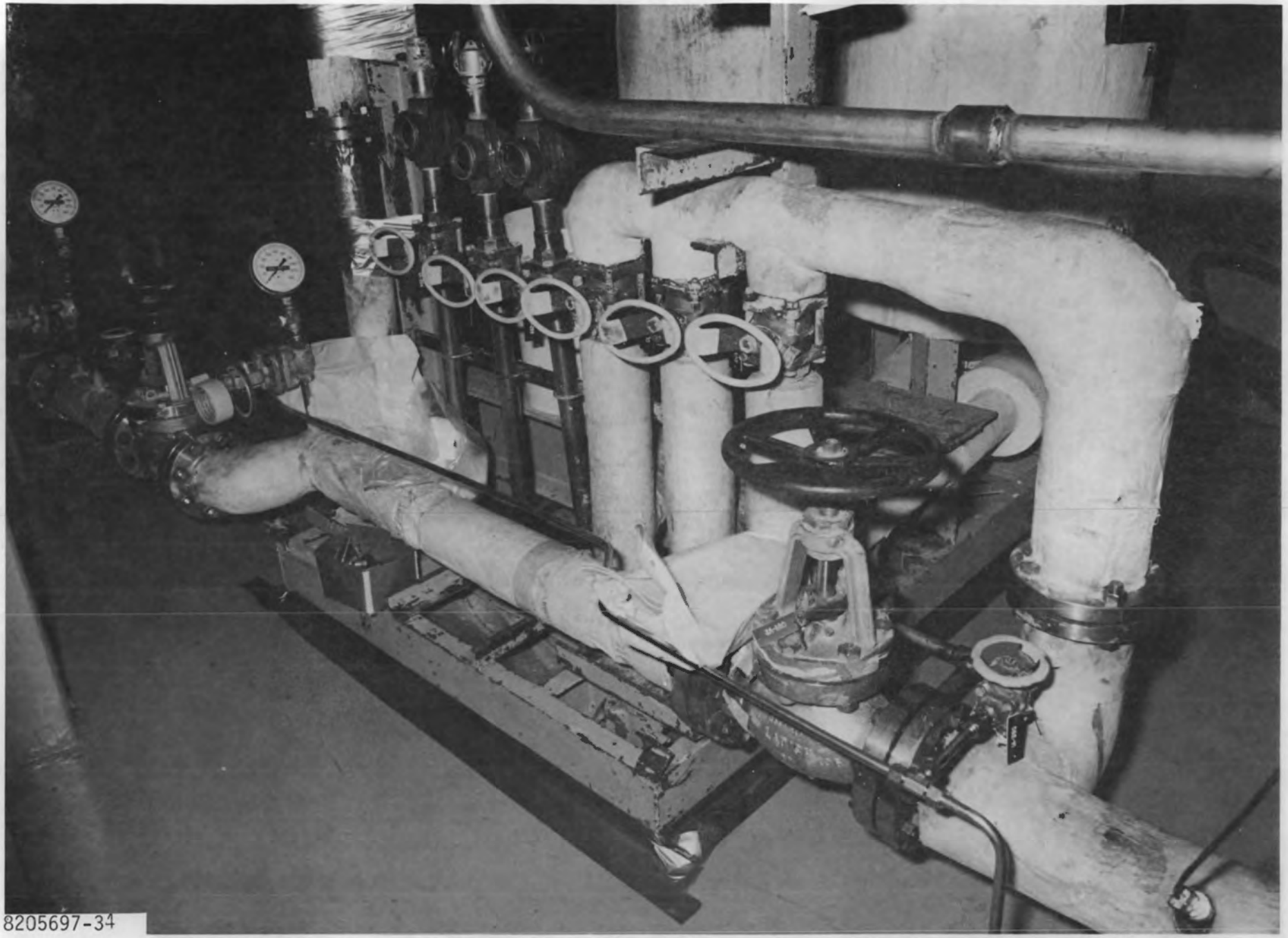

8205697-34

FIGURE 3-2. Ion Exchange Skid

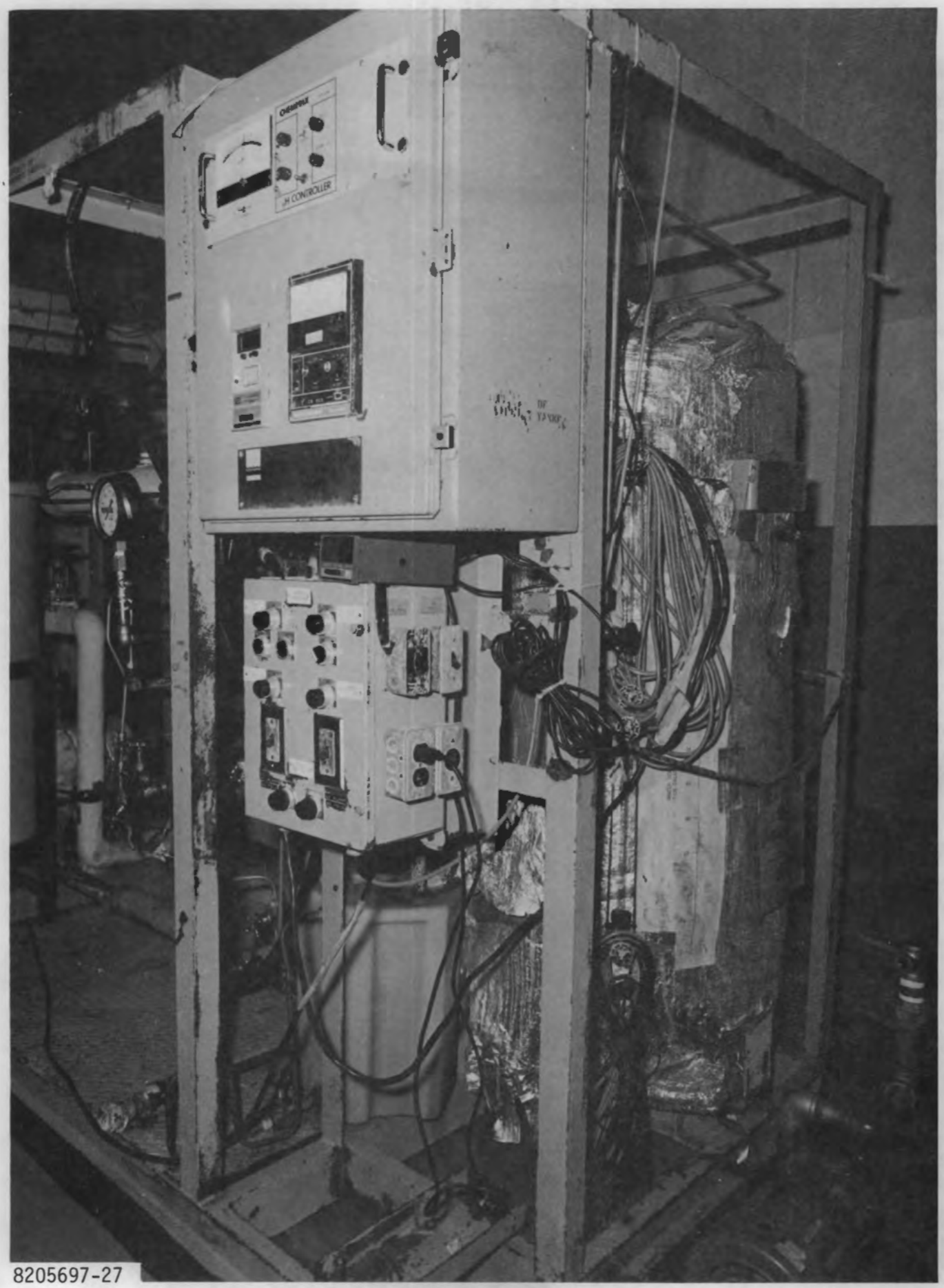

8205697-27

FIGURE 3-3. Ancillary Equipment Skid

FIGURE 3-4. Unloading the Cold Leg Decontamination Equipment

8205654-//

FIGURE 3-5. Moving the Decontamination Equipment into the SGEF

8205654-105

FIGURE 3-6. Size of Decontamination Equipment Compared with Available Space

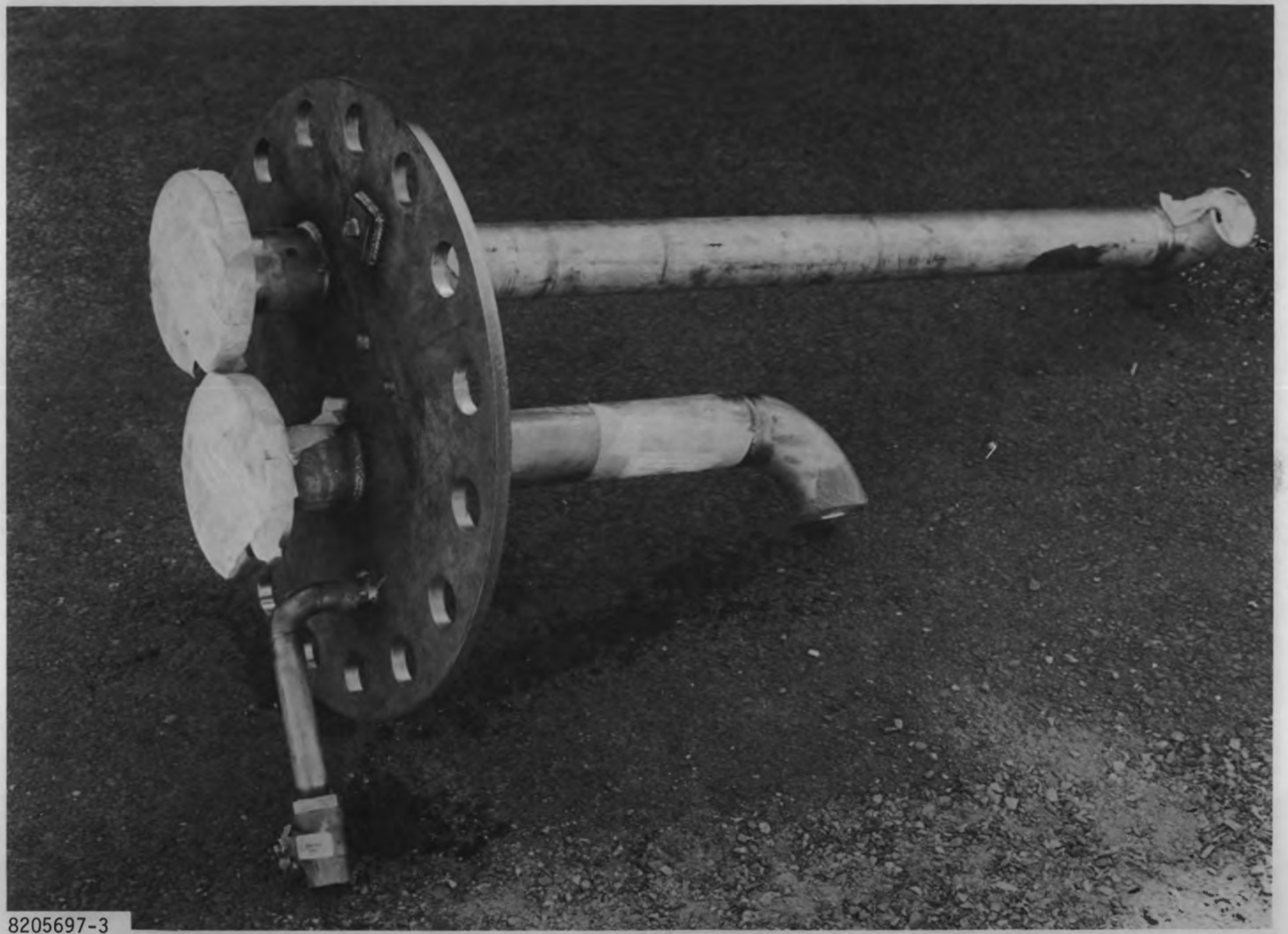

8205697-3

FIGURE 3-7. Nozzle and Return System Used for the Cold Leg Decontamination Operation

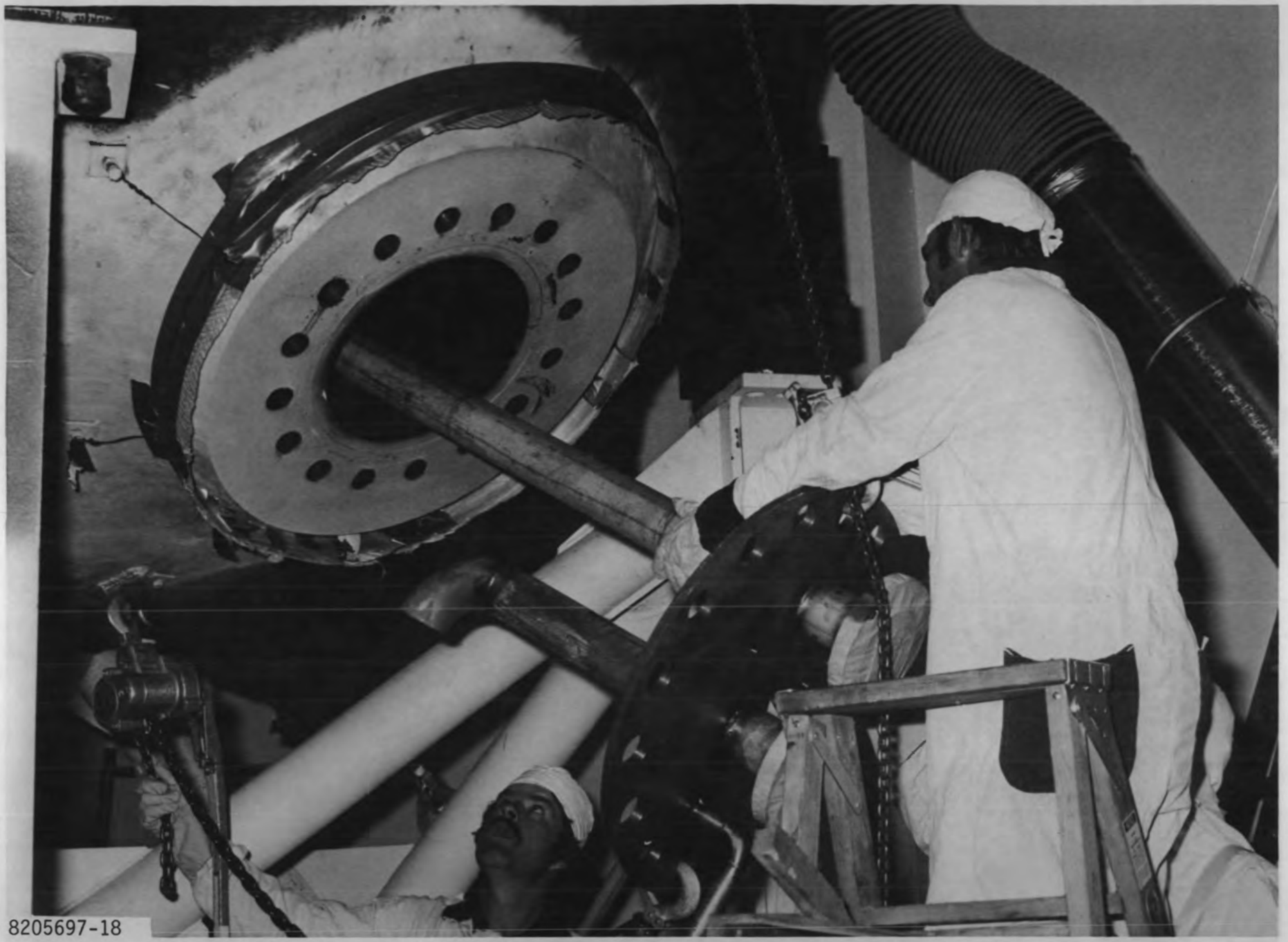

8205697-18

FIGURE 3-8. Installation of the Cold Leg Manway Cover and Nozzle System

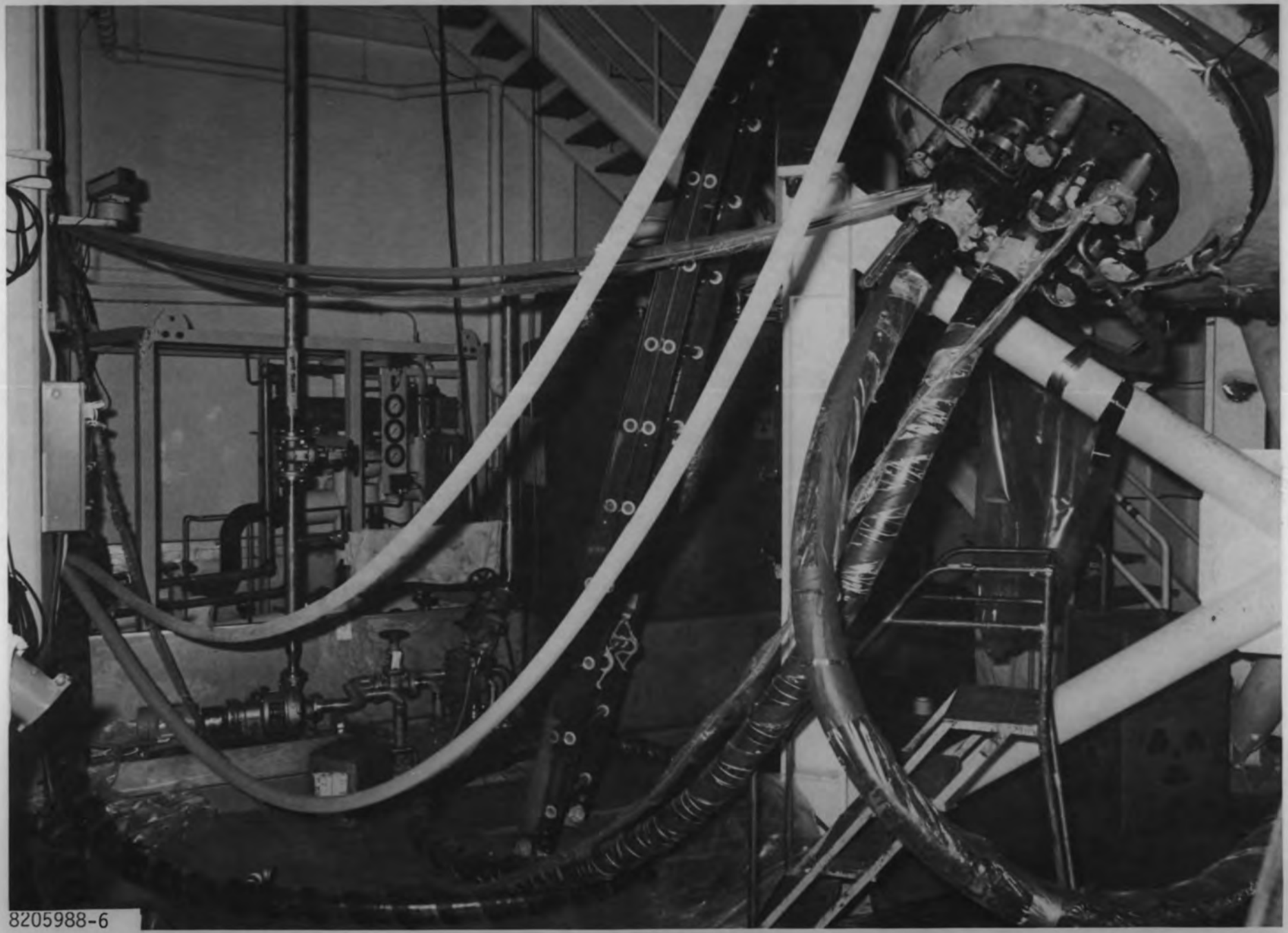

FIGURE 3-9. Installed Cold Leg Decontamination System in the Tower Basement

8207468-14

FIGURE 3-10. Control Room and Remote TV System Used to Monitor the Decontamination Operations

the hot leg side, resulting in the collection of about 130 ℓ of contaminated water. Conductivity and pH measurements on this hot leg condensate verified the absence of any chemicals from the cold leg operation. The final excursion occurred at the end of the second oxidation cycle, when the solution level increased approximately 0.6 m above the tube sheet for a few minutes. An examination of accessible secondary side areas did not show any evidence of leakage due to this excursion.

Process Results - The results of the cold leg decontamination operation are presented in the LNS report and other sections of this report. However, the following summaries, figures and comments are provided:

- Dissolved metal concentration - the effect of the alternating oxidizing and reducing steps on the concentration of Fe, Cr and Ni in the decontamination solution is presented in Figure 3-11. As expected, Cr removal occurred primarily during the film conditioning (oxidation) steps. The Fe concentration readings include a contribution from corrosion of the carbon steel nozzle cover.

- Co-60 concentration - the effect of the decontamination steps on Co-60 removal is shown in Figure 3-12. It should be noted that the 1.6 Ci removed during the second reduction step also includes the contamination washed out of the tubes by the water refluxing action during the preceding oxidation step. As in the case of the dissolved metals, the concentration of Co-60 decreases with time due to its removal by the ion exchange system.

- Radiation readings - the radiation readings after completion of both the cold leg and the hot leg decontaminations (to minimize shine contributions) are shown in Figure 3-13 as a function of position. The corresponding change from the pre-decontamination readings is summarized in Figure 3-14. As discussed in Section 5, the major contributor to the remaining radiation level inside the channel head is tube shine.

- Surface appearance - the appearance of the three major surface areas (Inconel 600 tube sheet, Inconel 600 divider plate and 309 stainless steel bowl) is shown before decontamination (Figure 3-15), after the two decontamination cycles (Figure 3-16) and after the high-pressure water rinse operation (Figure 3-17). The comparatively well-cleaned (film-free) area on the divider plate and adjoining tube sheet (Figures 3-16 and 3-17) correlates with the outlet of the nozzle (Figure 3-7) used to introduce the decontamination solution. This evidences an apparent beneficial effect of higher flow rates or increased solution agitation in removing the contaminated surface film. Although the decontamination cycles removed substantial contamination and adequately reduced the radiation level inside the channel head, there was still a highly-smearable, readily-detachable film on all three surfaces as shown in Figure 3-16. This was removed using a 5-7 MPa water jet to produce the comparatively clean, less-smearable surface shown in Figure 3-17. The water cleaning operation was conducted using the high-pressure spray system and special manway cover illustrated in Figure 3-18.

COLD LEG DECONTAMINATION - EFFECT OF PROCESS STEPS ON DISSOLVED METAL CONCENTRATION

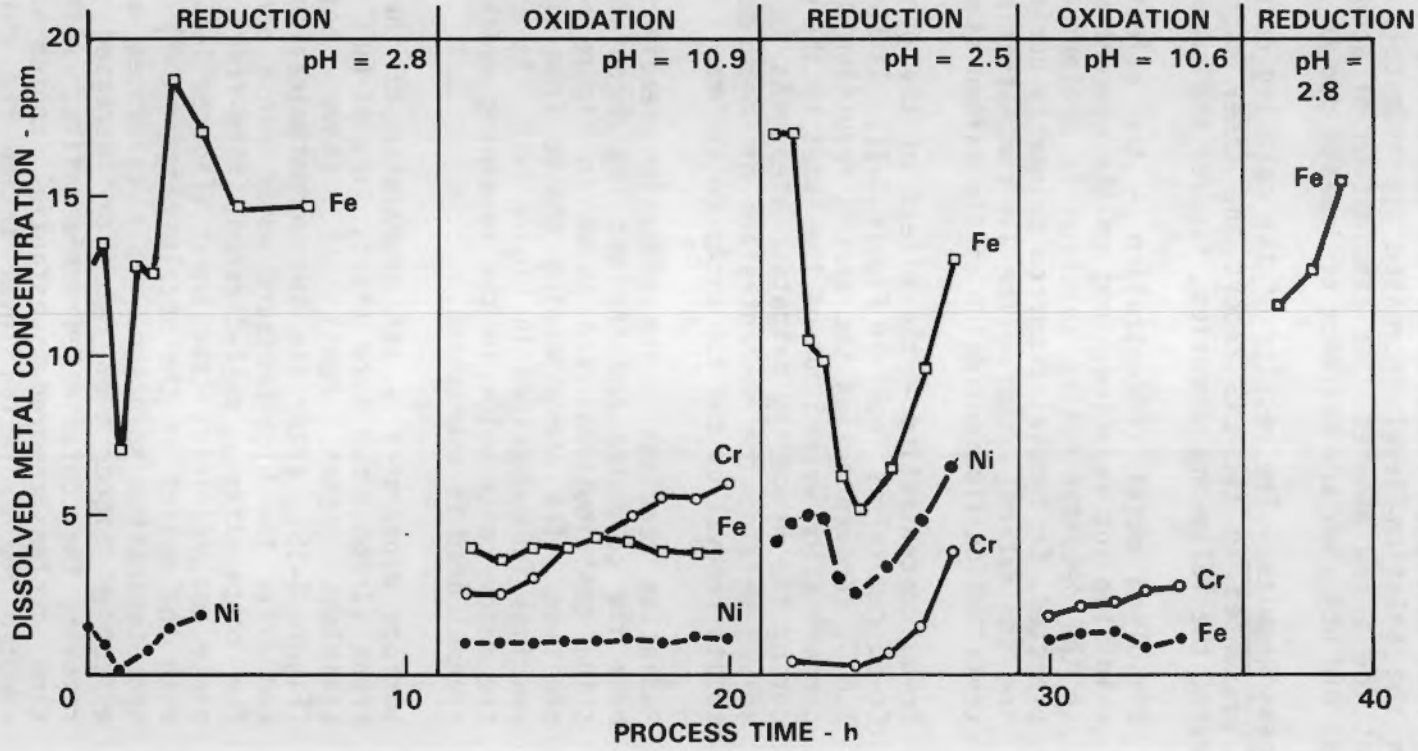

FIGURE 3-11.

COLD LEG DECONTAMINATION - EFFECT OF PROCESS STEPS ON ^{60}Co CONCENTRATION

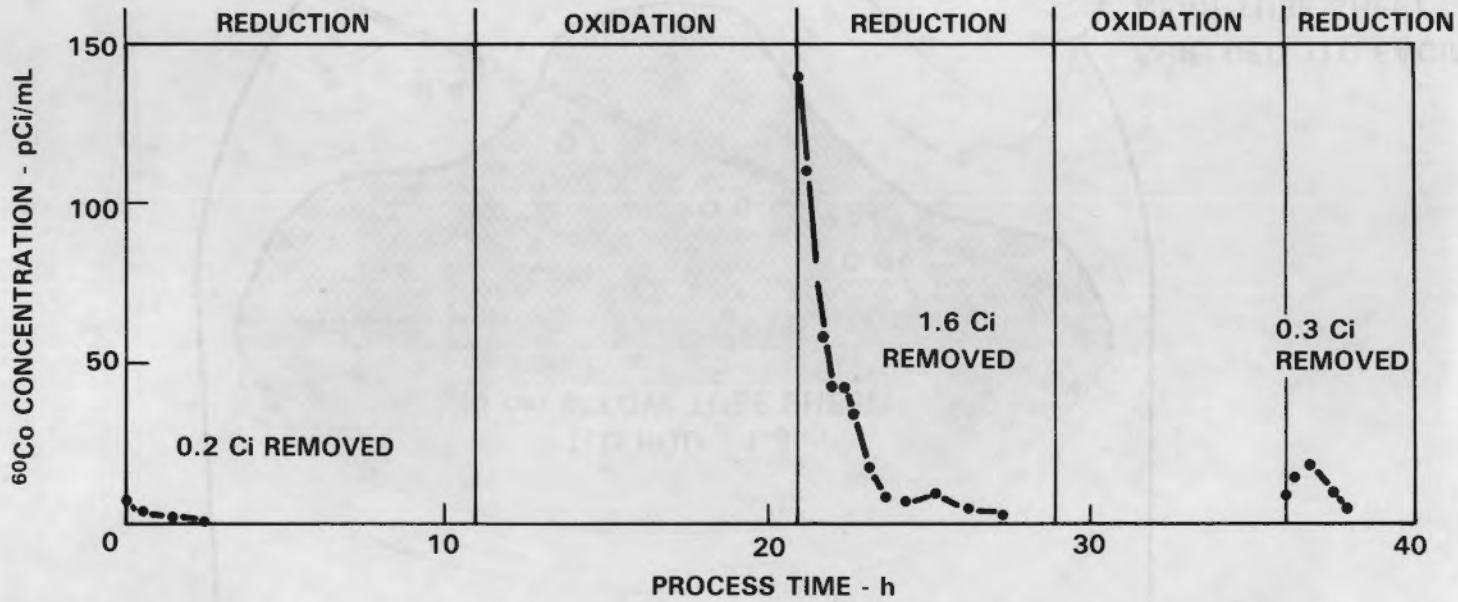

FIGURE 3-12.

FINAL RADIATION READINGS
(COLD LEG - R/h)

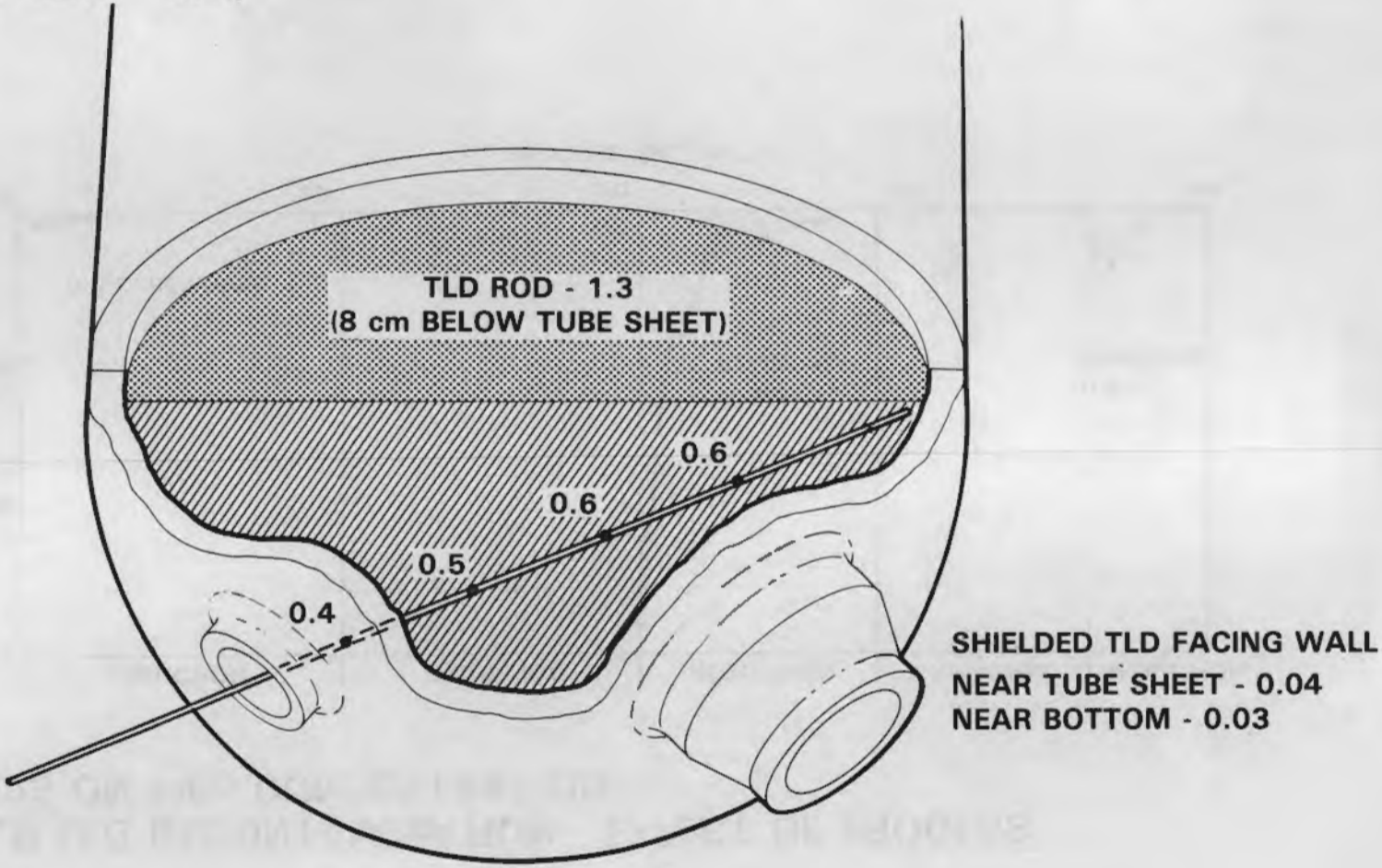

FIGURE 3-13.

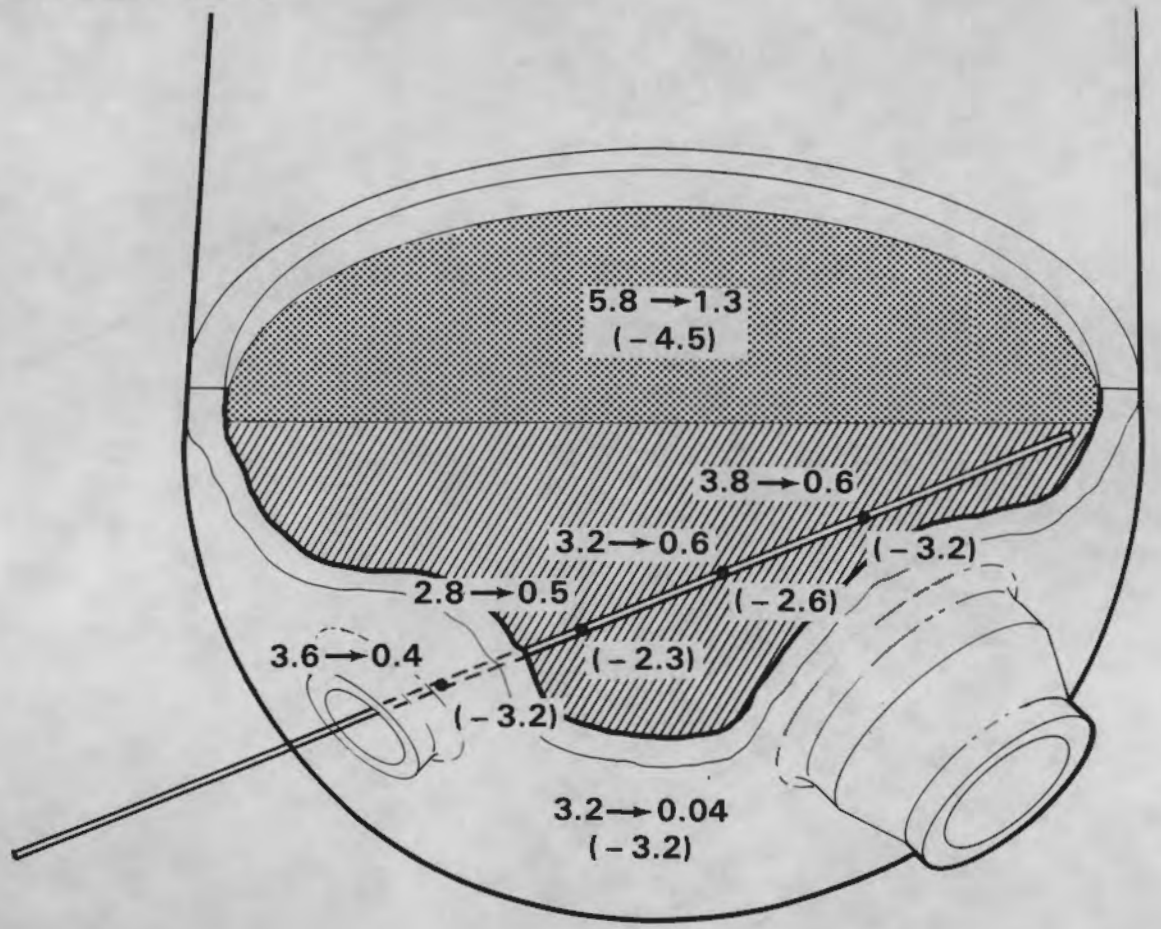
RADIATION READING CHANGE
(COLD LEG - R/h)
5.8 → 1.3
(-4.5)
3.8 → 0.6
3.2 → 0.6
(-3.2)
2.8 → 0.5
(-2.6)
3.6 → 0.4
(-2.3)
(-3.2)
3.2 → 0.04
(-3.2)

FIGURE 3-14.

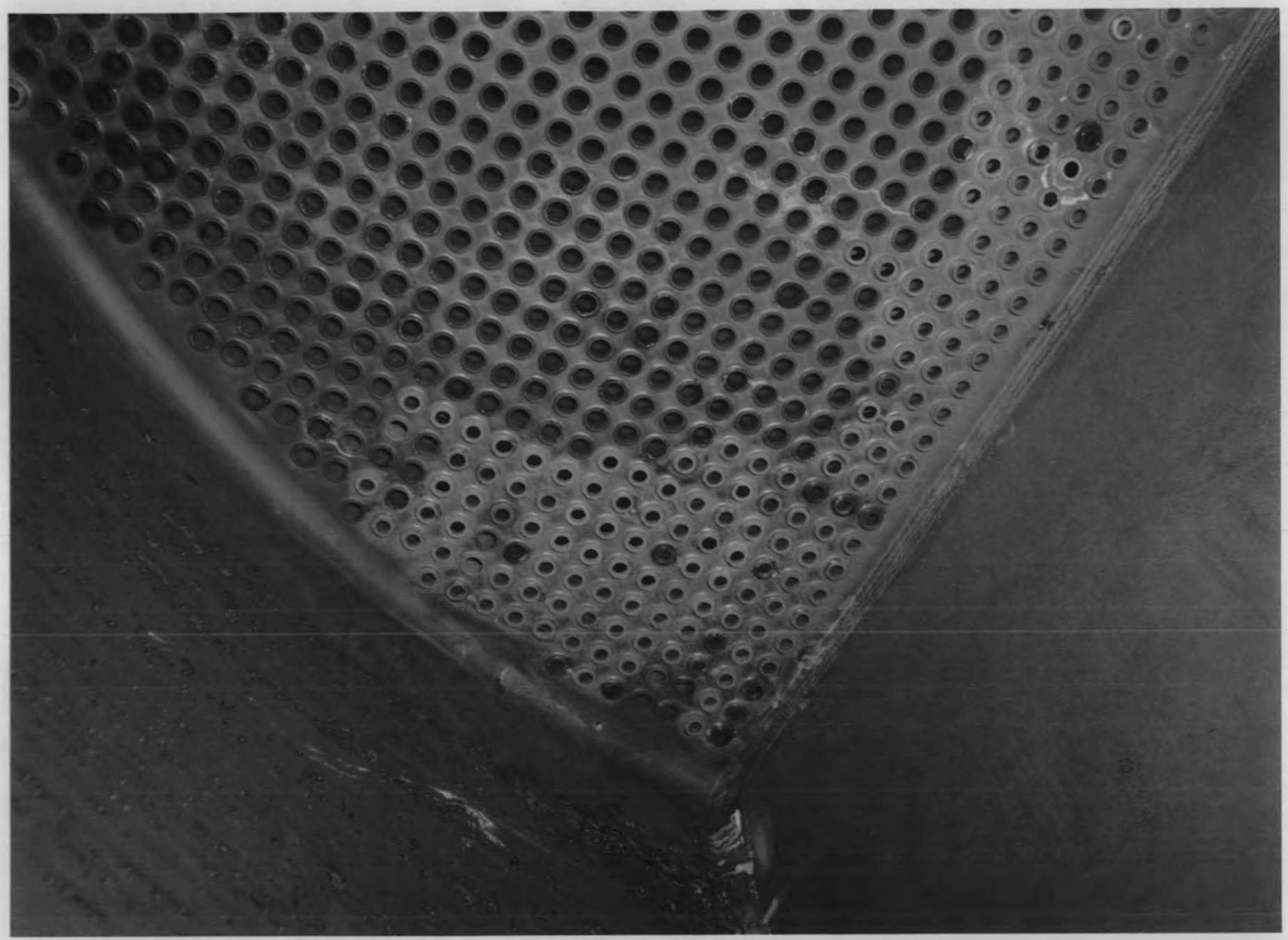

8202467-5

FIGURE 3-15. Cold Leg Surfaces Before Decontamination

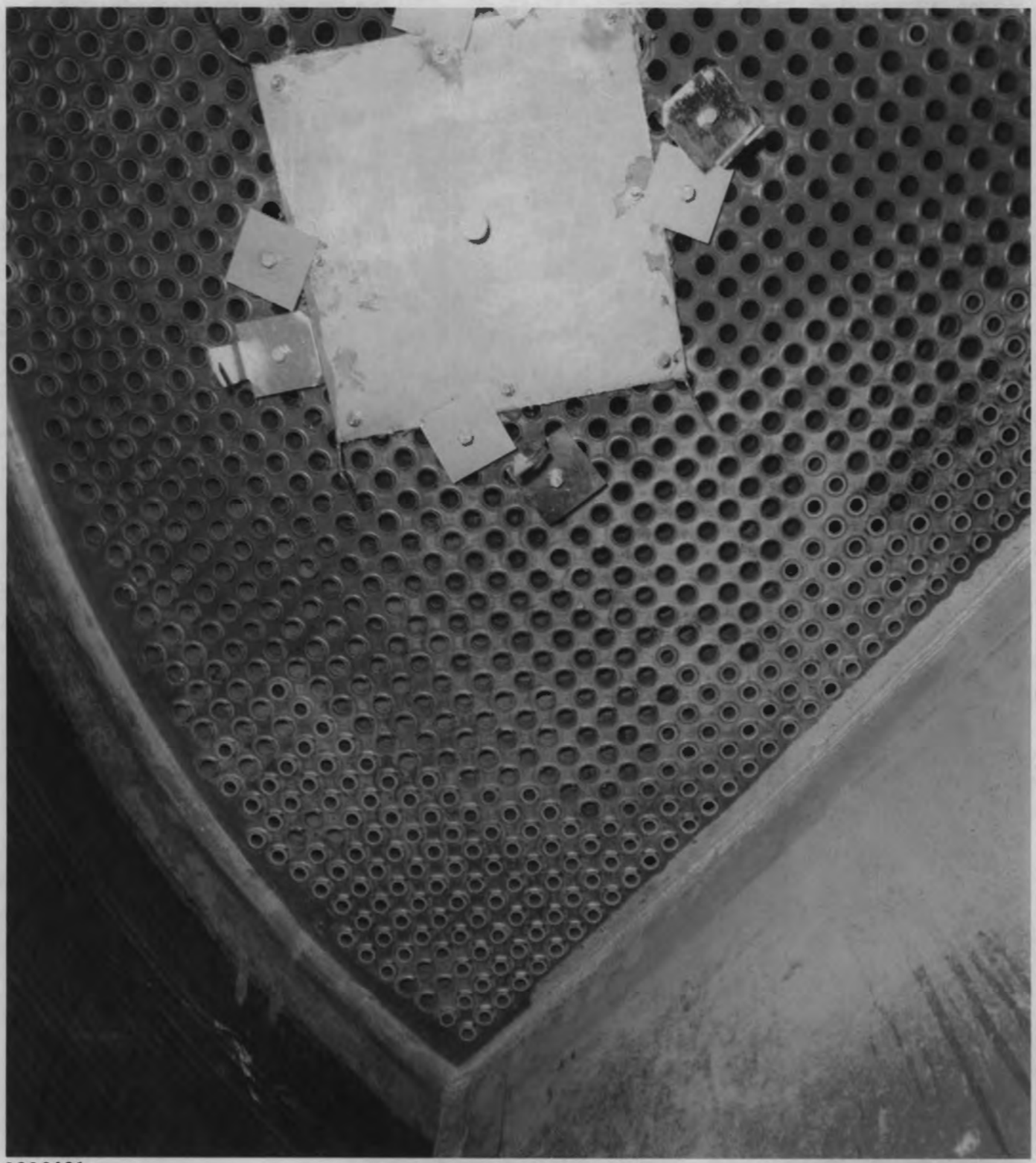

8206491

FIGURE 3-16. Cold Leg Surfaces After Two Decontamination Cycles

8207341-13

FIGURE 3-17. Cold Leg Surfaces After High-Pressure Water Rinse

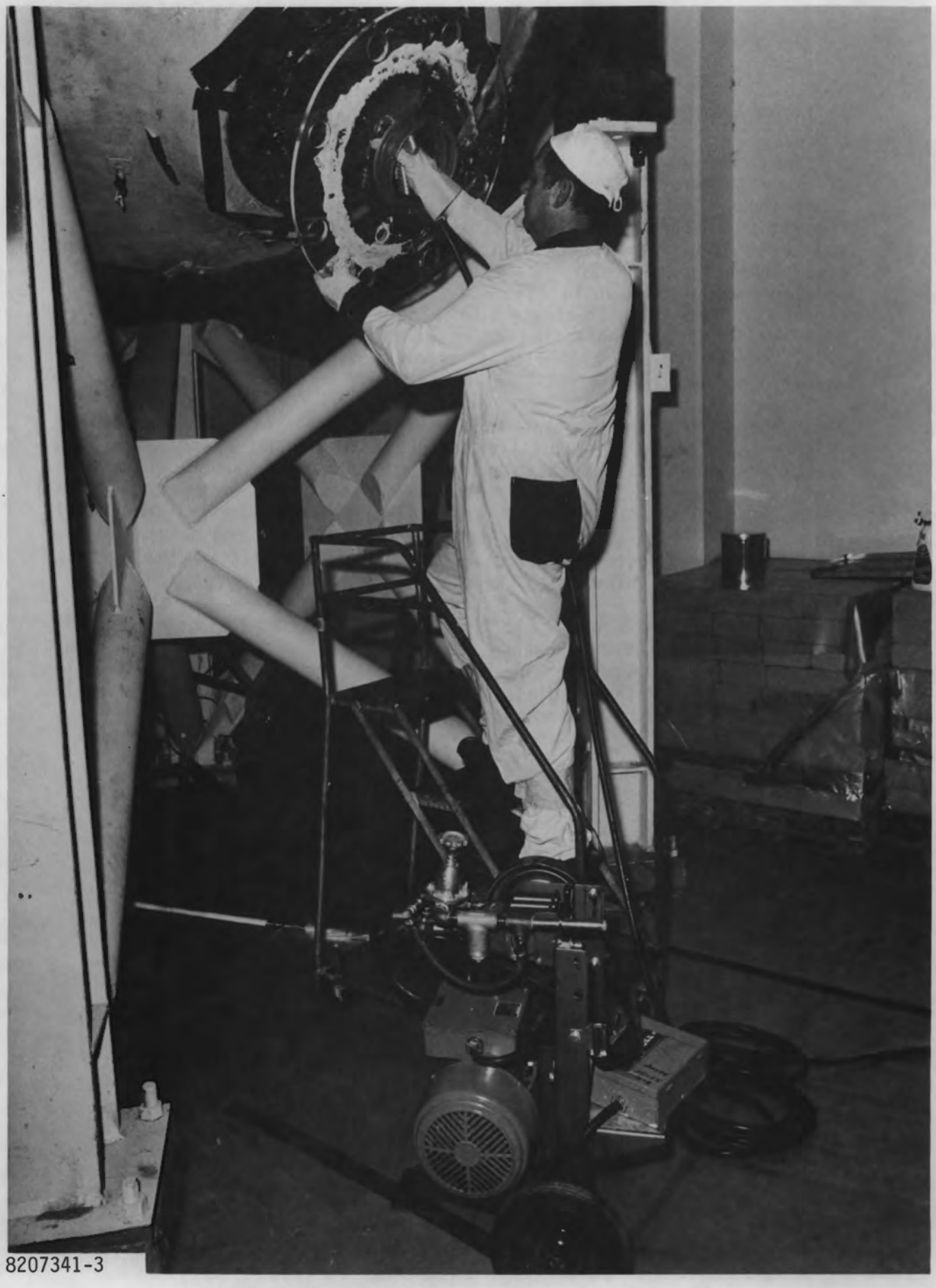

8207341-3

FIGURE 3-18. High-Pressure Water Rinse Operation

Resin Slurry Operation - At the conclusion of the decontamination process, the activity removed by the recirculating decontamination solution was contained within the three cation and mixed-bed ion exchange columns on the shielded ion exchange column skid inside the truck lock. The contaminated resin from each 265-ℓ-capacity column was removed as a slurry using approximately 420 ℓ of water from a 110 ℓ/min supply in the truck lock. The slurry stream was split and channeled simultaneously into four 208 ℓ waste disposal drums using the PNL-developed header shown in Figure 3-19. The slurry operation was conducted remotely as illustrated in Figure 3-20 to minimize exposure. After filling, the palletized drums were stored in the tower basement until completion of the liquid removal and liquid waste transfer operations (Section 2).

Once the liquid waste tank was emptied, the resin was dewatered (Figure 3-21) using a mesh filter to separate the water and resin, and the excess water was pumped into the waste tank. The drums, which then contained about 35 vol% damp resin, were next filled remotely with adsorbent material (Figure 3-22) and sealed from behind a shielding wall (Figure 3-23). The drums were then remotely clamped and hoisted up to the truck lock (Figure 3-24), rolled to the door and lifted onto a truck (Figure 3-25) for shipment to the disposal site.

Approximately 85-90% of the activity removed from the cold leg was collected on the cation exchange resin in one of the columns. The four waste drums that received the resin from this column read from 3 to 5 R/h at contact. The readings for the eight drums containing the resin from the other two columns ranged from 85 to 285 mR/h.

FIGURE 3-19. Header Used to Divide the Slurry Stream

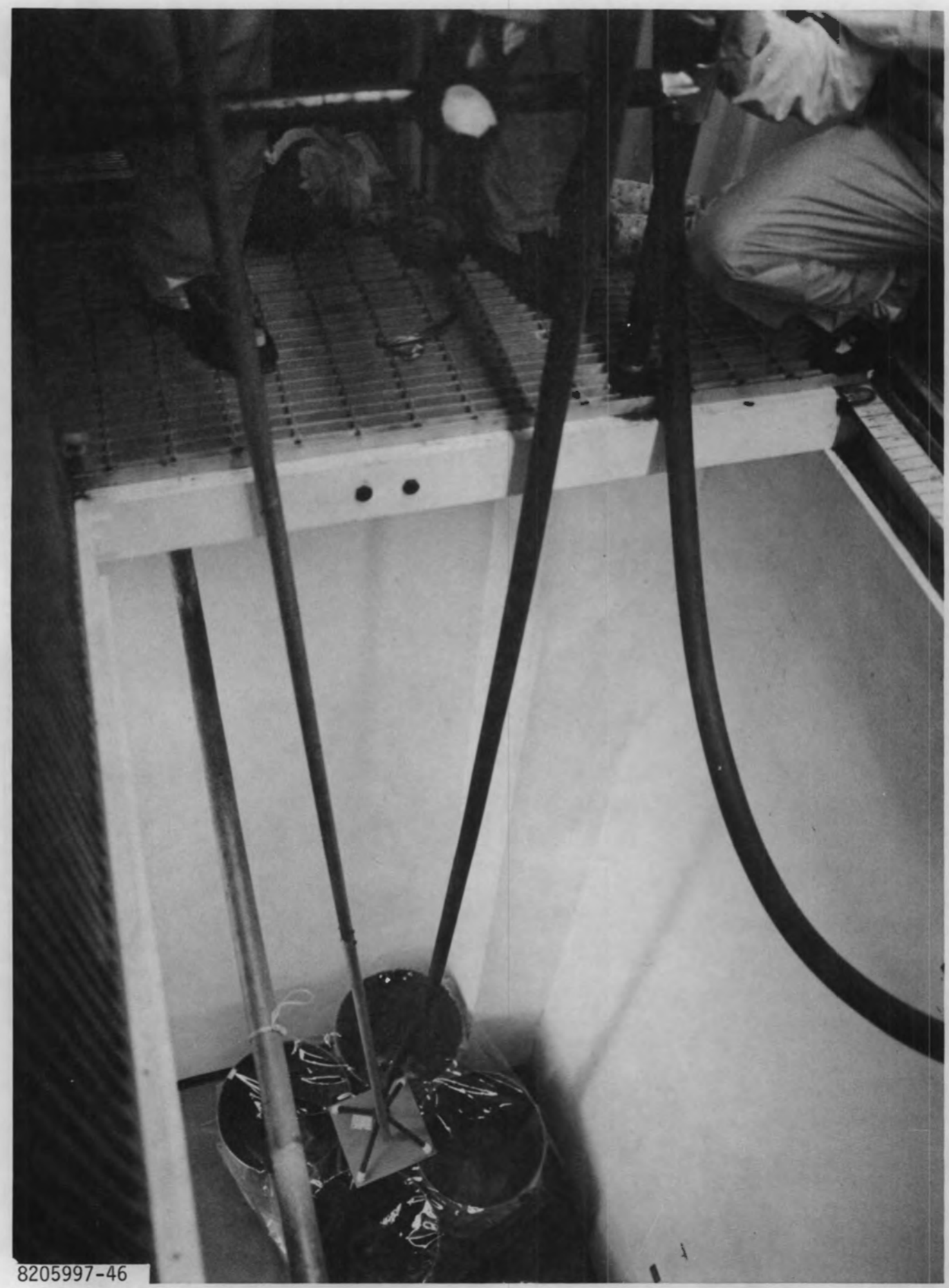

8205997-46

FIGURE 3-20. Remote Filling of the Waste Disposal Drums

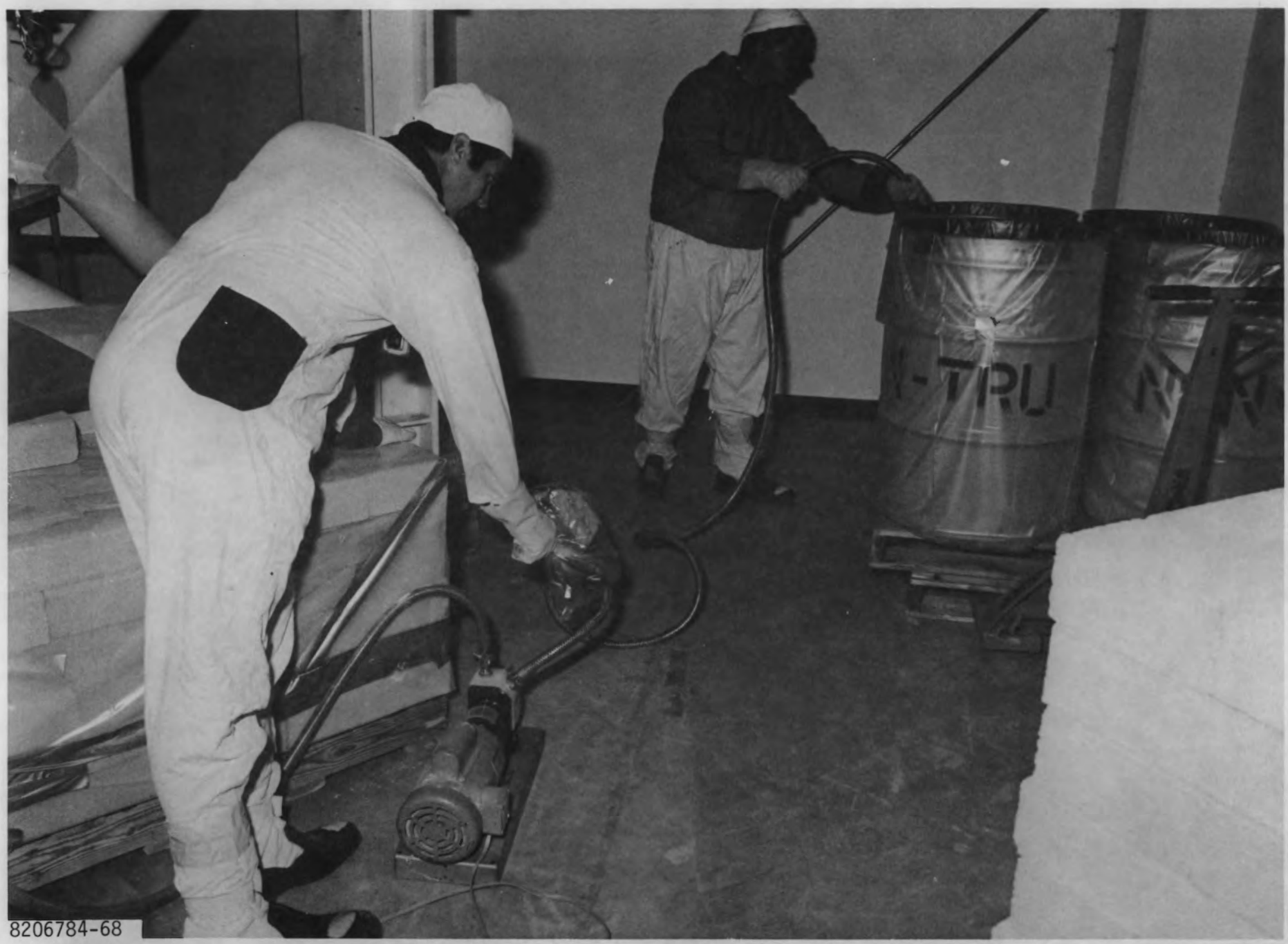

8206784-68

FIGURE 3-21. Dewatering the Resin

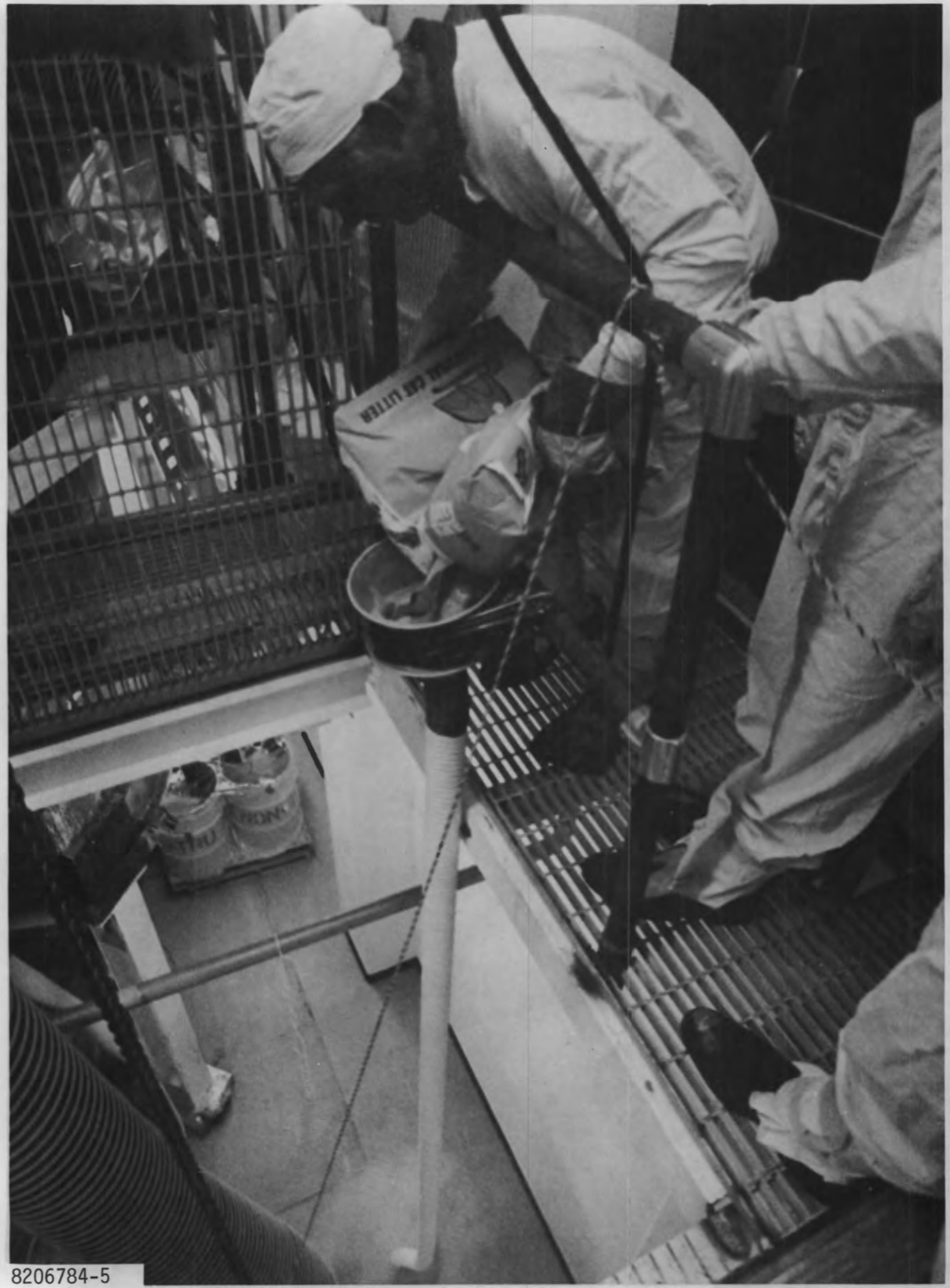

8206784-5

FIGURE 3-22. Remote Addition of Adsorbant Material

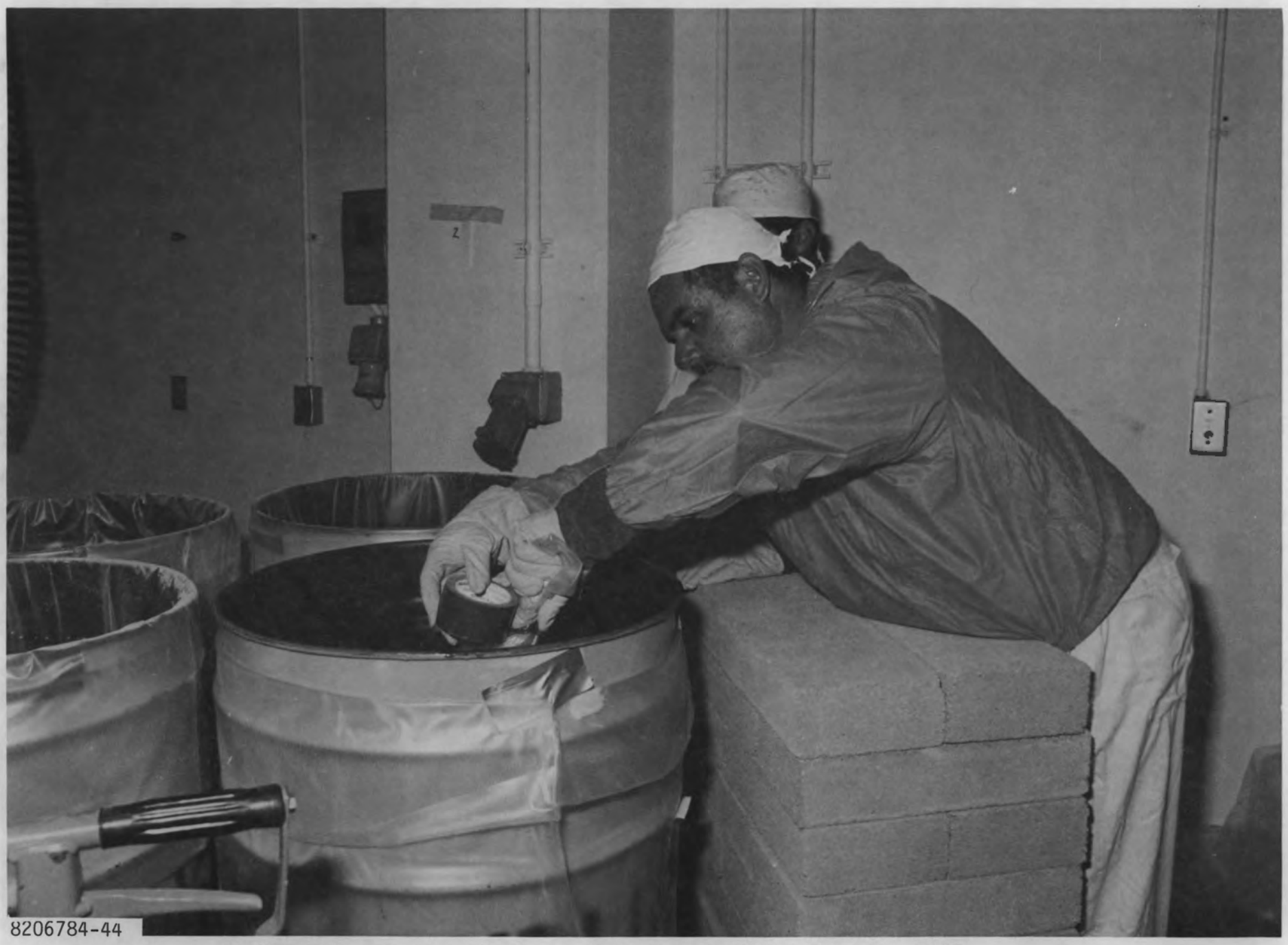

8206784-44

FIGURE 3-23. Sealing the Waste Drums From Behind a Shielding Wall

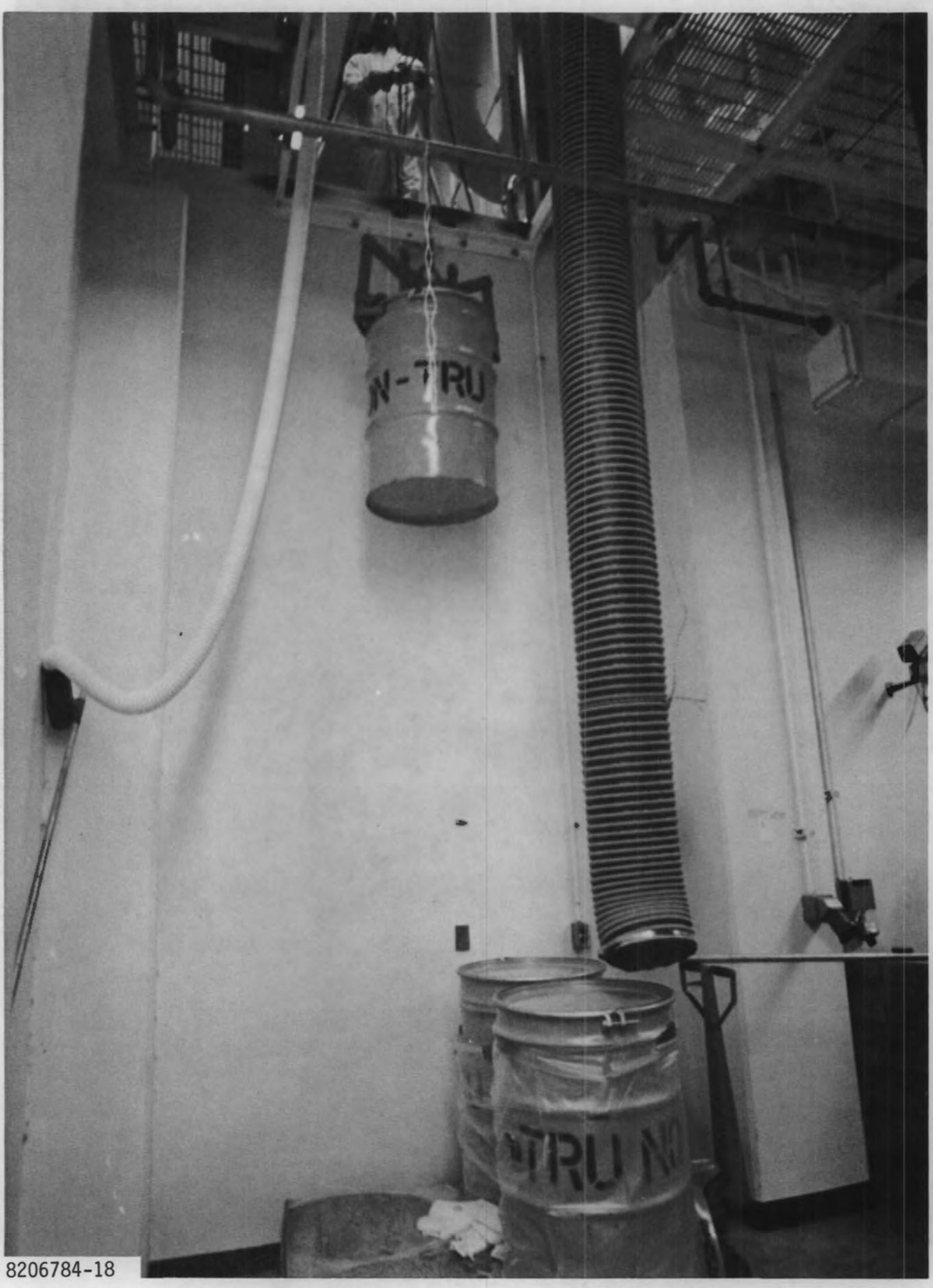

8206784-18

FIGURE 3-24. Remote Clamping and Hoisting System

8206784-80

FIGURE 3-25. Loading the Drums for Shipment to the Disposal Site

4. HOT LEG DECONTAMINATION

The hot leg region of the Surry steam generator channel head was decontaminated during the November 2-10, 1982 time period by Quadrex Corporation in cooperation with Babcock-Woodall Duckham, Ltd. and the Central Electricity Generating Board using the LOMI dilute chemical decontamination process supplemented by other film pretreatment and dissolution steps. This section of the report contains the project report prepared by the decontamination contractors followed by a PNL addendum providing supplemental details and figures.

DECONTAMINATION OF THE RETIRED SURRY STEAM GENERATOR CHANNEL HEAD AT BATTELLE

Summary of the Project
Completed November 16, 1982

Prepared by:
D. Bradbury*, A. N. McLean**, M. E. Pick*,
and C. N. Spalaris***

* Berkeley Nuclear Laboratories CEGB
** Babcock Woodall - Duckham Ltd.
*** Quadrex Corporation

TABLE OF CONTENTS

ABSTRACT

Decontamination of a pressurized water reactor steam generator (steam-head portion) was performed at Battelle Pacific Northwest Laboratory. The steam generator was the Surry Nuclear Power Station component, retired from service in 1979 and transported to Richland, Washington for studies.

The dilute chemical process LOMI (low oxidation state metal ion) was used for the first step and POD (pressurized water reactor oxide decontamination) process was used during the second step. Decontamination factors for stainless steel surfaces were 50, for Inconel 600, 6 to 10 and the overall space readings were 10 times lower than those originally. Electropolishing was used as a demonstration which reduced surface radiation reading even further. Details of the decontamination campaign are described in this report.

1.0 OVERALL STATEMENT

Decontamination factors obtained using two successive dilute chemical methods are as follows. For the stainless steel channel head surfaces, measured DFs are 50, estimated DFs for Inconel 600 surfaces are 6 to to 10, and overall internal space readings (including shine from the tube bundle) show DFs of 10. Stainless specimens (original manway cover) suspended from the tube sheet and submerged into the chemical solutions show DFs as high as 700. Inconel 600 tube specimens (removed from the tube bundle) were submerged into the chemical solutions and exhibited DFs of four to six*. Corrosion rates of the specimens were minimal and no stress corrosion cracking was experienced by the U-bend surveillance coupons prototypic of the structural alloys of steam generator internals.

The chemical operations were applied very successfully; the thermal and hydraulic operation of the system was uneventful. Overall housekeeping and radiation protection was maintained within Battelle operating ALARA guidelines.

2.0 BACKGROUND

This project was initiated by a request for proposal by Battelle PNL (Richland) on April 22, 1982 (Battelle-F1668). Quadrex submitted a proposal on May 21, 1982 to perform the work, using the LOMI (Low Oxidation State Metal Ion) technique with electropolishing as a back up. Quadrex received a Notice of Selection on July 13, 1982.

Application of the LOMI process was possible through a joint program with Babcock-Woodall Duckham, Ltd. (BWD) of UK, who in turn were assisted by Central Electricity Generating Board (CEGB) chemists who developed the process.

---

*The tubular samples were mounted over a teflon rod, with an estimated annulus of 1/4", which may have restricted solution entry into the interior surfaces where the activity was present.

The major technical requirement of the RFP was for the process to achieve DFs of 10 or greater at the channel head surfaces.

3.0 TECHNICAL AND OPERATIONAL DETAILS

The mechanical/hydraulic system performed satisfactorily. Temperature control of the liquids was achieved to within ±2°C, heat-up time to 90°C was 10-12 hours (as predicted), maximum possible agitation was achieved by means of a special jet nozzle affixed to the pump discharge hose entering the steam head. The liquid level in the steam generator steam channel head was regulated by an overflow loop to within ±2 inches at the tube sheet level as required by Battelle.

Operations manpower was provided by Quadrex, BWD and CEGB. Battelle provided radiological measurements, analytical chemistry services, corrosion characterization, health physics, safety training, monitoring services, waste removal, and personnel for facility operation.

The LOMI process application required four days round-the-clock shifts, and the AP/POD (second step) spanned another four days. Selective electropolishing was done around the manway cover and the Inconel separator plate.

All operations were preceded by readiness reviews of the key procedural elements. Battelle management and operations personnel participated in these meetings and offered suggestions where needed.

Removal of wastes from the 2,000 gallon storage tank was carried out by Battelle, using a transfer tank of 400 gallons capacity. This method of waste removal was selected by Battelle, in preference to collecting the activity in ion exchange columns. Ion exchange was originally proposed by Quadrex as an option for the LOMI process but at added cost (see sections 5.4 and 6.0, this report). Each time the storage tank needed emptying, the operation consumed two shifts, a requirement

which was the reason for using the AP/POD process for the second step. Because POD (pressurized reactor oxide decontamination) requires no intermediate rinse between the oxidation and reduction steps, the volume of total liquid wastes was limited to less than 2,000 gallons total for the second step. The AP (alkaline permanganate) part of the POD process was needed to preoxidize the Inconel 600 oxide surfaces.

4.0 CHEMICAL PROCESSES AND ANALYTICAL CONTROL

4.1 Application of NP/LOMI

As the system temperature approached 90°C, a solution containing potassium permanganate and nitric acid was prepared in the reagent tank. It was added to the circulating DI water as soon as the desired temperature of 90°C in the channel head was reached. Measured permanganate concentration and pH were close to the target values. The permanganate concentration and pH were monitored at 15 minute intervals for the first hour, then 30 minute intervals for the next 6 hours and then at 1 hour intervals thereafter; chromium, iron and nickel concentrations were also measured. After about an hour, it was apparent that the pH of the solution was rising steadily. However, the permanganate concentration was showing no change, hence the rise in pH was not due to permanganate self-destruction. After 2 hours, when the pH had risen by 0.2 units, it was decided to add nitric acid; this returned the pH to the desired value and it remained constant at that value for the rest of the run. The NP reagent was applied for 20 hours. At the end of this period oxalic acid and nitric acid were added to destroy the permanganate and manganese dioxide which forms on surfaces and as a suspension in the solution. These reagents were dissolved in cold DI water in the reagent tank and were added at a rate of about 6 dm^3 min^{-1}. This controlled rate ensured that the pH remained within the desired range and also ensured that carbon dioxide, which is generated when the chemicals react, was not given off too

rapidly. The final pH of the solution was correct and there were no problems with carbon dioxide evolution. The run was terminated 1 hour after oxalic and nitric acid addition commenced and the solution was dumped to the waste tank.

The channel head and hoses were then rinsed until analysis of rinse water for nitrate ion showed that when the water for LOMI was added there was less than 3 ppm nitrate present.

The system was then filled and while the water was heating up to 90°C it was deoxygenated using a nitrogen sparge. Remaining traces of oxygen were removed by addition of hydrazine hydrate solution. A solution of picolinic acid and sodium hydroxide was prepared in deoxygenated DI water in the reagent tank. When dissolved this was added to the circulating water. It was allowed to circulate for a short period before adding vanadous formate solution at a rate of about 5 dm^3 min^{-1}. The concentration of the vanadous picolinate complex was monitored continuously using a flow colorimeter. Samples of the circulating solution were taken at 15 minute intervals to monitor radioactivity, iron, chromium and nickel. The run was terminated about 2.6 hours after vanadous formate addition commenced, the solution was then dumped to the waste tank. The channel head and hoses were then rinsed and the manway cover was removed to permit a visual examination and dose-rate measurements in the channel head. In addition, the DF's on the specimens mounted in the channel head were determined.

4.2 Application of AP/POD

Before final reassembly and filling with DI water the hoses and channel head were rinsed again. The conductivity of the circulating water after refill was 4μS. When the temperature approached 90°C, the AP solution was prepared in the reagent tank.

The AP solution was applied for 11 hours, the pH was then lowered by the controlled addition of nitric acid to give NP conditions. Samples of solution were taken at 30 minute intervals initially at the start of the AP and NP conditions and at 1 hour intervals thereafter. The samples were monitored for pH, permanganate, radioactivity, chromium, iron and nickel. After about 5 hours in NP conditions, a solution containing oxalic acid and nitric acid was added to the circulating solution from the reagent tank. 1 hour after this addition commenced a solution containing oxalic acid and citric acid was added.

This solution was applied for about 2 hours. It was then dumped to the waste tank. The channel head was then rinsed and the manway cover removed.

4.3 Hydrolasing

After the decontamination of the cold leg side, Battelle had performed a hydrolasing operation which removed a considerable amount of activity. It was decided to perform a similar hydrolasing operation on the hot leg side, however, very little activity was removed.

5.0 RESULTS

5.1 NP/LOMI

5.1.1 Reagent Monitoring

After the early rise in pH which was rectified, the pH in the NP reagent remained roughly constant. The reason for the initial rise was probably dissolution of scale, e.g. calcium carbonate, in the channel head. The presence of calcium was confirmed by atomic absorption analyses of the circulating solution. The pH after permanganate and manganese destruction was as expected. The permanganate concentration declined at a fairly constant slow rate.

This was about the loss rate expected from prediction based on the surface area of hoses and metal in the system. A significant proportion of the loss (possibly the majority) was probably due to the hoses. As regards process chemistry the loss was of no consequence.

In the LOMI stage the pH remained constant and the stability of the vanadous picolinate complex was as predicted.

5.1.2 Metals and Radioactivity Release

Chromium, iron and nickel concentrations were monitored throughout the run. Chromium release took place at a steady rate throughout the NP run. Nickel was also released at a steady rate. There was no iron release in the NP stage.

After addition of oxalic and nitric acid to destroy the permanganate there was a further release of metals probably from oxide dissolution and a little corrosion.

There was very little release of radioactivity in the NP stage and the results are neglibible compared with subsequent values. The average concentration of 60 Co was only about 2.0×10^{-3} $\mu Ci\ cm^{-3}$. When the oxalic and nitric acid were added there was a rise to give a final value of 5.7×10^{-3} $\mu Ci\ cm^{-3}$ which corresponded to a total release of about 40 mCi.

Radioactivity release in LOMI is plotted in figure 1. The release of radioactivity and metals from the chromium depleted oxide took place quickly and radioactivity release levelled off at a value of about 0.95 $\mu ci\ cm^{-3}$ after about an hour, representing a total release of about 0.62 Ci. There was then some further release of

metals from corrosion before the solution was dumped after 2.6 hours. In retrospect, data show that the solution could have been dumped after an hour when it was clear that radioactivity release had ceased. In an operating reactor it would have been dumped in order to minimize corrosion, although the actual metal loss represented by the extra duration was less than 1μm.

5.1.3 Decontamination Factors and Dose Rates

The DFs obtained on the specimens inserted in the channel head are listed in table I. On the stainless steel manway cover specimens, DF of 21 - 30 were obtained, which is very good. On the Inconel 600 tube specimens, DFs were much lower, between 1 - 4 and 1 - 6. However, reagent access to the primary circuit oxide may have been restricted resulting in lower DF's. In laboratory tests higher DFs have been obtained on similar specimens.

A shielded TLD on the stainless-steel channel - head bowl surfaces showed that the surface dose rate had been reduced from 2.7 R/hour to 0.42 R/hour, i.e., a DF of 6.5 (table II). Dose rates in the volume of the channel head were measured using TLDs mounted at 6" intervals on a rod running from the manway cover into the furthest corner of the channel head by the tube sheet. Initial, pre-cleaning measurements ranged from about 3.0 R/hour just inside the manway to 4.9 R/hour adjacent to the tube sheet (table III). After NP/LOMI these dose rates had been reduced to about 1.0 R/hour to 1.9 R/hour by the tube sheet. The average area DF was about 2.7. These results are, of course, affected by tube shine. This probably accounts for about 10% of the original dose; if this is factored out of the data, then the average DF rises to about 3.3 (table III).

5.1.4 Corrosometer Probe Readings

In NP the Inconel 600 probes showed a metal loss of about 1.4μm, with the loss diminishing near the end of the run. There was no further corrosion when the oxalic and nitric acid were added at the end of the run. The stainless steel probe showed a more erratic behavior, although there was a general rising trend. At the end of the run the cumulative loss was small, about 0.20μm. The behavior of the carbon steel probe was interesting; the corrosion rate actually dropped from that in hot water when the NP chemicals were added to the circulating water indicating that NP was passivating the carbon steel. There was about 1 μm loss after 3 hours, the rate then dropped further and the total loss after 20 hours was 2 μm. At the end of the run when oxalic and nitric acid were added there was a small rise in corrosion as expected.

In LOMI, the Inconel 600 probe showed no detectable corrosion. With stainless steel there was no corrosion up to 1 hour; the rate then increased but the total loss at the end was only 0.35 μm. As mentioned previously, if the solution had been dumped after an hour this loss, although quite small, would have been avoided. The carbon steel probe showed a steadily increasing rate giving a total loss of about 6 μm.

5.1.5 Visual Examination

Before decontamination, photographs showed that the stainless steel bowl surfaces were black and of a fairly rough appearance. Concentric ridges formed during the clad welding process were visible in some ares, but others appeared to be obscured by oxide. The divider plate was of a dark brown appearance characteristic of Inconel 600 oxide. The tube sheet was a lighter brown. Visual examination by the authors after NP/LOMI treatment showed that the bowl surfaces were now a reddish brown color.

5.2 AP/POD

5.2.1 Reagent Monitoring

The potassium permanganate concentration after 11 hours in AP conditions was a little less than the starting concentration. The rate of loss was a little higher than in the NP phase in the first run. However, it was expected that the loss rate would be higher from laboratory tests on the degradation of permanganate on hose specimens in NP and AP solutions. After 5 hours in NP conditions in the channel head the loss rate was back to that expected for NP. There appeared to be a step loss of about 5% when the pH was changed from AP to NP. The pH of the AP solution remained constant throughout the run. During the NP stage the pH rose very gradually; however, no further additions were judged to be necessary. After addition of the oxalic and nitric acids the pH fell to near the target value. Addition of the citric and oxalic acids for the final phase lowered the pH to within the desired range.

5.2.2 Metals and Radioactivity Release

Metals and activity released were measured during the run. As previously in the oxidation phase there was very little release of radioactivity (less than 2.0×10^{-3} $\mu Ci\ m^{-3}$) and these results are not recorded. The bulk of the chromium release took place in the first 3 hours and in fact more than half had been released after about 40 minutes. There was no release of iron or nickel observable in the AP phase, however, neither metal is very soluble under alkaline conditions. In the period of NP conditions chromium release recommenced, more rapidly than during the AP stage. Nickel was also released.

The release of radioactivity after addition of the oxalic and nitric acid followed by citric and oxalic acids is shown in figure 2. Samples taken 1 hour after the addition of oxalic and nitric acid showed a small release of radioactivity (7.1×10^{-3} $\mu Ci\ cm^{-3}$, equivalent to about 40 m Ci). Chromium and nickel concentrations had increased and iron had also appeared in solution. When the citric and oxalic acids were added there was a sharp jump in the radioactivity in solution. This represented a total release of 0.58 Ci. There was further release of metals from corrosion and when the solution was dumped the cumulative metals had increased by about 50%. As with LOMI in the first run, the solution could probably have been dumped soon after 30 minutes - 1 hour when it was clear that radioactivity relase had ceased, although actual metal loss represented by the extra metal dissolved was <1μm.

5.2.3 Decontamination Factors and Dose Rates

The DFs obtained on the stainless steel and Inconel specimens are listed in table I. DFs on the manway specimens had now risen to between 360 to 706 with one specimen showing a DF of 3979. The DFs on these specimens after NP/LOMI were already 21-30 which in terms of dose reduction was already an excellent DF. Inconel specimen DFs ranged from 4.0 - 5.6, in spite of the fact that these specimens were mounted over a teflon rod, allowing only a narrow annular space between it and the inner diameters of the tubular specimens. Laboratory tests on these specimens showed that if they had been mounted in a manner which would have allowed more liquid to contact the contaminated surfaces, DFs would have been higher.

Dose rates measured on the TLD rod ranged from about 0.3 R/hour at the manway entrance to 0.8 R/hour by the tube sheet

(table III). The average area DF was about 6.2. However, allowing for tube shine the corrected value was ~16. A shielded TLD measurement on the channel bowl was not taken until after hydrolasing had been carried out. The hydrolasing probably did not remove much radioactivity from the bowl and the value of 0.052 R/hour representing a DF of 52 is probably applicable to the two decontamination cycles (table II).

5.2.4 Corrosometer Probe Readings

The Inconel 600 probe showed no obvious corrosion in AP conditions. After changing to NP conditions some corroson took place; 0.8μm loss occurred in the first 2 hours, the rate then appeared to drop. However, there was a jump of about 0.3μm after addition of citric and oxalic acid. The total corrosion overall was about 1.5μm. The stainless steel probe showed very erratic behavior and the only conclusion that could be drawn was that little corrosion took place. For carbon steel the probe showed negligible corrosion in AP and NP conditions as expected, because they passivate carbon steel. After addition of citric and oxalic acids there was a step loss of about 11μm but then the probe showed no further loss.

5.2.5 Visual Examination

The bowl surfaces and tube sheet now looked very clean and major portions of the area were free of oxide. Patches of grey thinned oxide remained on some areas on the bowl and appeared to follow the contours of the ridges formed during clad welding. In these areas the oxide may have been particularly thick initially. (This may be because of variable intermixing of the channel head base metal with the weld overlay, leading to surfaces or to an accumulation of deposited oxides on the corrugated surfaces which corroded

more during operation.) The divider plate was still a light brown color although some areas which had obviously been struck by the water jets in rinsing were cleaned to the base metal.

5.3 Hydrolasing

In the hydrolasing operation performed by Battelle an estimated 0.1 Ci of activity were removed in the water which was colored reddish bown at the end. The dose rates recorded on the TLD rod afterwards were slightly lower around the inside of the manway but those by the tube sheet where shine was dominant showed little change.

5.4 Ion Exchange Demonstration Experiments

For the purposes of demonstrating the ion exchange of the CEGB decontamination solutions, four litre batches of the NP and LOMI solutions were collected at the end of the runs. The solutions were deionised in a recirculatory mode. For NP 50 cm^3 of cation resin and 100 cm^3 of anion resin were used and the flow rate was up to 70 bed volumes per hour on the cation column. The conductivity of the effluent was 1μS, the experiment was run until the solution conductivity fell to the target of 10μS. For deionisation of LOMI 100 cm^3 of cation resin and 200 cm^3 of anion resin were used. Again, the flow rate was quite high and reached 120 BV /h on the cation column, towards the end of the experiment. The effluent conductivity was 3.6μS and the experiment was terminated when the target of 10μS was reached in the bulk solution.

The dose rate on the reservoir, initially 50 mR/h had fallen to less than 0.5 mR/h at the end of the experiment.

5.5 Corrosion Rates of Surveillance Specimens and Corrosometer Data

The value of any chemical decontamination technique will be judged on the basis of reagent interaction with the structural materials of the

component being cleaned. Corrosion measurements taken during the Battelle-Surry decontamination activities can be classified as follows:

a. General corrosion was determined by weight loss, dimensional changes and resistance measurements of wires using a corrosometer.

b. Corrosion under stress was determined by means of "U"-bends fabricated according to ASTM G30-72 standards.

c. Crevice corrosion was determined using double "U"-bends as per ASTM G30-72 standards.

All samples were exposed directly into the bulk liquid volume of chemical solutions contained within the steam generator. Some of the specimens were suspended from the tube sheet, while others were fixed onto the manway covers.

Types of alloys used in the corrosion surveillance were Inconel 600, types 304, 316, 347 stainless, and AISI 410 all cut from flat stock, as well as Inconel 600 tubing. Tubular specimens were also removed from the steam generator tube bundle and were held by teflon spacers. Sections of the original manway cover were also exposed to determine corrosion rates as well as degree of decontamination.

Upon removal, inspection of U-bend specimens under 16X magnification revealed no stress or crevice corrosion. Dye penetrant was also used to increase the degree of sensitivity for surface crack inspections. No cracks were detected for any of the alloys typical of steam generator surfaces subjected to decontamination.

Inconel 600 and 300 series stainless surfaces exhibited general corrosion losses of much less than 0.5 mil during the entire decontamination cycle. These determinations were made by weight loss measurements. More accurate corrosion rate measurments will be reported at a later date, along with results of metallographic examination aimed to determine microstructural surface condition.

Corrosometer data indicate losses of 0.03 mils for the type 304 stainless wire, 0.1 mils for Inconel 600, and less than 1 mil for the carbon steel during the LOMI plus AP/POD runs.

6.0 ELECTROPOLISHING*

Electropolishing was offered originally to Battelle as a backup process to LOMI in order to meet the decontamination factor of 10 stipulated in the contract. Thus, there was no obligation or need to undertake electropolishing of the entire steam head surface. Instead, it was decided to demontrate the compability of electropolishing steam head surfaces, using semi-remotely operated devices. The areas chosen for electropolishing were the manway entrances into both sides of the steam head, and an area of about 2 square feet of the hot leg side of the Inconel divider plate.

Small hand-held swab type in-situ devices were used for the electropolishing. The insulator on the devices was Type-T Scotch Brite. The electrolyte was 75% phosphoric acid supplied at the rate of about 2-3 gal/hr, and the current density was about 2.5 A/in^2. Actual electropolishing time for any given point on the test area was about one minute for each electropolishing step. Following electropolishing, the test areas were rinsed with cold water, scrubbed with wet rags and wiped with a foaming cleanser. Smears were taken over the entire electropolished area and counted with an Eberline CP or E-140 with a P-11 pancake probe.

The surface condition in the test areas differed widely depending on the material of construction. The stainless steel surface was rough and irregular, with a series of high and low points in a wave-like pattern, the result of the weld overlay during its fabrication. The Inconel surface in comparison was smooth and flat. The results of electropolishing the test areas in the hot leg are shown below:

*Work described in section 6 was performed by Michael McCoy.

Area Description	2 ft^2 area Divider Plate	Manway Entrance
Material	(Inconel)	(stainless steel)
Smearable Contamination before EP	100 mrad/hr	24 mrad/hr
Smearable contamination after EP	80K counts/minute 6K counts/minute 2K counts/minute	6K counts/minute 25K counts/minute 8K counts/minute 2K counts/minute 6K counts minute <200 counts/minute

The Inconel surface was covered with the reddish-brown film. This film was rapidly removed by electropolishing, leaving a shiny, clean-looking surface. The above table shows that residual smearable contamination remained after the initial electropolishing. Two additional electropolishing steps, 3-4 minutes total electropolishing time, were required to reduce this area to background. The 2000 c/m final level was probably due to cross-contamination of the smears while removing them from the channel head.

The stainless steel test area was also covered with the redish-brown film observed on the Inconel. Like the Inconel surface, this film was rapidly removed by electropolishing revealing areas of the original black oxide film. The black film was mainly concentrated in the valley-like areas of the surface whereas the crest-like areas of the surface were shiny. Additional electro-polishing caused the smearable contamination level of the surface to increase as though contamination was embedded in the stainless steel and was being released by the repeated electro-polishing steps. Smearable contamination remained even after all visible traces of the black film were removed. The total electropolishing time to decontaminate a given point on the stainless steel was about ten

minutes. This is in marked contract to the time of one minute required to decontaminate stainless steel coupons cut from the flat, machined manway cover insert.

7.0 DISCUSSION

Application of the NP/LOMI and AP/POD processes took place with no major problems. The stability of the reagents was very good and in the case of NP and AP might have been even better if alternative flexible hoses had been used. There were no major problems in rinsing between stages. Deoxygenation of the system for LOMI application was carried out with no problems.

The DFs obtained were within the expected range for the processes used. For the first application of NP/LOMI it was anticipated that DFs on stainless steel would be 5-10 and on Inconel about 2. Actual DFs recorded on stainless steel were 6.5 on the bowl and 21-30 on manway cover specimens. DFs for Inconel specimens were a little lower than anticipated, but this was probably because the specimens were mounted in a manner that restricted full access of chemicals to contact the contaminated surfaces. It was not possible to obtain a direct measurement of the DF on the Inconel surfaces in the bowl. However, calculations based on the dose rates and radioactivity released suggested that the DF was in the range 1.5-3. The DFs at the end after AP/POD, as expected after a second decon application, had been increased to very high values on the stainless steel specimens and 50 on the bowl. On the Inconel surfaces within the bowl the estimated DFs were in the range 5-15.

Ion exchange of the NP, AP, LOMI and POD soulutions has been amply demonstrated in experiments at Berkeley Nuclear Laboratories. Results of this work were reported at the ANS/CNA decontamination conference held at Niagara Falls and discussed in the following publications:

a. Bradbury, Segal, Sellers, Swan and Wood, 1982; Pick, 1982). (Pick, M.E. 1982, "Development of Nitric Acid Permanganate Pre-oxidation and Its Application in the POD Process for PWR

Decontamination", Proc. Int. Conf. Decontamination of Nuclear Facilities, ANS/CNA, Niagara Falls, Canada.)

b. (Bradbury, D., Segal, M. G., Sellers, R. M. Swan, T. and Wood, C. J. 1982, "Decontamination Systems of BWRs and PWRs Based on LOMI Reagents", Proc., Int. Conf. Decontamination of Nuclear Facilities, ANS/CNA, Niagara Falls, Canada, September 1982.)

There are no problems in ion exchanging any of these solutions or combinations and resin requirements typically are in the range 50-80 dm^3 per m^3 of solution. The ease of activity removal by means of ion exchange was shown by the demonstration experiments at Battelle on the NP and LOMI solutions.

Electropolishing was found to be an effective method for removing oxides from steam generator surfaces. Flat surfaces, such as the separator Inconel 600 plate, were much easier to electropolish than the stainless weld overlay. Electropolished surfaces were decontaminated to background levels.

8.0 LESSONS LEARNED

a. Removal of contamination is a very strong function of liquid agitation and/or flow (compare DFs between the specimens versus surfaces of the steam generator cavity).

b. Liquid waste volumes can be minimized through the application of a spinner head, designed to operate at high-pressures with spray heads set at multiple angles. (Quadrex's original proposal called for this method, but NRC requirements did not permit the use of a spinner head in order to keep chemicals out of the tubes.)

c. Mechanical, hydraulic, and electrical systems can be streamlined considerably. For commercial applications, the introduction of ion exchange capability will eliminate the generation of liquid wastes.

d. Handling of wastes can be done through the introduction of ion exchange capability. The principle was demonstrated at Battelle, using line samples taken from the process.

e. Electropolishing can reduce contamination of steam generator surfaces to background levels. Weld overlaid stainless is more difficult to electropolish than flat surfaces due to its corrugated surface roughness.

9.0 CONTRIBUTORS

- H. Arrowsmith - Quadrex
  - Proposal, cost estimates, assembly of components, and operations
- D. Skvara - Quadrex/Hydrite
  - Procurement of components, assembly, ans startup operations
  - System design
- C. N. Spalaris - Quadrex
  - Project integration
- M. McCoy - Quadrex
  - Procurement of chemicals, assembly of components, operations, cleanup, and disassembly/shipment to fixed-base facility
  - Electropolishing equipment and operations
- A. McLean - BWD
  - Initial system design, operations, and analysis
  - Systems engineering
- D. Bradbury - CEGB
  - Lomi process operations, analysis, chemical testing, and senior advisor
- M. Pick - CEGB
  - POD process, operations, analysis, chemical testing, and senior advisor
- L. Fetrow - Battelle
  - Lead person; assembly, operations, site supervision
- R. Allen - Quadrex and M. Lewis - Battelle
  - Lead project advisors, technical and contract coordination
  - Project evaluation
- K. Pool - Battelle
  - Senior chemist, analysis and control
- D. Reese and G. Hoenes - Battelle
  - Radiological services

- J. Remark - Quadrex
  - Project advisor, proposal preparation, and cost estimates
- G. Leonard and J. Coleman - Quadrex
  - Contract negotiations, legal and proposal preparation.

TABLE I

SURRY STEAM GENERATOR CHANNEL HEAD DECONTAMINATION DFs OBTAINED ON STAINLESS STEEL MANWAY COVER AND INCONEL 600 SG TUBE SPECIMENS

Specimen No.	Decontamination factor (DF)	
	After NP/LOMI	Cumulative at the end after AP/POD
Stainless Steel		
HA-8	28	669
HA-9	27	3979
HA-10	29	540
HB-8	21	358
HB-9	27	706
HB-10	30	411
Inconel 600		
R-1	1.4	4.0
R-6	1.5	4.7
R-8	1.6	5.0
R-10	1.6	5.6

TABLE II

DFs IN CHANNEL HEAD

Stainless Steel Bowl	6.5	52
Inconel 600	1.5-3.0 (estimated)	5-15 (estimated)
Volume DF	2.7	6.2
	~3.2 (allowing for tube shine)	~16 (allowing for tube shine)

TABLE III

DECONTAMINATION OF SURRY STEAM GENERATOR CHANNEL HEAD (DETAILS)

Dose Rates Recorded Using Thermoluminescence Detectors
(Hot Leg)
Rates in Roentgen per hour

Position Inside* Steam Head 10' Rods	Before Decon	After LP-LOMI	After AP-Pod	After Hydrolaser
10		2.2		
9	4.9	2.1		
	4.3			0.62
8	4.2	1.8	0.78	0.80
	4.3		0.78	0.76
7	4.0	1.7	0.73	0.68
	3.4		0.69	0.65
6	3.8	1.6	0.65	0.62
	3.6		0.66	0.61
5	3.5	1.4	0.61	0.60
	3.5		0.62	0.58
4	3.2	1.3	0.57	0.57
	3.2		0.55	0.54
3	3.1	1.2	0.52	0.50
	3.0		0.49	0.46
2	2.9	1.1	0.44	0.52
	2.9		0.41	0.39
1	2.7	0.76	0.36	0.35
	3.4		0.34	0.34
0	2.3		0.31	0.33
Lead Bricks, (5" thickness to shield shine from tube bundle)				
Down	2.7	1.1	0.052	
Up		1.2		
		0.42	0.33	

Note: This was the measurement used to determine DF for contractual purposes. DF shown is equal to 52.

*Distance from manway opening in feet, rod placed diagonally into steam head.

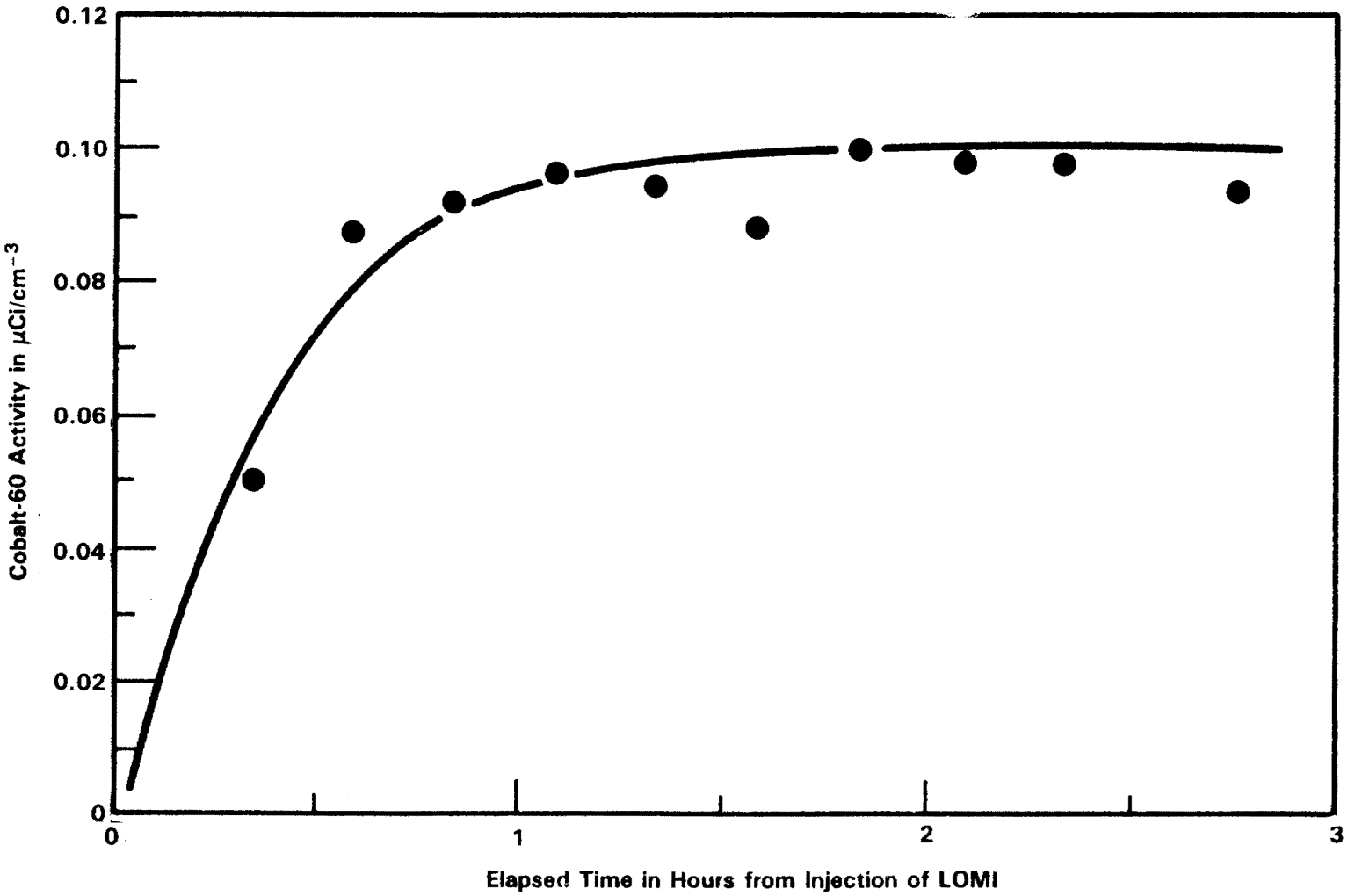

FIGURE 1. ACTIVITY RELEASE, COBALT 60 AS A FUNCTION OF TIME LAPSE SINCE INJECTION OF LOMI CHEMICALS

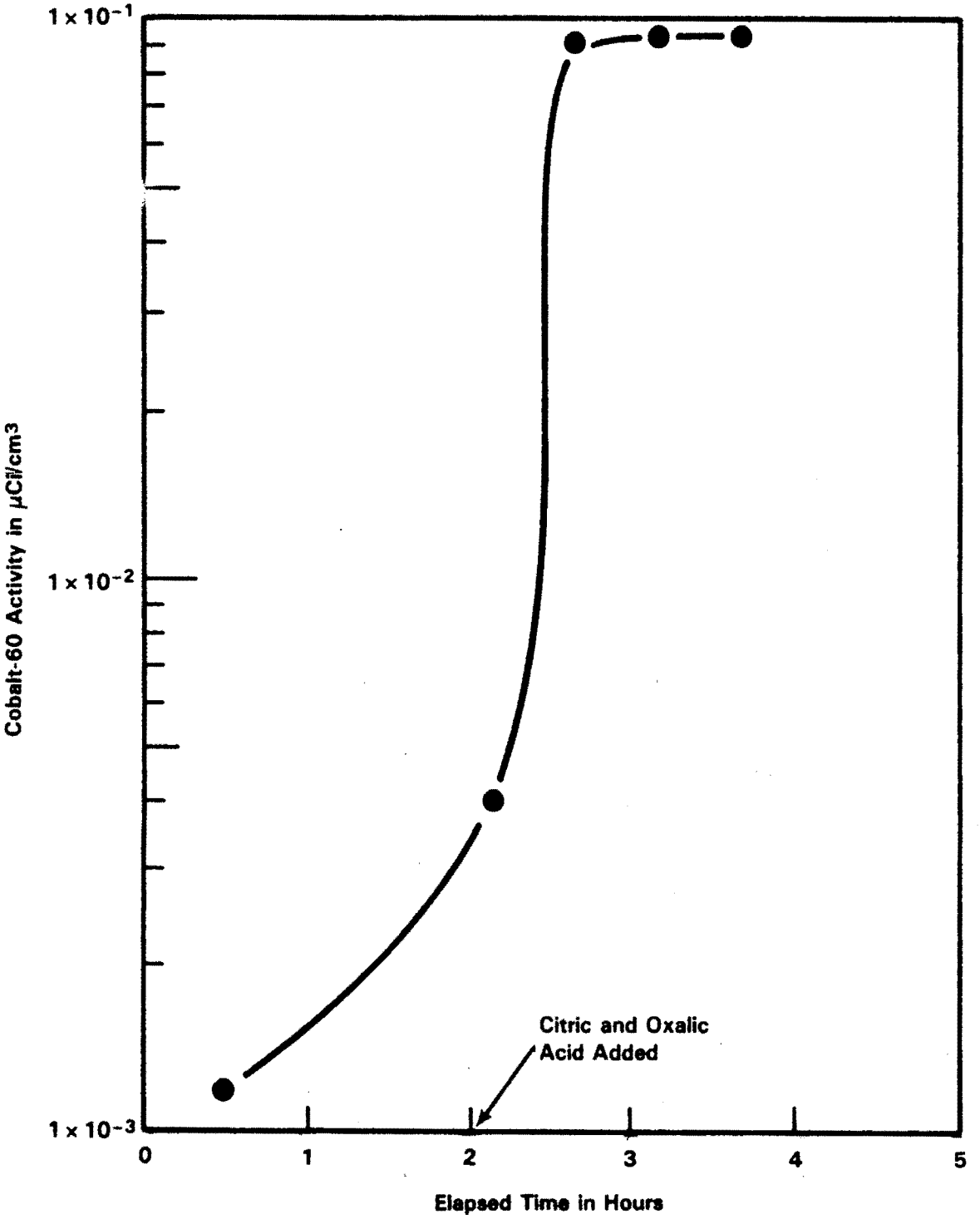

FIGURE 2. ACTIVITY RELEASED AT THE PERMANGANATE DESTRUCTION AND DECONTAMINATION PHASES OF THE AP/POD TREATMENT

PNL Addendum

The following subsections provide additional information and figures relating to the hot leg decontamination operation and results:

Decontamination Processes - The LOMI (Low Oxidation State Metal Ion), NP (Nitric Acid Permanganate Preoxidation) and POD (Pressurized Reactor Oxide Decontamination) processes, major features and chemistry are described in papers by Bradbury et al. (1982) and Pick (1982).

Equipment Installation - The Quadrex Corporation equipment consisted of a chemical addition/mixing tank that was installed inside the tower near the truck lock entrance (Figure 4-1), and a surge tank containing the heater and pump that was installed in the tower basement in the secondary containment area next to the liquid waste tank (Figure 4-2). Installation of the equipment was facilitated by its smaller size and the ability to place it all within the tower. However, it should be noted that an ion exchange system, while offered at extra cost by the contractor, was not utilized for the hot leg operation.

Decontamination Operations - The hot leg decontamination operation went well in all respects. This was attributable in part to changes and modifications made based on the cold leg decontamination experience. Pump problems were minimized by using a seal-less immersible centrifugal design. Increased agitation and better circulation of the decontamination solutions within the channel head was effected by using a special jet mixing nozzle (Figure 4-3) to introduce the solutions and by attaching the main return line to the channel head nozzle as shown in Figure 4-4. Exact control of the liquid level just above the bottom of the tube sheet was ensured by positioning the highest point of an overflow loop (Figure 4-5) at the desired control point and by equipping the sightglass with a sensor that provided the operators with a visual and audio alarm whenever the level fluctuated above the control point. Placement of the surge tank in the tower basement also ensured that most of the excess liquid inventory in the systen was below the level of the channel head.

Process Results - The results of the hot leg decontamination operation are presented in the Quadrex report and other sections of this report. The following is a summary of some of the more important information and findings:

- Dissolved metal concentration - the effect of the NP, LOMI, AP and POD process steps on the concentration of Fe, Cr and Ni in the decontamination solutions is summarized in Figure 4-6. It should be noted that these are cumulative values (no ion exchange) and that the Fe concentrations do not include a significant contribution from the coated channel head nozzle cover.

- Co-60 concentration - the effect of the various decontamination steps on Co-60 removal is shown in Figure 4-7. As discussed in Section 5, the difference in the amount of Co-60 removed from the

8207468-32

FIGURE 4-1. Chemical Addition/Mixing Tank for Hot Leg Decontamination

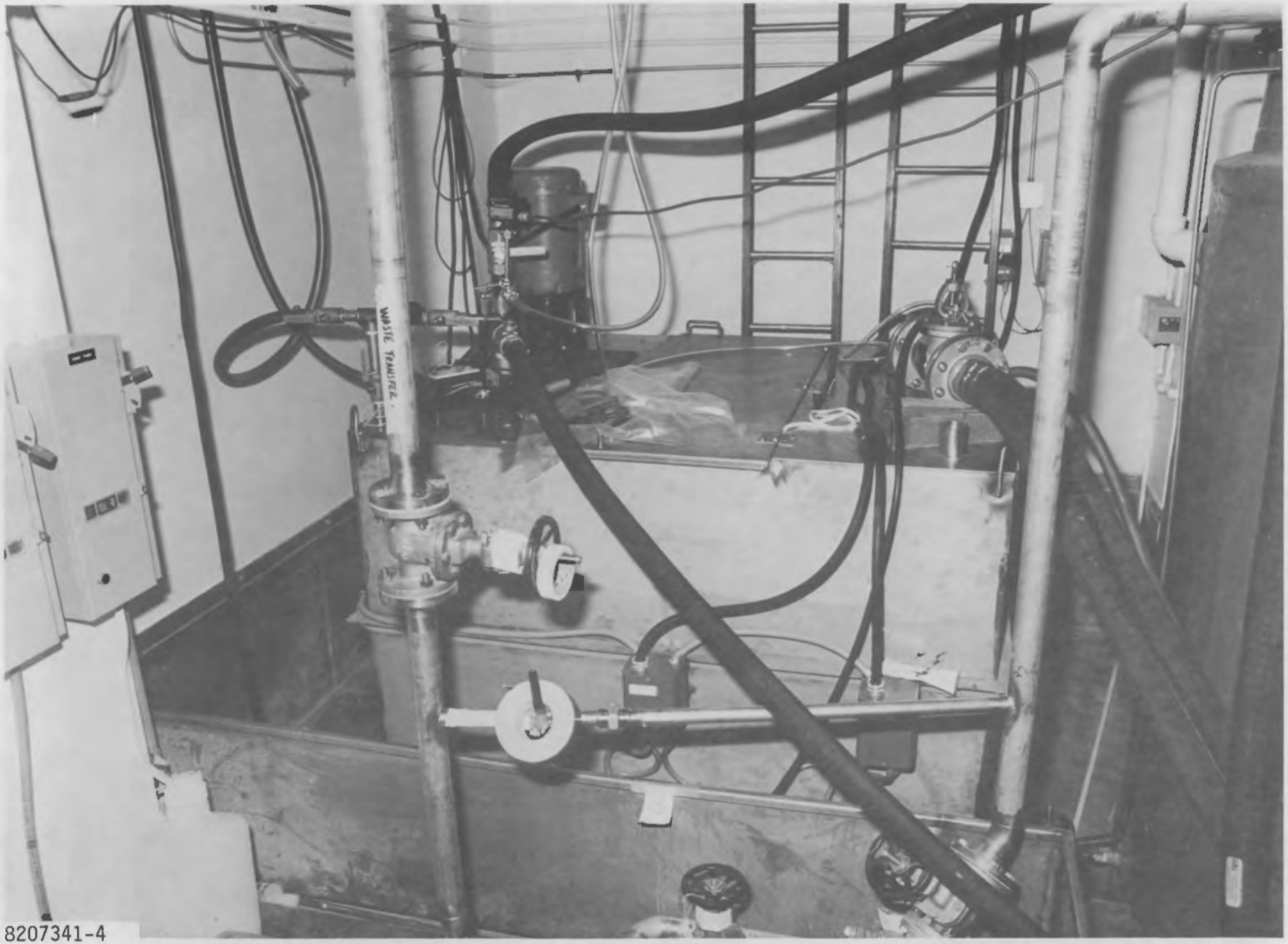

8207341-4

FIGURE 4-2. Surge Tank, Heater and Pump System for Hot Leg Decontamination

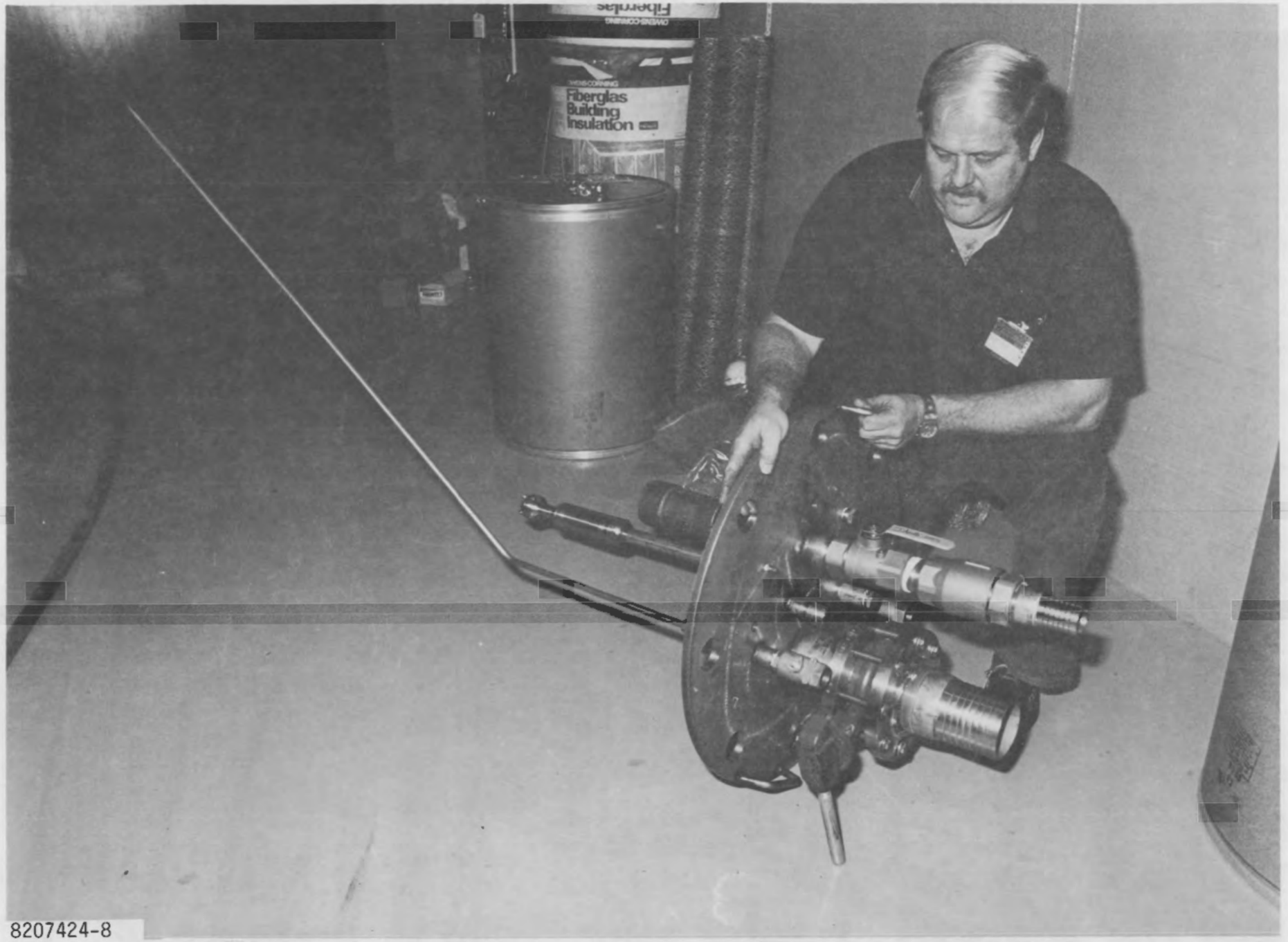

8207424-8

FIGURE 4-3. Jet Mixing Nozzle Used for the Hot Leg Decontamination Operation

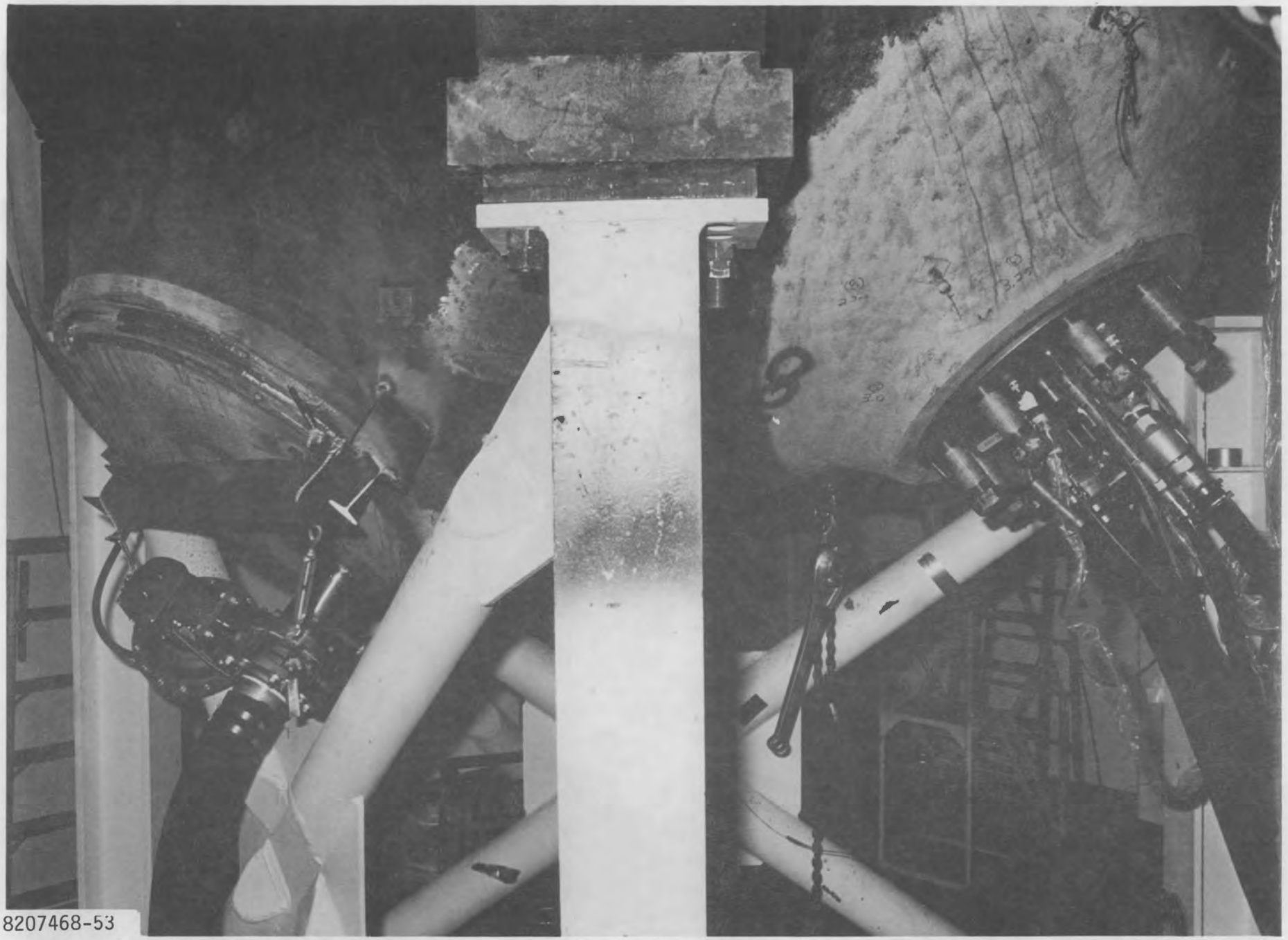

8207468-53

FIGURE 4-4. Main Solution Return Line From the Hot Leg Nozzle

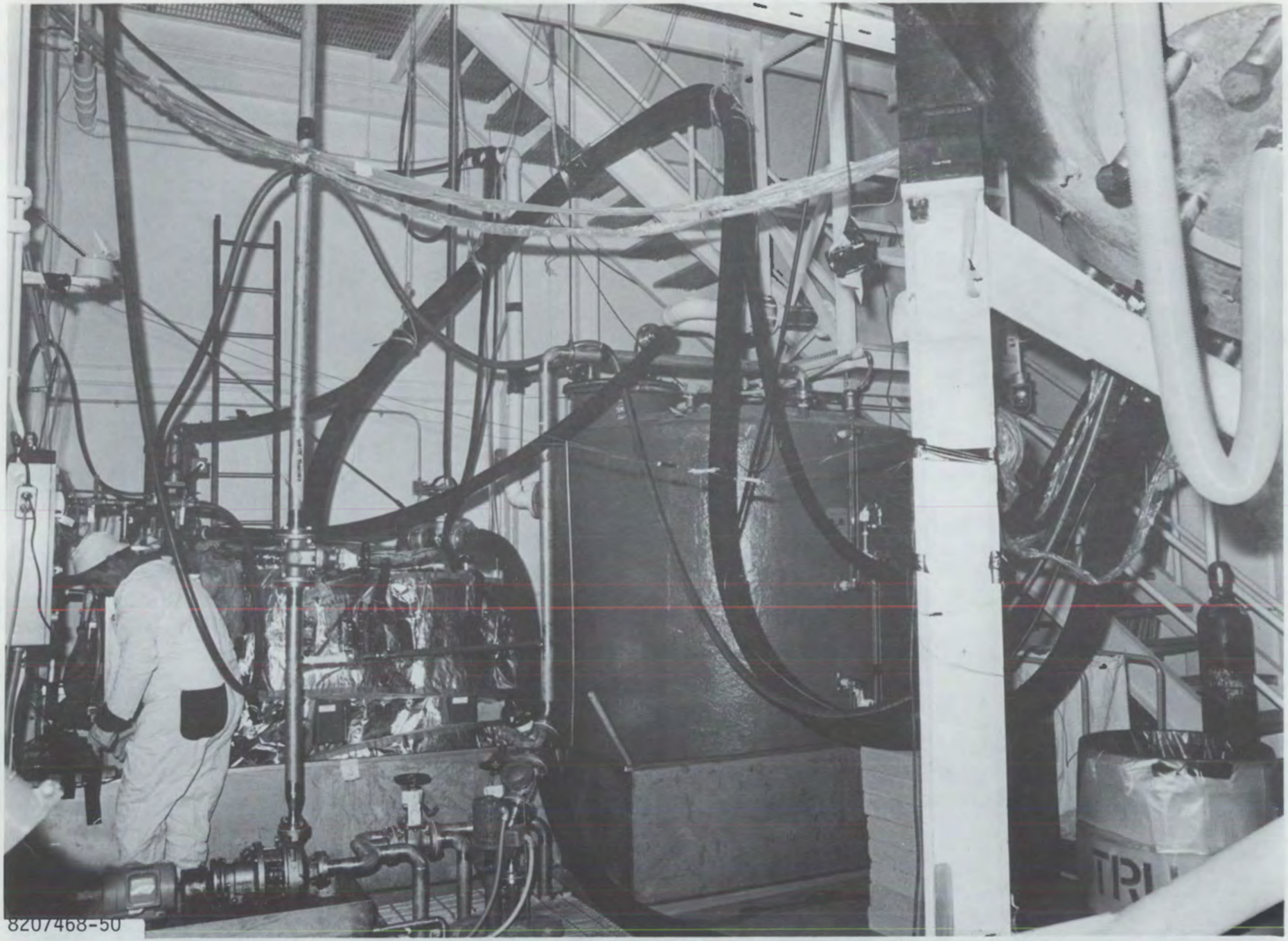

8207468-50

FIGURE 4-5. Overflow Loop Used to Control the Liquid Level in the Channel Head

HOT LEG CONTAMINATION - EFFECT OF PROCESS STEPS ON DISSOLVED METAL CONCENTRATION

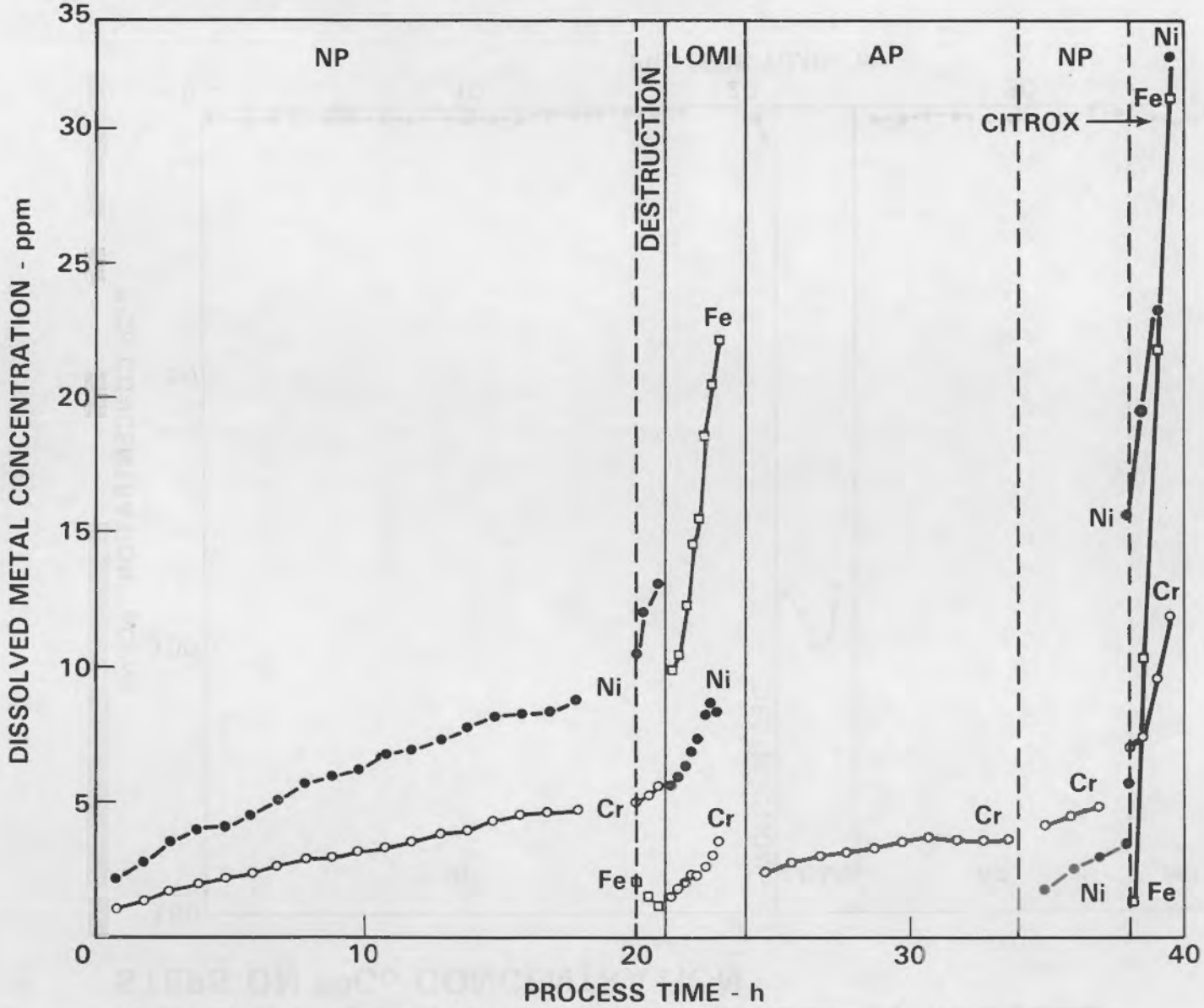

FIGURE 4-6.

HOT LEG DECONTAMINATION - EFFECT OF PROCESS STEPS ON ^{60}Co CONCENTRATION

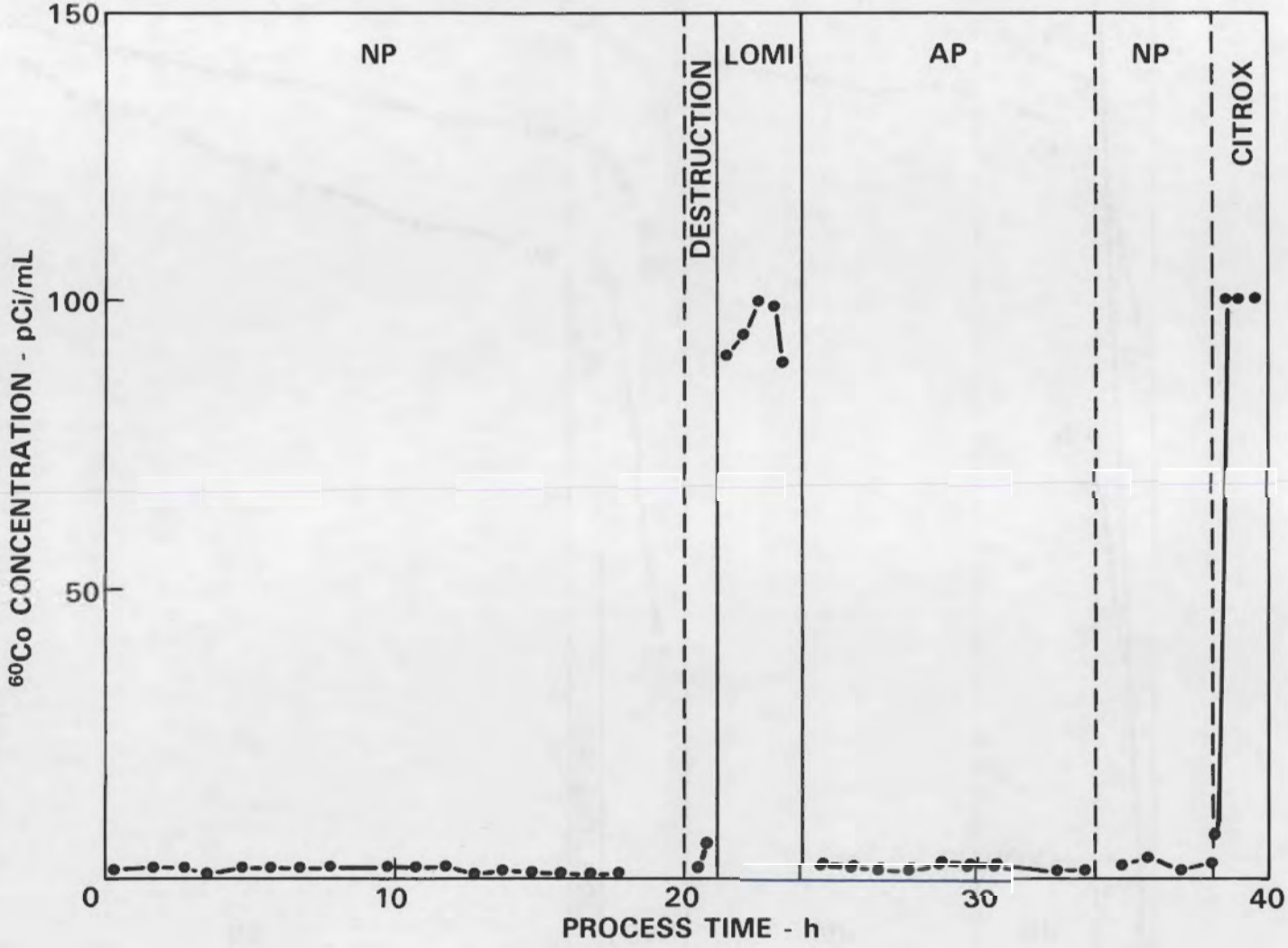

FIGURE 4.7.

hot leg and the cold leg surfaces is attributed primarily to the activity washed out of the tubes during the cold leg decontamination operations.

- Radiation readings - the radiation readings after completion of the hot leg decontamination (including high-pressure water rinse) are shown in Figure 4-8 as a function of position within the channel head. The corresponding change from the pre-decontamination readings is summarized in Figure 4-9. A comparison of the final values for the hot leg and cold leg regions shows that both decontamination processes were equally effective in reducing the internal and surface radiation levels, with the final levels on both sides reflecting the contribution from tube shine.

- Surface appearance - the appearance of the three major surface areas (Inconel 600 tube sheet, Inconel 600 divider plate and 309 stainless steel bowl) is shown before decontamination (Figure 4-10), after the NP/LOMI step (Figure 4-11), and after the AP/POD process (Figure 4-12). The appearance after the high-pressure water rinse operation was essentially unchanged. There was no indication of flow distribution problems. However, there did appear to be more dark surface material left as compared with the cold leg decontamination, although the final surface TLD measurements indicated comparable radiation levels. This residual film was quite adherent immediately after completion of the decontamination and water rinsing operations, but became more smearable with time. A comparison made in mid-February, 1983 gave 100 cm^2 smear values of 5-10 mR/h for the upper divider plate and 4-6 mR/h for the tube sheet on the hot leg side as compared with 2-5 mR/h for the upper divider plate and 3 mR/h for the tube sheet on the cold leg side. The values for the bowl areas were essentially identical.

- Electropolishing operation - as noted in the Quadrex report, the use of in situ electropolishing techniques rapidly and completely removed the contamination from the Inconel surfaces. The 309 stainless steel weld overlay material was more difficult to decontaminate due to the apparent presence of embedded contamination. Figures 4-13 and 4-14 show the in situ electropolishing operation and the resulting cleaned area on the Inconel divider plate.

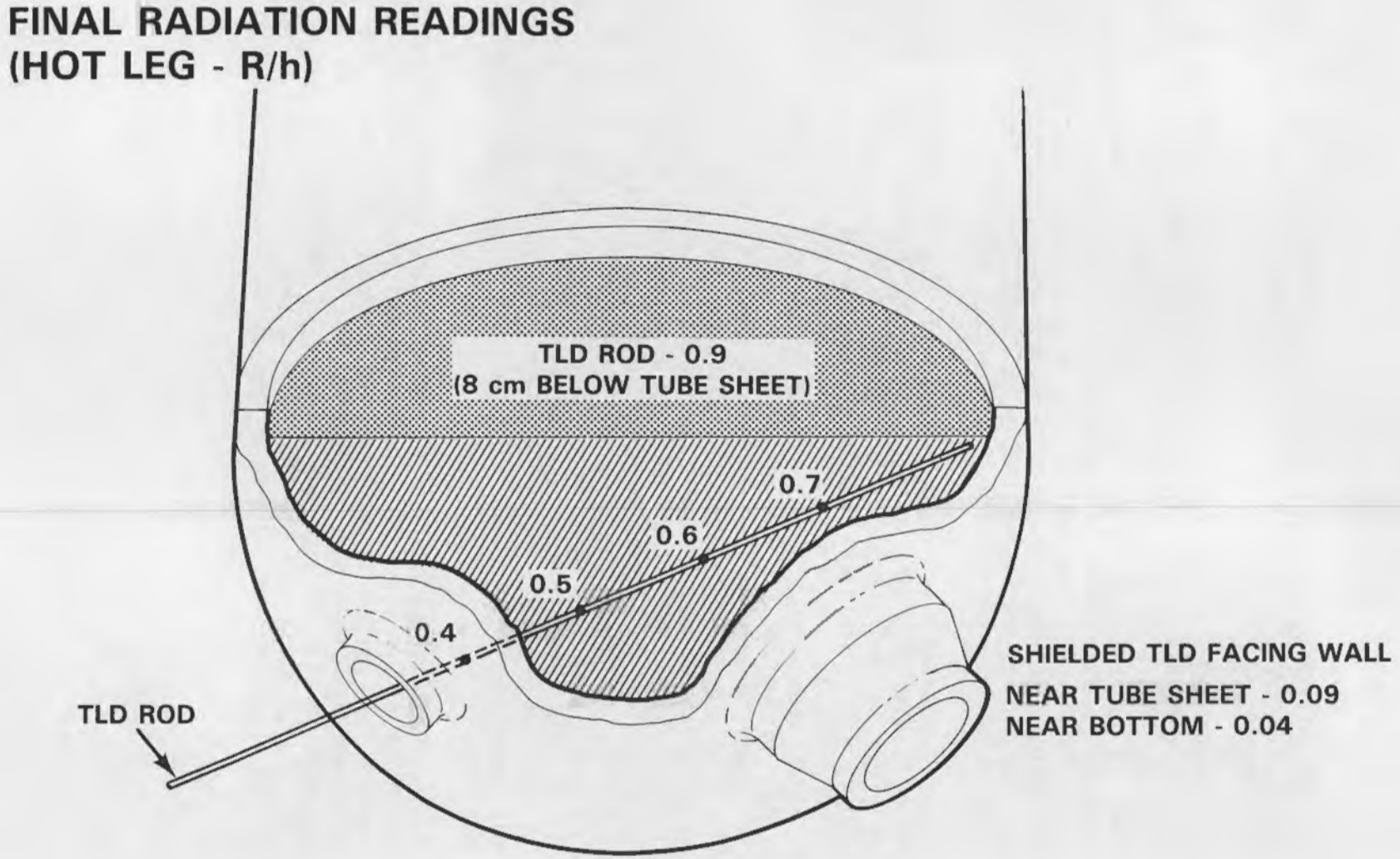
FINAL RADIATION READINGS
(HOT LEG - R/h)
TLD ROD - 0.9
(8 cm BELOW TUBE SHEET)
0.7
0.6
0.5
0.4
TLD ROD
SHIELDED TLD FACING WALL
NEAR TUBE SHEET - 0.09
NEAR BOTTOM - 0.04

FIGURE 4-8.

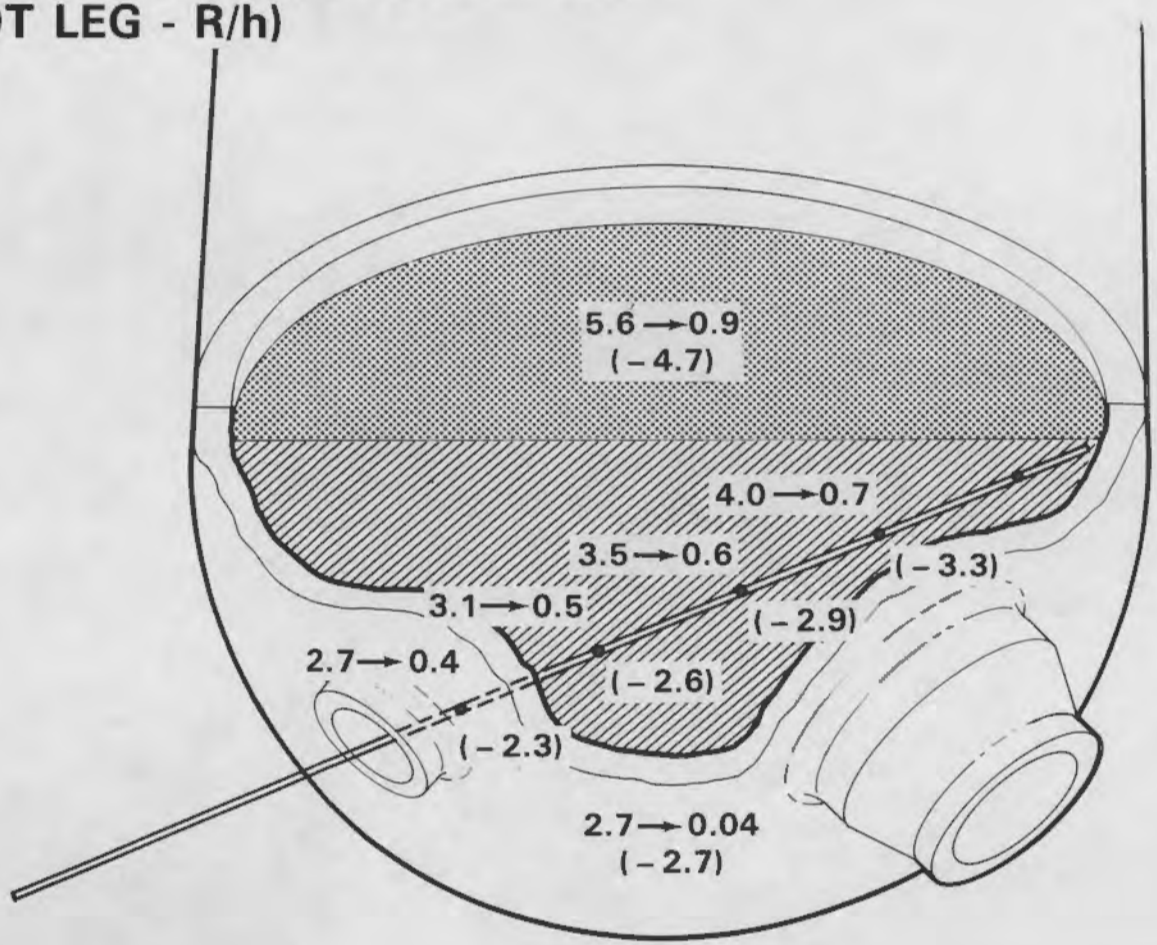
RADIATION READING CHANGE
(HOT LEG - R/h)
5.6 → 0.9
(-4.7)
4.0 → 0.7
3.5 → 0.6
(-3.3)
3.1 → 0.5
(-2.9)
2.7 → 0.4
(-2.6)
(-2.3)
2.7 → 0.04
(-2.7)

FIGURE 4-9.

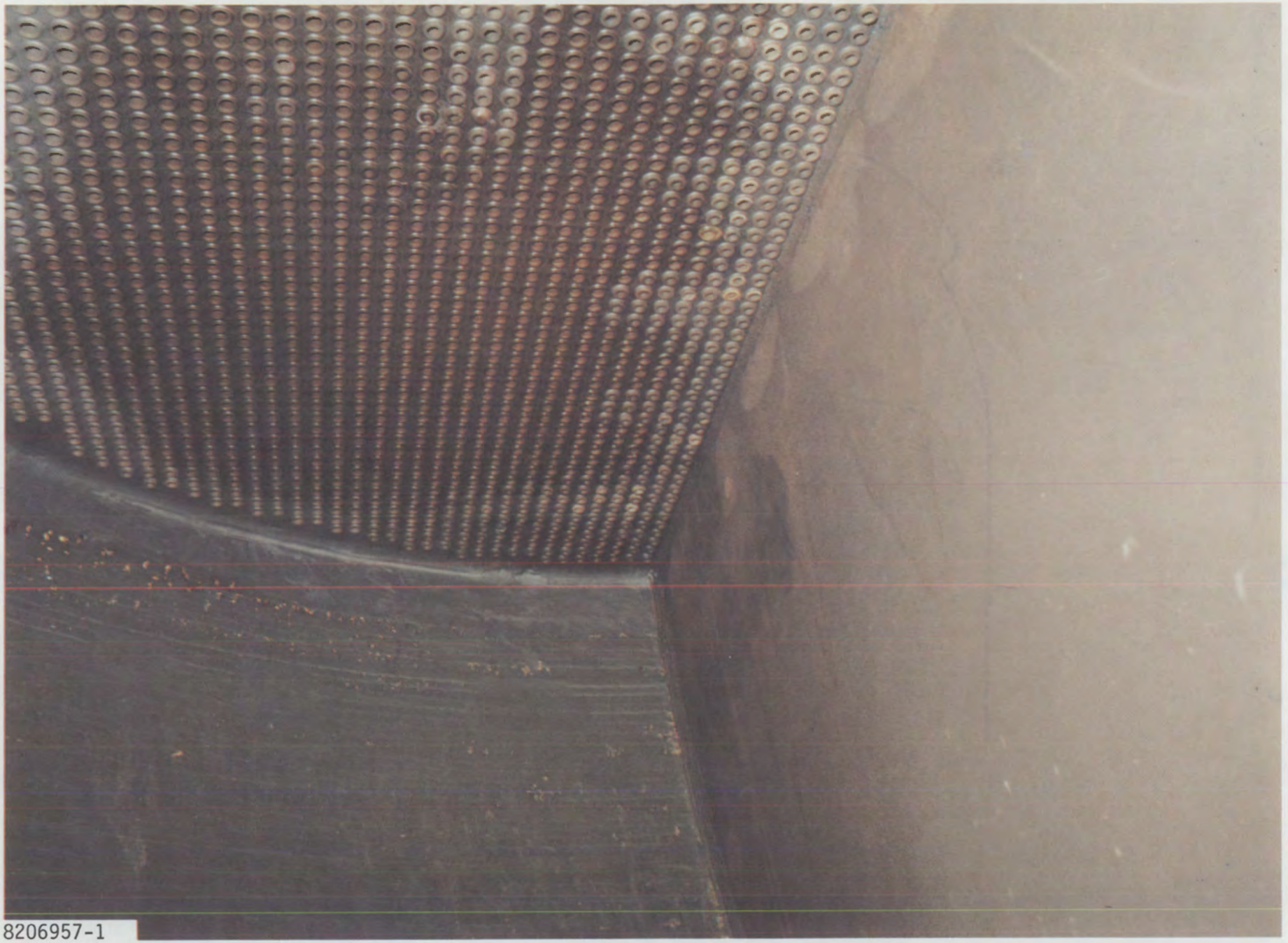

8206957-1

FIGURE 4-10. Hot Leg Surfaces Before Decontamination

8207739-1

FIGURE 4-11. Hot Leg Surfaces After the NP/LOMI Process

8207891-1

FIGURE 4-12. Hot Leg Surfaces After the AP/POD Process

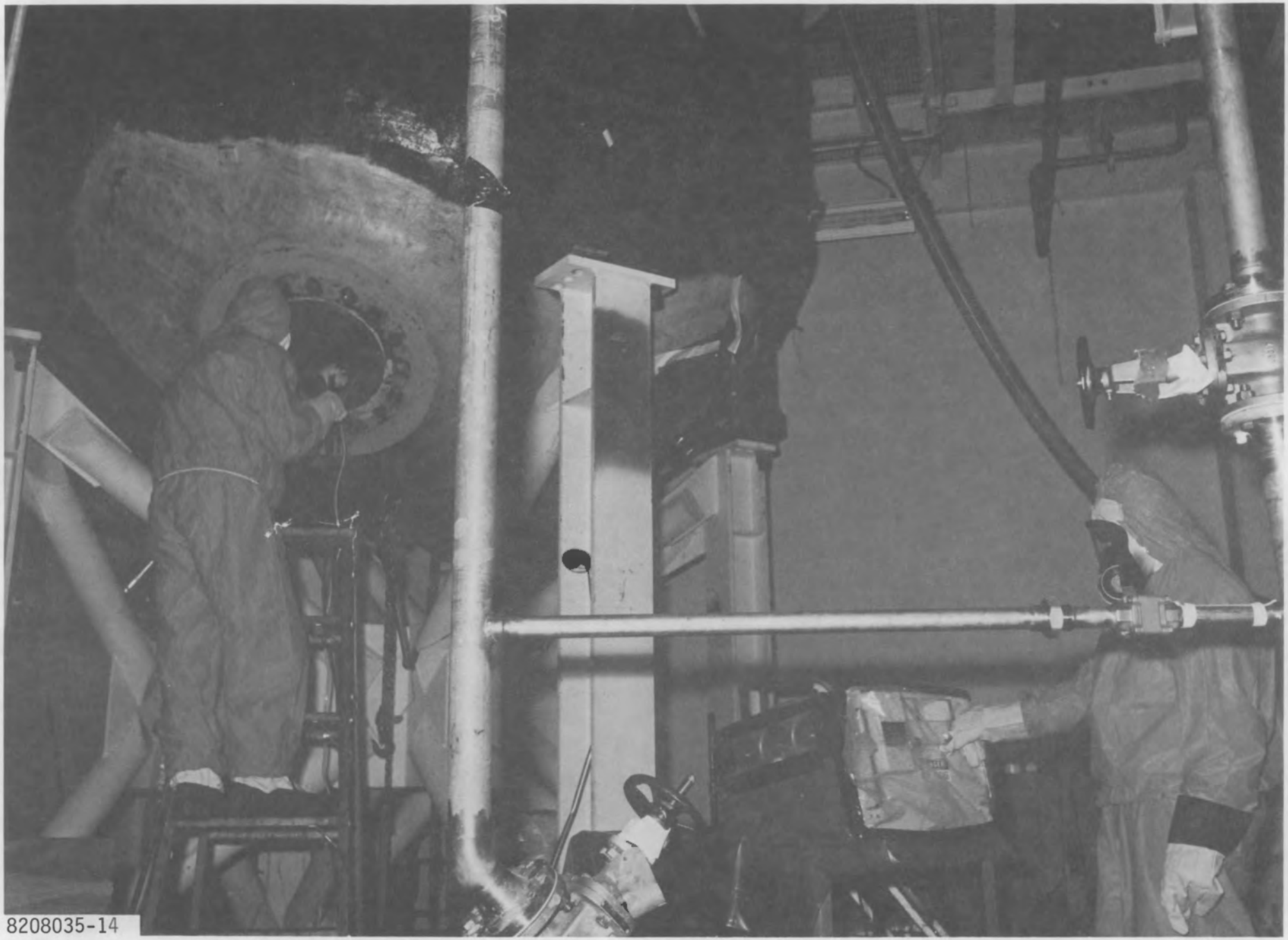

8208035-14

FIGURE 4-13. In Situ Electropolishing Decontamination Operation

8208035-1

FIGURE 4-14. Electropolished Area on the Inconel 600 Divider Plate

5. RADIOLOGICAL MEASUREMENTS

Summary of Conditions Prior to Decontamination

A variety of measurements of the radiation fields in and around the Surry steam generator prior to decontamination served as the basis for assessing the effectiveness of each decontamination technique and, using simple distribution models, allowed calculation of the radionuclide inventory. These measurements are described in the "Interim Topical Report, Steam Generator Group Project, Health Physics - Task 3" (Reece and Hoenes 1983). A summary of the results of the measurements is presented here as an aid to the reader.

Energy spectral measurements made with portable lithium drifted germanium detectors (hand held Ge(Li)) showed Co-60 to be the only detectable gamma emitter. Modeling efforts using the field measurements have shown that the Co-60 inventory is not uniformly distributed in the heat exchanger tubes. Strings of TLD-700's (LiF thermoluminescent dosimeters) inside rigid plastic tubing placed 3 in. under the tube sheet gave readings showing a gamma field which averaged 5.8 R/h, with a low of 5.6 R/h and a high of 6.2 R/h. The gamma fields in the hot and cold legs of the channel head were measured by inserting 10-ft-long plastic tubes with TLD strings through the manways to the far upper corner of the intersection of the bowl and divider plate. This gave a depth profile along the rods ranging from 1.6 to 4.1 R/h in the cold side and from 2.3 to 4.9 R/h in the hot leg side (see Table 5-1 and Figures 5-1 and 5-2).

TABLE 5-1. Comparison of Pre-Decontamination Channel Head Gamma Fields (Depth Profile #1)

Depth Inside Bowl Along Rod (ft)	Cold Leg (R/h)	Hot Leg (R/h)
9	4.1	4.9
8	3.9	4.2
7	3.8	4.0
6	3.7	3.8
5	3.2	3.5
4	3.2	3.2
3	2.8	3.1
2	2.9	2.9
1	3.6	2.7
at manway	1.6	2.3

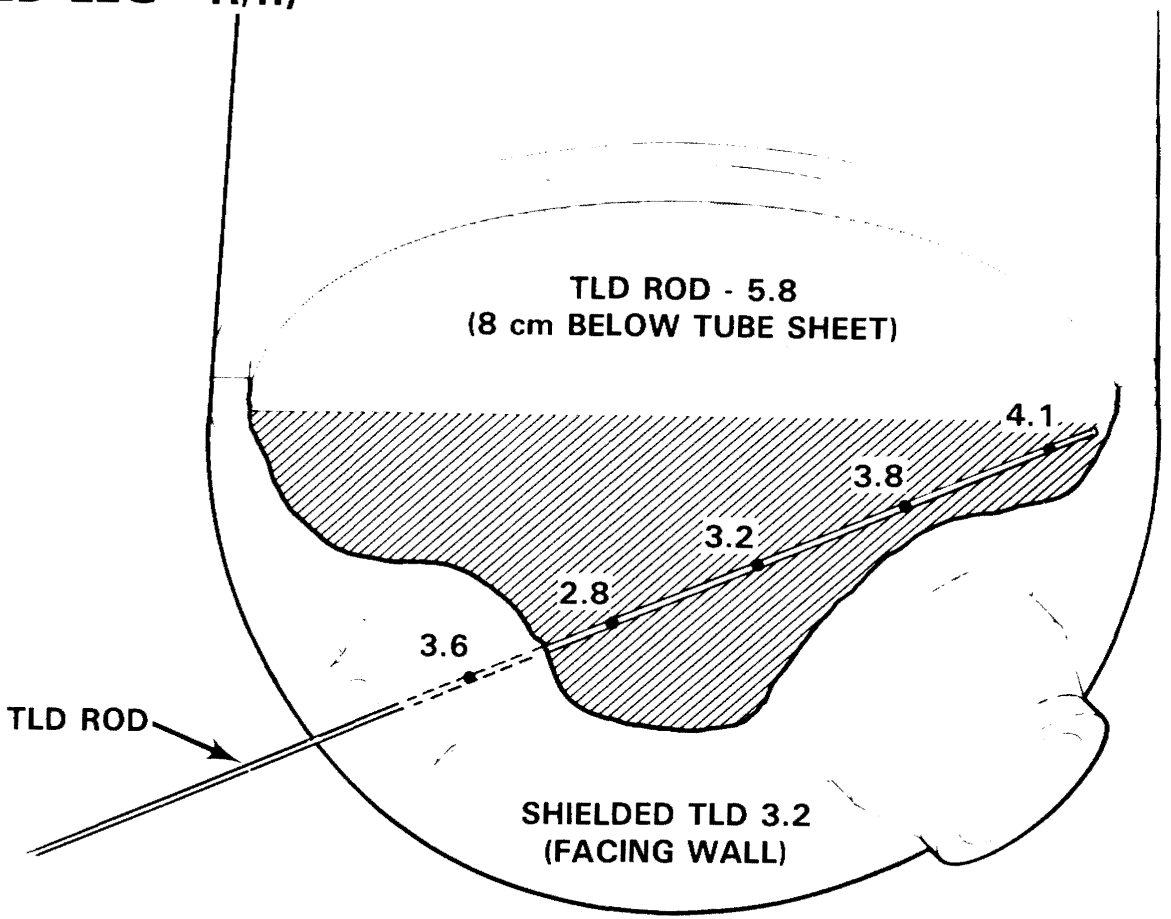
INITIAL RADIATION READINGS
(COLD LEG - R/h)
TLD ROD - 5.8
(8 cm BELOW TUBE SHEET)
4.1
3.8
3.2
2.8
3.6
TLD ROD
SHIELDED TLD 3.2
(FACING WALL)

FIGURE 5-1.

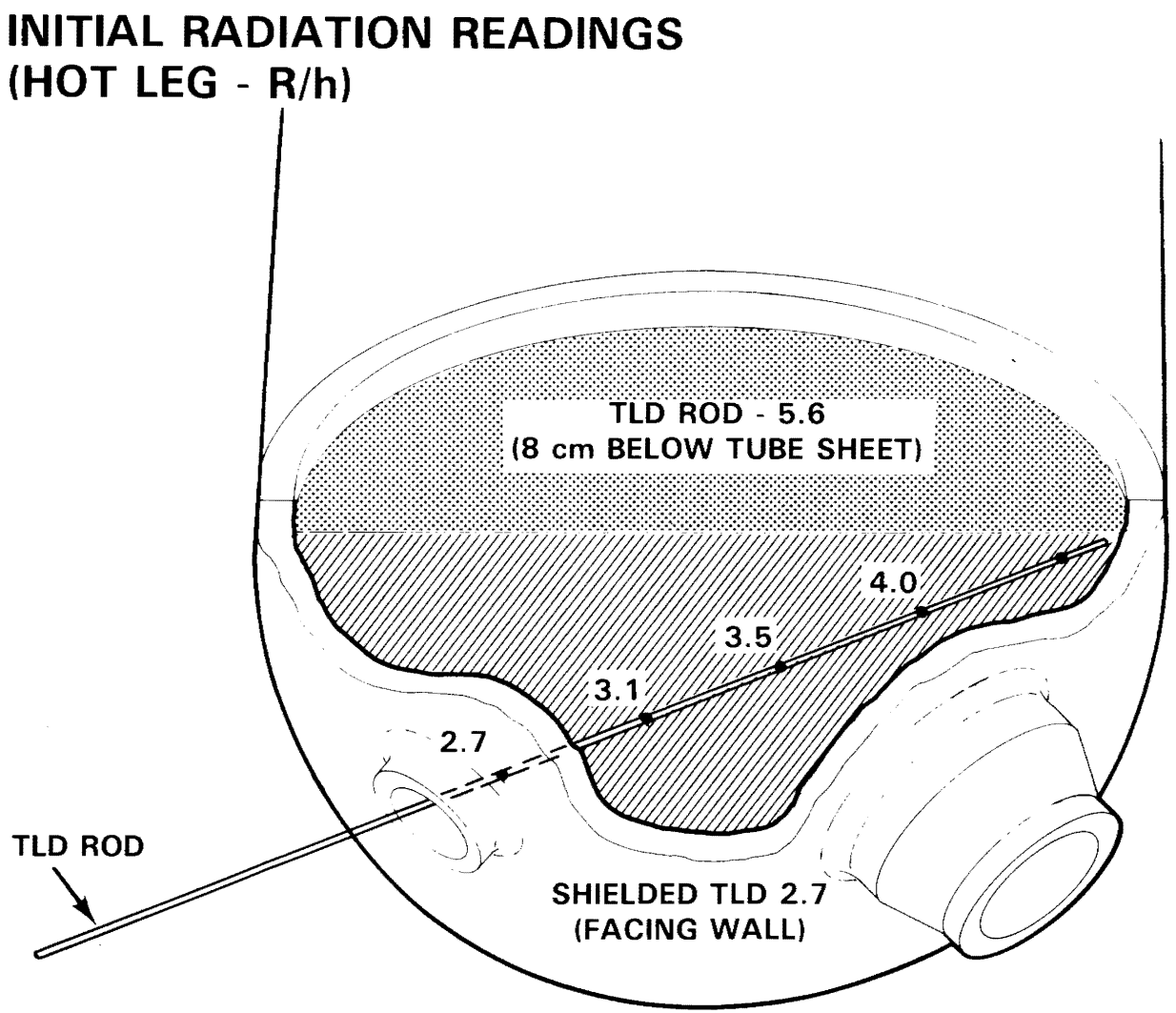
INITIAL RADIATION READINGS
(HOT LEG - R/h)
TLD ROD - 5.6
(8 cm BELOW TUBE SHEET)
4.0
3.5
3.1
2.7
TLD ROD
SHIELDED TLD 2.7
(FACING WALL)

FIGURE 5-2.

A second study of the dose inside the channel head used tubes inserted through the manway up to the intersection of the bowl and the tube sheet at a point directly opposite the divider plate (Figure 5-3). As seen in Table 5-2, the field in this area proved to be slightly higher.

TABLE 5-2. Comparison of Pre-Decontamination Channel Head Gamma Fields (Depth Profile #2)

Depth (ft)	Cold Leg (R/h)	Depth (ft)	Hot Leg (R/h)
6.1	5.2	3.5	6.3
5.1	4.1	3.0	4.7
4.1	3.5	2.0	3.3
3.1	3.2	1.0	2.8
2.1	3.3	0.0	3.5
1.1	3.5		
0.1	2.1		

Lead bricks were used as shields over TLD's to indicate the exposure due to the contamination at one spot on the channel head walls (as opposed to tube shine and other contributions to the general field). The TLD's were taped to a machined insert in the brick and placed dosimeter side down next to the inner channel head surface 1 ft from the manway hole. The average TLD exposure rates using this procedure were:

Hot Leg	2.7 R/h
Cold Leg	3.2 R/h

Swipes of the surface of the channel head produced smear samples having a dose of tens of mrem/h.

Computer codes using simple isotope distribution patterns calculated the Co-60 inventory inside the tubes above the tube sheet to be between 69 and 85 curies. The Co-60 inventory in the channel head was estimated by hand calculations to lie between 1.1 and 1.8 curies for each side of the channel head.

Data Obtained During Decontamination

During each of the decontamination efforts, which are described in detail elsewhere in this report, the process streams were monitored for Co-60. Samples of the process streams were taken periodically (every fifteen minutes being the most frequent) and aliquots were counted using

LOCATION OF TLD STRINGS FOR SECOND STUDY (LOOKING DOWN ON CHANNEL HEAD)

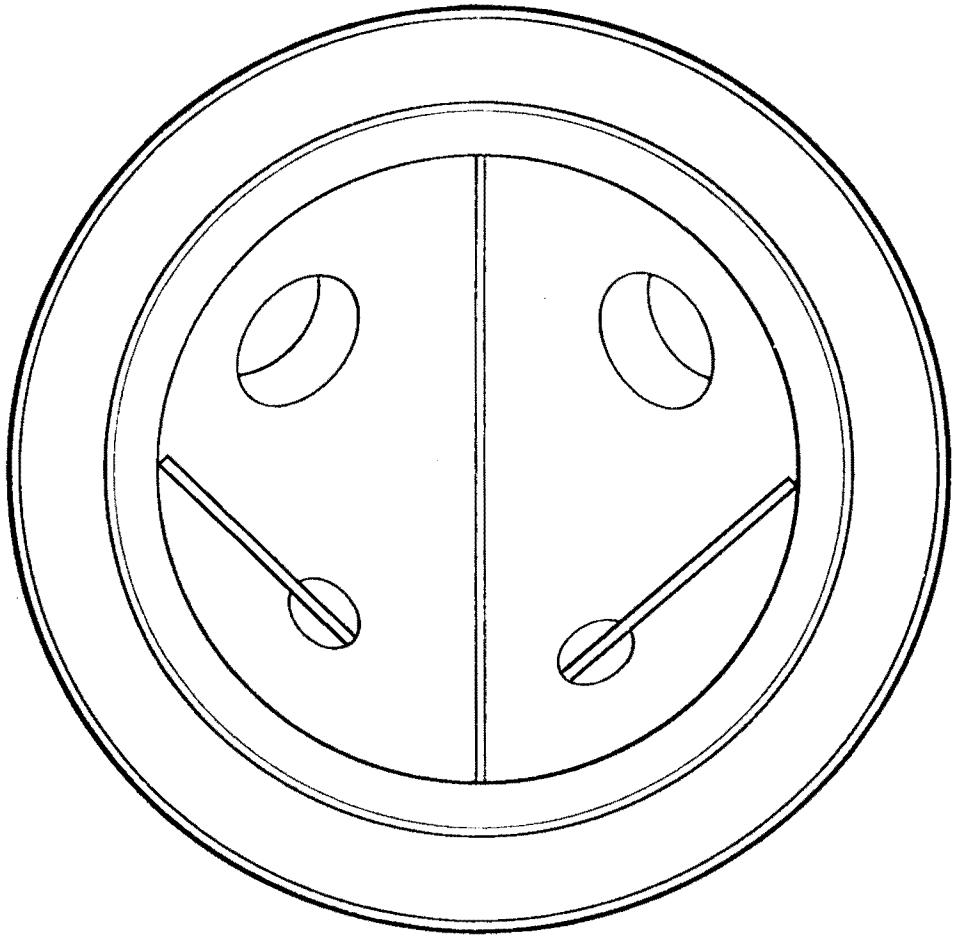

FIGURE 5-3.

a lithium drifted germanium detector previously calibrated against standard solutions of Co-60. Knowing the Co-60 concentration and the volume of the decontamination solution, or flow rates, real-time estimates of the contamination removal and the speed of the attack on the film were possible. Graphs of Co-60 removal during the decontaminations are shown in Figures 5-4 and 5-5.

All personnel entering the radiations zone wore pocket ionization chambers and all doses were tracked during the decontamination processes by individual and by working groups (i.e., crafts, engineers, etc.). Table 5-3 shows exposures by group and calendar quarter during the decontamination efforts. The total exposure to all personnel during London Nuclear's cold leg operation was 9.0 man-rem and 5.4 man-rem during Quadrex's operations on the hot leg. The differences in exposure to the different contractor teams is discussed below.

TABLE 5-3. Personnel Radiation Exposures by Group

	Total Personnel Exposure - man-rem					
	FY-1982				FY-1983	Total
	Q1	Q2	Q3	Q4	Q1	
Engineers & Tech.	0	2.472	0.831	4.351	4.151	11.805
Crafts	0	4.125	0.975	2.933	0.629	8.662
Visitors	0	0.005	0.079	0.093	0	0.177
London Nuclear*	0	0	0	1.600	0	1.600
Quadrex**	0	0	0	0.020	0.634	0.654
Totals/qtr.	0	6.602	1.885	8.997	5.414	22.898

*Cold Leg Decontamination
**Hot Leg Decontamination

During decontamination of both legs of the channel head, interim measurements of the radiation field in the channel head were made to determine the degree of decontamination following one cycle of decontamination solutions. In both cases one decontamination cycle was insufficient (i.e., both the surface decontamination factor and the general field decontamination factor were less than ten) and another cycle was initiated.

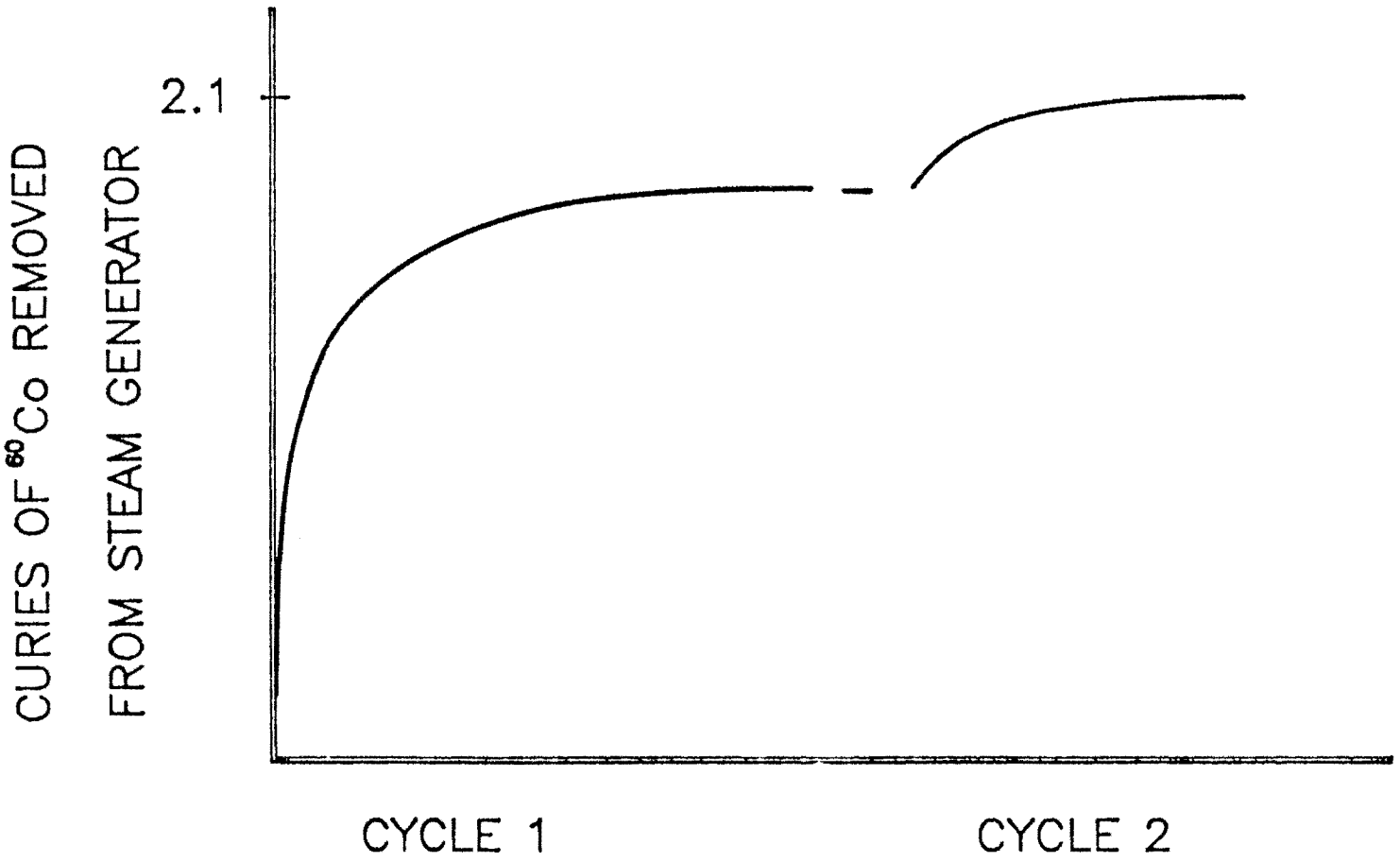

FIGURE 5-4. Cobalt-60 Removal During the Cold Leg Decontamination

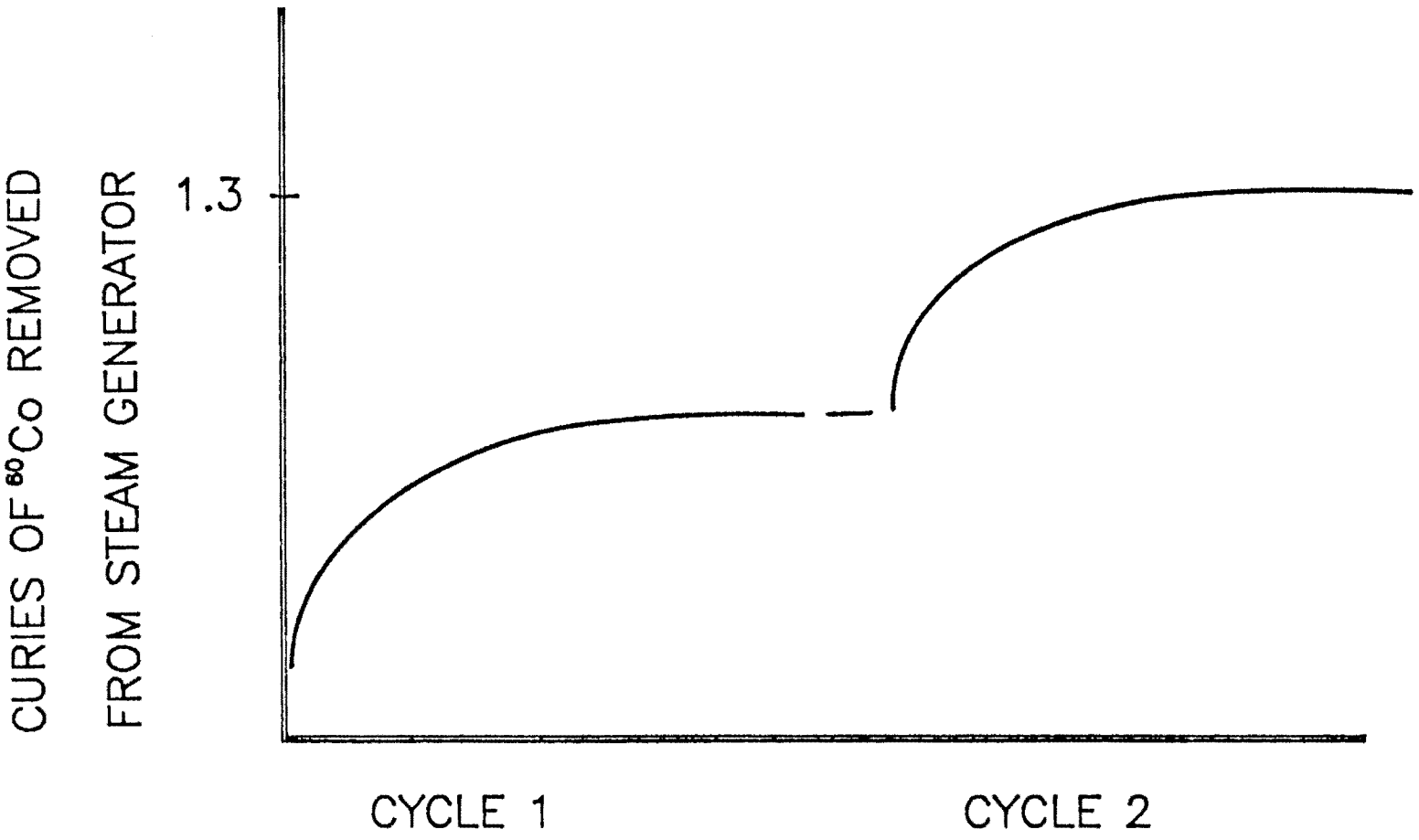

FIGURE 5-5. Cobalt-60 Removal During the Hot Leg Decontamination

Measurements Following Decontamination

After each of the decontamination procedures by London Nuclear or Quadrex and high-pressure water washes by Battelle staff, several types of measurements were taken to determine the strength of the radiation field remaining, and its distribution on the walls on each side of the channel head. As before, TLD-700 dosimeters inside a rigid plastic tube were inserted through the manway openings and also suspended 3 in. below the tube sheet to measure the gamma field. A summary of these measurements is given in Tables 5-4 and 5-5. Four lead bricks with dosimeters attached were placed in the channel head, two bricks with dosimeters facing up and two with dosimeters facing down to get a measure of tube shine/backscatter. Results of these exposures are shown in Table 5-6.

The high reading of the lead-shielded dosimeter facing down in the cold leg side may reflect its position near the bottom of the bowl. To check this, lead bricks with single pockets for encapsulated TLD chips were propped up at various heights within the hot and cold legs. A single brick for beta measurement was also placed inside each leg. The shielded dosimeters were exposed for 66 to 68 h. Results of this exposure in the cold leg amounted to 30 mR/h to 51 mR/h on the sides. A single shielded dosimeter placed on the outlet cover, which appeared to have a heavy oxide film, produced a reading of 413 mR/h. This may have been due to redeposition of Co-60 from the decontamination solution onto the cover. The four shielded dosimeters placed along the wall on the hot side varied from 40 mR/h to 168 mR/h. The bricks included for beta measurement were exposed less than two hours and any exposures due to beta were below the error of the measurement. These results are summarized in Table 5-7. As can be seen, the beta component of the radiation field contributes a negligible amount to the dose received by the TLD chip.

Since the London Nuclear decontamination of the cold leg side of the channel head collected more Co-60 than calculations indicated could be present in the channel head, further measurements were made above the tube sheet to determine possible changes in the Co-60 inventory in the tubes due to refluxing as discussed in Section 3. Rigid plastic tubes containing strings of TLD-700 dosimeters were inserted through shell penetrations P-1 and P-4 into the interstices between tubes on the secondary side (see Figure 5-6 for the location of the penetrations through the shell). As seen in Table 5-8, the field across the steam generator at the height of the P-1 penetration dropped by approximately 25%. The field near the top of the steam generator at the P-4 penetration remained unchanged (see Table 5-9). Figures 5-7 and 5-8 show the data graphically. Using simple models for distribution of the Co-60 in the tubes, this change in the field represents the loss of 0.5 to 1.2 curies from the tubes.

TABLE 5-4. Cold Leg Radiation Field Measurements (R/h)

	Before Decon	After Decon by Subcontractor	After High-Pressure Water Wash	After Hot Leg Decon
2-ft Rods (3 in. below tube sheet)				
Right	6.2	2.1	2.2	
	5.8	2.7	2.8	
	5.6	2.8	2.7	
	5.7	2.3	2.4	
	5.6	1.9	1.8	
Average	5.8	2.4	2.4	
Left	5.7	1.7	1.6	
	5.8	2.3	2.0	
	5.9	2.5	2.3	
	5.6	2.2	2.1	
	5.7	1.8	1.6	
Average	5.7	2.1	1.9	
10-ft Rods (inserted through manway)				
10	--	1.2	--	--
9-1/2	3.6	--	--	--
9	4.1	1.4	--	--
8-1/2	3.9	--	1.3	0.56
8	3.9	1.3	1.4	0.65
7-1/2	3.9	--	1.4	0.68
7	3.8	1.3	1.4	0.65
6-1/2	3.7	--	1.2	0.58
6	3.7	1.2	1.1	0.58
5-1/2	3.4	--	1.1	0.53
5	3.2	1.2	1.0	0.55
4-1/2	3.2	--	1.0	0.55
4	3.2	1.1	1.0	0.52
3-1/2	3.0	--	0.99	0.51
3	2.8	1.1	0.95	0.52
2-1/2	3.0	--	0.94	0.49
2	2.9	1.1	0.88	0.47
1-1/2	3.0	--	0.85	0.43
1	3.6	0.84	0.84	0.41
1/2	2.3	--	0.79	0.41
0	1.6	0.28	0.74	0.40

Lead Brick	Before Decon	Interim	After Decon	After Water Wash	After Hot Leg Decon
Down	3.2	1.2	0.55	0.70	0.64
Down		1.5	0.55	0.81	
Up			0.64	0.47	0.30

TABLE 5-5. Hot Leg Radiation Field Measurements (R/h)

	Before Decon	After LP-LOMI	After AP-Citrox	After High-Pressure Water Wash
2-ft Rods (3 in. below tube sheet)				
Right		3.2	0.81	
		3.2	0.84	
		3.1	0.99	
		3.3	0.97	
		3.4	0.79	
Average		3.2		
Left		3.2	0.82	
		3.1	0.90	
		3.1	1.1	
		2.9	0.93	
		3.0	0.77	
Average		3.1		
10-ft Rods (inserted through manway)				
10		2.2		
9	4.9	2.1		
	4.3			0.62
8	4.2	1.8	0.78	0.80
	4.3		0.78	0.76
7	4.0	1.7	0.73	0.68
	3.4		0.69	0.65
6	3.8	1.6	0.65	0.62
	3.6		0.66	0.61
5	3.5	1.4	0.61	0.60
	3.5		0.62	0.58
4	3.2	1.3	0.57	0.57
	3.2		0.55	0.54
3	3.1	1.2	0.52	0.50
	3.0		0.49	0.46
2	2.9	1.1	0.44	0.52
	2.9		0.41	0.39
1	2.7	0.76	0.36	0.35
	3.4		0.34	0.34
0	2.3		0.31	0.33
Lead Bricks				
Down	2.7	1.1	0.052	
		1.2		
Up		0.42	0.33	

TABLE 5-6. Lead-Brick-Shielded TLD Measurements (Bowl Bottom)

	mR/h	
Cold Leg		
Dosimeter facing up	301	
Dosimeter facing down	637	(see text)
Hot Leg		
Dosimeter facing up	333	
Dosimeter facing down	52	

TABLE 5-7. Lead-Brick-Shielded TLD Measurements (Bowl Sides)

	mR/h	
Cold Leg		
Sample 1	413	
Sample 2	51	
Sample 3	30	
Sample 4	35	
Beta Sample	64	vs. 51 beta + gamma
Hot Leg		
Sample 1	168	
Sample 2	82	
Sample 3	102	
Sample 4	40	
Beta Sample	75	vs. 82 beta + gamma

To determine the distribution of the fields remaining in the channel head, strings of TLDs were encased in plastic and hung from various tubes by inserting rubber stoppers with the string attached into the tubes. Dosimeters placed at 6 in. increments gave readings recorded by position in the channel head from 0 to 60 in. from the bottom of tube sheet (Figures 5-9 through 5-19). The average exposure rates and ranges for each level are listed in Table 5-10:

SHELL PENETRATION LOCATIONS ON SURRY STEAM GENERATOR

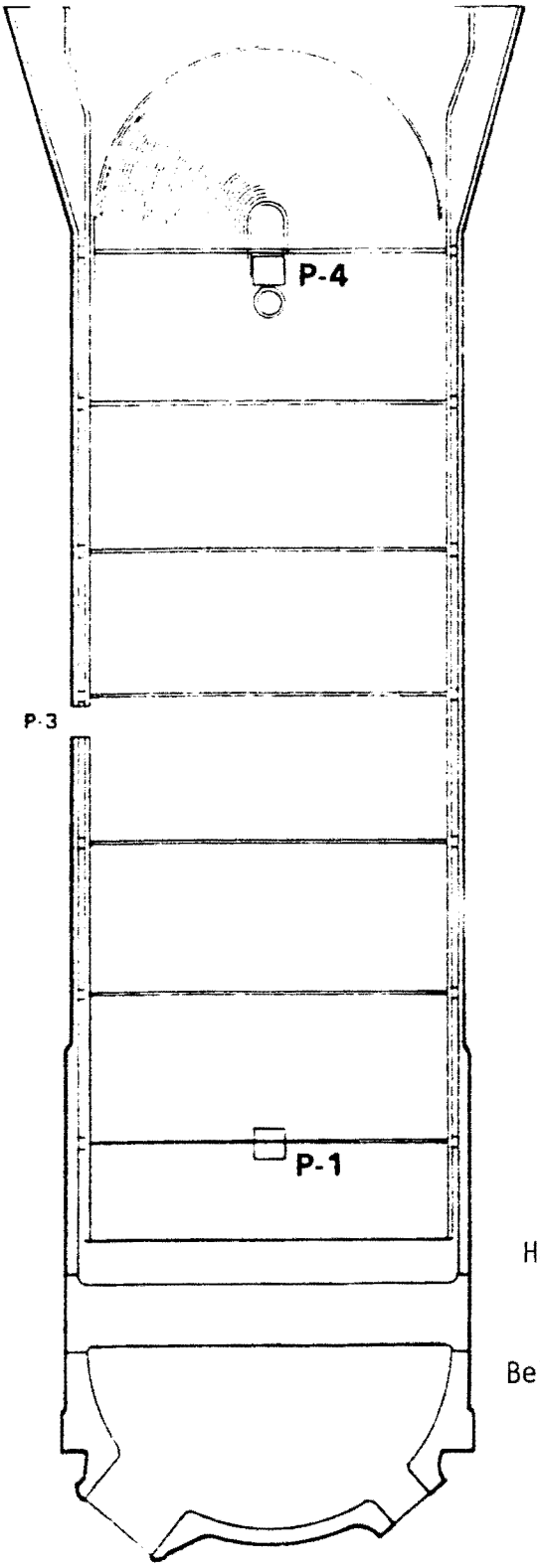

FIGURE 5-6.

TABLE 5-8. Dose Rates Across Steam Generator at P-1 Penetration (Corrected for decay of Co-60 to 1/1/83)

Distance Inside Steam Generator (measured from P-1 opening) -in.	Before Decon (R/h)	Distance Inside Steam Generator (measured from P-1 opening) -in.	After Decon (R/h)
3	3.3	0	0.5
9	5.3	6	1.1
15	7.3	12	2.4
21	9.0	18	4.8
27	9.8	24	6.2
33	9.7	30	7.1
39	9.2	36	7.2
45	9.8	42	6.9
51	9.8	48	7.1
57	9.0	54	7.3
63	8.5	60	6.9
69	8.0	66	6.8
75	8.8	72	5.9
81	8.2	78	6.5
87	8.8	84	6.5
93	8.2	90	6.6
99	8.6	96	6.7
105	9.1	102	6.6
		108	7.1

TABLE 5-9. Dose Rates Across Steam Generator at P-4 Penetration (Corrected for decay of Co-60 to 1/1/83)

Distance Inside Steam Generator (measured from P-4 opening) -in.	Before Decon (R/h)	Distance Inside Steam Generator (measured from P-4 opening) -in.	After Decon (R/h)
5	3.1	0	0.2
11	5.9	6	4.3
17	7.5	12	6.4
23	9.2	18	8.3
29	8.7	24	9.4
35	9.4	30	9.5
41	9.0	36	9.5
47	9.5	42	9.8
53	9.8	48	10.0
59	9.4	54	9.6
65	9.4	60	9.4
71	9.0	66	9.6
77	9.1	72	9.1
83	8.9		

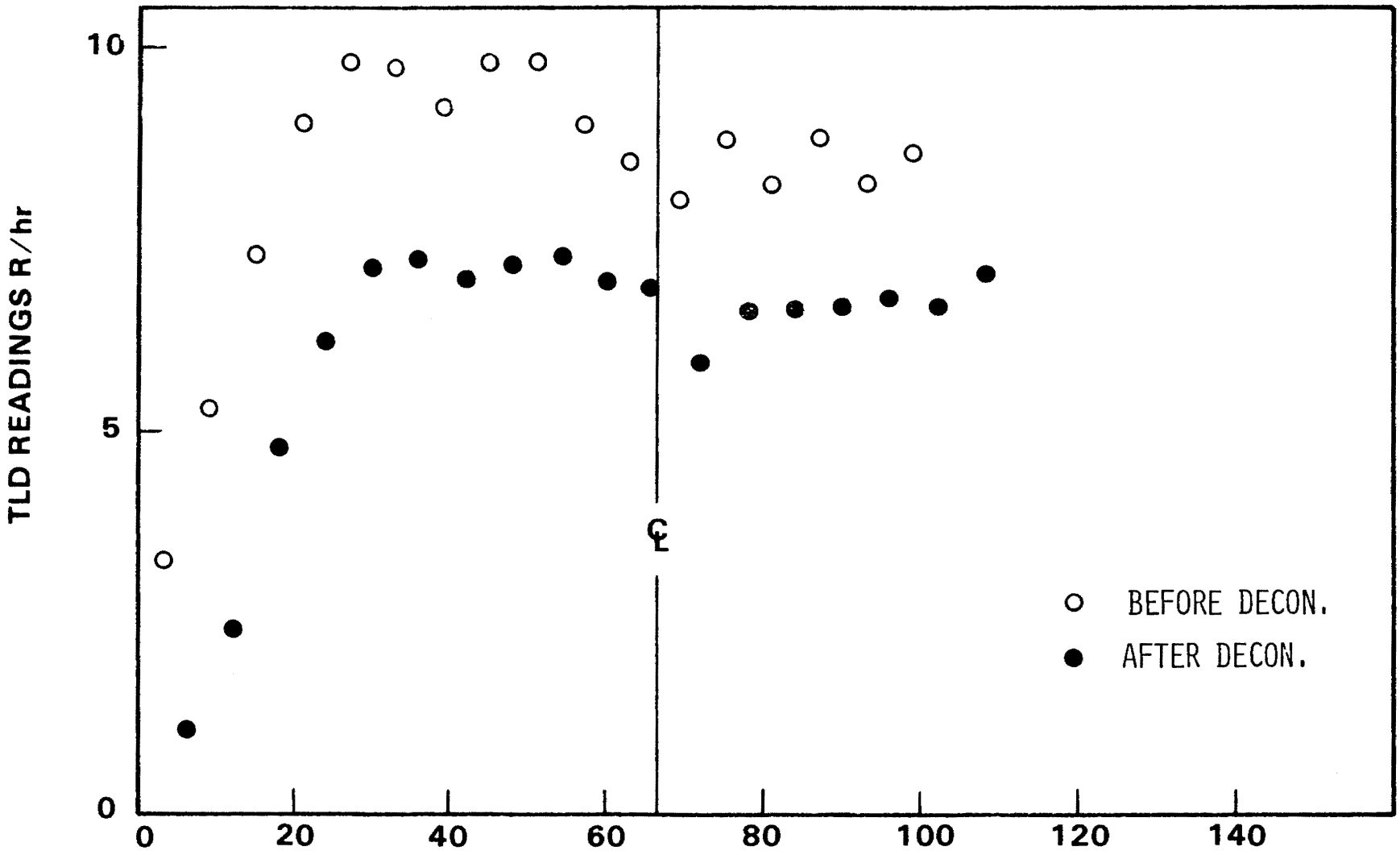

FIGURE 5-7. Pre- and Post-Decontamination Field Versus Distance Inside From the P-1 Penetration

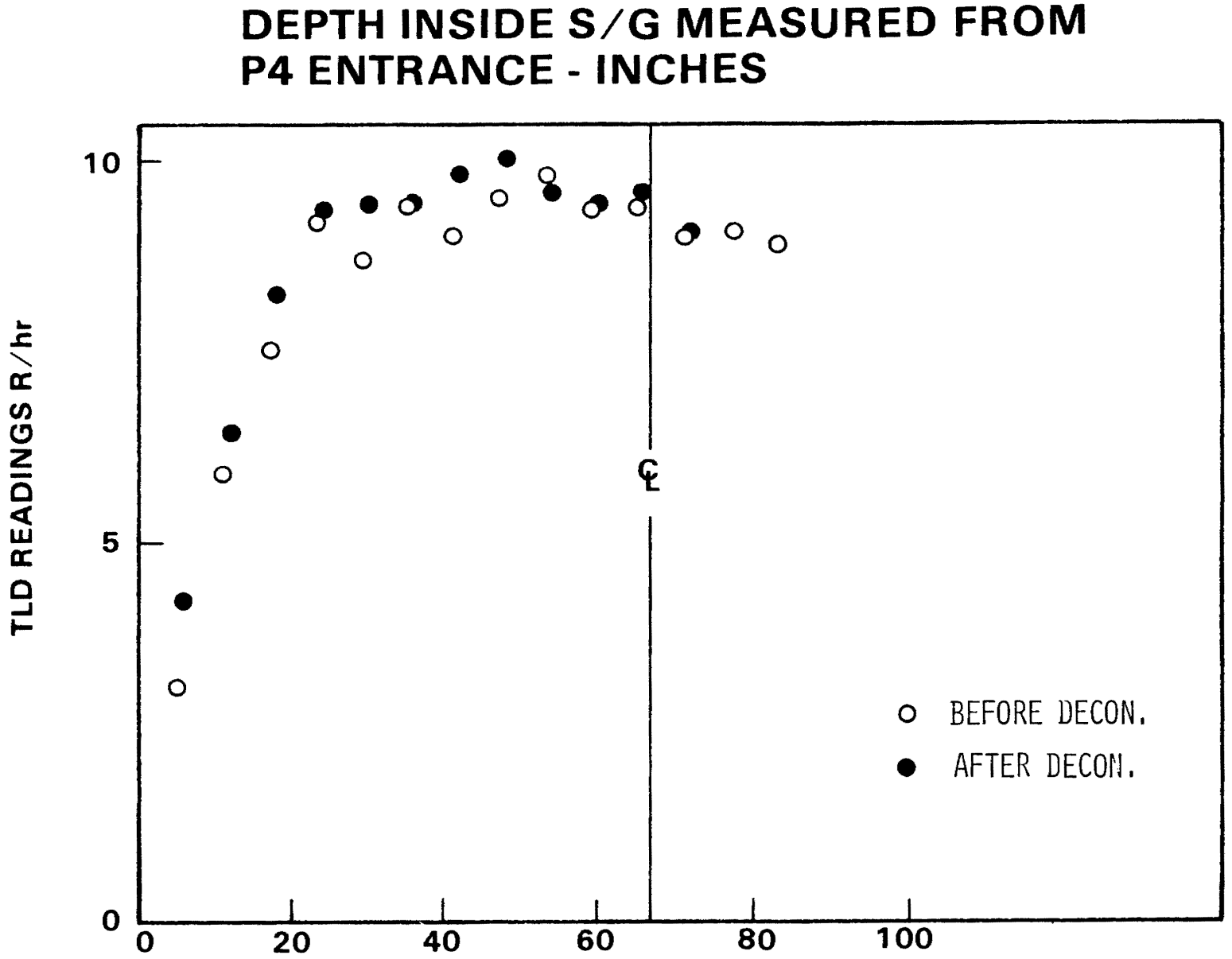

FIGURE 5-8. Pre- and Post-Decontamination Field Versus Distance Inside From the P-4 Penetration

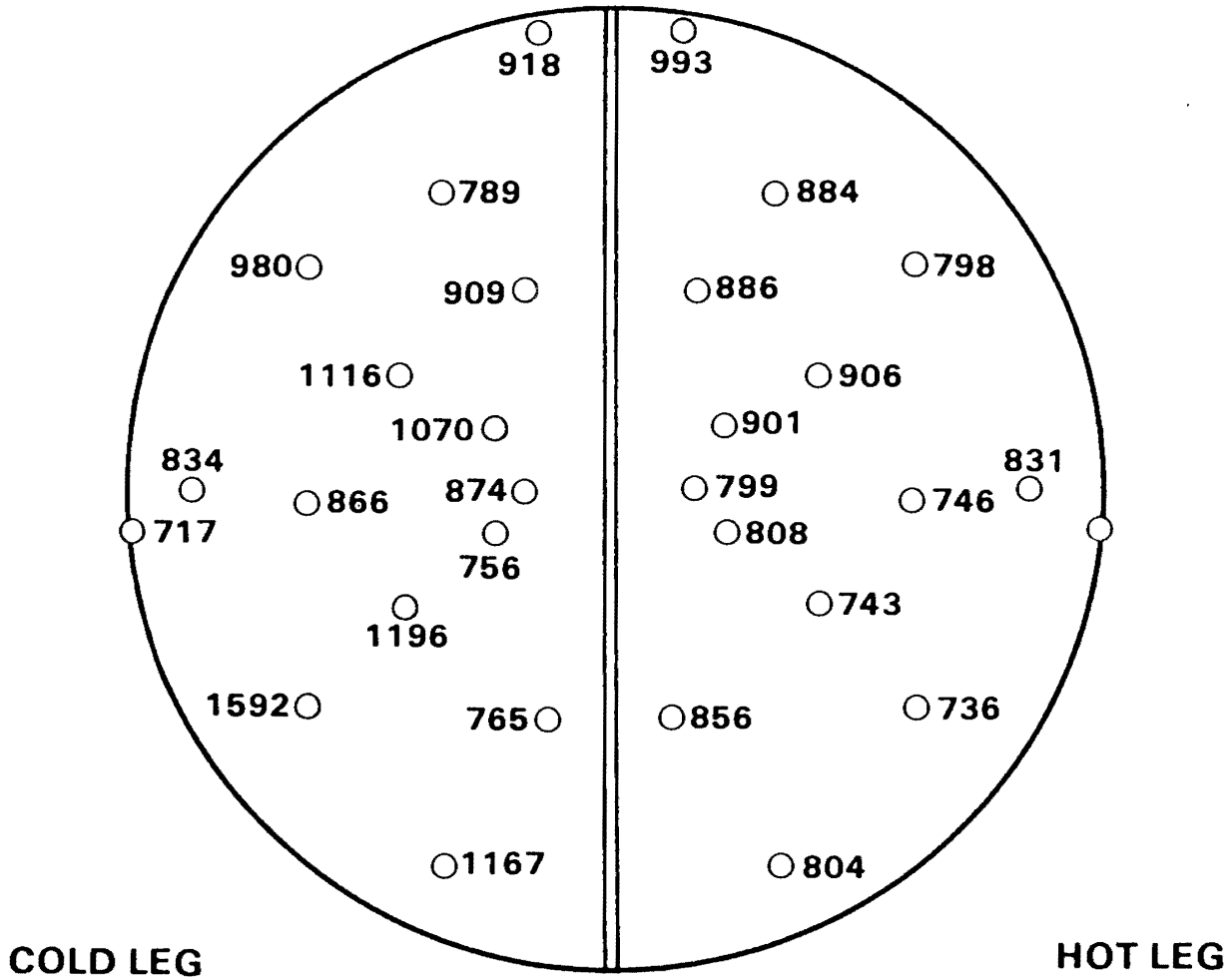
DOSE RATE (mR/hr) IN CHANNEL HEAD
0 INCHES FROM TUBE SHEET
918
993
789
884
980
798
909
886
1116
906
1070
901
834
831
866
874
799
746
717
808
756
743
1196
1592
765
856
736
1167
804
COLD LEG
HOT LEG

FIGURE 5-9.

DOSE RATE (mR/hr) IN CHANNEL HEAD 6 INCHES FROM TUBE SHEET

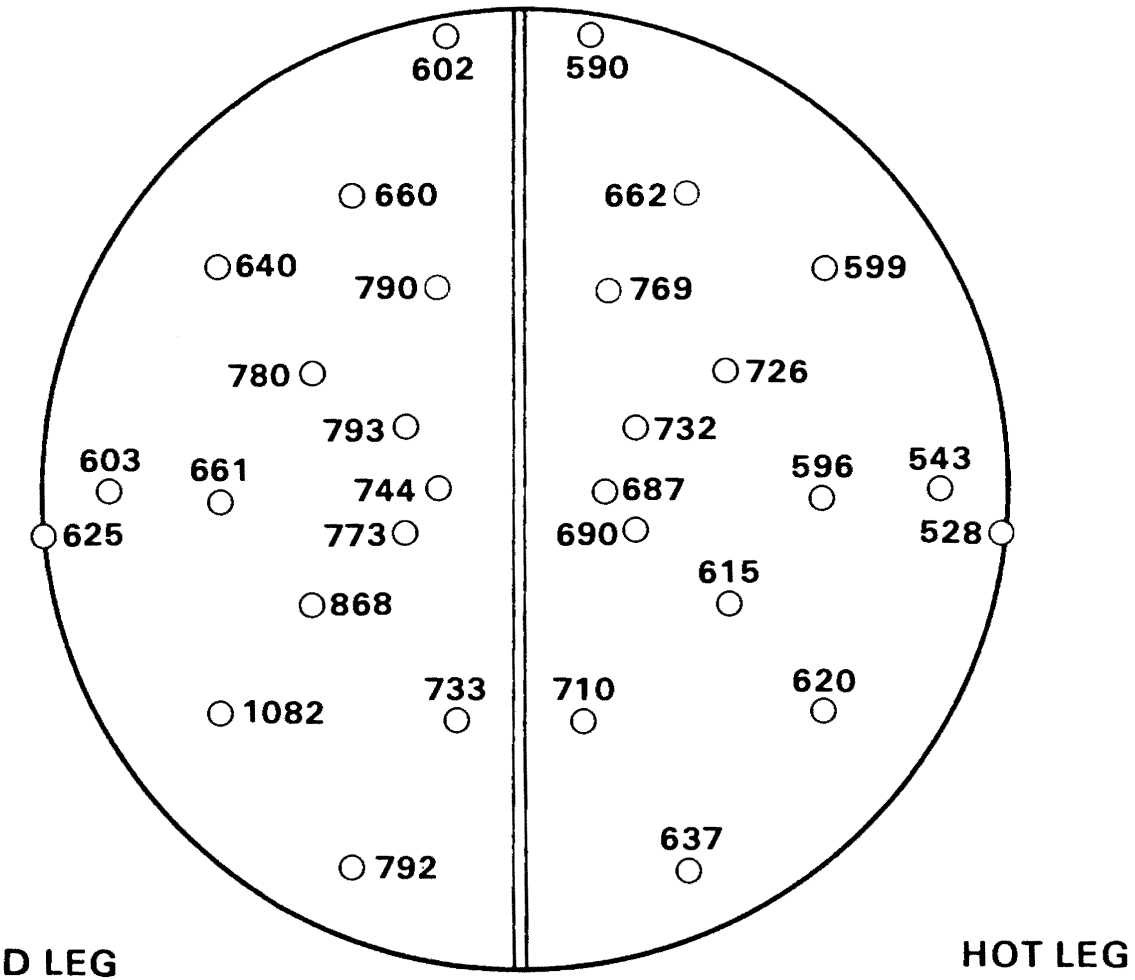

FIGURE 5-10.

DOSE RATE (mR/hr) IN CHANNEL HEAD 12 INCHES FROM TUBE SHEET

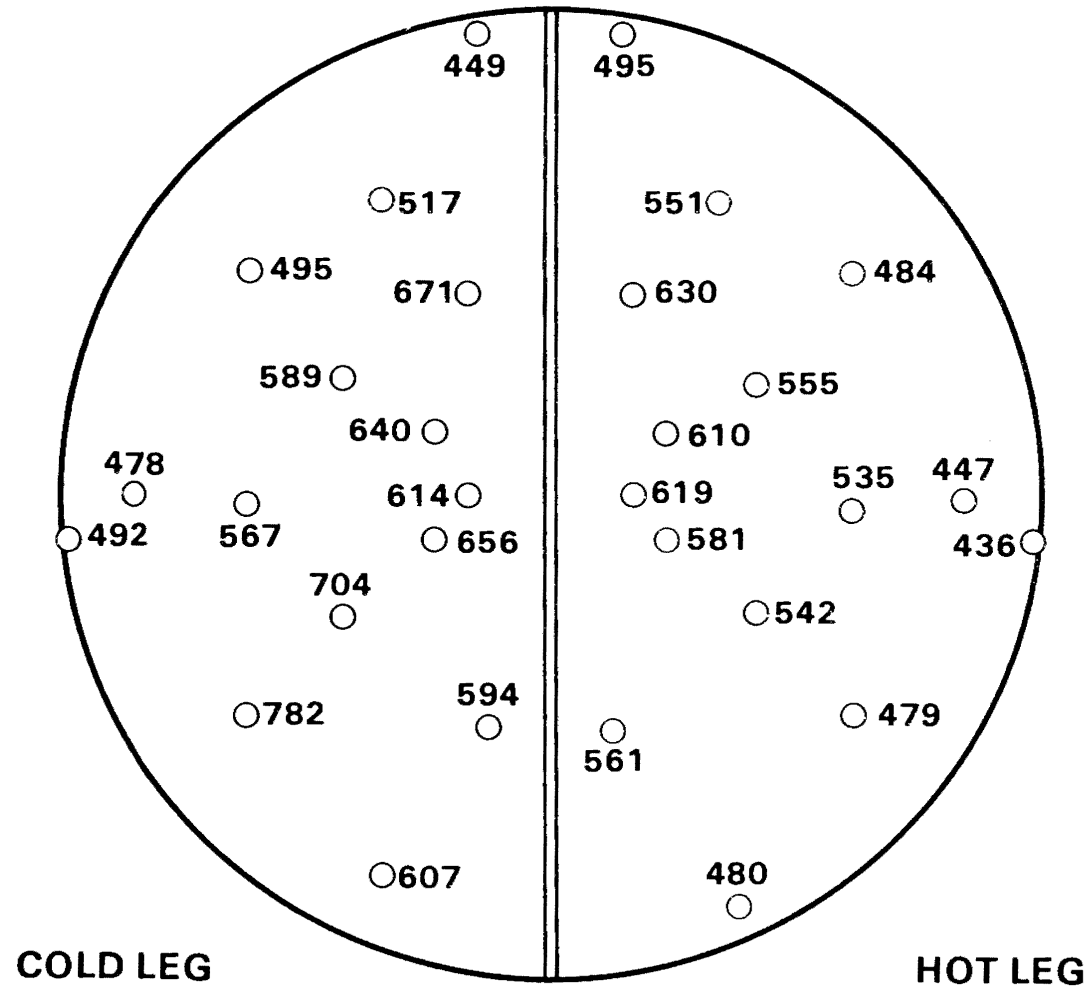

FIGURE 5-11.

DOSE RATE (mR/hr) IN CHANNEL HEAD 18 INCHES FROM TUBE SHEET

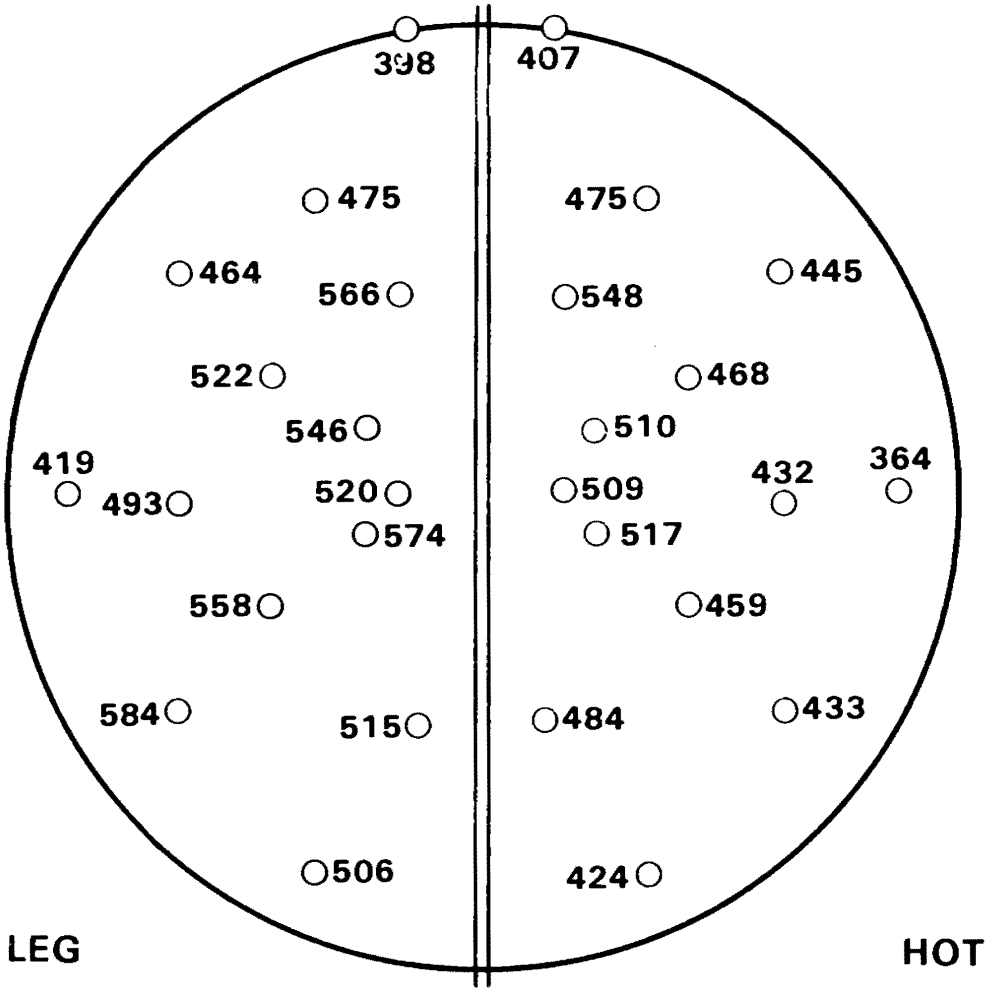

FIGURE 5-12.

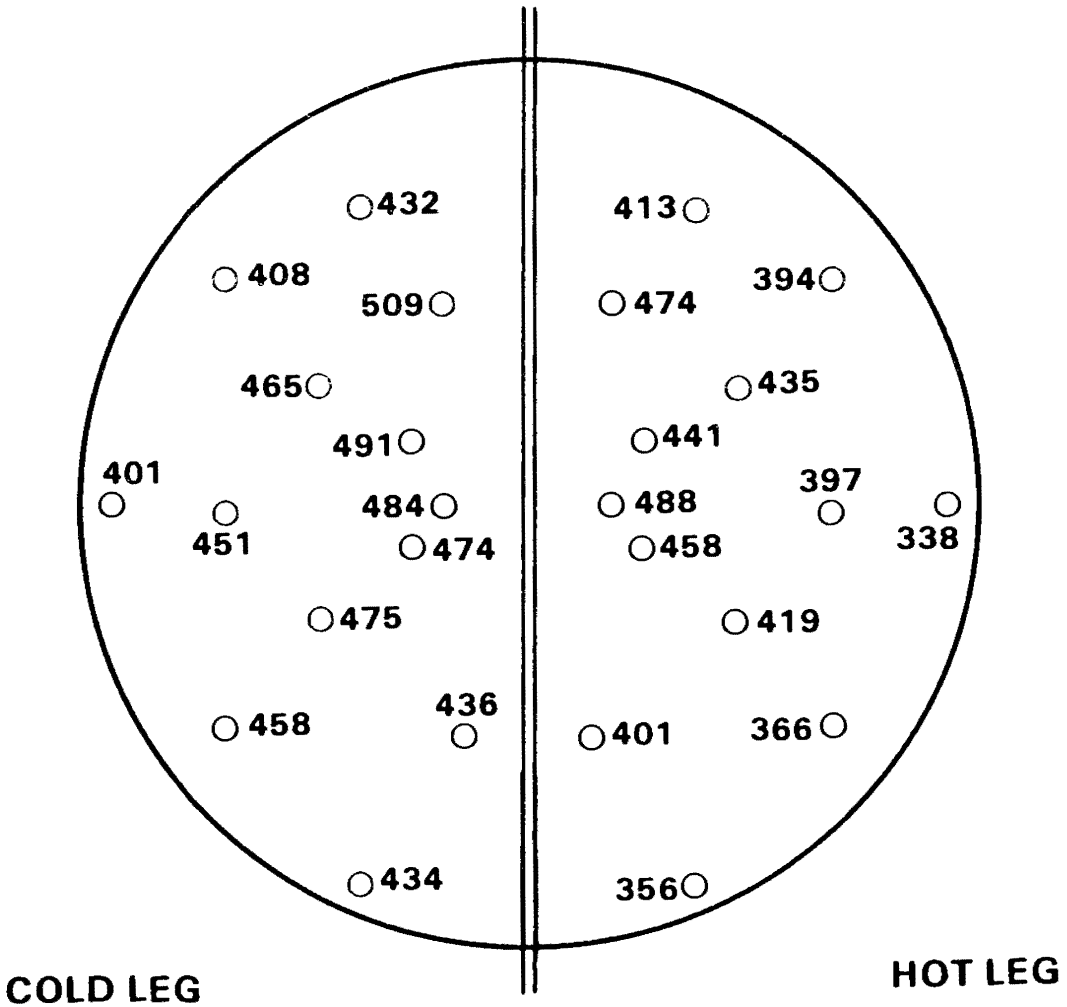
DOSE RATE (mR/hr) IN CHANNEL HEAD
24 INCHES FROM TUBE SHEET
432
408
509
465
491
401
484
451
474
475
458
436
434
413
394
474
435
441
397
488
338
458
419
401
366
356
COLD LEG
HOT LEG

FIGURE 5-13.

DOSE RATE (mR/hr) IN CHANNEL HEAD 30 INCHES FROM TUBE SHEET

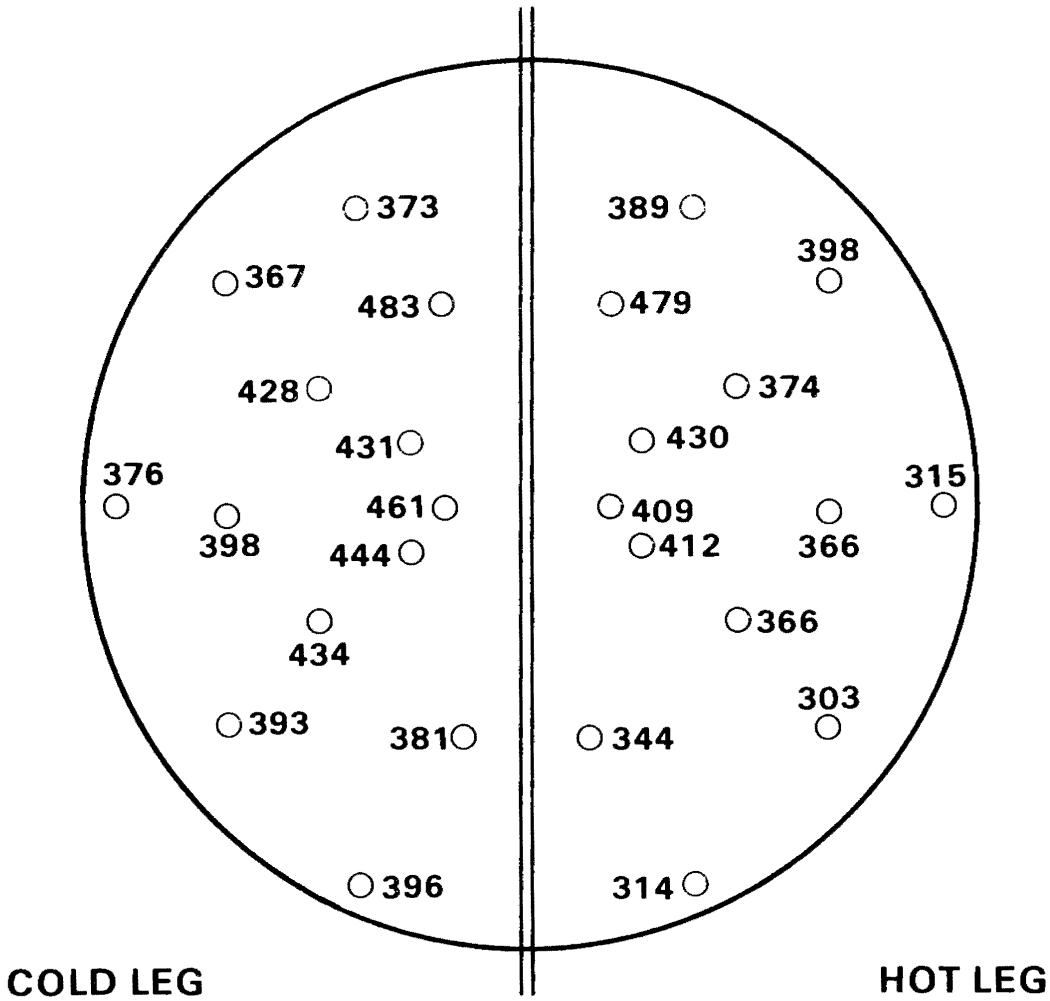

FIGURE 5-14.

DOSE RATE (mR/hr) IN CHANNEL HEAD 36 INCHES FROM TUBE SHEET

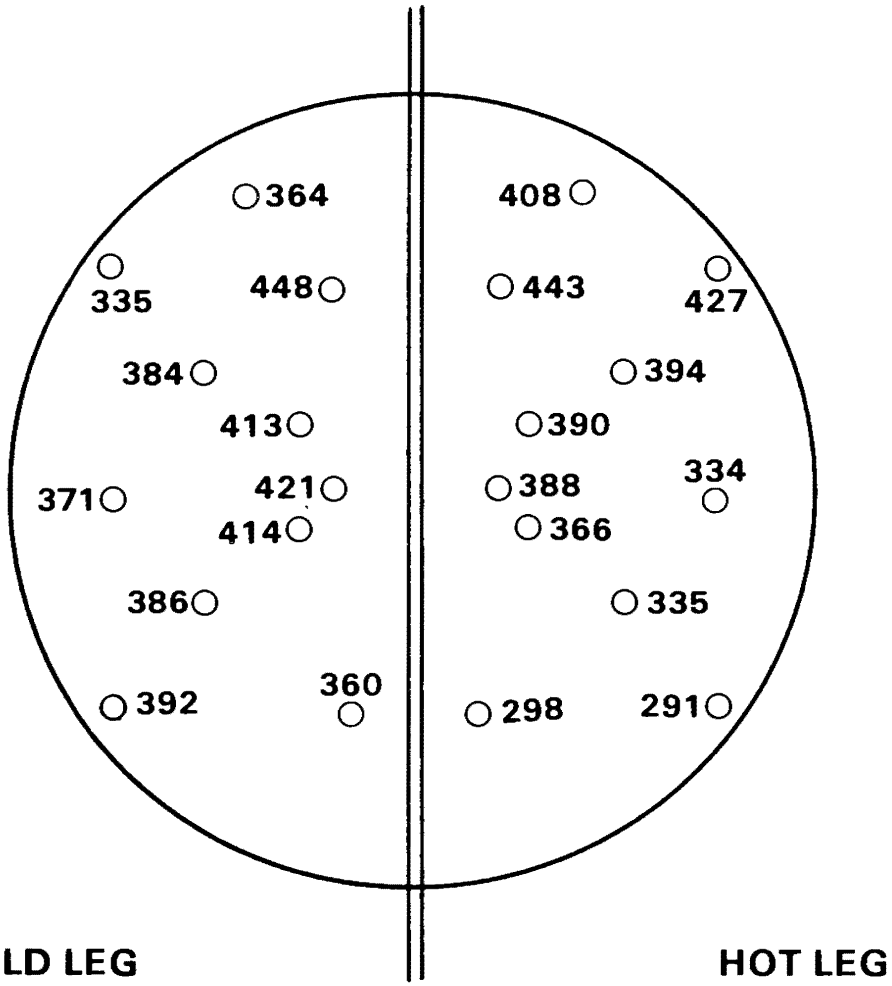

FIGURE 5-15.

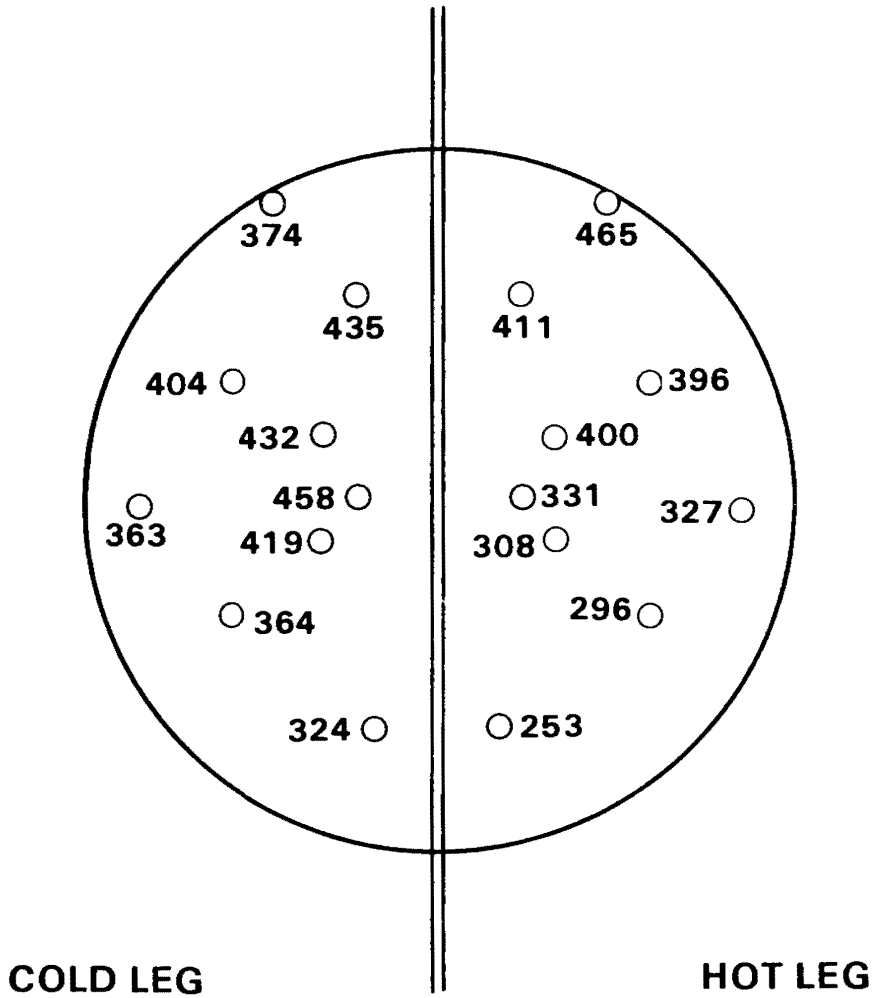
DOSE RATE (mR/hr) IN CHANNEL HEAD
42 INCHES FROM TUBE SHEET
374
465
435
411
404
396
432
400
458
331
327
363
419
308
364
296
324
253
COLD LEG
HOT LEG

FIGURE 5-16.

DOSE RATE (mR/hr) IN CHANNEL HEAD 48 INCHES FROM TUBE SHEET

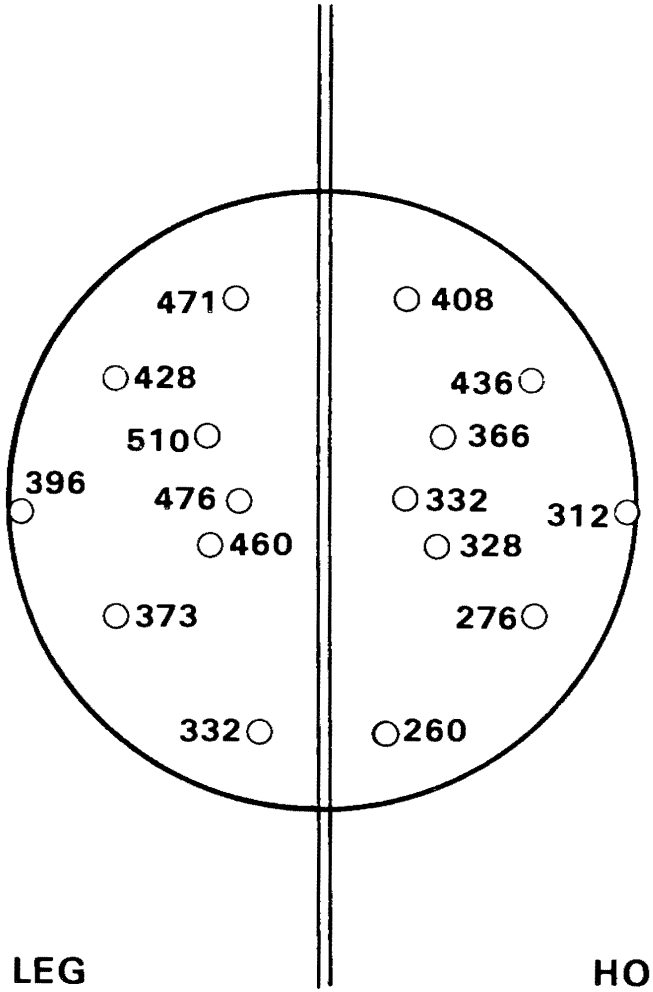

FIGURE 5-17.

DOSE RATE (mR/hr) IN CHANNEL HEAD 54 INCHES FROM TUBE SHEET

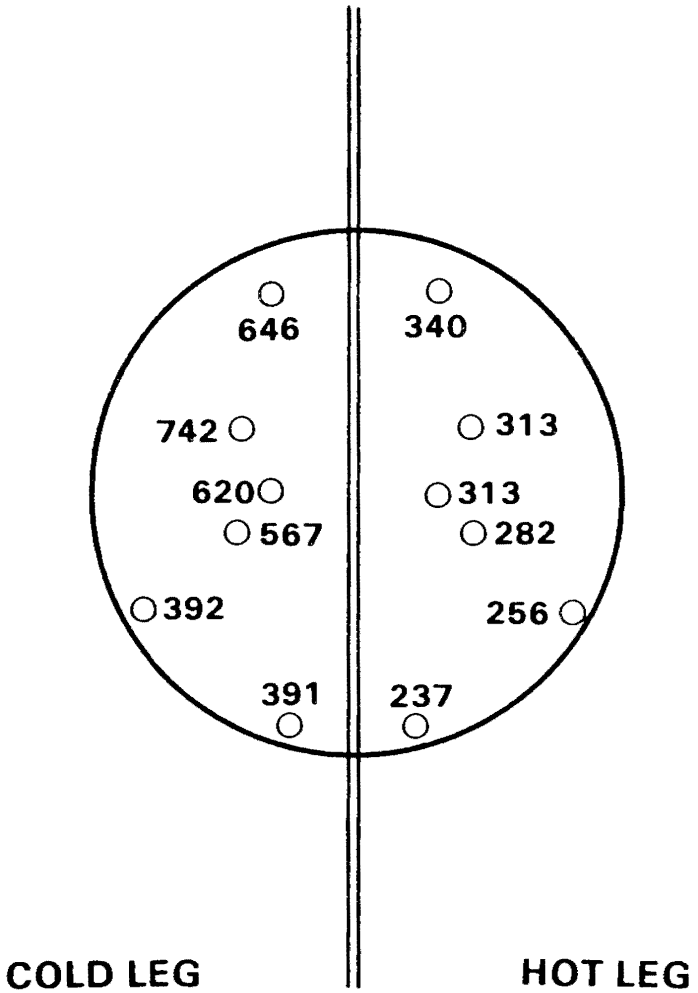

FIGURE 5-18.

DOSE RATE (mR/hr) IN CHANNEL HEAD 60 INCHES FROM TUBE SHEET

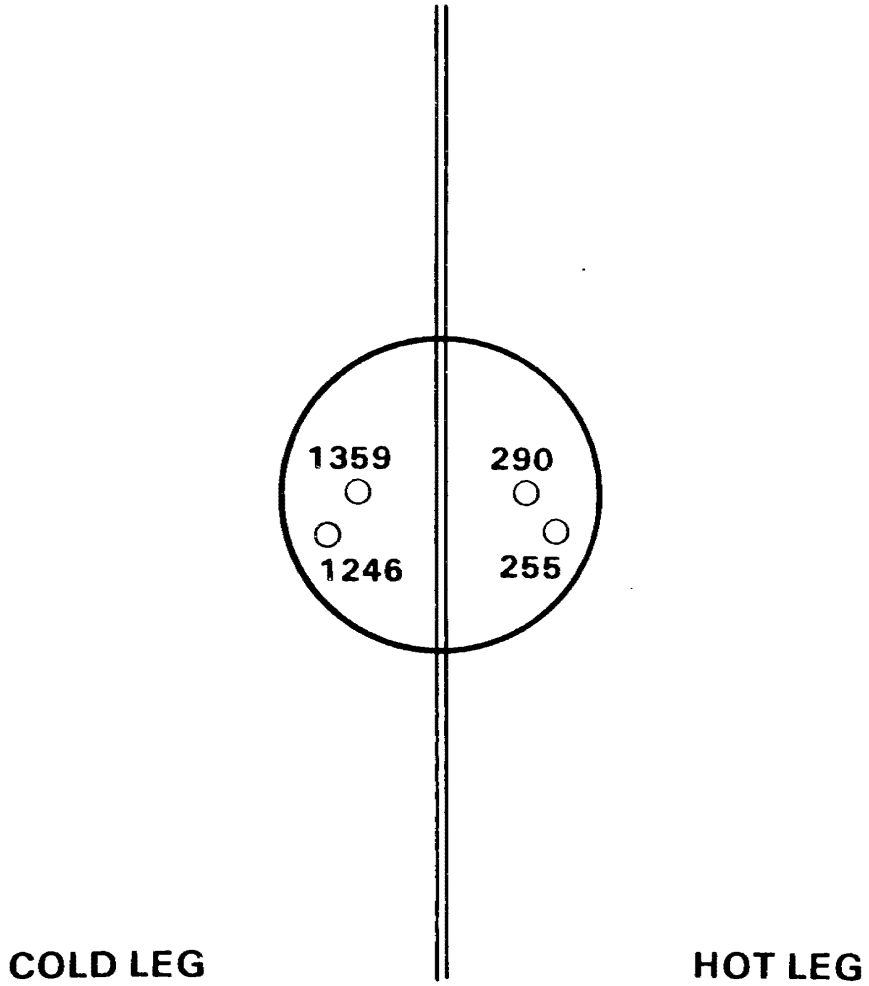

FIGURE 5-19.

TABLE 5-10. Average Post-Decontamination Channel Head Exposure Rates and Ranges Measured Using TLDs Suspended From the Tube Sheet

Distance Below Tube Sheet (in.)	Hot Leg (mR/h)	Cold Leg (mR/h)
0	833 (743-993)	970 (717-1596)
6	647 (354-769)	743 (602-1082)
12	534 (436-630)	590 (449-782)
18	463 (364-548)	510 (398-584)
24	414 (338-488)	455 (401-509)
30	377 (303-479)	413 (367-483)
36	370 (291-443)	390 (335-448)
42	354 (253-465)	397 (324-458)
48	340 (260-436)	431 (332-510)
54	290 (237-340)	560 (391-742)
60	273 (225-290)	1303 (1246-1359)

At each level, exposure rates were slightly greater in the cold leg than in the hot leg. This may be due in part to an increased inventory in the tubes leading to increased tube shine in the cold leg side of the channel head. There is definite indication of contamination in the lower sections of the cold side of the channel head, probably on the divider plate.

General Health Physics Overview of the Decontamination Efforts

Due to the different technical approaches to decontamination, each contractor presented separate challenges on ways to reduce personnel exposure. During the decontamination of the cold leg side of the channel head, the Co-60 released from the oxide film was stripped from the process stream by in-line ion exchange columns. The radiation field around the ion exchange columns rose to over 10 R/h as the Co-60 was concentrated in the columns. Since the columns were isolated from the main working environment and were shielded by temporary brick walls, the radiation fields were lowered for most of the personnel involved in the decontamination work. However, the shipping and disposal of the spent resin afterwards reduced the savings in overall exposure.

When the hot leg side of the channel head was decontaminated by the second contractor, the dissolved Co-60 was left in the process streams and the total volume of the decontamination solutions was stored in the waste storage tank. Since the waste tank was adjacent to the major work

area, the exposure rate to the workers was raised. The fields were limited to some degree because of the dilution of the Co-60 by the volumes of the process streams, the extra water providing self shielding. Unfortunately, this also made for large volumes of waste to be handled.

A large portion of the extra exposure taken by the first contractor (see Table 5-3) was due to repeated mechanical failure of their main circulation pump. This led to increased exposure because of time spent in the radiation zone repairing the pump and because of the elevation of the general field caused by leaking contaminated solution each time the seals failed. Furthermore, the second contractor enjoyed lower general fields due to the previous decontamination efforts, and due to the general experience gained by Battelle in working on the first decontamination effort.

Final Decontamination Efforts

In order that drill operators in the channel head would be exposed to as low a gamma field as possible, and in view of indications of possible contamination in the cold leg of the channel head, Battelle personnel electropolished both sides of the divider plate. This effort lowered the fields near the divider plate by about 25% and lowered the gamma field throughout the channel head by approximately 10% (see Table 5-11 and Figures 5-20 through 5-30). The hot spots on the cold leg side were lowered by a factor of two.

Finally, to shield from the gamma rays streaming from the open tubes, tapered lead plugs were inserted into open ends of approximately 1000 tubes. The tubes receiving the plugs were chosen on the basis of the time the drill operators would spend under those tubes. The tubes near the divider plates received more plugs since the operators would work from this area and reach to the more cramped locations. The effects of the lead plugs are seen in Table 5-11 and Figures 5-31 to 5-41.

Summary and Conclusions

Although the exact decontamination factor for the channel head surfaces cannot be determined precisely due to the complicating factors of tube shine, uneven oxide film removal, and shine from the adjacent side of the channel head through the divider plate, the overall field was dropped by a factor of six at the minimum. For the tube unplugging operation, estimates of exposure indicate that the drill operators will receive on the order of 40 man-rem in the present fields. Thus, for this operation alone, over 200 man-rem will be saved by the sixfold reduction of the gamma field at a cost of no more than 14.4 man-rem for the decontamination operations. As future operations are done in the channel head, such as the nondestructive testing, even further exposure savings will be realized.

TABLE 5-11. Channel Head Gamma Fields After Each Field Reduction Effort

COLD LEG

Location Row	Location Column	Distance from Tube Sheet (in.)	Dilute Decontamination (mR/h)	Divider Plate Cleaned (mR/h)	Lead Plugs Installed (mR/h)
46	51	0	717.2	682.4	674.0
		6	625.4	591.5	494.6
		12	492.2	450.1	421.1
7	3	0	918.3	854.1	709.1
		6	601.5	547.1	456.2
		12	449.3	395.0	353.6
		18	397.8	340.9	301.6
40	47	0	834.5	776.1	616.9
		6	602.6	616.6	510.5
		12	478.0	485.1	436.2
		18	419.8	412.1	387.6
		24	401.0	362.7	358.7
		30	376.4	340.6	325.9
16	83	0	1166.9	921.1	898.5
		6	792.5	757.9	689.5
		12	606.6	577.6	519.5
		18	506.2	445.0	438.7
		24	433.5	371.8	368.9
		30	396.1	331.9	363.7
29	26	0	980.5	884.9	669.4
		6	640.2	597.3	494.4
		12	494.8	450.1	398.9
		18	464.1	408.2	339.0
		24	407.6	348.8	305.2
		30	367.2	290.3	281.7
		36	335.2	280.5	249.8
29	68	0	1592.5	1384.7	1240.4
		6	1082.3	949.4	892.1
		12	782.2	654.2	638.5
		18	584.1	539.3	499.4
		24	458.4	418.4	396.2
		30	392.9	348.1	324.7
		36	391.8	332.7	299.2

TABLE 5-11. (Continued)

Location Row	Location Column	Distance from Tube Sheet (in.)	Dilute Decontamination (mR/h)	Divider Plate Cleaned (mR/h)	Lead Plugs Installed (mR/h)
16	19	0	789.2	667.6	476.8
		6	660.3	574.3	473.6
		12	517.1	460.0	401.8
		18	474.6	409.4	344.5
		24	432.4	339.6	298.1
		30	373.1	299.4	274.7
		36	363.7	291.4	253.6
		42	373.5	271.3	237.2
29	48	0	865.8	814.2	659.7
		6	661.4	658.4	555.5
		12	566.9	577.1	493.6
		18	492.7	461.2	405.2
		24	451.2	393.4	357.5
		30	398.0	341.1	301.1
		36	370.8	314.4	275.7
		42	363.1	286.5	259.8
		48	396.4	261.2	259.1
20	36	0	1115.6	955.2	720.9
		6	780.2	676.6	542.0
		12	589.3	546.7	455.6
		18	521.7	470.3	386.8
		24	464.6	394.2	325.2
		30	428.3	338.4	284.8
		36	383.7	320.0	273.8
		42	403.8	295.2	262.0
		48	427.8	307.5	277.0
20	58	0	1196.2	956.2	850.9
		6	867.6	770.4	701.1
		12	703.7	602.0	548.0
		18	557.9	501.9	450.2
		24	474.9	384.3	378.7
		30	433.5	364.0	298.6
		36	386.1	324.1	290.4
		42	363.7	306.3	263.3
		48	373.3	295.1	270.8
		54	391.5	336.3	287.0

TABLE 5-11. (Continued)

Location Row	Location Column	Distance from Tube Sheet (in.)	Dilute Decontamination (mR/h)	Divider Plate Cleaned (mR/h)	Lead Plugs Installed (mR/h)
6	69	0	764.2	738.1	673.4
		6	732.9	686.7	596.4
		12	594.1	516.9	465.6
		18	514.8	484.4	380.2
		24	435.5	374.1	349.3
		30	380.6	349.7	255.0
		36	360.4	287.0	236.0
		42	324.1	259.3	255.0
		48	331.6	250.0	237.4
		54	390.8	282.6	307.3
8	28	0	908.8	722.7	639.5
		6	790.4	584.1	548.0
		12	670.9	462.2	462.9
		18	565.6	398.3	379.9
		24	509.2	352.1	319.4
		30	482.8	320.3	285.2
		36	448.5	296.2	283.2
		42	435.1	300.7	284.8
		48	470.8	346.9	353.5
		54	645.5	564.4	542.2
11	41	0	1070.5	836.8	791.7
		6	793.1	660.6	610.7
		12	640.1	540.8	486.1
		18	546.0	438.0	411.8
		24	491.1	366.7	350.6
		30	430.9	349.5	305.2
		36	412.8	309.7	297.2
		42	431.8	293.9	293.0
		48	509.6	344.7	327.0
		54	742.0	460.2	468.2
11	51	0	756.3	641.7	608.0
		6	772.8	618.3	605.3
		12	656.3	544.1	489.3
		18	573.5	458.7	395.2
		24	474.2	392.2	361.7
		30	444.0	336.9	334.9
		36	414.2	304.7	297.4
		42	418.6	290.0	293.7
		48	459.6	310.1	324.2
		54	567.4	340.5	441.6
		60	1245.9	254.1	842.6

TABLE 5-11. (Continued)

Location Row	Location Column	Distance from Tube Sheet (in.)	Dilute Decontamination (mR/h)	Divider Plate Cleaned (mR/h)	Lead Plugs Installed (mR/h)
8	47	0	873.8	740.6	713.6
		6	744.5	588.9	585.9
		12	614.4	497.8	484.4
		18	519.9	401.3	399.1
		24	484.5	369.9	324.8
		30	461.4	328.8	303.9
		36	420.8	316.8	292.1
		42	457.9	313.1	290.4
		48	476.3	326.1	304.1
		54	620.5	349.4	402.0
		60	1359.1	229.4	703.3
HOT LEG					
46	51	0	830.6	711.9	621.5
		6	527.8	420.4	448.7
		12	436.3	359.5	376.4
7	4	0	993.0	706.5	636.9
		6	590.4	454.8	477.7
		12	495.2	340.2	332.3
		18	407.4	280.5	275.2
40	47	0	811.9	666.9	651.8
		6	542.6	510.5	469.6
		12	446.7	393.2	427.6
		18	364.1	326.4	328.9
		24	337.8	303.6	312.8
		30	314.6	273.9	252.1
16	83	0	803.5	678.9	740.4
		6	637.4	556.0	599.0
		12	480.4	419.0	461.9
		18	424.3	339.5	352.8
		24	356.4	297.1	315.5
		30	313.9	279.0	272.2
29	26	0	798.1	696.7	545.3
		6	598.8	510.5	455.9
		12	483.5	406.6	398.8
		18	445.3	341.5	372.0
		24	393.9	312.6	292.9
		30	398.5	303.1	301.0
		36	426.7	314.6	325.6

TABLE 5-11. (Continued)

Location Row	Location Column	Distance from Tube Sheet (in.)	Dilute Decontamination (mR/h)	Divider Plate Cleaned (mR/h)	Lead Plugs Installed (mR/h)
29	68	0	735.6	676.9	
		6	619.9	598.9	
		12	478.7	458.7	
		18	433.1	377.9	
		24	365.5	312.4	
		30	302.7	283.8	
		36	291.0	248.9	
16	19	0	883.8	656.4	565.8
		6	661.6	530.3	485.0
		12	551.2	417.5	388.6
		18	474.9	348.9	343.8
		24	413.0	334.0	294.4
		30	389.0	279.1	286.9
		36	408.3	275.6	323.5
		42	465.3	295.4	312.1
29	48	0	746.2	672.1	555.6
		6	596.1	565.1	450.2
		12	535.3	482.3	419.5
		18	432.2	391.7	359.1
		24	397.4	356.3	304.2
		30	366.2	317.1	279.3
		36	334.5	275.9	280.5
		42	326.6	261.4	258.9
		48	311.6	249.7	252.2
19	35	0	906.0	868.3	725.4
		6	726.3	574.6	560.7
		12	555.4	469.7	444.7
		18	467.6	378.6	413.6
		24	434.9	329.8	353.7
		30	374.0	324.9	331.9
		36	394.4	290.8	290.2
		42	396.1	306.0	314.8
		48	436.0	315.2	313.2
20	58	0	742.7	690.1	640.1
		6	614.8	542.3	546.9
		12	542.4	450.0	481.6
		18	459.3	374.9	409.3
		24	419.0	317.8	398.2
		30	365.5	285.3	301.1
		36	335.3	270.5	259.6
		42	296.5	236.3	238.3
		48	276.1	212.1	211.4
		54	255.7	179.7	168.7

TABLE 5-11. (Continued)

Location Row	Location Column	Distance from Tube Sheet (in.)	Dilute Decontamination (mR/h)	Divider Plate Cleaned (mR/h)	Lead Plugs Installed (mR/h)
6	69	0	856.1	658.2	
		6	710.1	539.0	
		12	561.4	456.5	
		18	484.2	362.9	
		24	400.8	294.5	
		30	343.7	245.8	
		36	298.2	230.1	
		42	252.6	214.6	
		48	260.4	187.4	
		54	236.7	184.7	
8	28	0	885.6	657.0	668.7
		6	769.3	599.7	555.7
		12	630.5	461.8	461.6
		18	547.5	373.2	380.9
		24	474.4	326.6	341.3
		30	479.1	297.3	318.0
		36	442.8	263.3	284.2
		42	410.6	254.6	279.5
		48	407.8	253.2	259.9
		54	339.7	209.6	247.8
11	41	0	901.3	742.7	728.0
		6	732.1	566.8	576.6
		12	610.4	435.3	478.5
		18	510.2	390.8	383.9
		24	441.1	341.4	333.6
		30	430.5	292.9	302.7
		36	389.5	270.9	274.9
		42	400.2	273.3	266.8
		48	366.1	262.9	250.9
		54	312.8	227.3	235.9
11	51	0	807.5	592.0	620.7
		6	690.1	496.8	577.7
		12	581.3	416.3	420.7
		18	516.9	377.5	403.9
		24	457.8	321.4	355.9
		30	412.0	292.6	337.2
		36	365.5	264.7	285.8
		42	307.6	254.7	253.7
		48	327.7	218.1	225.8
		54	282.3	204.6	202.2
		60	255.0	211.7	205.2

TABLE 5-11. (Continued)

Location Row	Location Column	Distance from Tube Sheet (in.)	Dilute Decontamination (mR/h)	Divider Plate Cleaned (mR/h)	Lead Plugs Installed (mR/h)
8	47	0	798.9	660.1	622.7
		6	686.8	558.5	557.8
		12	619.4	490.2	472.6
		18	509.0	402.2	402.5
		24	488.4	334.1	343.6
		30	409.1	290.5	298.3
		36	388.1	280.4	266.1
		42	331.3	253.1	247.8
		48	332.5	235.8	237.2
		54	313.3	233.0	215.1
		60	290.0	208.7	232.0

DOSE RATE (mR/hr) IN CHANNEL HEAD 0 INCHES FROM TUBE SHEET, DIVIDER CLEANED

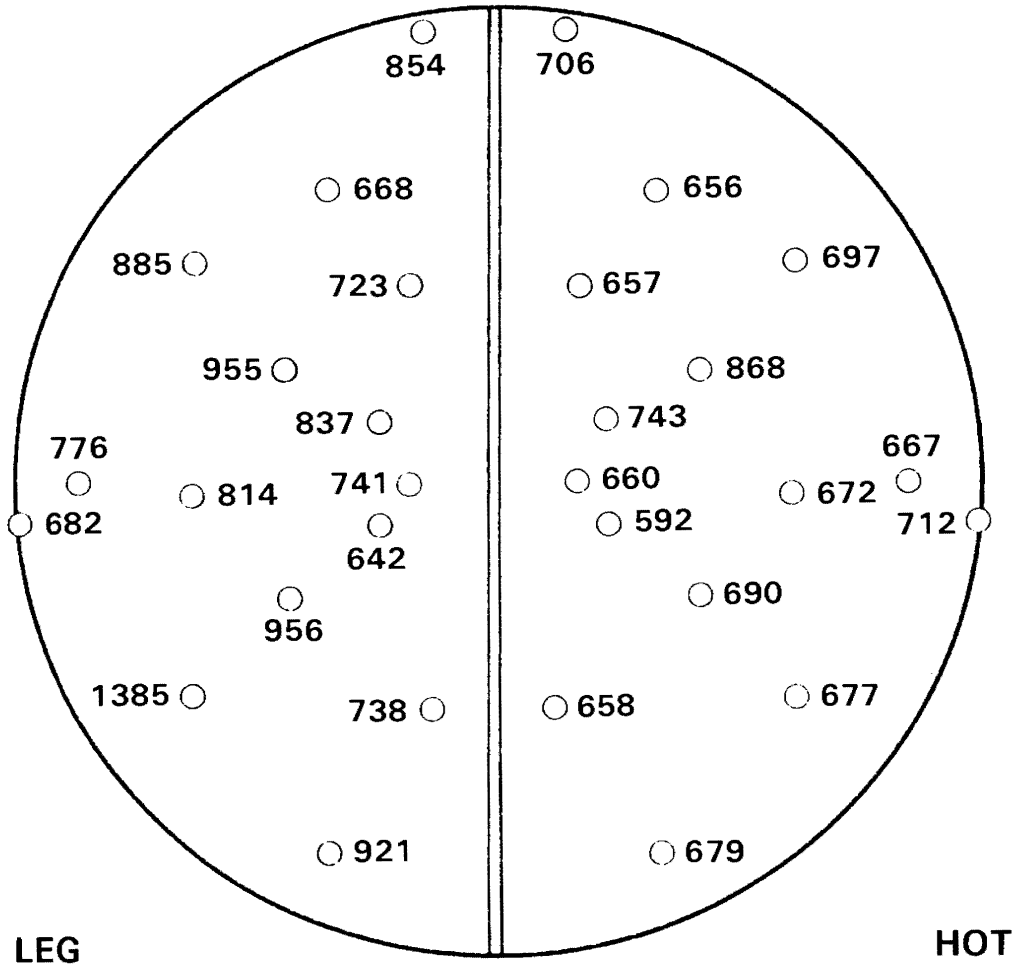

FIGURE 5-20.

DOSE RATE (mR/hr) IN CHANNEL HEAD 6 INCHES FROM TUBE SHEET, DIVIDER CLEANED

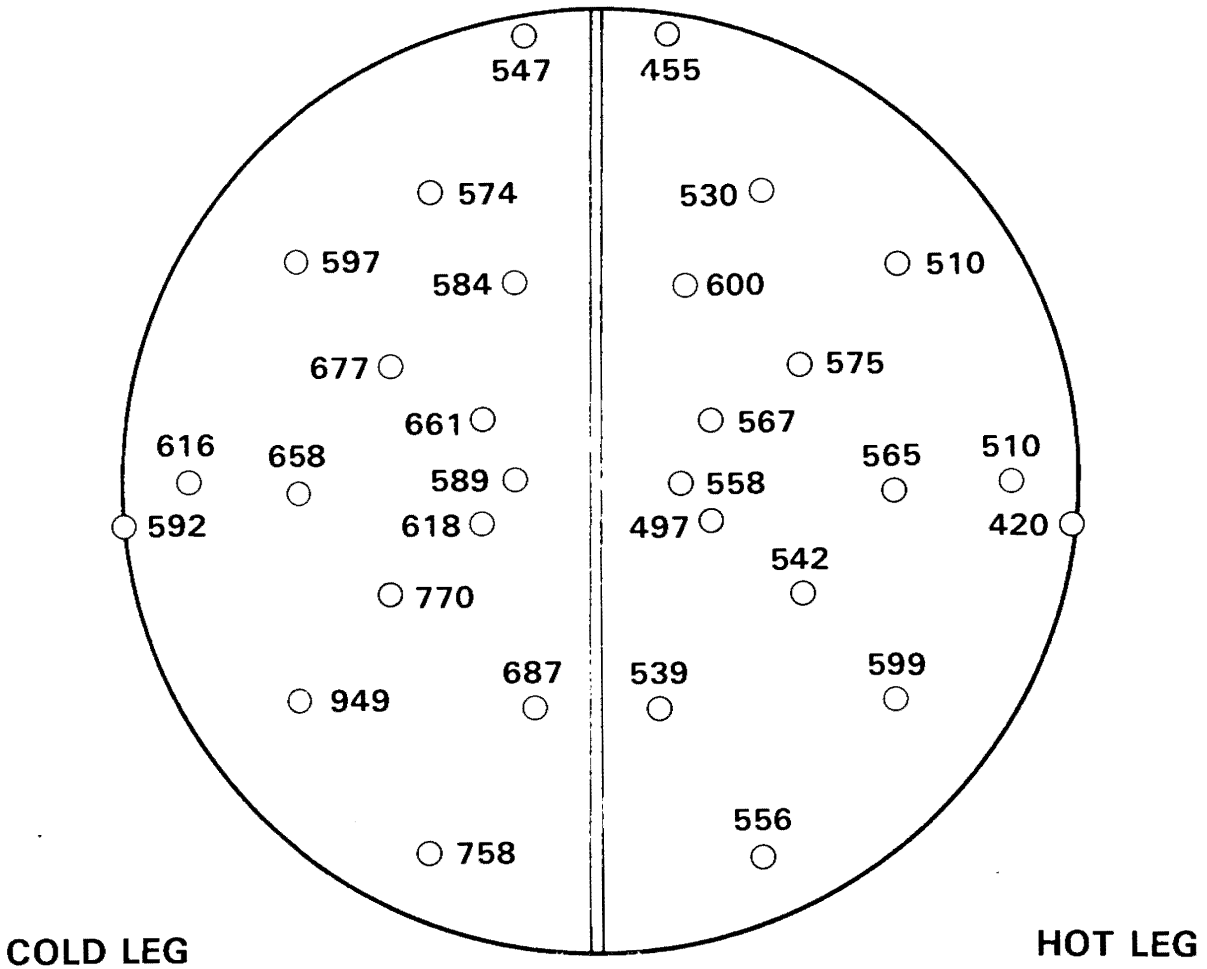

FIGURE 5-21.

DOSE RATE (mR/hr) IN CHANNEL HEAD 12 INCHES FROM TUBE SHEET, DIVIDER CLEANED

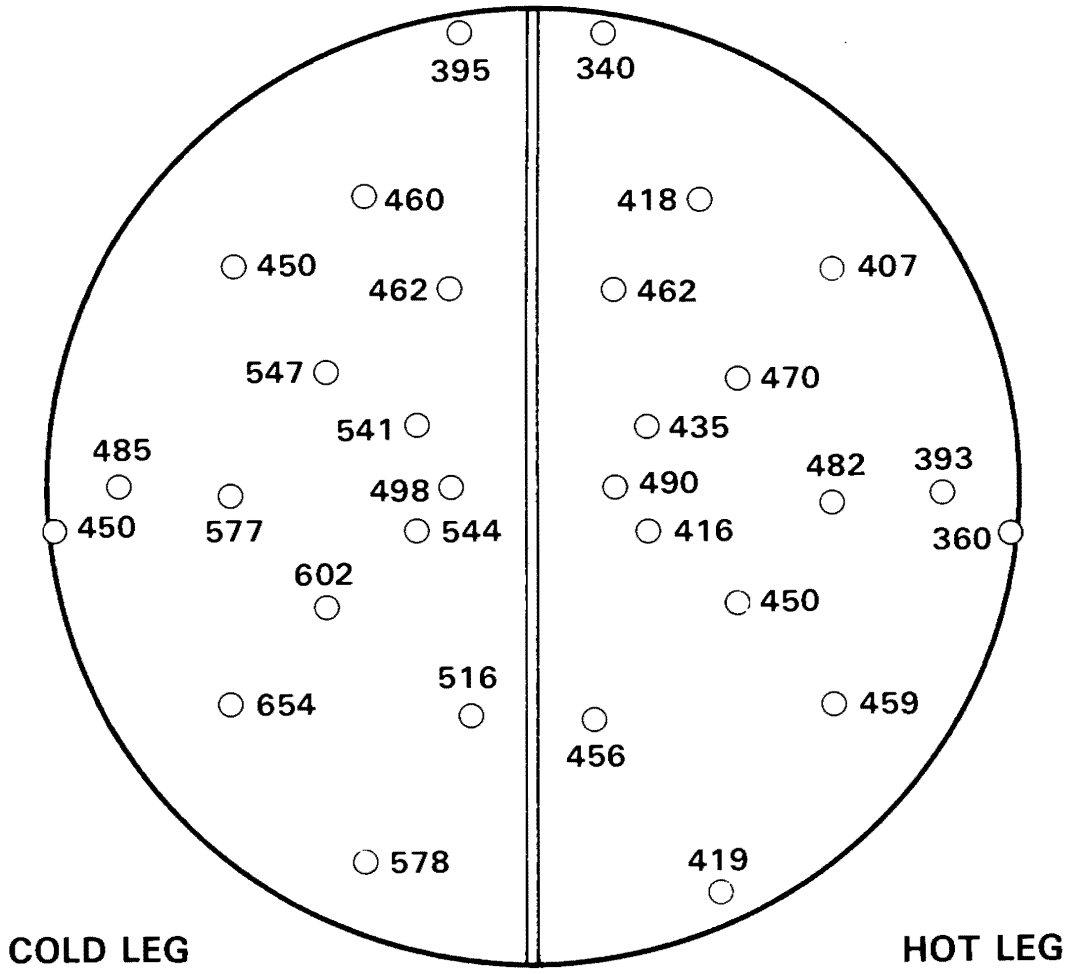

FIGURE 5-22.

DOSE RATE (mR/hr) IN CHANNEL HEAD 18 INCHES FROM TUBE SHEET, DIVIDER CLEANED

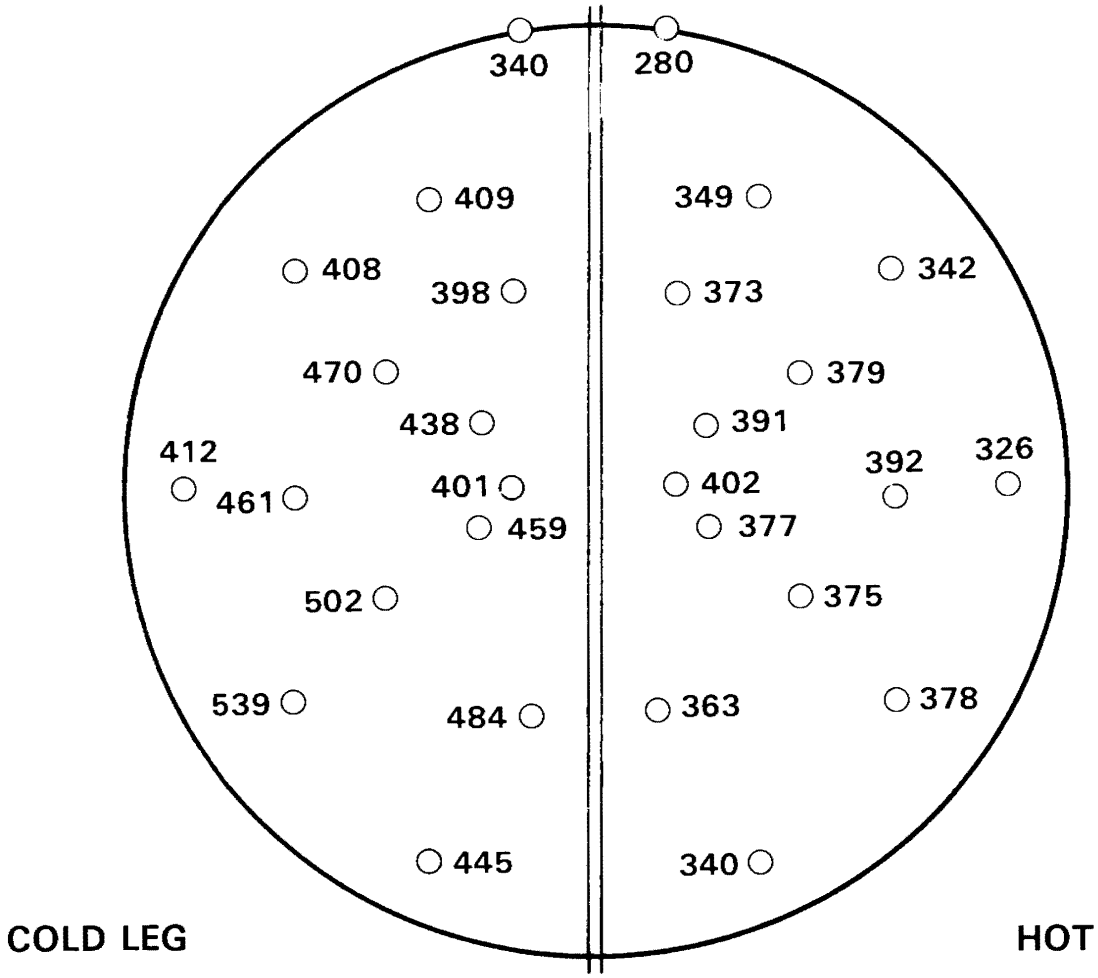

FIGURE 5-23.

DOSE RATE (mR/hr) IN CHANNEL HEAD 24 INCHES FROM TUBE SHEET, DIVIDER CLEANED

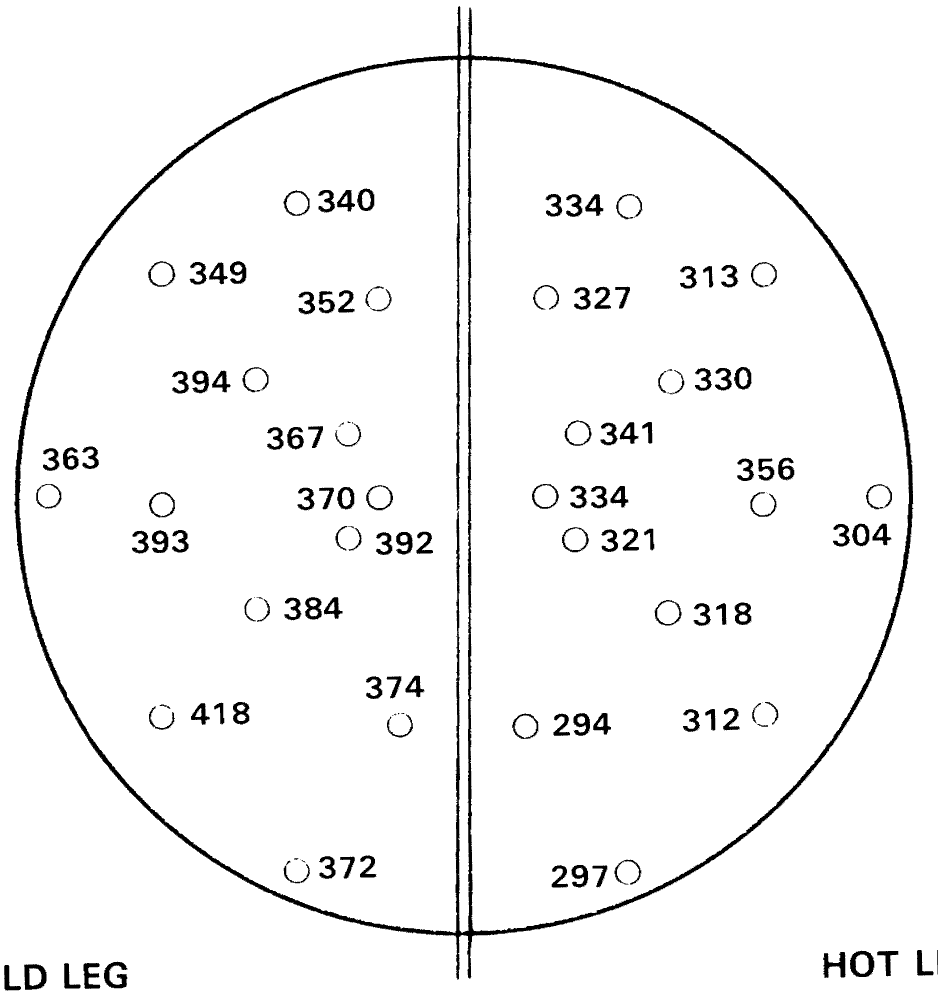

FIGURE 5-24.

DOSE RATE (mR/hr) IN CHANNEL HEAD 30 INCHES FROM TUBE SHEET, DIVIDER CLEANED

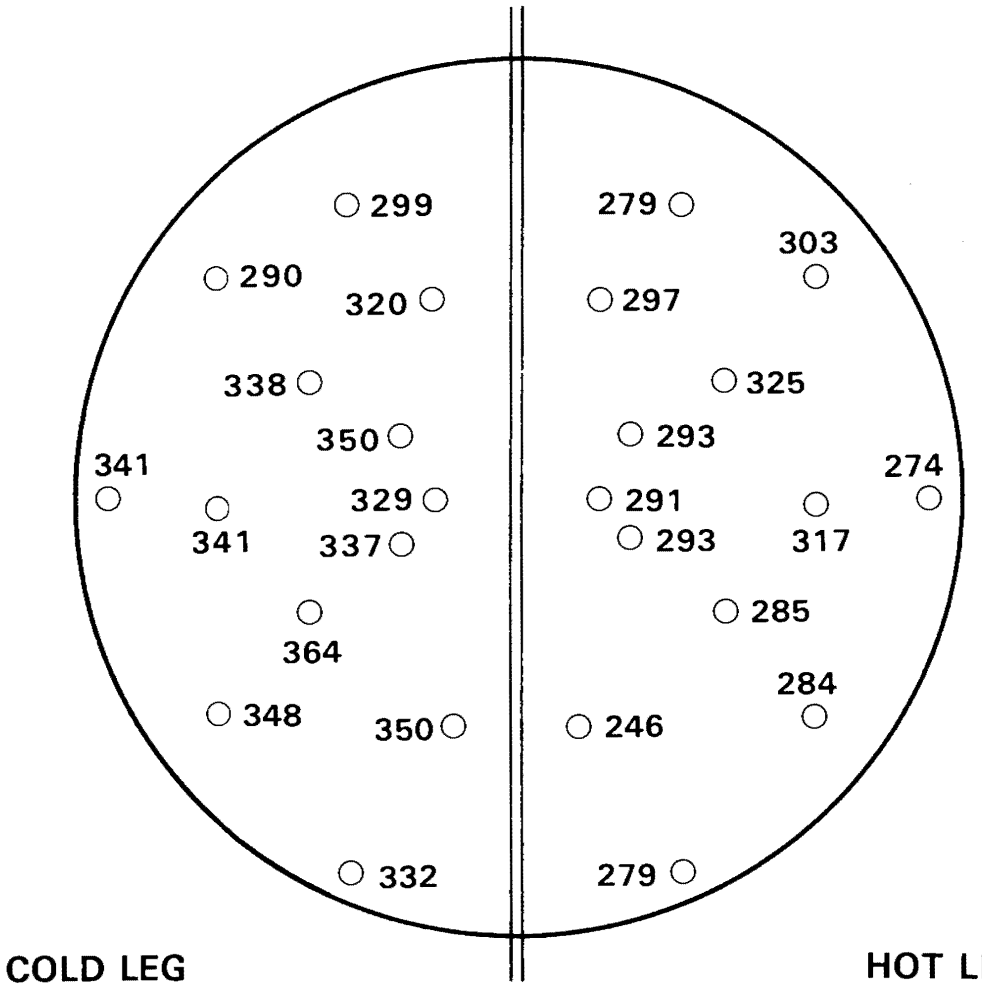

FIGURE 5-25.

DOSE RATE (mR/hr) IN CHANNEL HEAD 36 INCHES FROM TUBE SHEET, DIVIDER CLEANED

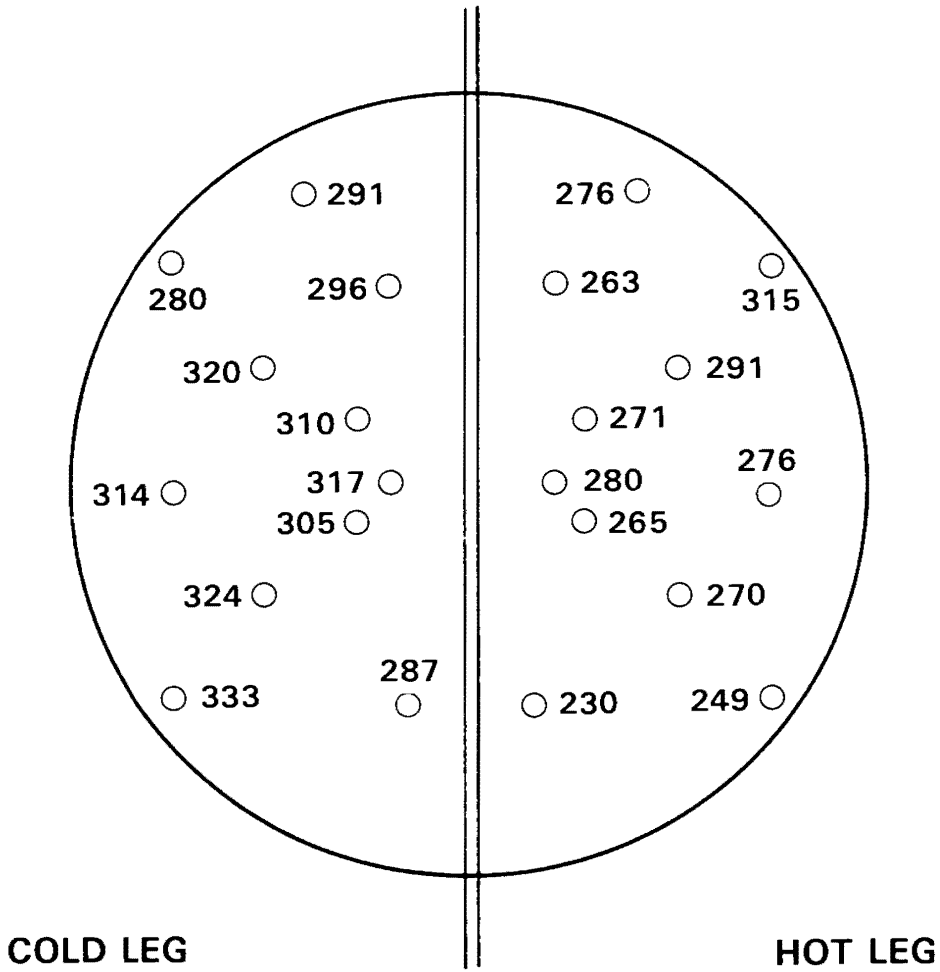

FIGURE 5-26.

DOSE RATE (mR/hr) IN CHANNEL HEAD 42 INCHES FROM TUBE SHEET, DIVIDER CLEANED

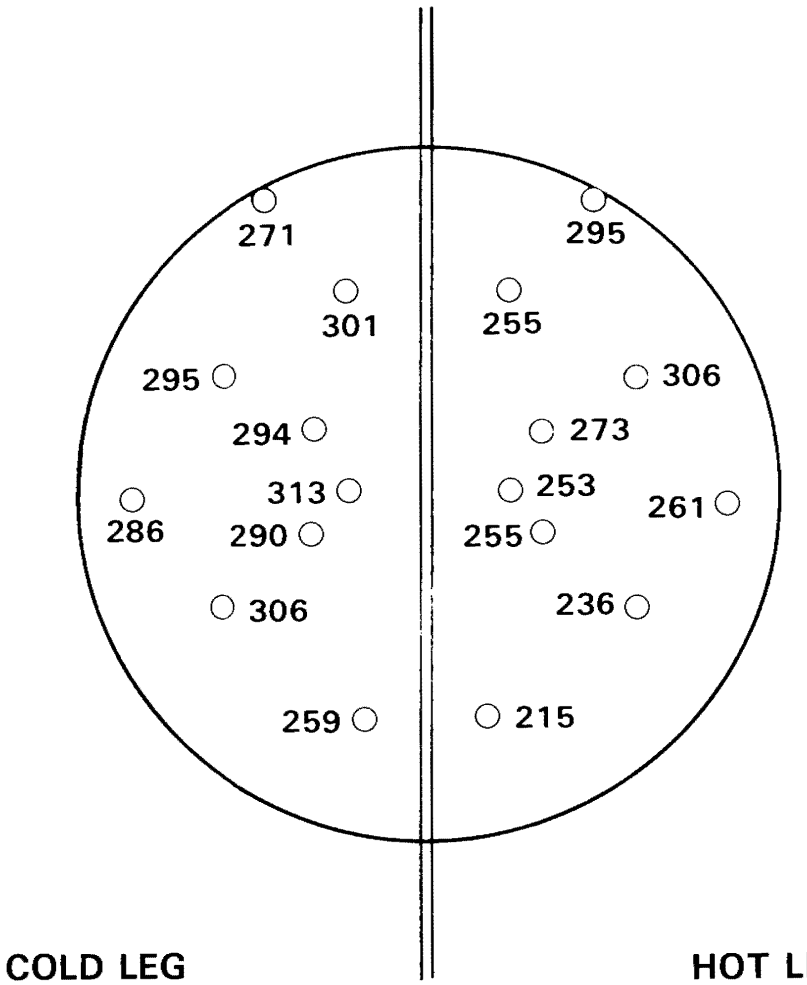

FIGURE 5-27.

DOSE RATE (mR/hr) IN CHANNEL HEAD 48 INCHES FROM TUBE SHEET, DIVIDER CLEANED

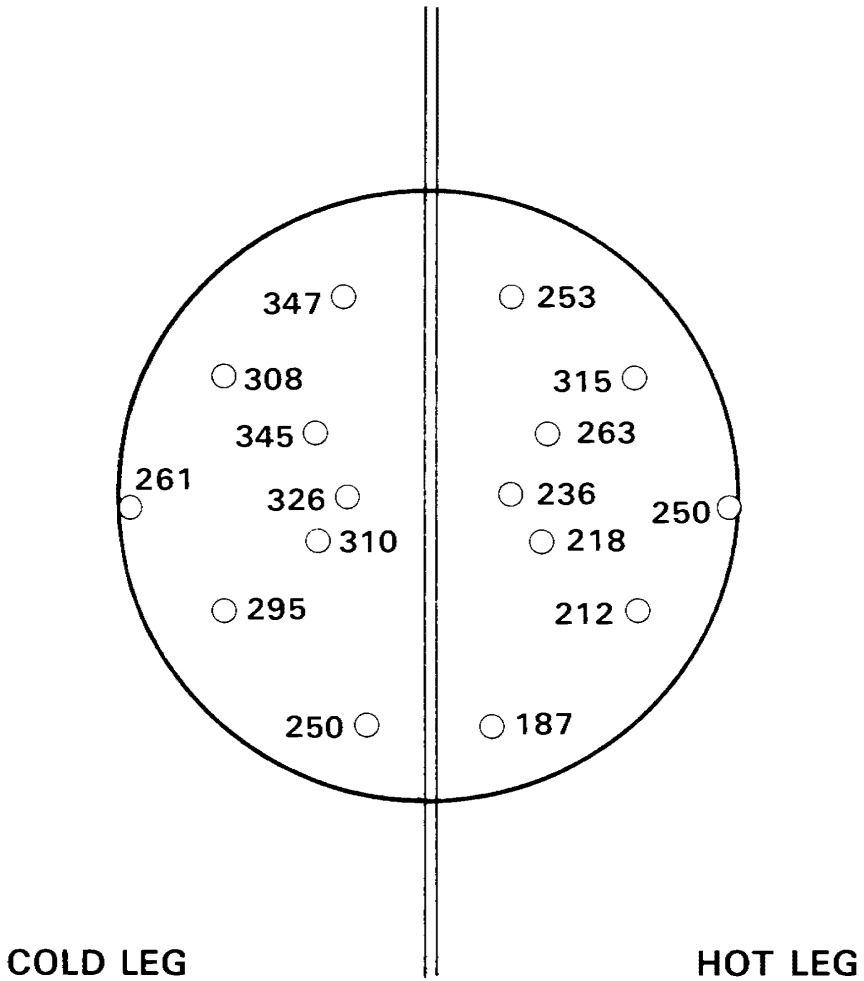

FIGURE 5-28.

DOSE RATE (mR/hr) IN CHANNEL HEAD 54 INCHES FROM TUBE SHEET, DIVIDER CLEANED

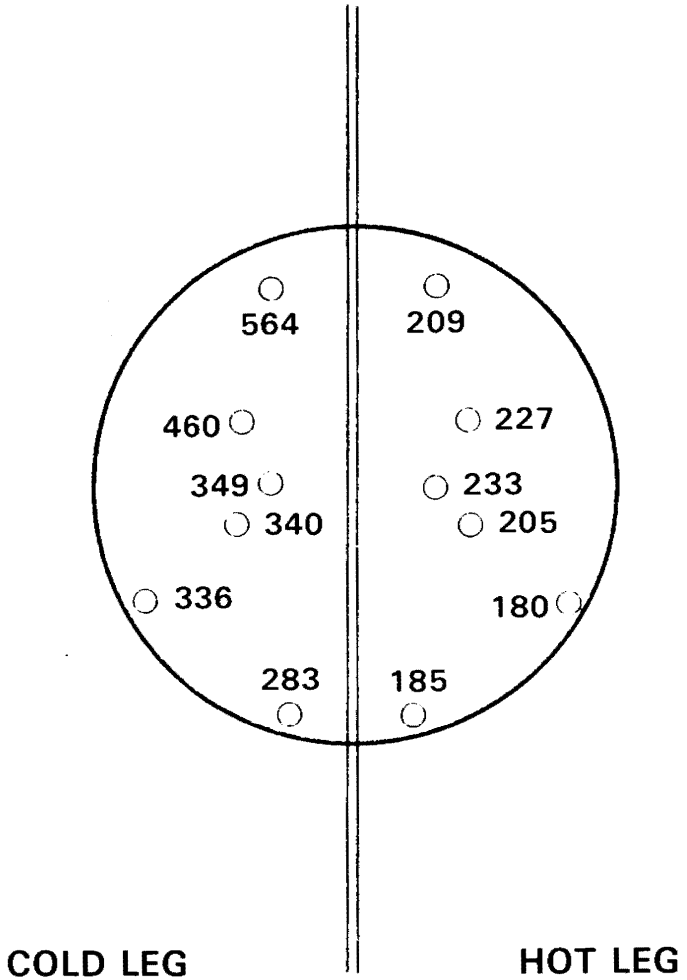

FIGURE 5-29.

DOSE RATE (mR/hr) IN CHANNEL HEAD 60 INCHES FROM TUBE SHEET, DIVIDER CLEANED

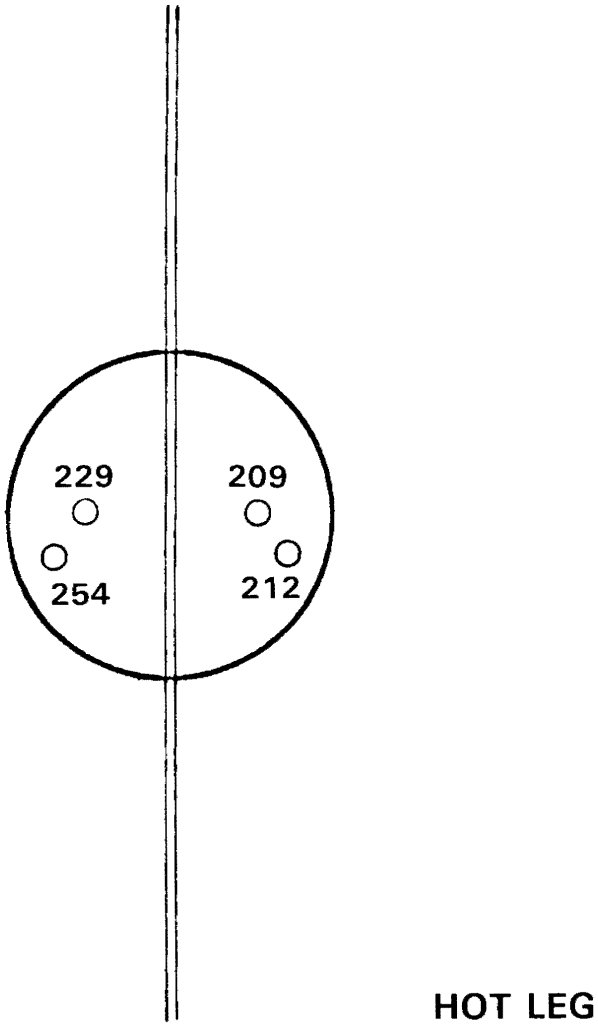

FIGURE 5-30.

DOSE RATE (mR/hr) IN CHANNEL HEAD 0 INCHES FROM TUBE SHEET, DIVIDER CLEANED AND LEAD PLUGS IN PLACE

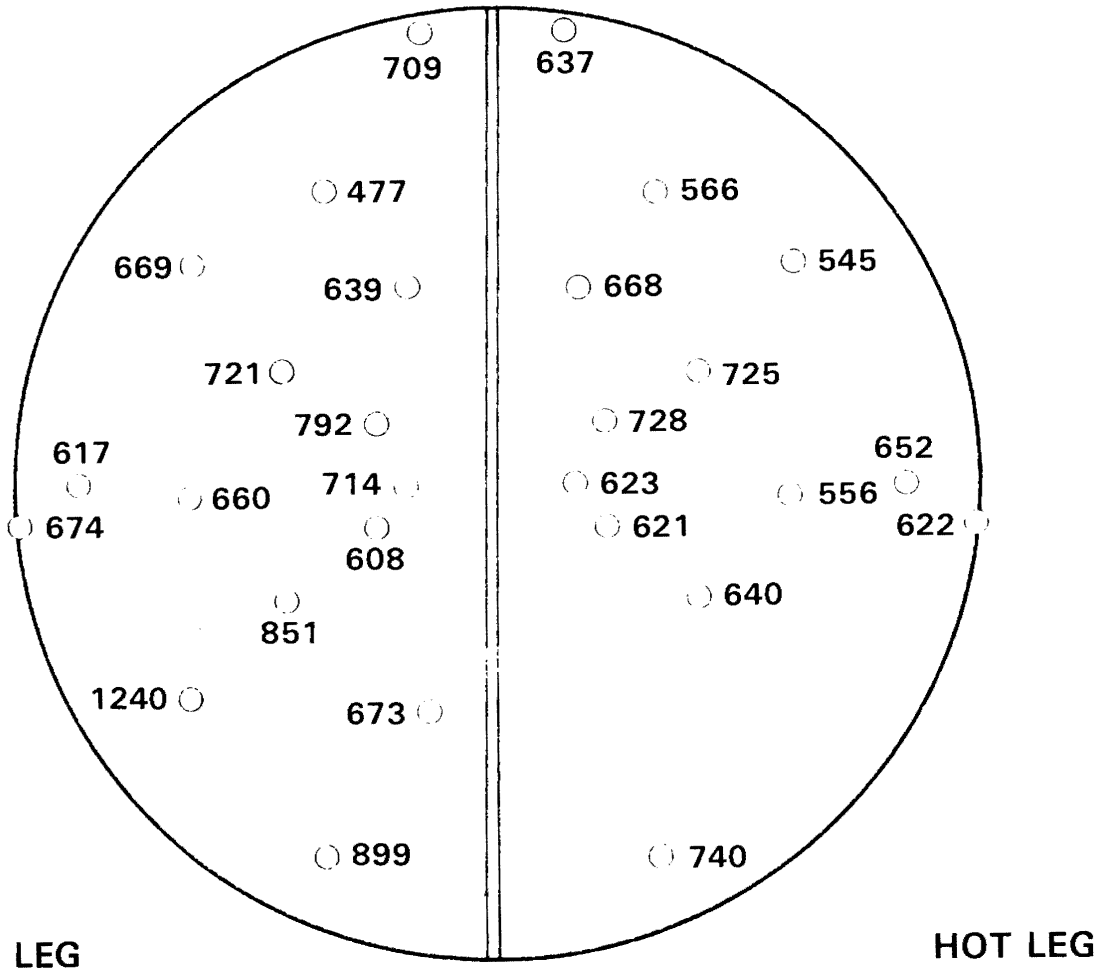

FIGURE 5-31.

DOSE RATE (mR/hr) IN CHANNEL HEAD 6 INCHES FROM TUBE SHEET, DIVIDER CLEANED AND LEAD PLUGS INSTALLED

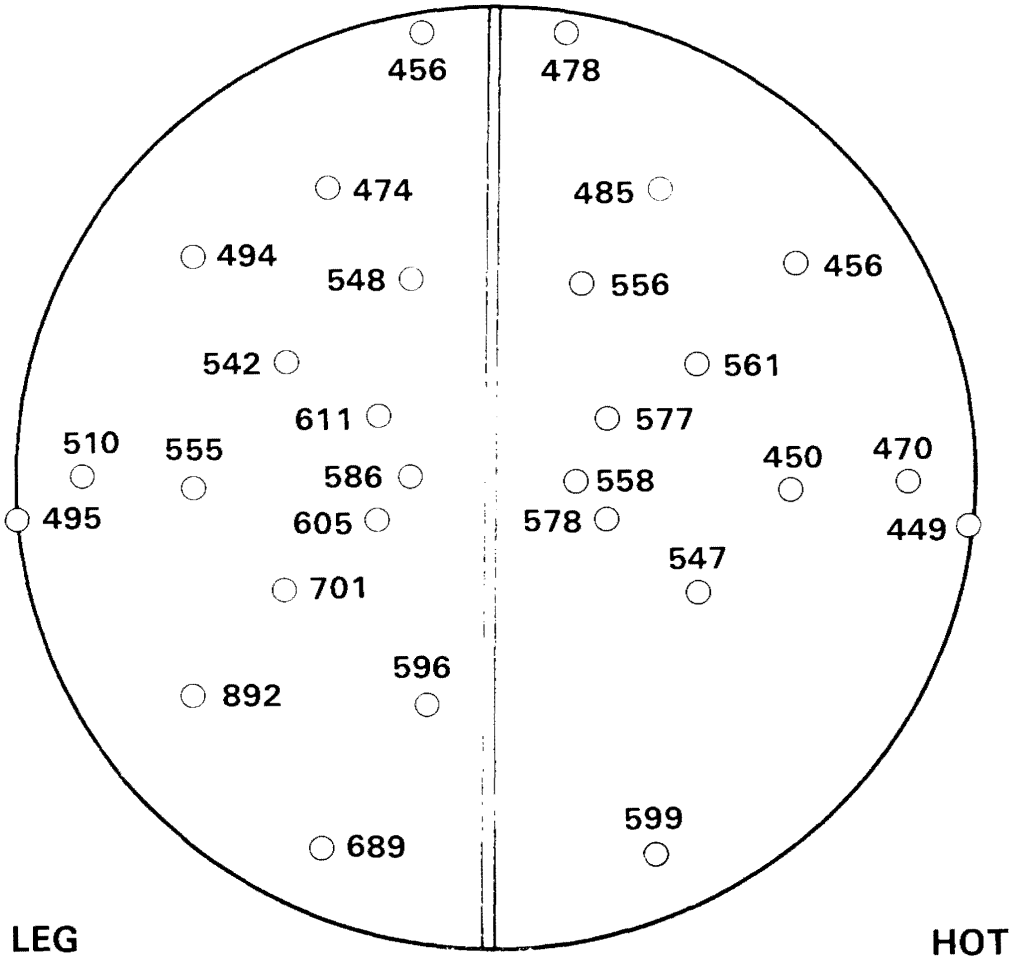

FIGURE 5-32.

DOSE RATE (mR/hr) IN CHANNEL HEAD 12 INCHES FROM TUBE SHEET, DIVIDER CLEANED AND LEAD PLUGS INSTALLED

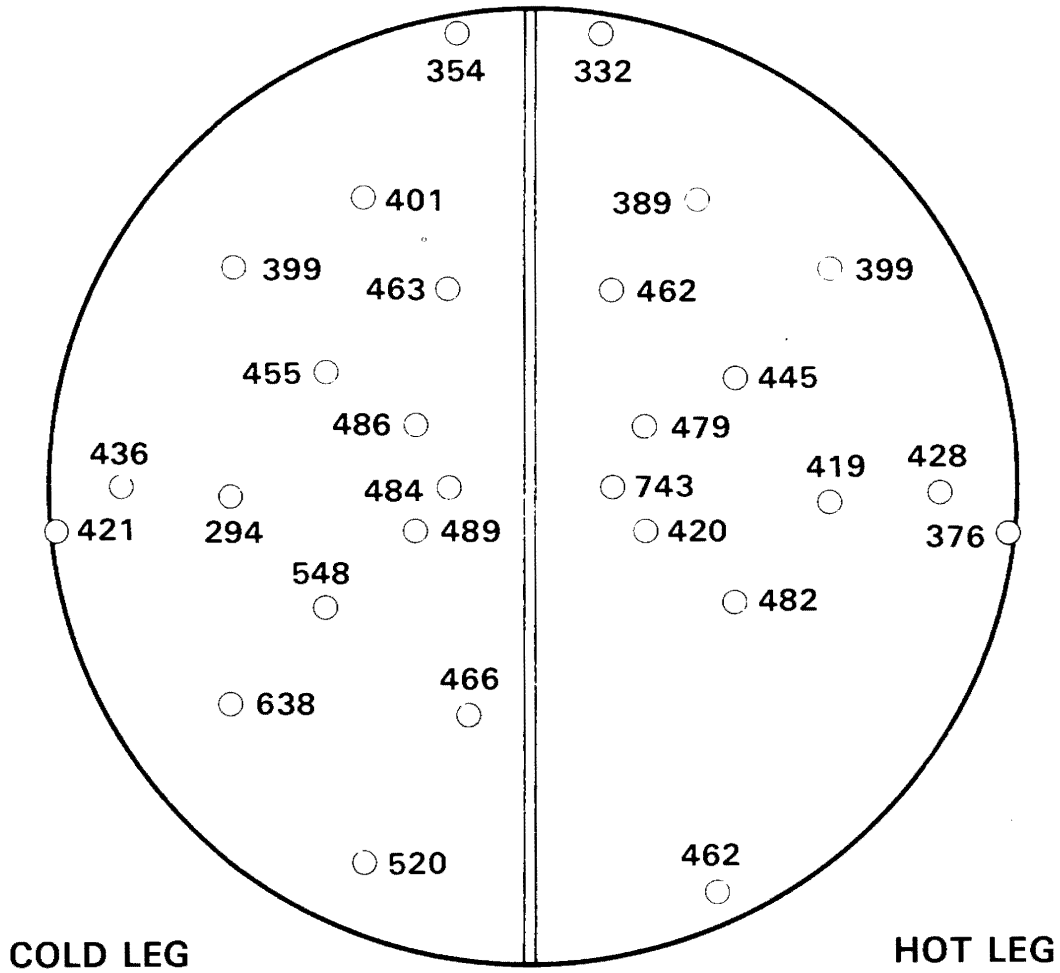

FIGURE 5-33.

DOSE RATE (mR/hr) IN CHANNEL HEAD 18 INCHES FROM TUBE SHEET, DIVIDER CLEANED AND LEAD PLUGS INSTALLED

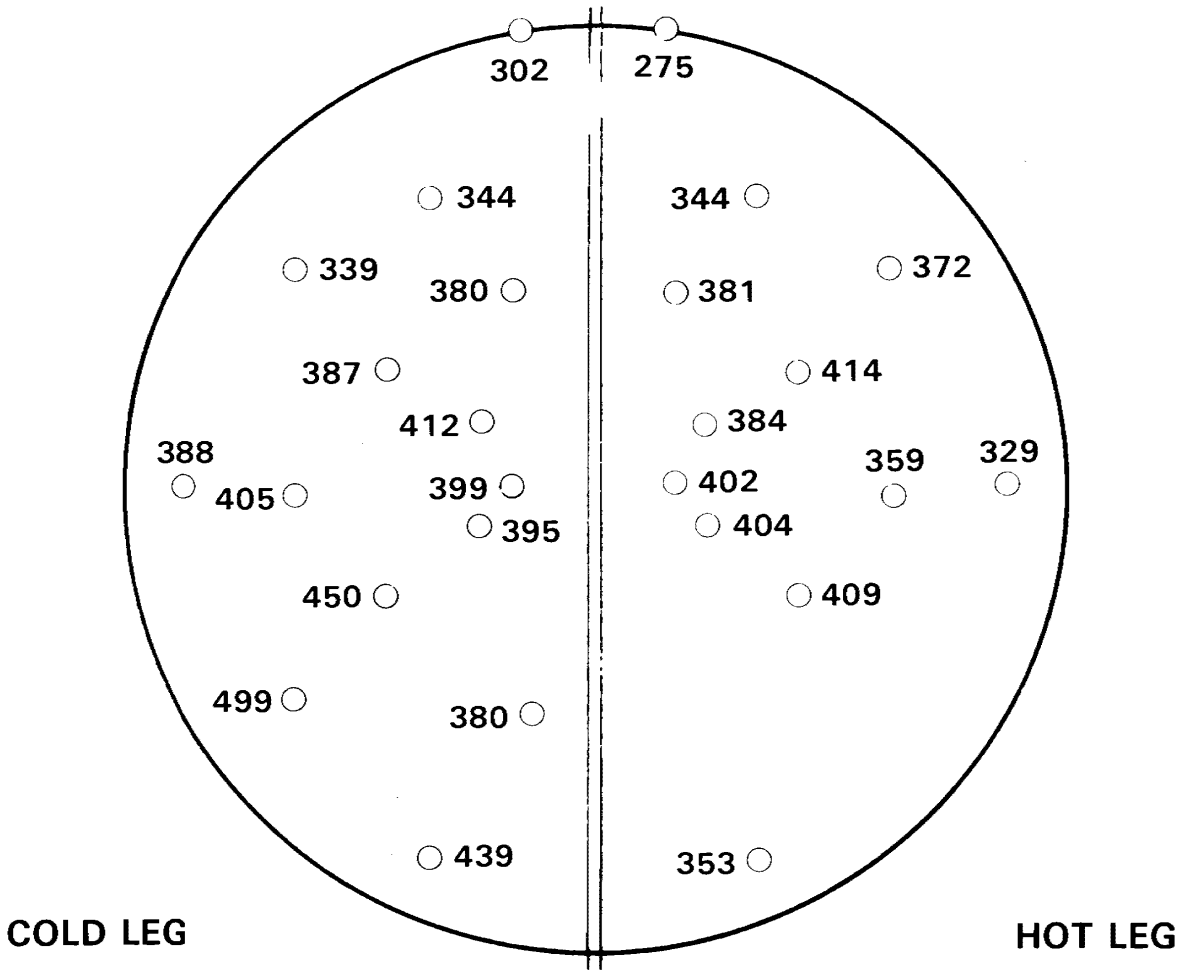

FIGURE 5-34.

DOSE RATE (mR/hr) IN CHANNEL HEAD 24 INCHES FROM TUBE SHEET, DIVIDER CLEANED AND LEAD PLUGS INSTALLED

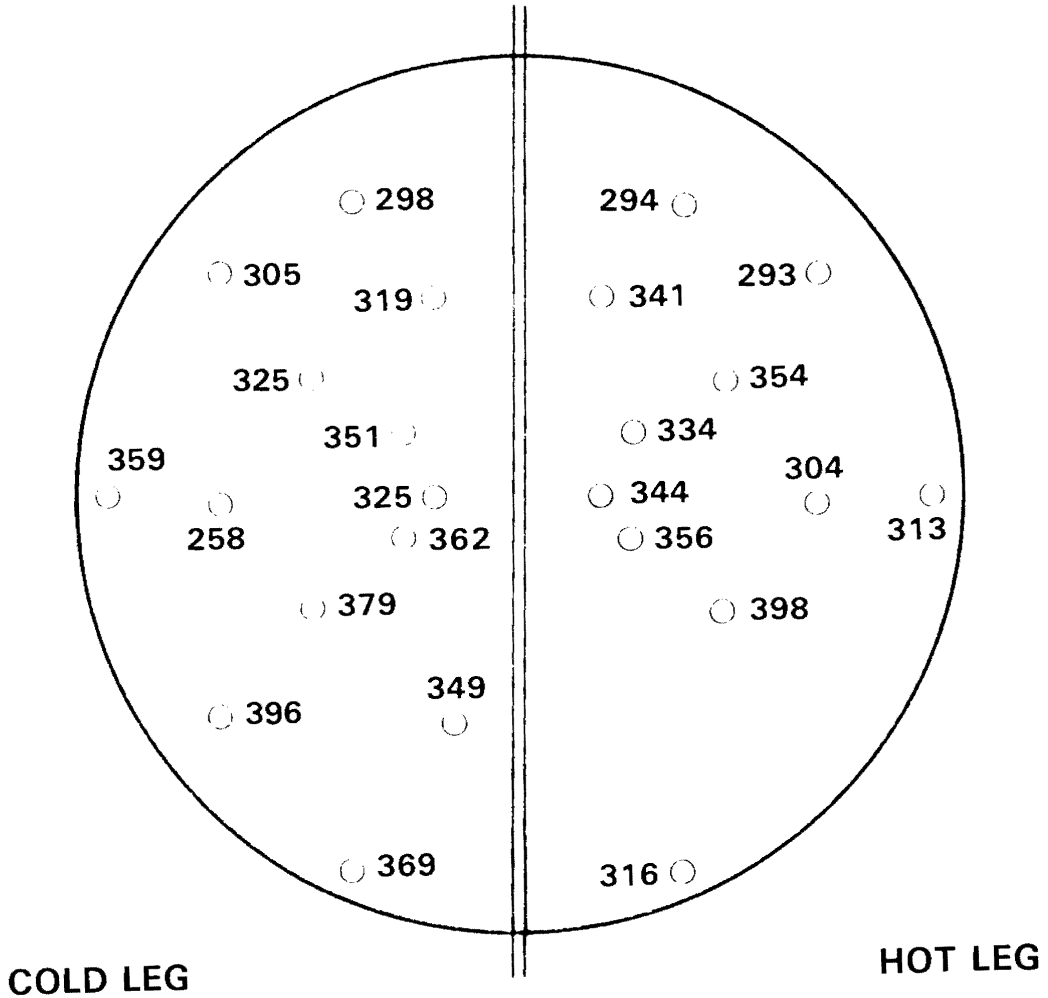

FIGURE 5-35.

DOSE RATE (mR/hr) IN CHANNEL HEAD 30 INCHES FROM TUBE SHEET, DIVIDER CLEANED AND LEAD PLUGS INSTALLED

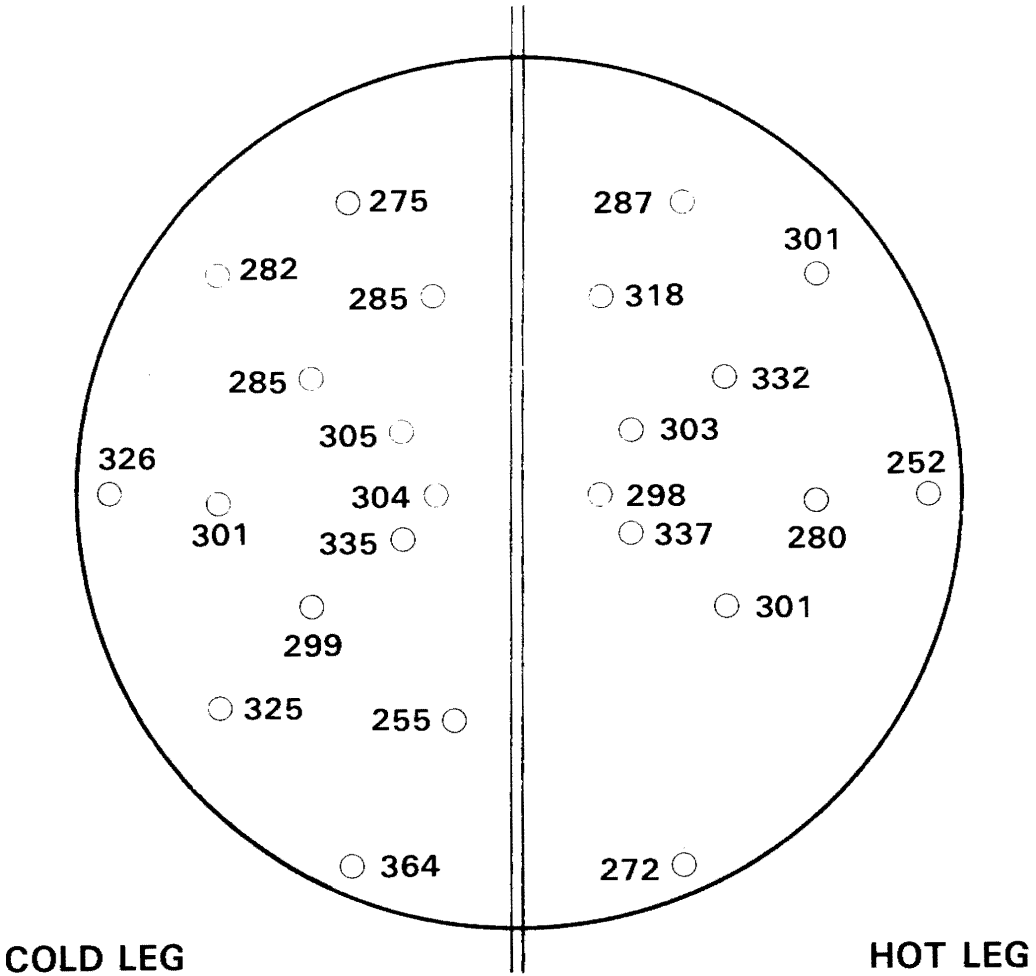

FIGURE 5-36.

DOSE RATE (mR/hr) IN CHANNEL HEAD 36 INCHES FROM TUBE SHEET, DIVIDER CLEANED AND LEAD PLUGS INSTALLED

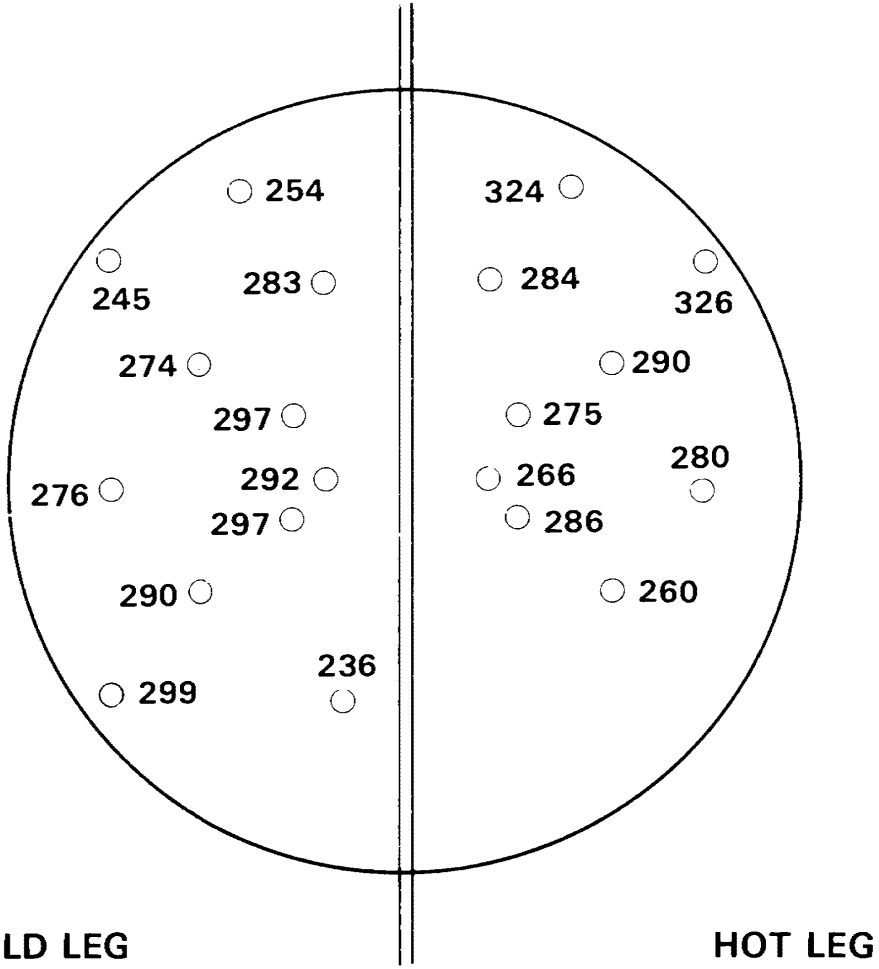

FIGURE 5-37.

DOSE RATE (mR/hr) IN CHANNEL HEAD 42 INCHES FROM TUBE SHEET, DIVIDER CLEANED AND LEAD PLUGS INSTALLED

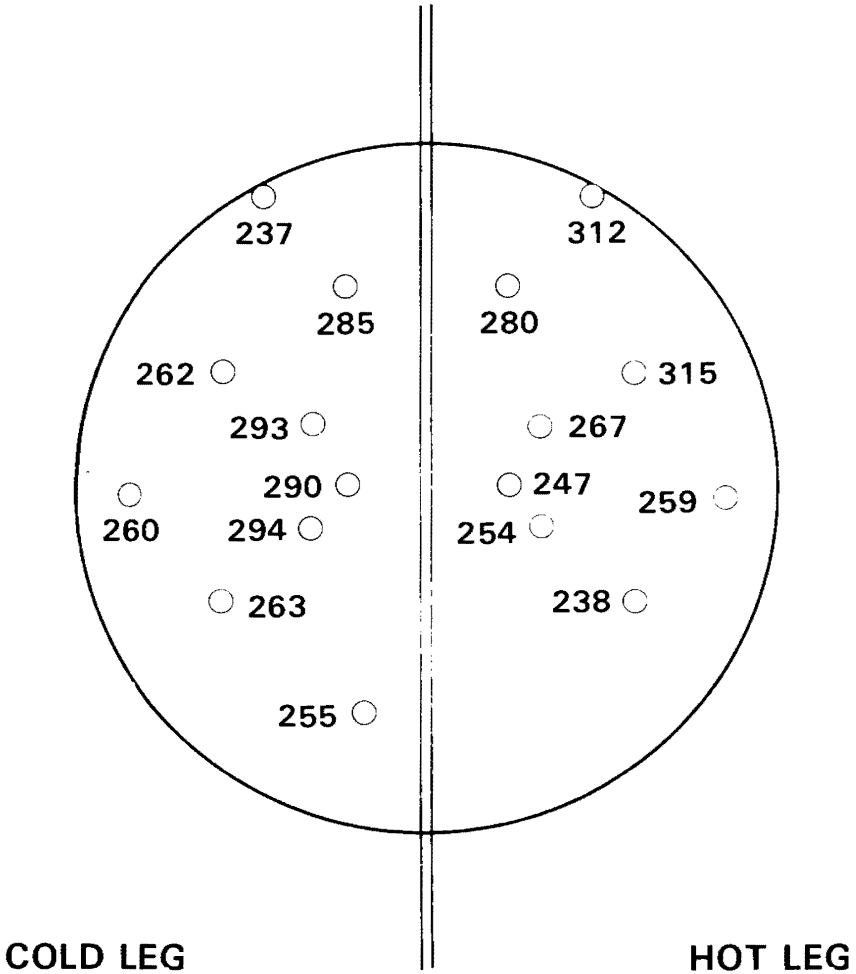

FIGURE 5-38.

DOSE RATE (mR/hr) IN CHANNEL HEAD 48 INCHES FROM TUBE SHEET, DIVIDER CLEANED AND LEAD PLUGS INSTALLED

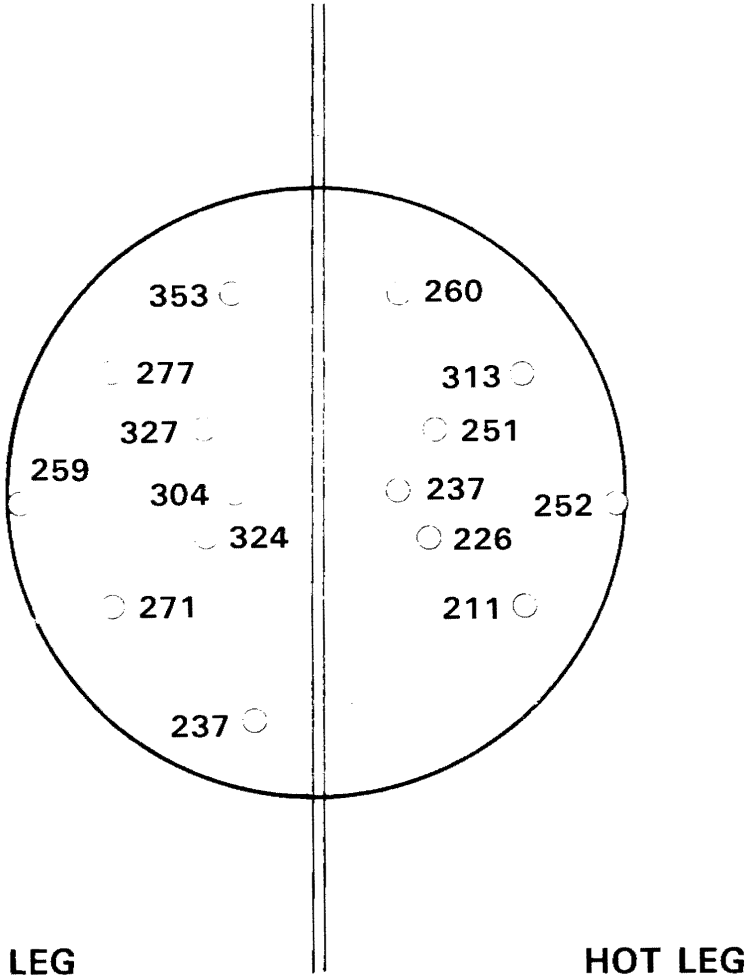

FIGURE 5-39.

DOSE RATE (mR/hr) IN CHANNEL HEAD 54 INCHES FROM TUBE SHEET, DIVIDER CLEANED AND LEAD PLUGS INSTALLED

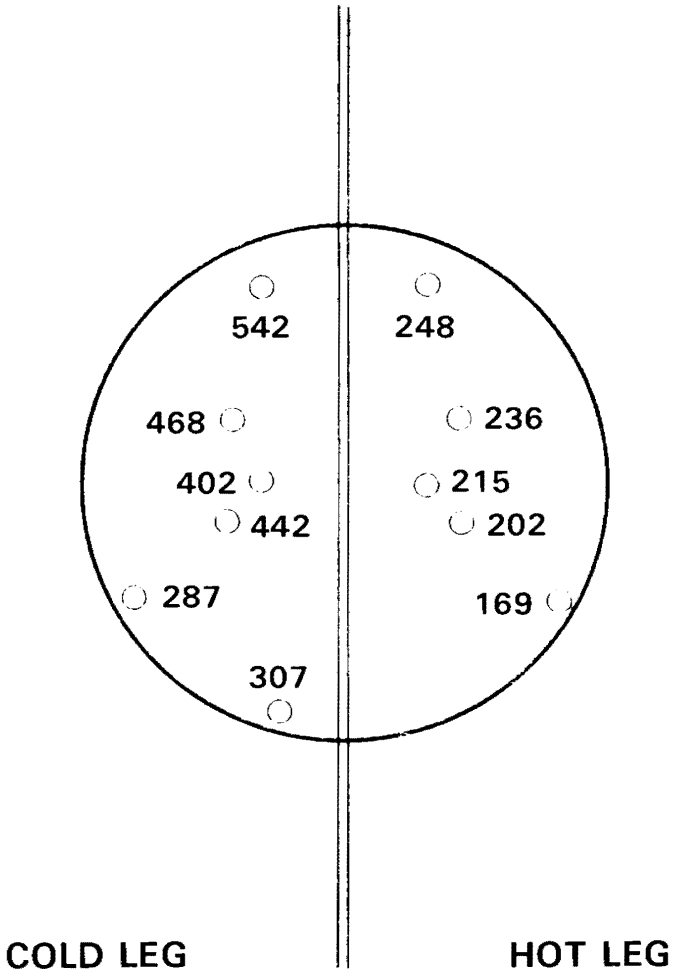

FIGURE 5-40.

DOSE RATE (mR/hr) IN CHANNEL HEAD 60 INCHES FROM TUBE SHEET, DIVIDER CLEANED AND LEAD PLUGS INSTALLED

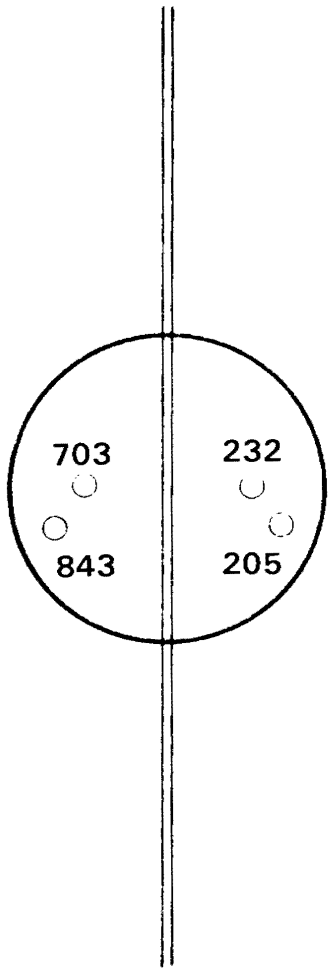

COLD LEG HOT LEG

FIGURE 5-41.

6. CORROSION TESTING AND WATER CHEMISTRY ANALYSES

This section of the report summarizes the results of the corrosion tests and film characterization studies conducted by PNL as part of the channel head decontamination task. For review, the cold leg decontamination was performed by London Nuclear Services, Inc. and the hot leg was decontaminated by Quadrex Corporation in cooperation with Babcock-Woodall Duckham, Ltd. (BWD) and the Central Electricity Generating Board (CEGB). The cold leg and hot leg were both decontaminated by two-step dilute chemical processes:

Cold Leg - The complete cycle involved a PWR film conditioning step followed by CAN-DECON. Two complete cycles were applied.

Hot Leg - 1) NP pre-treatment followed by LOMI.
2) AP, NP pre-treatment followed by Citrox.

London Nuclear used two different ion exchange beds as part of their process, while liquid waste from the Quadrex operation was stored in existing tankage.

Purpose

Uncertainties about the effects of chemical decontamination on reactor materials of construction have inhibited industry acceptance of chemical decontamination for operating plants. Chemical decontaminations have been applied to entire PHWR primary systems and on BWR subsystems (feedwater heaters). The decontamination of the Surry steam generator channel heads was the first full-scale application of chemical decontamination to a large component from a commercial U.S. PWR. These decontamination operations provided an opportunity to closely examine the corrosion effects of dilute chemical decontamination on PWR materials. The corrosion monitoring program for Task 6 had two aspects:

- Standard corrosion testing to determine the extent of corrosion of stainless steel, Inconel 600, and carbon steel caused by the chemical decontamination.
- Characterization of actual Surry steam generator specimens (before and after decontamination) to determine how chemical decontamination affected primary side surfaces.

Approach

The specific components of the corrosion testing and film characterization studies for both the cold leg and hot leg decontamination processes included:

- Racks containing both corrosion coupons and steam generator specimens were installed in the channel head during decontamination.

- Electrical resistance (corrosometer) corrosion probes made of 304 stainless steel and A-36 carbon steel (and Inconel 600 for the hot leg decontamination) were installed in the manway covers.

- Grab samples from the decontamination solutions were analyzed for dissolved metals and radioactivity.

- Channel head surfaces were smeared for deposited material and visually examined for corrosion after the decontamination.

- Specimens from the channel head bowl, tube sheet primary side surface, manway cover insert, and steam generator tubing were characterized before and after decontamination.

Assessments of the materials impacts of the two decontaminations were obtained using this multi-faceted approach.

Experimental Equipment and Methods

Corrosion coupons and coupon rack components were obtained from Metal Samples, Inc.; Table 6-1 lists the types of specimens included in the coupon racks for both decontaminations. Corrosion specimens were prepared in accordance with ASTM recommended practices G1, G30 and G58. Metal Samples, Inc. performed a sensitization heat treatment for selected stainless steel coupons (1 h at 650°C in air) and Inconel 600 coupons (12 h at 700°C in air). Inconel 600 and 304 stainless steel coupons that had been prefilmed in deionized water (300°C, 50 ppb dissolved oxygen, 800 h) were also included. The coupon racks also contained ring sections from a Surry steam generator tube (Inconel 600) and coupons cut from the manway cover inserts (304 stainless steel) for determining specimen decontamination factors. The coupon racks were suspended from the tube sheet as shown in Figure 2-5.

ASTM recommended practices G1, G4, and G38 were used as guidelines for conducting and evaluating the corrosion coupon tests. Corrosion coupons were degreased with methanol and weighed to the nearest 0.0001 g before and after decontamination. Stainless steel coupons from the hot leg manway cover insert were included in the hot leg coupon racks, and coupons from the cold leg manway cover insert were in the cold leg coupon racks. Inconel 600 ring sections from steam generator tube R1C94 were common to both racks. Selected manway coupons and ring sections that were used in the cold leg decontamination were recycled in the hot leg coupon racks to determine the effects of repeated decontamination. Selected coupons, and all steam generator specimens, were counted before and after the decontaminations to determine Co-60 levels. Selected carbon steel coupons were descaled to a constant weight with CP-9 (hydrochloric acid solution inhibited with formaldehyde) before reweighing. Coupons were examined under a microscope at magnifications up to 70X for pitting. U-bend specimens were cleaned with methanol and examined for cracking under a microscope using Spot-Check dye penetrant.

TABLE 6-1. Corrosion Coupons Used for the Surry Steam Generator Channel Head Decontaminations

Quantity	Coupon Type	Materials	Comments
4	Flat	304 stainless steel Sensitized 304 stainless steel 304L stainless steel Sensitized 304L stainless steel Inconel 600 Sensitized Inconel 600 A-36 carbon steel	Hot leg and cold leg
6	Flat, welded galvanic couple	304 stainless steel/Inconel 600 304 stainless steel/A-36 carbon steel	Hot leg and cold leg
2	U-bends	304 stainless steel Sensitized 304 stainless steel 304L stainless steel Sensitized 304L stainless steel Inconel 600 Sensitized Inconel 600 A-36 carbon steel	Hot leg and cold leg
4	U-bends, weld at the apex	304 stainless steel 304L stainless steel Inconel 600 Sensitized Inconel 600 A-36 carbon steel	Hot leg and cold leg
2	Prefilmed, flat	304 stainless steel Inconel 600	Hot leg and cold leg
4	Rings from a Surry steam generator tube	Inconel 600 (radioactive)	Hot leg and cold leg

TABLE 6-1. (Continued)

Quantity	Coupon Type	Materials	Comments
6	Coupons from manway cover inserts	Stainless steel (radioactive)	Hot leg and cold leg
4	Flat	309 stainless steel	Hot leg only
5	Flat	A-508 steel	Hot leg only
3	Surry steam generator tube rings previously decontaminated in the cold leg channel head	Inconel 600 (radioactive)	Hot leg only
3	Cold leg manway cover insert coupons previously decontaminated in the cold leg channel head	Stainless steel (radioactive)	Hot leg only

In general, identical testing procedures were used for both the cold and hot leg decontaminations. The only significant difference involved the post-decontamination handling of the corrosion coupons. The cold leg coupons were left in the channel head for three weeks before removal and evaluation while the hot leg coupons were removed immediately after the decontamination and stored in plastic bags for 10 days before evaluation. Unlike the hot leg corrosion coupons, the radioactive steam generator specimens were processed immediately after the hot leg decontamination. Storage of the hot leg coupons may have slightly affected the extent of the observed corrosion, but did not compromise the overall results as indicated by agreement between the corrosion coupons and 1) in situ inspection of the channel head surfaces, 2) corrosion on the steam generator specimens, 3) the corrosometer results, and 4) the water chemistry data.

Resistance element corrosion probes and a corrosometer (Rohrback Instruments) were used to follow real-time corrosion during the actual decontaminations. A corrosometer measures the increase in electrical resistance of a probe element due to corrosion. Since resistance is a function of cross-sectional area, penetration rates can be calculated from a plot of resistance as a function of time. Table 6-2 lists the materials and sensitivities for the corrosometer probes used in the hot leg and cold leg decontaminations. Linear polarization corrosion rate determinations were not made due to the anticipated strong redox nature of the decontamination solutions.

TABLE 6-2. Corrosometer Probes Used During the Surry Channel Head Decontaminations

Number	Rohrback Model Number	Material	Type	Penetration Sensitivity (μm)	Comments
1-1	37424/8002/T-20	carbon steel	tube	0.25	cold leg
1-2	20534/8013/W-40	304 stainless steel	wire	0.25	cold leg
1-3	20534/8014/W-40	304L stainless steel	wire	0.25	cold leg
2-1	20534/8057/W-40	Inconel 600	wire	0.25	hot leg
2-2	20534/8003/W-40	carbon steel	wire	0.25	hot leg
2-3	20534/8013/T-4	304 stainless steel	tube	0.05	hot leg

Radioactivity (Co-60) measurements on the corrosion specimens and Surry steam generator specimens were made using a Ge(Li) gamma detector and multi-channel analyzer. Dissolved metals in the decontamination solutions were determined using flame atomic absorption spectrometry (AAS), which had a 0.1 ppm detection limit. Deposits on channel head smears were qualitatively analyzed using bulk energy-dispersive X-ray fluorescence (XRF). Specimens were also characterized using X-ray diffraction (XRD) and scanning electron microscopy (SEM) with energy dispersive X-ray analysis (EDX). Approximate compositions (weight percents) were calculated from baseline-corrected Kα X-ray peak height ratios. Although this method systematically overestimates Cr, and underestimates Ni, it provides a basis for determining trends between closely related specimens.

Corrosion Coupons

Inconel 600, 304 stainless steel, and A-36 carbon steel were common to both hot and cold leg decontaminations. Coupons of 309 stainless steel and A-508 steel were also included in the hot leg corrosion racks. Inconel is used for the tube sheet cladding and divider plate. The channel head bowl is made of 309 stainless steel cladding over A-508 steel. Since 309 stainless steel has better corrosion characteristics than 304 stainless steel, tests using 304 stainless steel are conservative. Both A-36 and A-508 carbon steel corrosion coupons behaved similarly during the hot leg decontamination.

Overall corrosion coupon results for the hot leg and cold leg decontaminations were as follows:

- Carbon steel uniformly corroded during both decontaminations.

- Trace films formed on stainless steel (both sensitized and mill annealed) during both decontaminations. The filming (or staining) was more pronounced after the hot leg decontamination than after the cold leg decontamination.

- Generalized superficial pitting of Inconel 600 (both sensitized and mill annealed) occurred during the hot leg decontamination (4-6 μm penetration), and surface staining occurred during the cold leg decontamination. Inconel 600 corrosion during the hot leg decontamination was similar to that previously reported for the $HNO_3/KMnO_4$ POD process (Pick 1982).

- Metallographic cross sections of specimens from both decontaminations showed no intergranular (IG) attack.

- Dark brown deposits (probably manganese dioxide) were found in crevice regions after both the hot and cold leg decontaminations.

  In all cases, corrosion in crevice regions was less than that on exposed surfaces.

- Carbon steel corrosion was similar for both the cold leg and hot leg processes, as was stainless steel corrosion. Inconel 600 showed more susceptibility to corrosion (superficial pitting) under the hot leg process than under the cold leg process. A separate EPRI program, RP2296-4, is currently underway to better evaluate the corrosion characteristics of the NP/LOMI portion of the process used in the hot leg decontamination.

Cold Leg Weight Loss Coupons

The range of average penetrations (calculated from corrosion coupon weight losses) are shown in Figure 6-1: 80 μm for A-36 carbon steel, 0.05 μm for 304 stainless steel (sensitization slightly decreased the range of calculated penetrations for both 304 and 304L), and 0.15 μm for Inconel 600 (sensitization also decreased the range of observed weight losses). Significant radioactivity was deposited on the corrosion specimens as a result of the cold leg decontamination. Figure 6-2 summarizes measured dose rates (mR/h) at contact on the cold leg corrosion coupons after decontamination; A-36 carbon steel had more deposited activity than either stainless steel or Inconel 600. Comparison of Figure 6-2 with Figure 6-1 shows that the level of deposited radioactivity correlates with the extent of corrosion on the coupons, suggesting a surface roughness effect.

Significant dark brown deposits (probably manganese dioxide) were found in the crevice regions between the Teflon insulating spacers and the coupons after both the hot leg and cold leg decontaminations. These deposits were easily removed with a wet paper towel and tended to protect the underlying base metal from corrosion. About 50% of the deposited radioactivity was located in those regions. Figure 6-3 shows that a heavier tarnish formed on Inconel 600 than on stainless steel. Galvanic coupling of A-36 carbon steel with 304 stainless steel increased the stainless steel corrosion, while 304 stainless steel and Inconel 600 galvanic coupling did not (Figure 6-3). A highly-radioactive, powdery deposit was also found on the exposed coupon surfaces after decontamination, as seen on the endplate of rack #2 in Figure 6-4.

Hot Leg Weight Loss Coupons

As shown in Figure 6-1, average penetrations were about five times higher for the 304 stainless steel and Inconel 600 specimens exposed in the hot leg than for those exposed in the cold leg. However, even the hot leg penetrations were still relatively small (<1.0 μm). Corrosion coupon data indicated that 309 stainless steel penetrations were lower than 304 stainless steel penetrations. This suggests that extrapolation of corrosion tests based on 304 stainless steel to actual steam generators, having 309 stainless steel cladding, should be conservative. Corrosion of A-508 and A-36 steel was similar, with uniform penetrations of 40 to 60 μm.

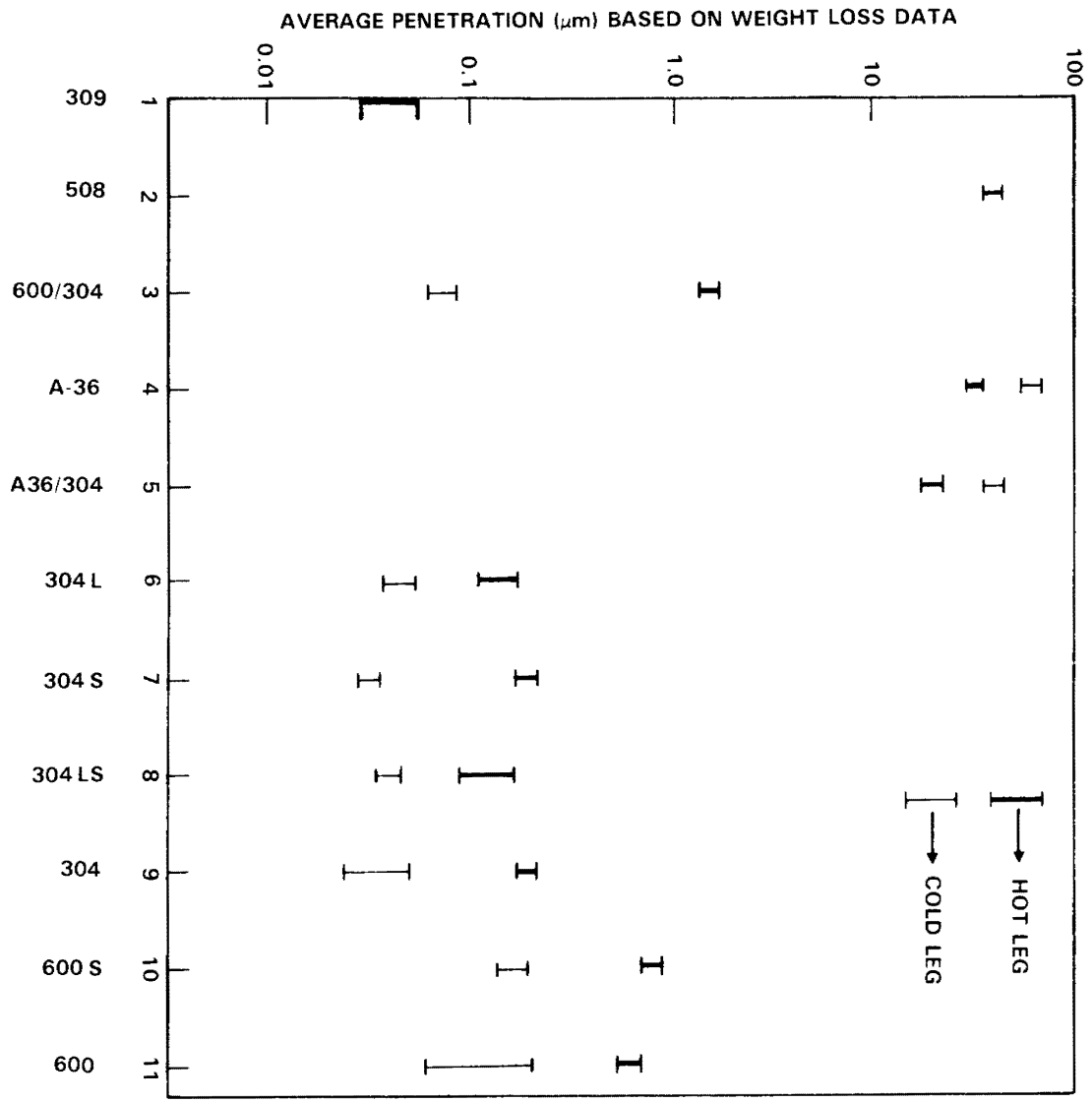

FIGURE 6-1. Corrosion Coupon Penetrations Based on Weight Loss Data

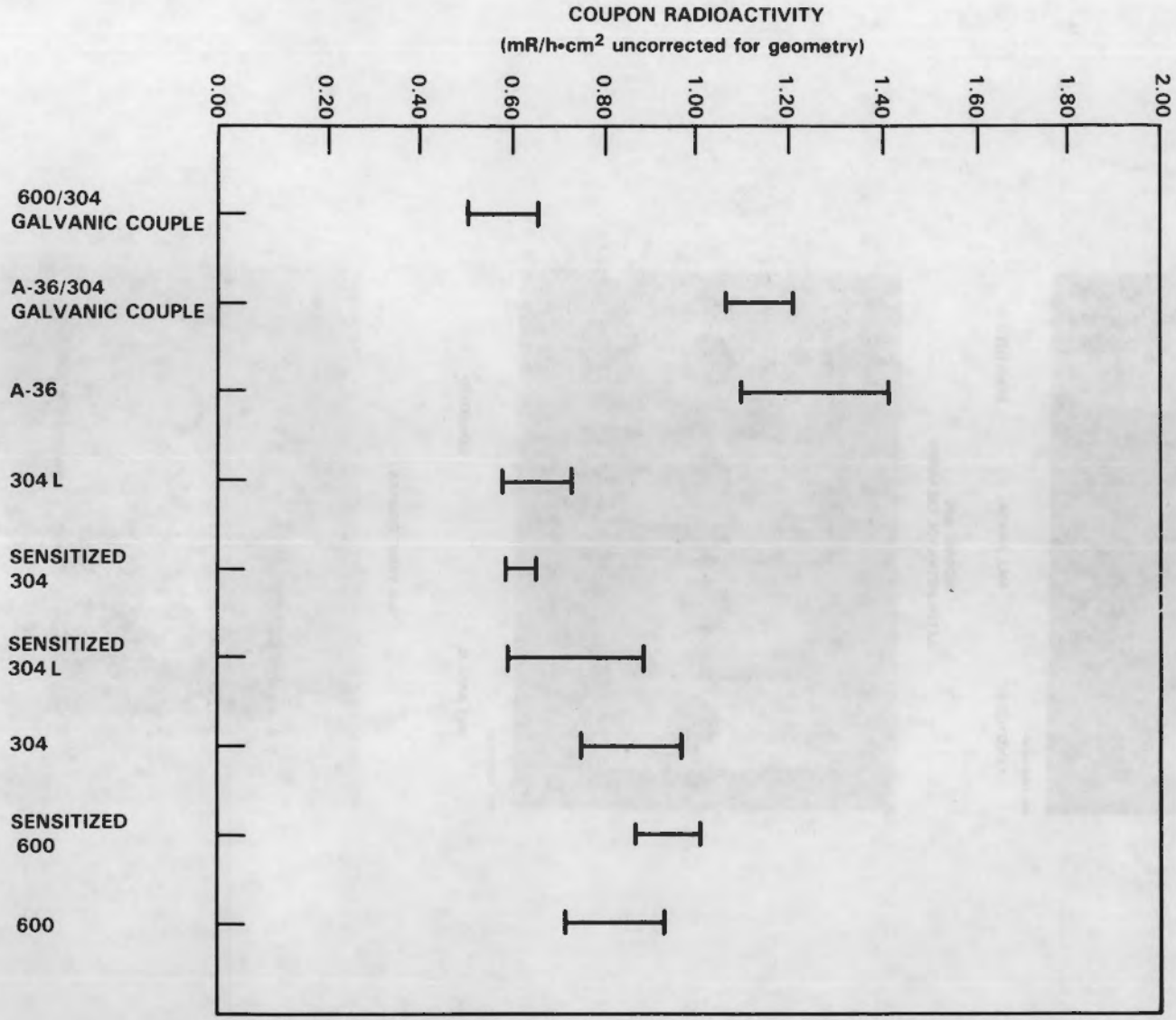

FIGURE 6-2. Deposited Radioactivity on Corrosion Coupons After the Cold Leg Decontamination

304 AND 304L STAINLESS STEEL
(AFTER METHANOL CLEANING)

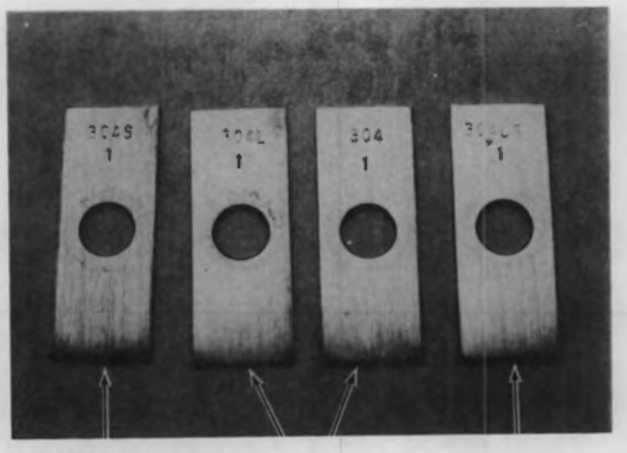

NEG. 8208355-50

SENSITIZED MILL ANNEAL SENSITIZED

INCONEL 600
(AFTER METHANOL CLEANING)

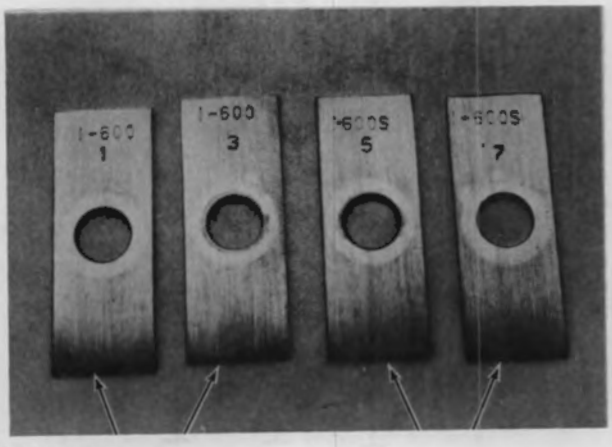

NEG. 8208355-20

MILL ANNEAL SENSITIZED

GALVANIC COUPLES

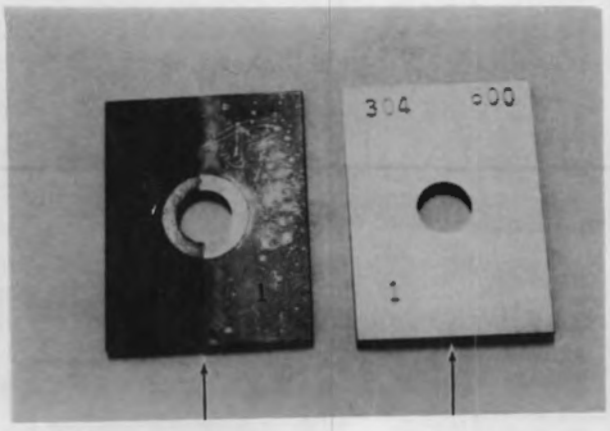

NEG. 8208355-51

DESCALED
A-36/304

METHANOL CLEANED
304/INCONEL 600

FIGURE 6-3. Corrosion Coupon Appearance After the Cold Leg Decontamination

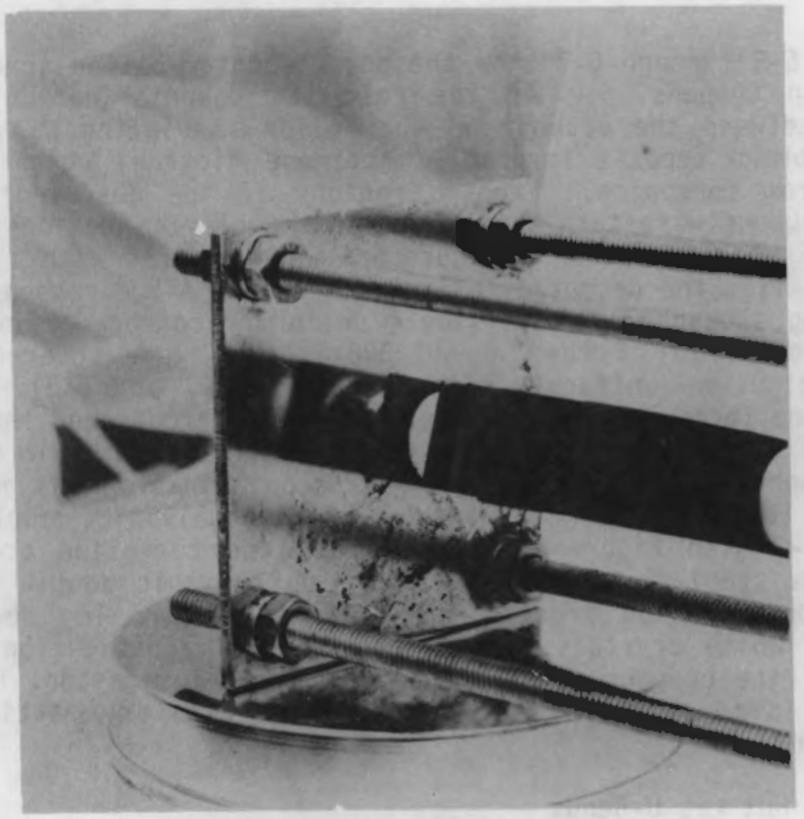

RACK #2

NEG. 8206771-63

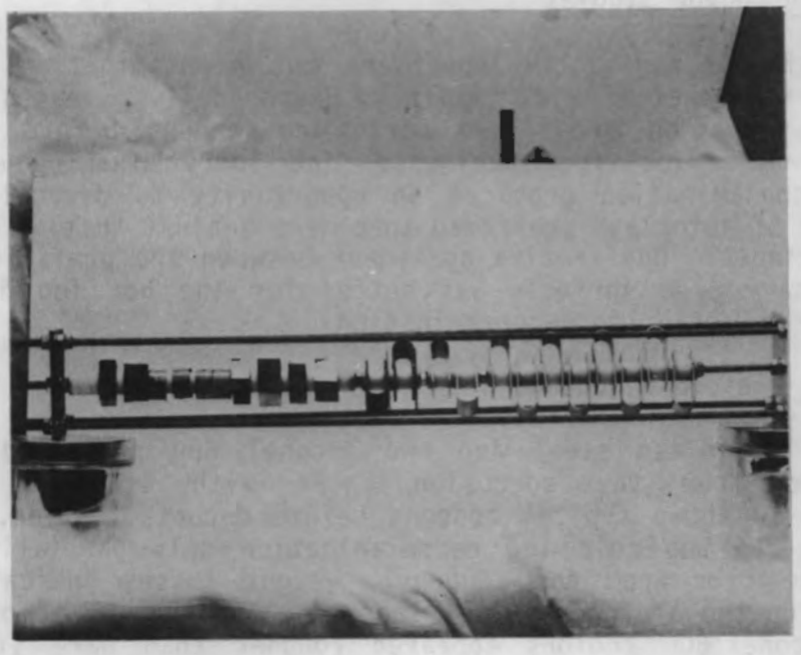

RACK #3

NEG. 8206771-3

FIGURE 6-4. Corrosion Coupon Rack Appearance After the Cold Leg Decontamination

Figures 6-5 through 6-7 show the post-decontamination appearance of the corrosion coupons. As in the cold leg decontamination, the crevice region between the coupon and the Teflon insulating washer was filled with a brown deposit (probably manganese dioxide) which protected the metal from corrosion. Exposed regions of the descaled 304 stainless steel coupons were tarnished, but not the crevice regions (Figure 6-5). The A-36 steel coupons in Figure 6-6 were covered with a powdery black deposit after the decontamination as were the A-508 coupons (not shown). Descaling showed that both steels uniformly corroded during the decontamination. All of the Inconel 600 coupons were covered with a dark film, which was uniformly pitted (Figures 6-7 and 6-8). Corrosion on sensitized Inconel coupons was slightly more pronounced than on the mill annealed specimens. For comparison, the superficial film on the Inconel 600 coupons following the cold leg decontamination was much less pronounced (Figure 6-3). Comparison of the galvanic couple coupons in Figure 6-9 with Figure 6-3 shows that less corrosion occurred on the stainless steel portion of the A-36/304 galvanic couple after the hot leg decontamination process than after the cold leg decontamination. Residual white crystals were found (at 70X magnification) on the surfaces of the coupons after the hot leg decontamination; however, these crystals did not appear to be associated with any particular type of corrosion.

Cold and Hot Leg U-Bends

No U-bend (ASTM G-30) failures were observed with the stainless steel, carbon steel or Inconel 600 specimens after either the cold leg or hot leg decontamination.

Prefilmed Coupon Studies

Acquisition of radioactive specimens for decontamination reagent development is generally difficult. Historically, reagent development efforts focus on pre-filmed corrosion coupons before proceeding to studies on radioactive specimens. The Surry steam generator channel head decontamination provided an opportunity to directly compare the behavior of autoclave prefilmed specimens against that of actual primary side surfaces. Qualitative agreement between the prefilmed coupons and the primary side surfaces was better for the hot leg decontamination than for the cold leg decontamination.

Cold Leg Prefilmed Coupons

Two 304 stainless steel and two Inconel 600 prefilmed coupons were suspended from the corrosion racks with stainless steel wire. Figure 6-10 shows typical coupons before decontamination. As shown in Figure 6-11, the cold leg decontamination only partially removed the autoclave film from the coupons. Weight losses indicated more film removal on the stainless steel specimens than on the Inconel ones. The bare Inconel 600 regions appeared rougher than bare stainless steel areas (Figure 6-12). Although the stainless steel and Inconel 600 coupons were partially defilmed (as were the steam generator specimens),

MILL ANNEALED COUPONS

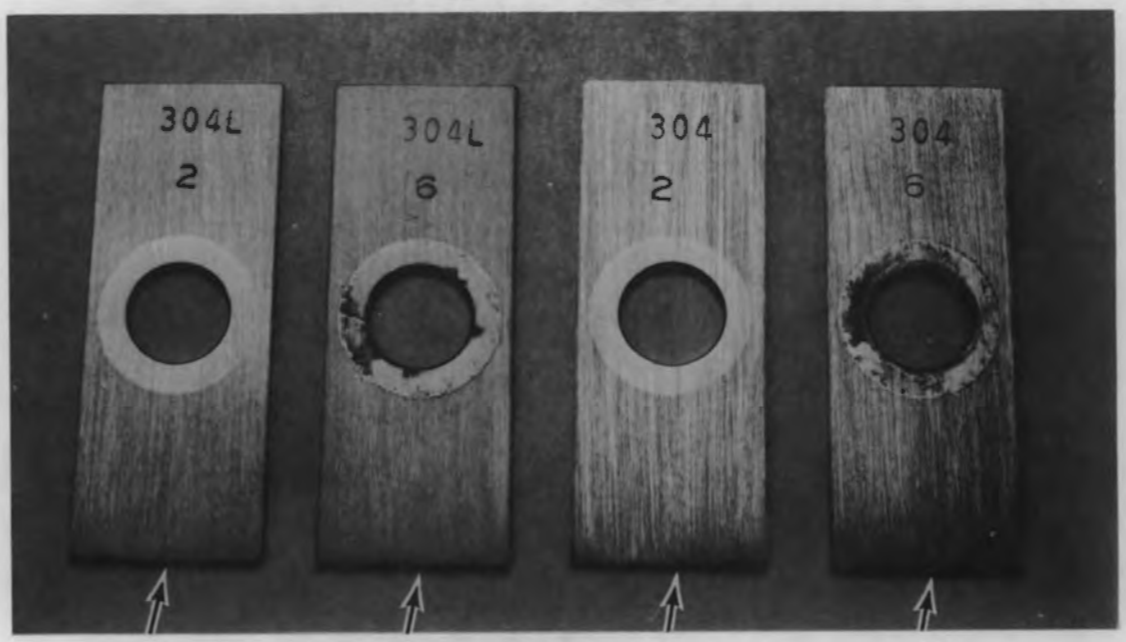

NEG. 8208355-47

METHANOL CLEANED 304	AS REMOVED 304	METHANOL CLEANED 304L	AS REMOVED 304L

SENSITIZED COUPONS

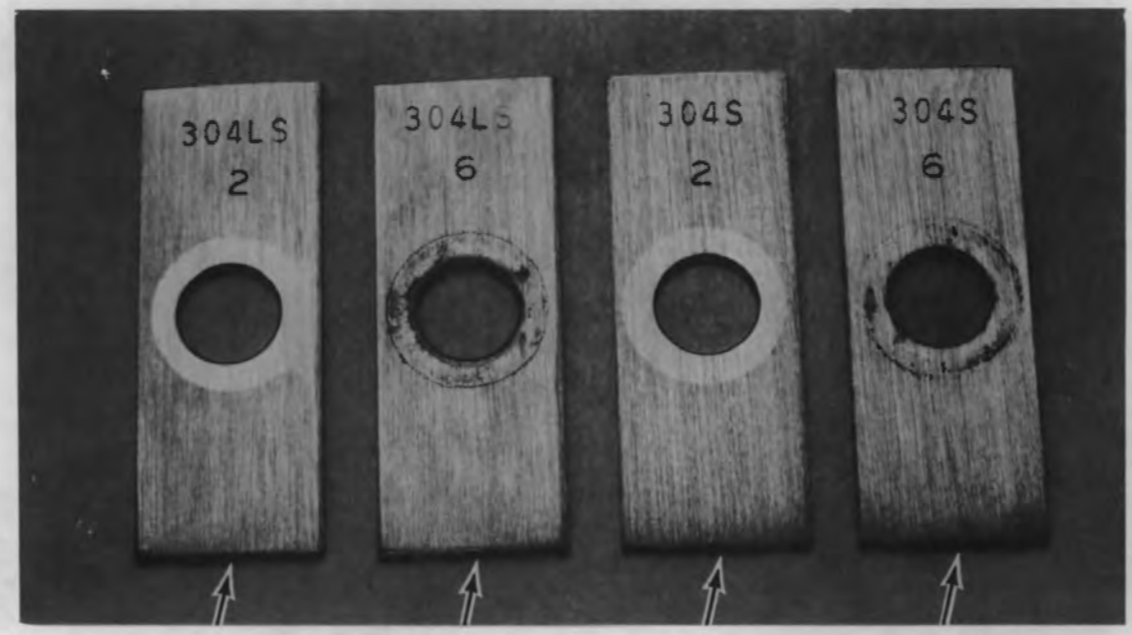

NEG. 8208355-46

METHANOL CLEANED	AS REMOVED 304L	METHANOL CLEANED	AS REMOVED 304

FIGURE 6-5. 304 Stainless Steel Corrosion Coupon Appearance After the Hot Leg Decontamination

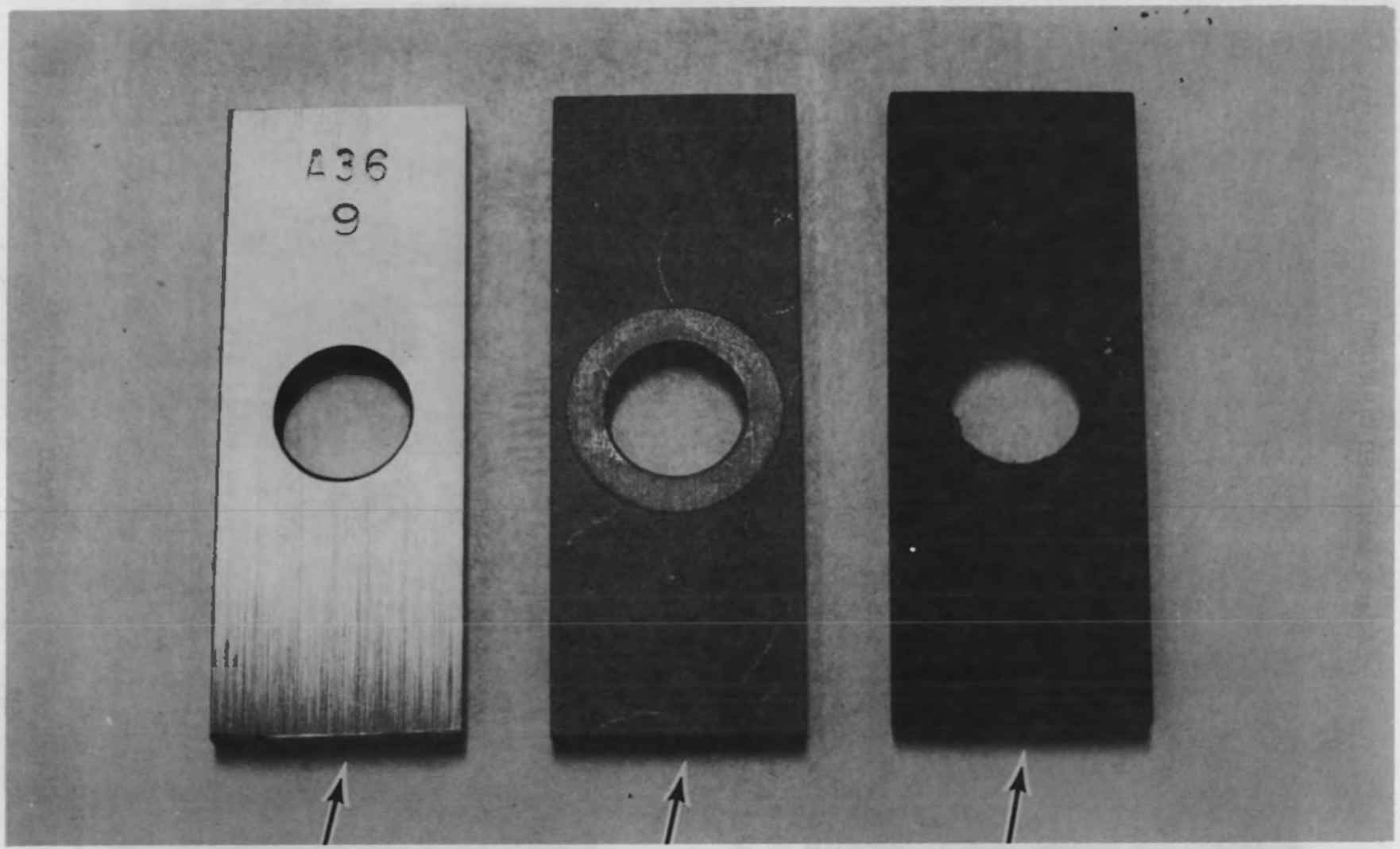

FIGURE 6-6. A-36 Carbon Steel Corrosion Coupon Appearance After the Hot Leg Decontamination

MILL ANNEAL

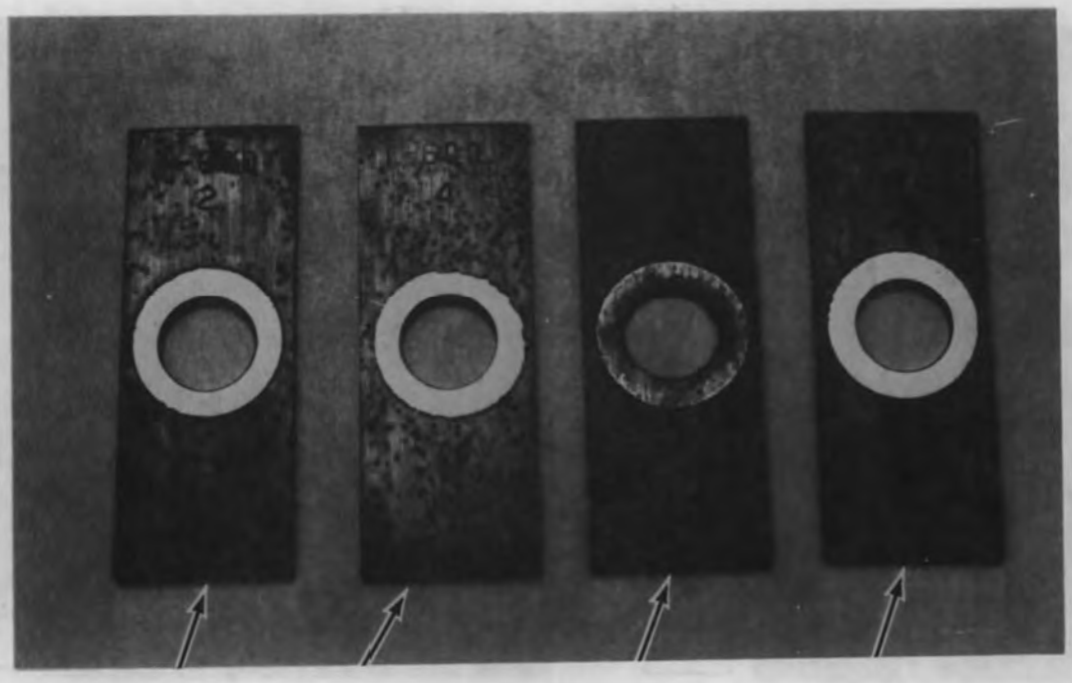

NEG. 8208355-17

DESCALED DESCALED AS REMOVED DESCALED

SENSITIZED

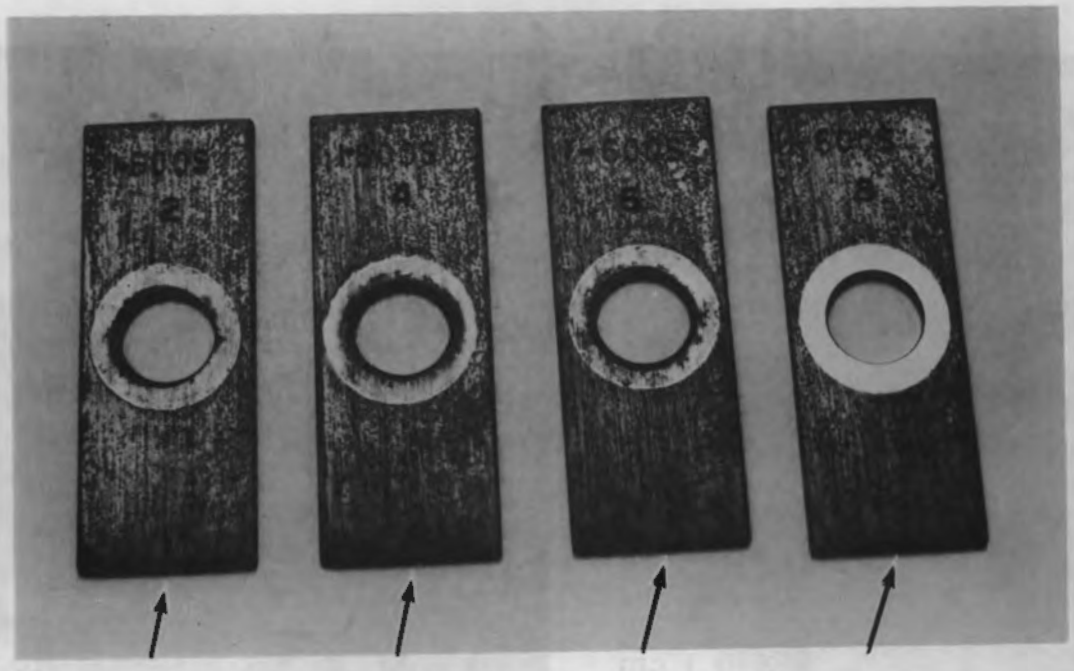

NEG. 8208355-21

AS REMOVED AS REMOVED AS REMOVED DESCALED

FIGURE 6-7. Inconel 600 Corrosion Coupon Appearance After the Hot Leg Decontamination

MILL ANNEAL

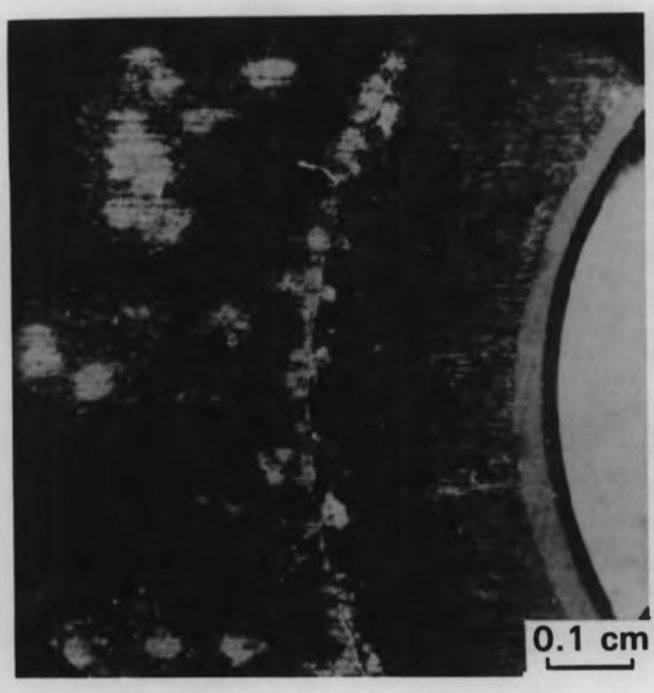

I600-6

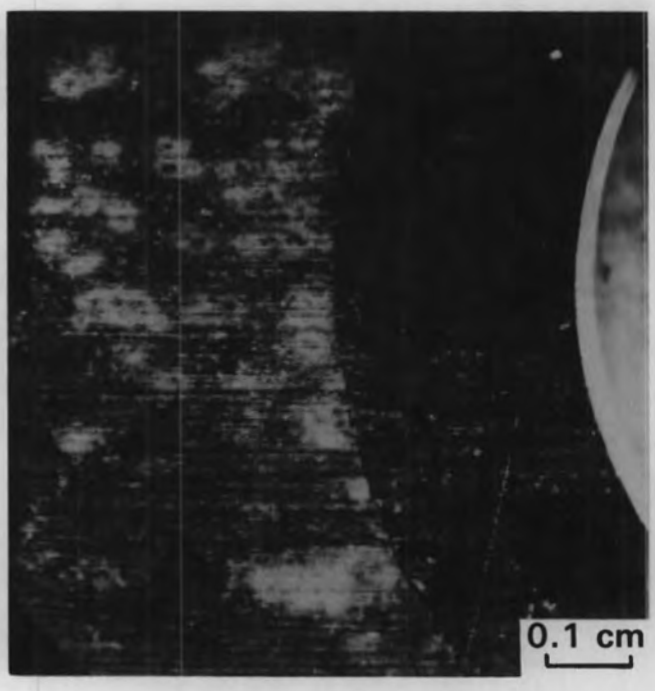

I600-8

SENSITIZED

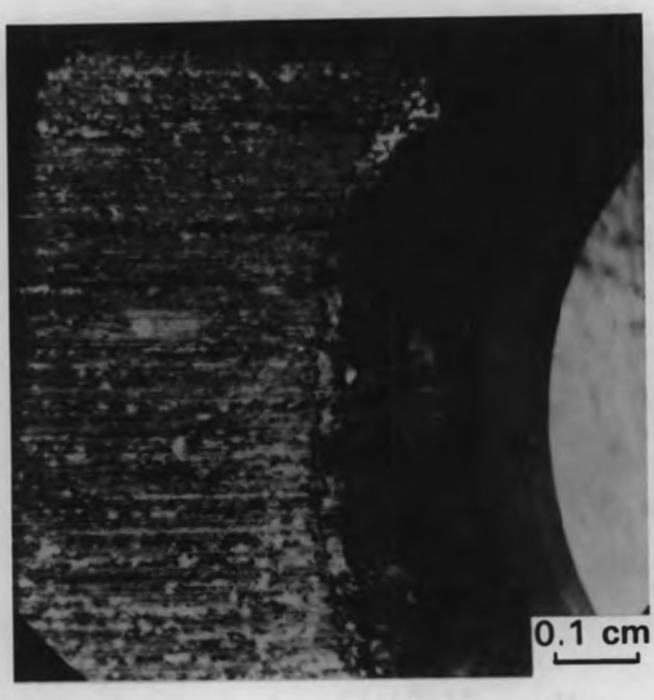

I600S-6

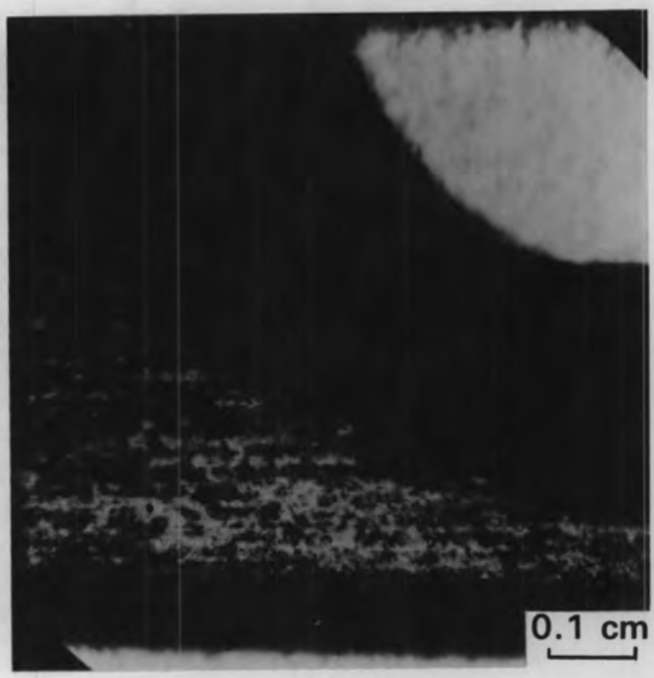

I600S-6

FIGURE 6-8. Inconel 600 Corrosion Coupon Appearance After the Hot Leg Decontamination

304/A-36 GALVANIC COUPLE

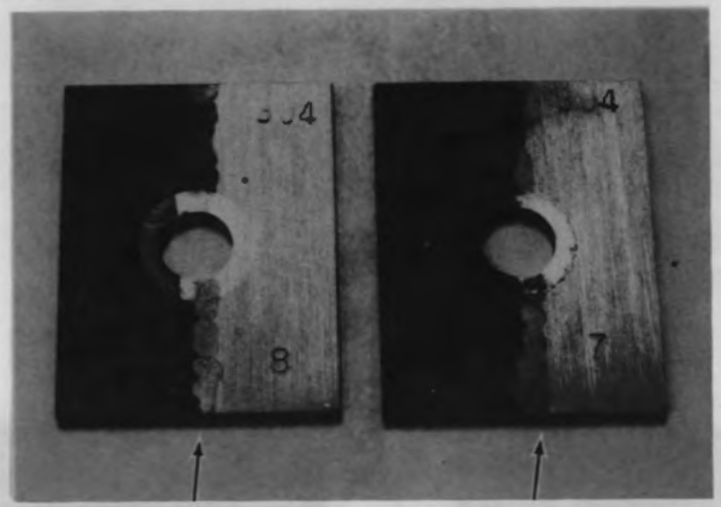

NEG. 8208355-31

DESCALED AS REMOVED

304/INCONEL 600 GALVANIC COUPLE

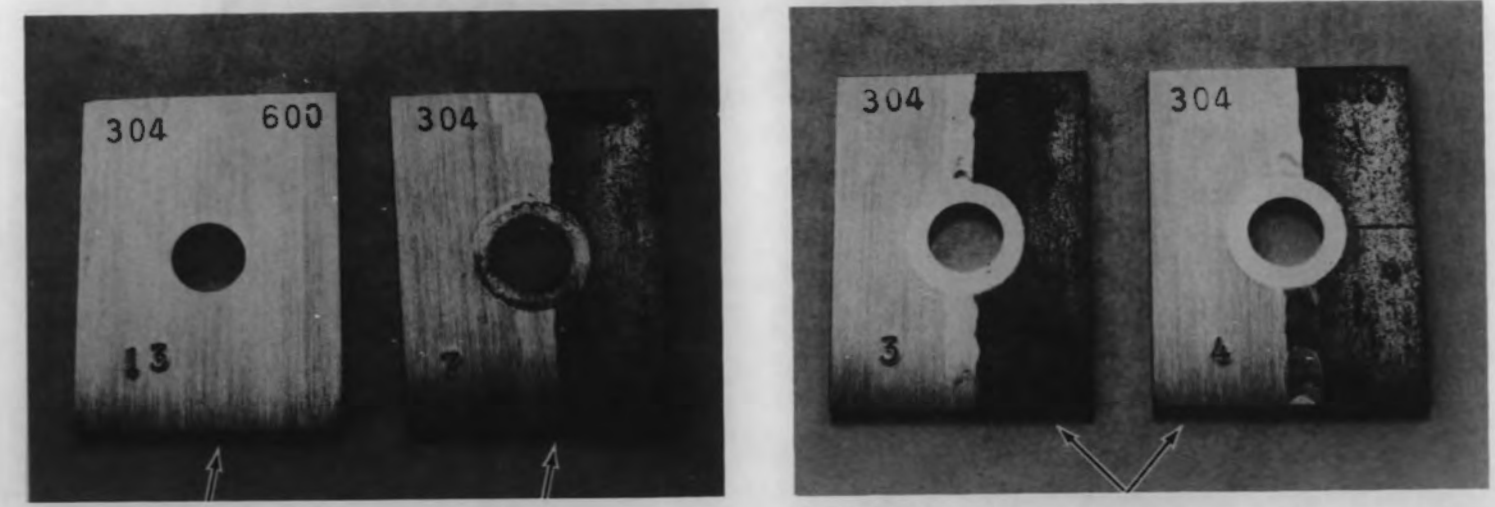

NEG. 8208355-25

UNEXPOSED AS REMOVED DESCALED

FIGURE 6-9. Galvanic Couple Corrosion Coupon Appearance After the Hot Leg Decontamination

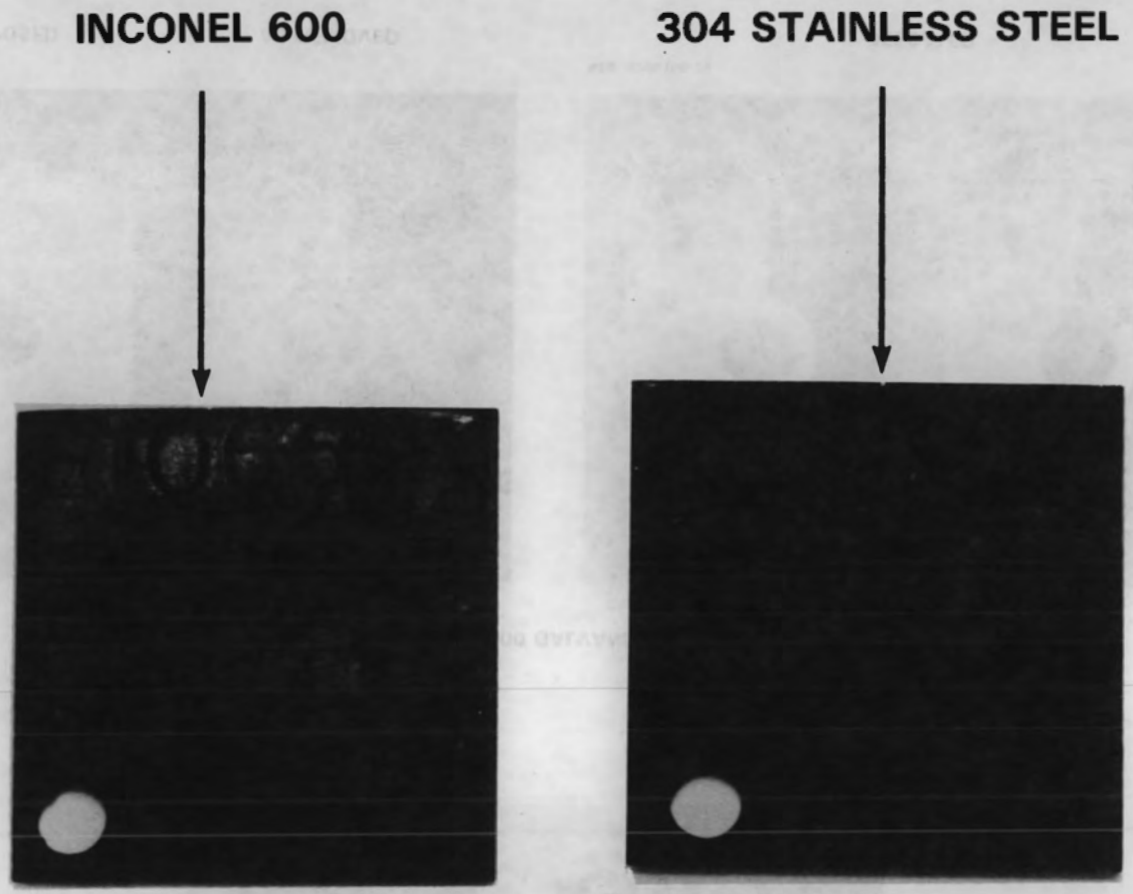

NEG 8208355-33

FIGURE 6-10. Appearance of the Prefilmed Coupons Before Decontamination

STAINLESS STEEL

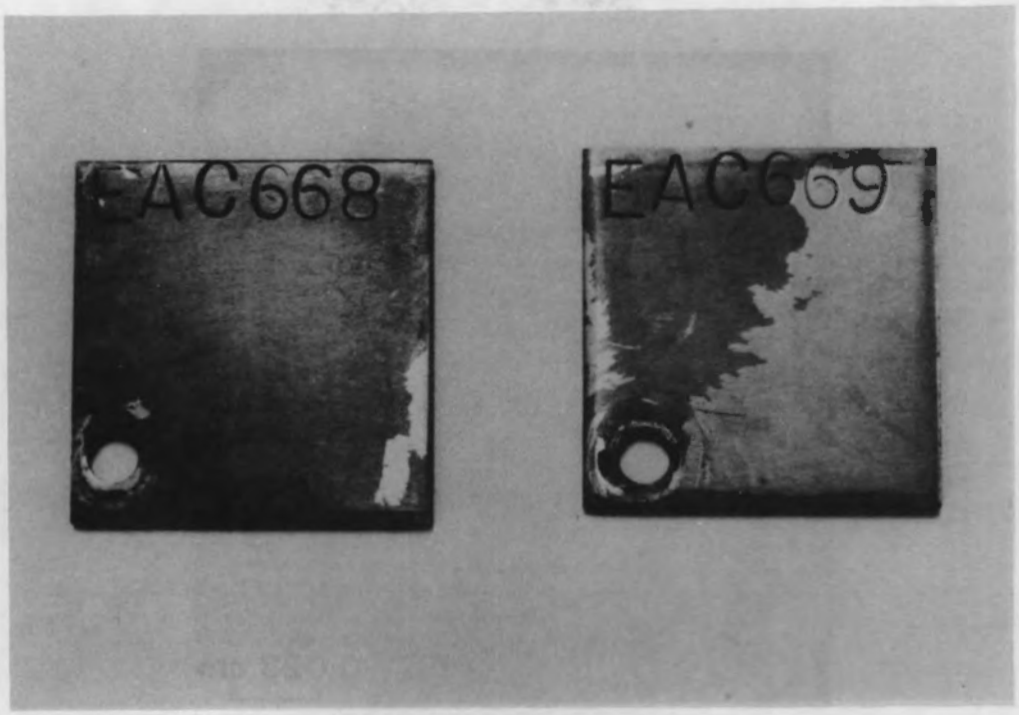

NEG. 8208355-13

INCONEL 600

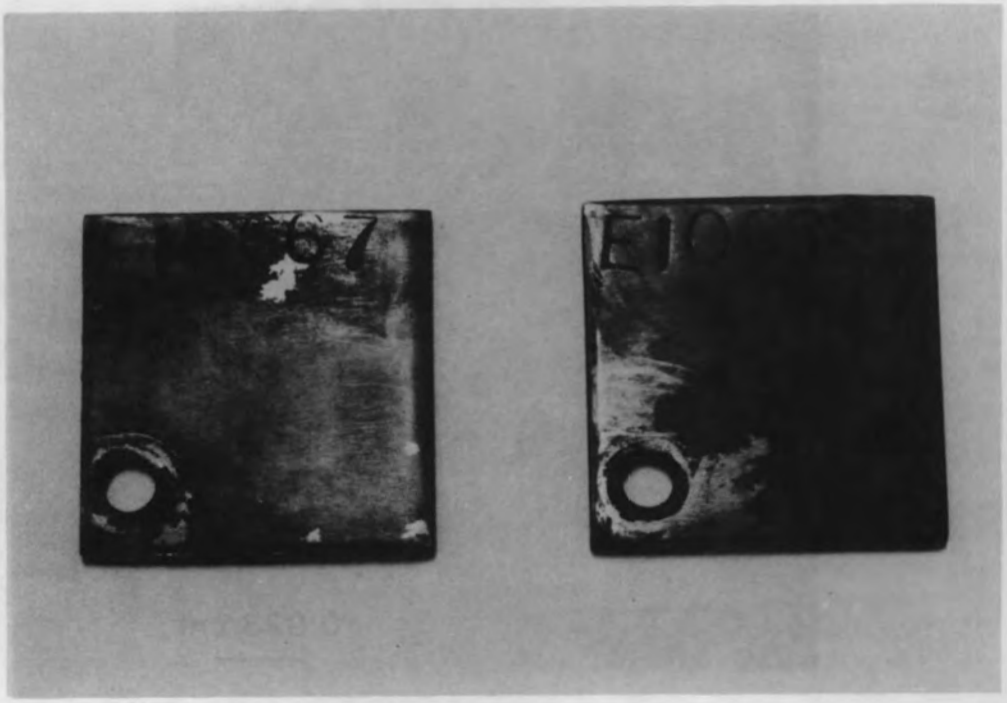

NEG. 8208355-5

FIGURE 6-11. Appearance of the Prefilmed Corrosion Coupons After the Cold Leg Decontamination

STAINLESS STEEL

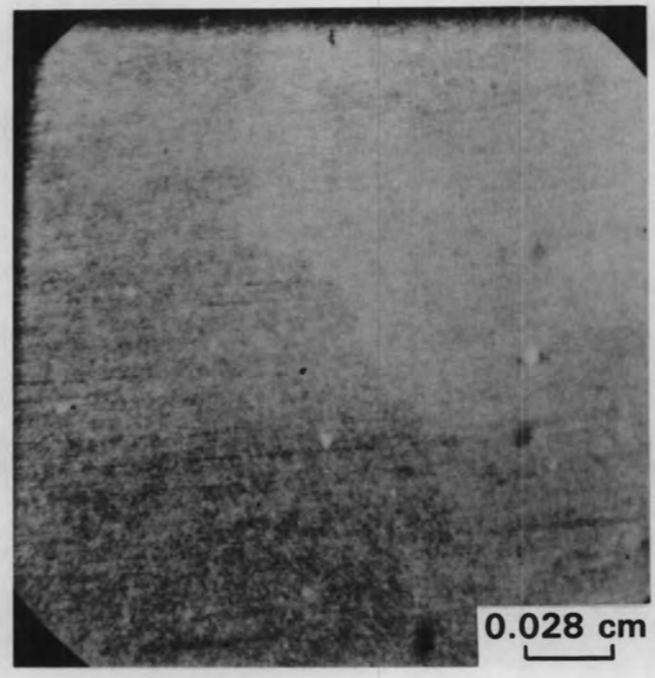

EAC-669

INCONEL 600

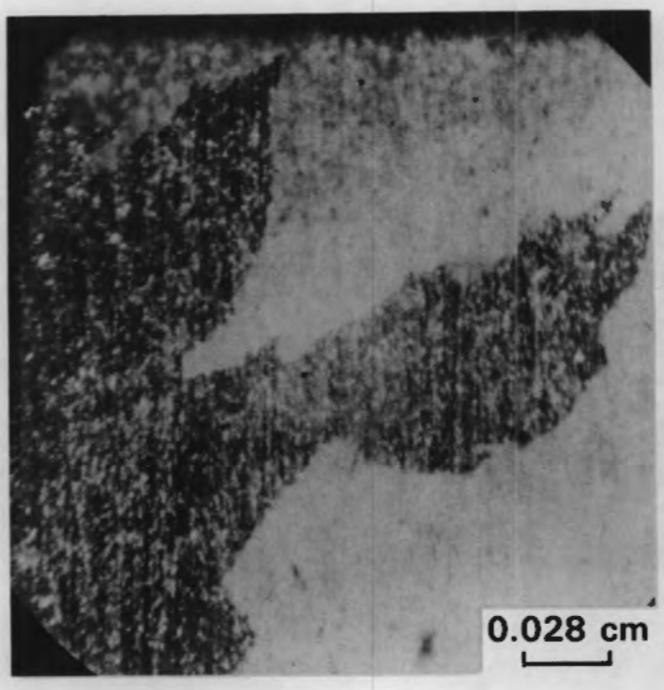

EIO-667

FIGURE 6-12. Prefilmed Corrosion Coupons After the Cold Leg Decontamination

differences between the coupons were much less than those between the stainless steel manway insert coupons and the Inconel 600 tube specimens (see Section 7).

Hot Leg Prefilmed Coupons

Results from the prefilmed coupons paralleled those for the hot leg weight loss coupons and steam generator specimens. The surface film was completely removed from the 304 stainless steel specimens and 95% removed for the Inconel 600 specimens (Figure 6-13). Very slight random staining occurred on the stainless steel specimens while uniform superficial pitting occurred on the Inconel specimens (Figure 6-14). Significantly, very little pitting occurred in regions covered by residual film. Film removal characteristics for the Inconel and stainless steel coupons showed greater similarity than for the manway coupons and steam generator tube specimens.

The defilming characteristics of the coupons for both the cold and hot leg decontaminations suggest that the stainless steel coupons predict stainless steel decontamination well. While the Inconel 600 steam generator coupons qualitatively matched with the Inconel 600 steam generator tube specimens, more film removal occurred on the coupons than on the tube specimens. This may have been due, in part, to the placement of the steam generator tube specimens or to differences between the coupon prefilm and the steam generator tube primary side film.

Real-Time Corrosion Monitoring

Corrosometers were used to follow real-time corrosion during both the hot and cold leg decontaminations. Probes of 1020 carbon steel, 304 stainless steel, and 304L stainless steel were used for the cold leg decontamination. An Inconel 600 probe was not available at the time of the cold leg decontamination, and corrosometer data was obtained for only the first full process cycle due to equipment availability. Inconel 600, 304 stainless steel, and 1020 carbon steel probes were used for the hot leg decontamination.

Cold Leg Corrosometer Results

Figure 6-15 shows carbon steel penetration (based on corrosometer readings) as a function of time for the initial cycle of the cold leg decontamination, and indicates that carbon steel corroded primarily during the reducing phases of the cold leg process. No attack on stainless steel was detected (304 or 304L) during this decontamination by the corrosometer (0.25 μm detection limit), which agrees with the coupon data.

Hot Leg Corrosometer Results

Figures 6-16 through 6-18 show metal penetration (based on corrosometer data) for carbon steel, Inconel 600 and 304 stainless steel as a function of time during the hot leg decontamination. Figure 6-16 shows that for carbon steel:

STAINLESS STEEL

NEG. 8208355-9

INCONEL 600

NEG. 8208355-1

FIGURE 6-13. Prefilmed Corrosion Coupons After the Hot Leg Decontamination

STAINLESS STEEL

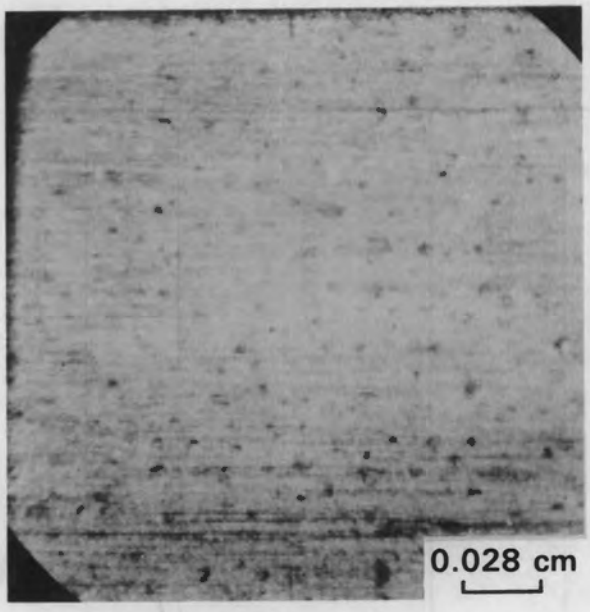

EAC-666

INCONEL 600

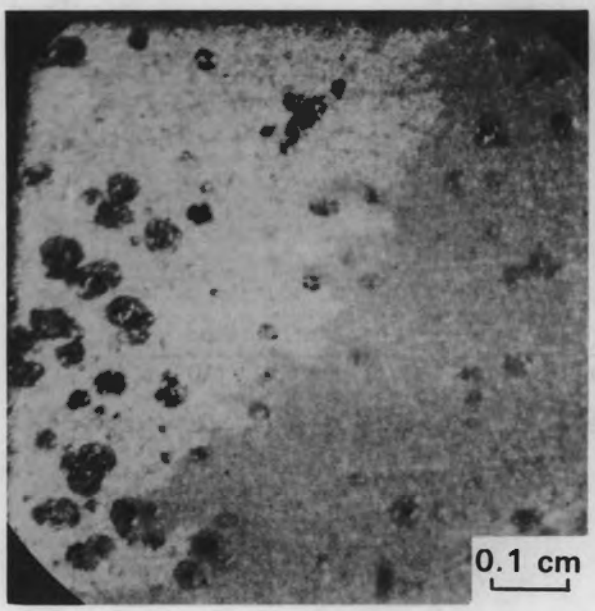

EIO-666

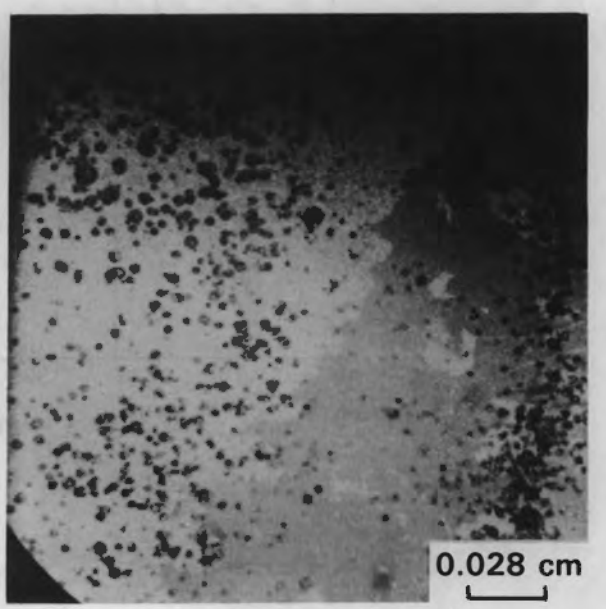

EIO-666

FIGURE 6-14. Prefilmed Corrosion Coupons After the Hot Leg Decontamination

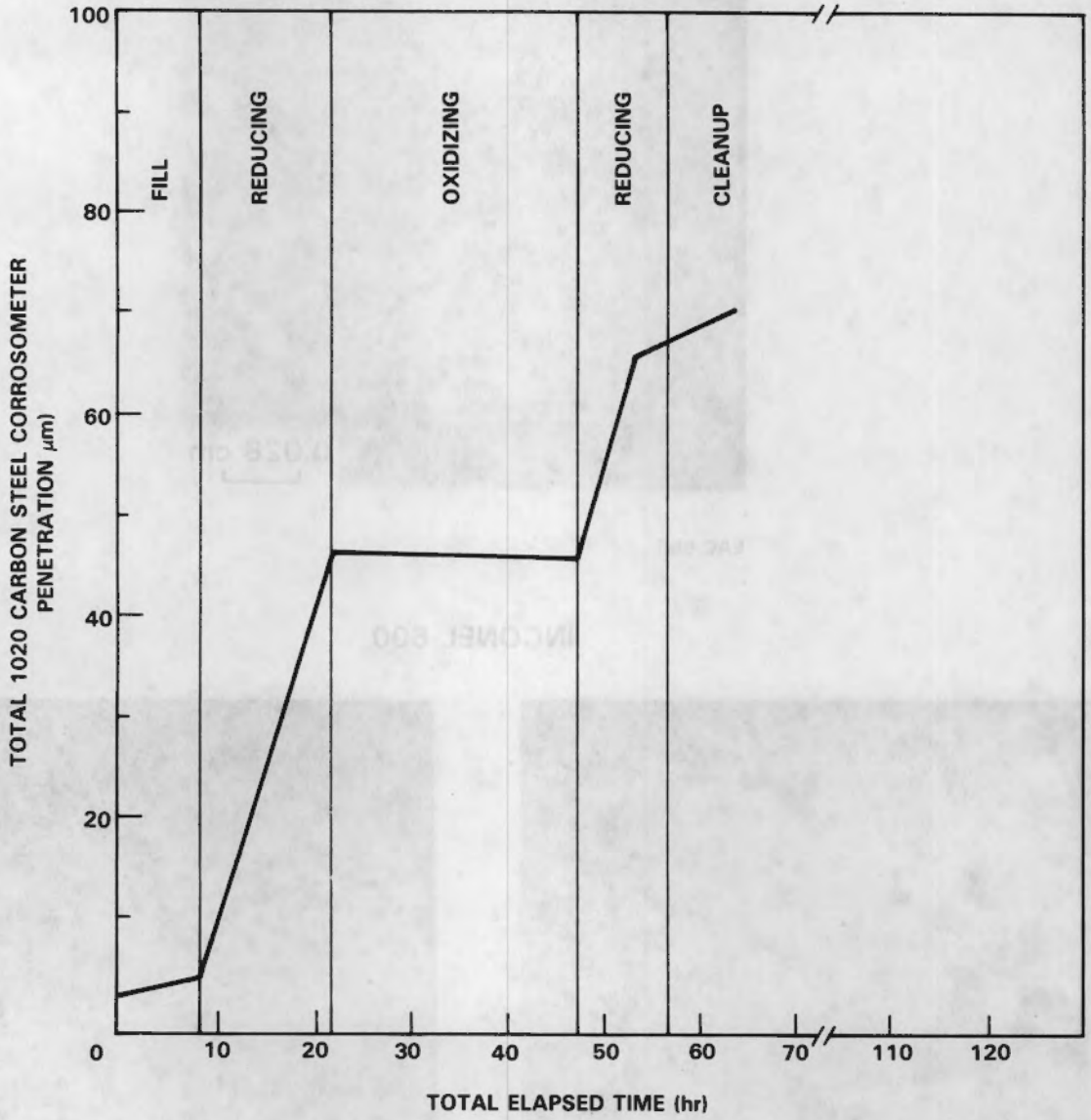

FIGURE 6-15. Total Corrosometer Penetration for 1020 Carbon Steel During the First Cold Leg Decontamination Cycle

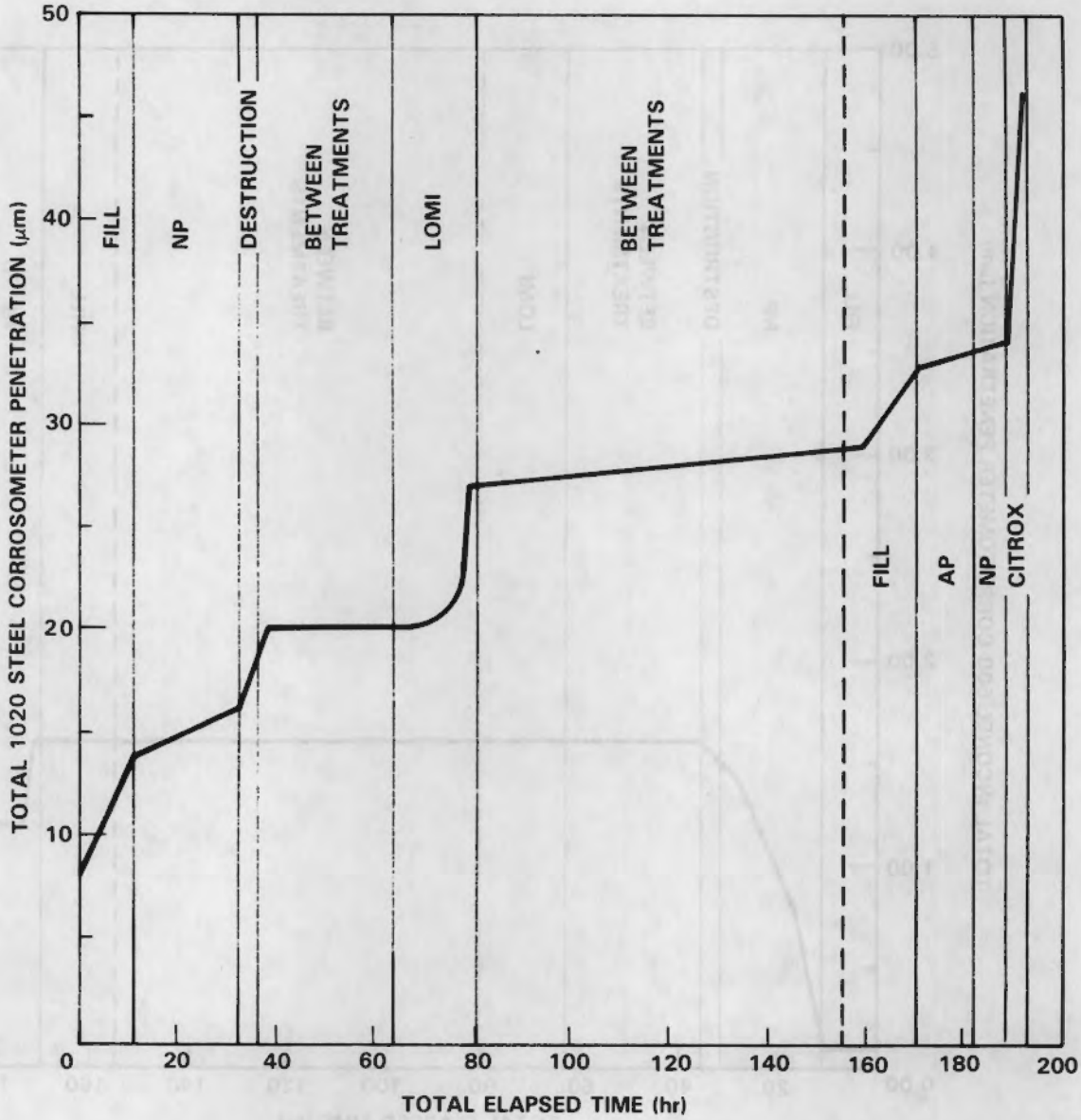

FIGURE 6-16. Total Corrosometer Penetration for 1020 Carbon Steel During the Hot Leg Decontamination

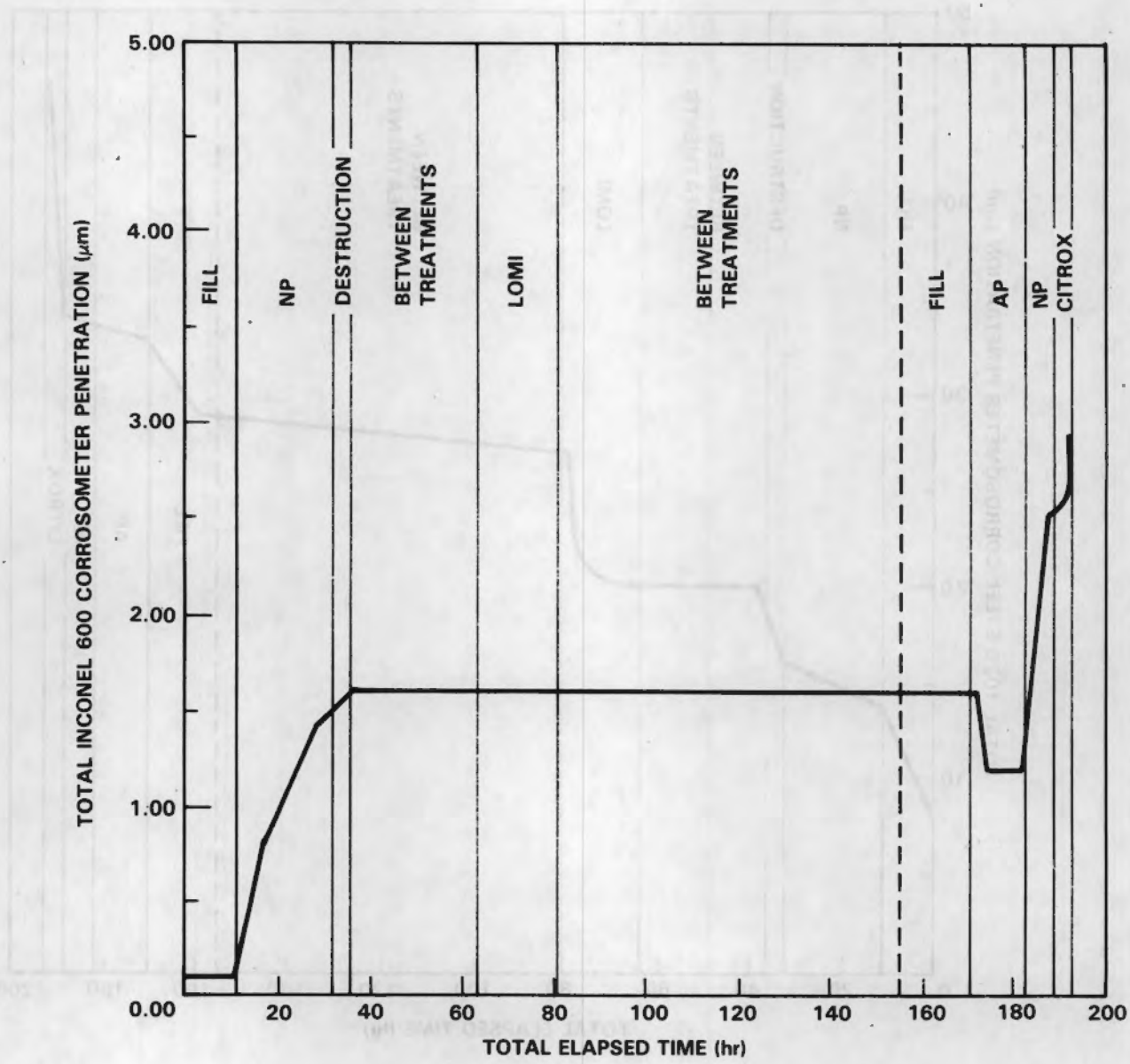

FIGURE 6-17. Total Corrosometer Penetration for Inconel 600 During the Hot Leg Decontamination

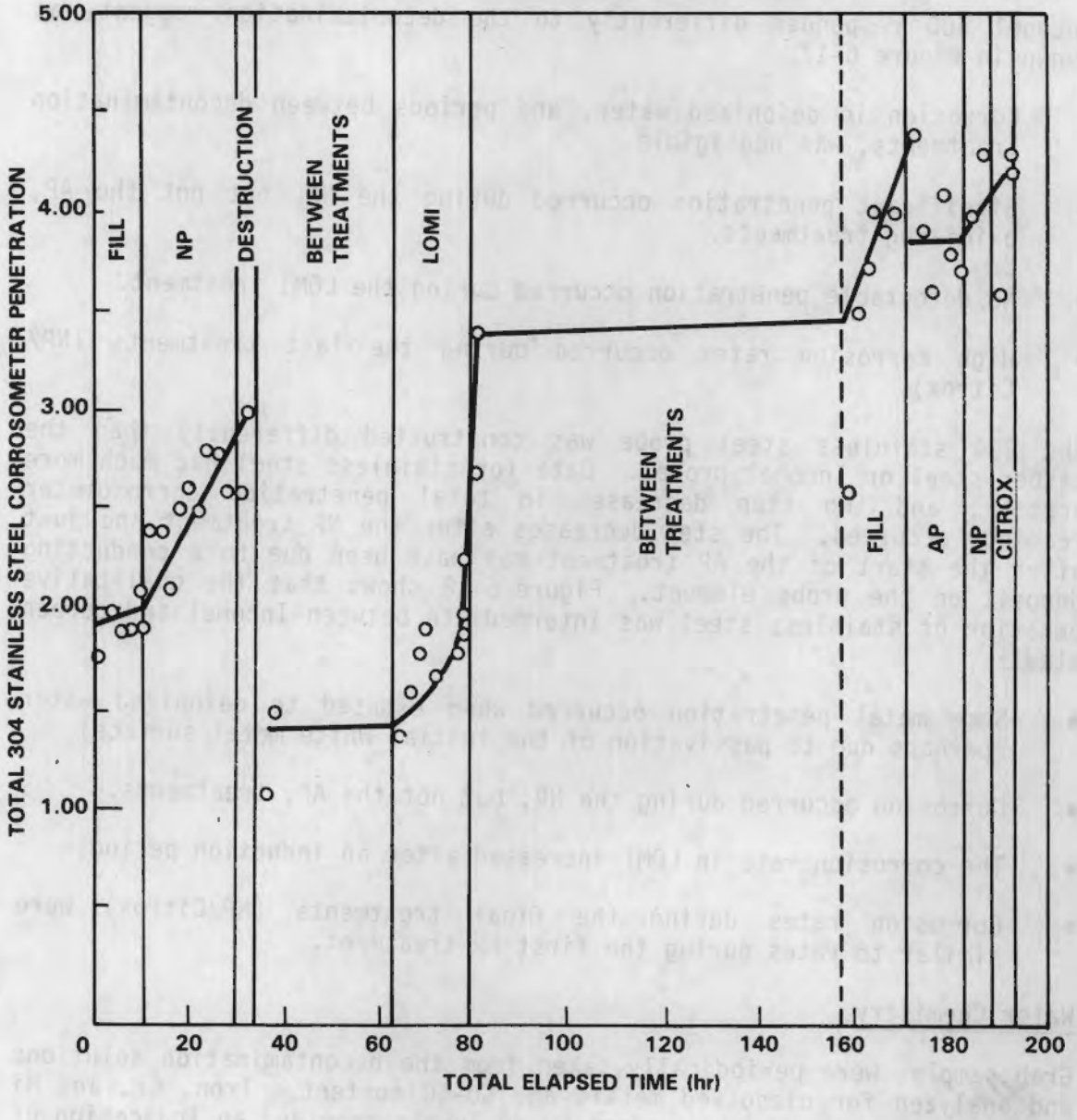

FIGURE 6-18. Total Corrosometer Penetration for 304 Stainless Steel During Hot Leg Decontamination

- The lowest corrosion rates occurred during the NP and AP steps.
- Corrosion in deionized water (probably oxygen saturated) was faster than corrosion under the strongly oxidizing conditions.
- Corrosion during NP-2 (destruction of the NP reagent) was similar to corrosion in deionized water.
- Corrosion rates were high in LOMI and Citrox after an induction period.

Inconel 600 responded differently to the decontamination reagent, as shown in Figure 6-17.

- Corrosion in deionized water, and periods between decontamination treatments, was negligible.
- Significant penetration occurred during the NP, but not the AP, oxidizing treatments.
- No detectable penetration occurred during the LOMI treatment.
- High corrosion rates occurred during the last treatments (NP/Citrox).

The 304 stainless steel probe was constructed differently than the carbon steel or Inconel probes. Data for stainless steel had much more scatter, and two step decreases in total penetration corrosometer readings occurred. The step decreases after the NP treatment and just after the start of the AP treatment may have been due to a conducting deposit on the probe element. Figure 6-18 shows that the qualitative behavior of stainless steel was intermediate between Inconel and carbon steel:

- Some metal penetration occurred when exposed to deionized water (perhaps due to passivation of the initial white metal surface).
- Corrosion occurred during the NP, but not the AP, treatments.
- The corrosion rate in LOMI increased after an induction period.
- Corrosion rates during the final treatments (NP/Citrox) were similar to rates during the first NP treatment.

Water Chemistry

Grab samples were periodically taken from the decontamination solutions and analyzed for dissolved metals and Co-60 content. Iron, Cr, and Ni concentrations normalized against Co-60 levels provided an indication of the corrosion occurring during decontamination. In addition, correlation of Co-60 levels with a particular stage in the decontamination process indicated the efficiency of a particular treatment. Since grab

samples were taken before and after passage through the ion exchange columns during the cold leg decontamination, the performance of the ion exchange columns also could be evaluated.

Cold Leg Water Chemistry Results

Iron, Cr, Ni, Mn, and Co-60 levels in the decontamination solution before the ion exchange column (BIX) are plotted in Figure 6-19, although complete analyses were not available for all stages of the decontamination. Iron levels were lowest (5 ppm and 2 ppm) during the two oxidizing treatments, and highest during the three reducing treatments (15 ppm, 45 ppm, and 20 ppm). Corrosion coupon and corrosometer results indicate that a significant fraction of the Fe may have come from corrosion of the carbon steel nozzle covers. High Cr concentrations started with the first oxidizing step, while high Ni concentrations started with the second reducing step. Manganese concentrations paralleled Co-60 levels in solution starting with the second reducing treatment. This suggests that most of the Co-60 removal may have occurred when residual Mn deposits, with entrained Co-60, were removed by the reducing treatments.

As noted in Section 3, cation and mixed-bed ion exchange columns were used to remove the dissolved metals and reagents for the cold leg decontamination. Figure 6-20 plots the "after ion exchange" (AIX) concentrations of Fe, Cr, Ni, Mn, and Co-60. Comparison of Figure 6-20 with Figure 6-19 shows that the Fe concentrations were decreased 50% to 70% by the cation exchange column during the first reducing treatment. The mixed-bed column also effectively removed Fe from the flow during clean up after the first reducing treatment, but added some Fe when used for clean up after the first oxidizing treatment. However, the primary purpose of the mixed-bed column was reagent removal, rather than Fe removal, from solution. During the second reducing treatment, approximately 80% of the Fe was removed from the flow by the cation column. No data was available to determine the efficiency of the mixed-bed column for Fe removal after the second reducing treatment. Figure 6-20 shows that during the third (and last) reducing treatment, the cation column also removed 80% of the Fe from the flow. In general, the cation column was more effective than the mixed-bed column for Fe removal during most phases of the decontamination.

Figure 6-19 indicated that little Cr was dissolved during the first reducing treatment. However, significant Cr went into solution during the first oxidizing treatment and some dissolution also occurred with the second reducing treatment. After the first oxidizing treatment, Cr levels dropped significantly during clean up when the mixed-bed ion exchange column was used (Figure 6-20). However, the cation column did not significantly reduce Cr concentrations during the second reducing treatment. A single data point suggests that the mixed-bed column was removing Cr during cleanup after the second oxidizing treatment. The mixed-bed ion exchange column appeared more effective for Cr removal than the cation column.

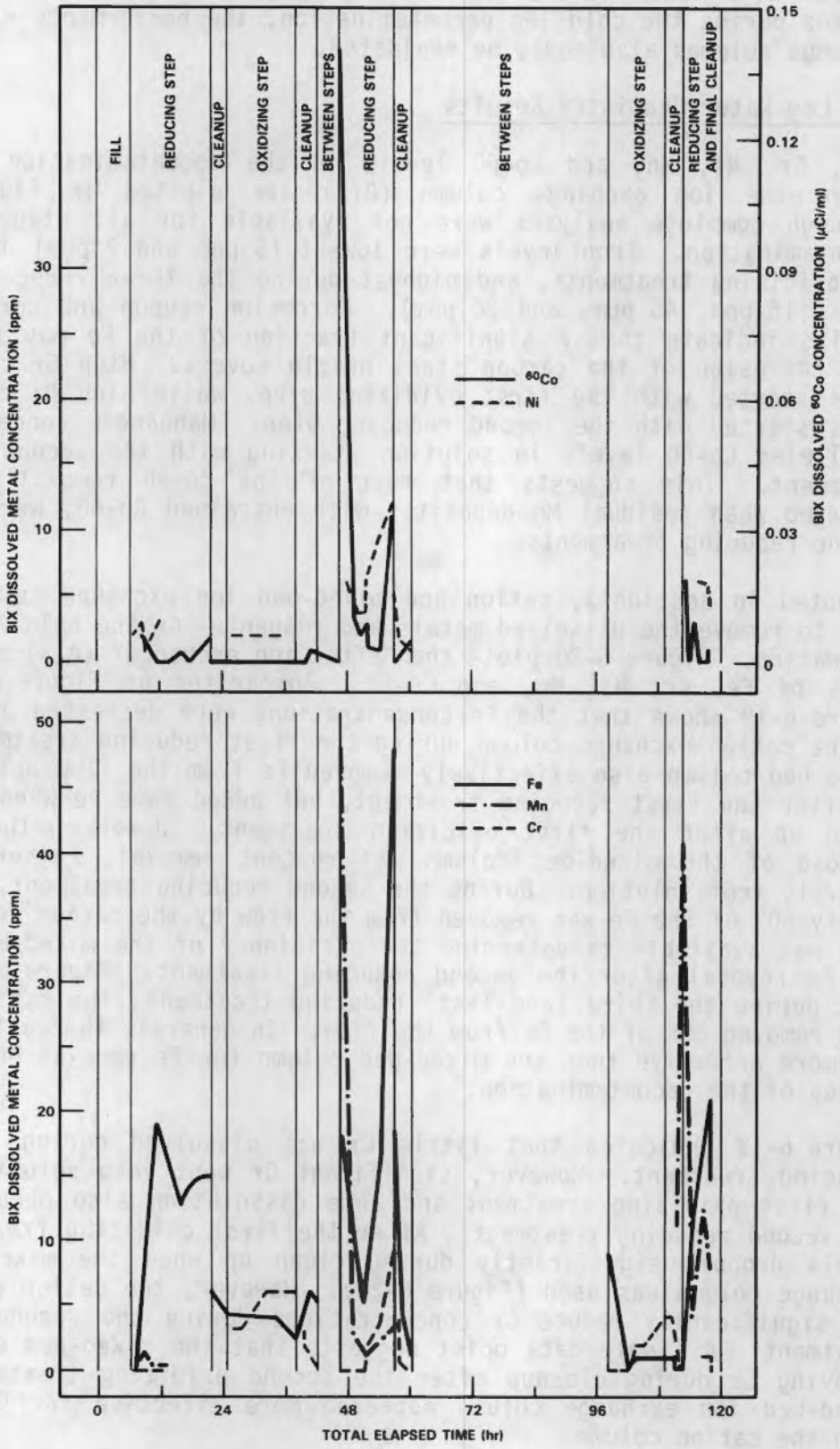

FIGURE 6-19. Fe, Cr, Ni, Mn, and Co-60 Concentrations in the Reagent Before Ion Exchange During the Cold Leg Decontamination

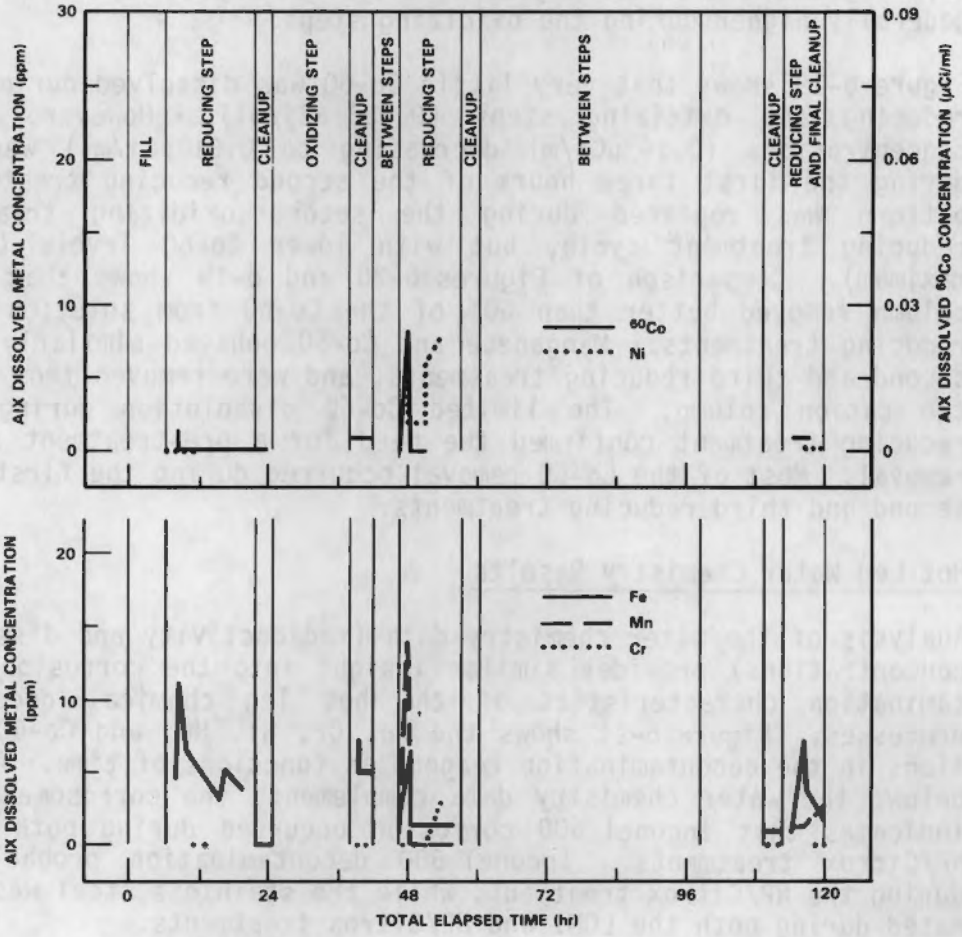

FIGURE 6-20. Fe, Cr, Ni, Mn, and Co-60 Concentrations in the Reagent After Ion Exchange During the Cold Leg Decontamination

Nickel concentrations were low except during the second and third reducing steps. Comparison of Figure 6-20 with Figure 6-19 shows that the cation column did not significantly remove Ni. However, the drop in Ni levels during cleanup (Figure 6-19) indicates that the mixed-bed column was removing Ni from the system. This suggests that the behavior of Cr and Ni was related since both were removed by the mixed-bed, but not the cation, ion exchange column. In addition, the initial oxidizing treatment appeared to facilitate Ni and Cr removal during subsequent reducing treatments, since concentrations were uniformly low during the first reducing treatment. Nickel was more soluble during subsequent reducing steps than during the oxidizing steps, while Cr levels were generally higher during the oxidizing steps.

Figure 6-19 shows that very little Co-60 was dissolved during the first reducing and oxidizing steps (0.005 μCi/ml). However, high Co-60 concentrations (0.14 μCi/ml decreasing to 0.01 μCi/ml) were observed during the first three hours of the second reducing treatment. This pattern was repeated during the second oxidizing treatment/third reducing treatment cycle, but with lower Co-60 levels (0.03 μCi/ml maximum). Comparison of Figures 6-20 and 6-19 shows that the cation column removed better than 60% of the Co-60 from solution during the reducing treatments. Manganese and Co-60 behaved similarly during the second and third reducing treatments, and were removed from solution by the cation column. The limited Co-60 dissolution during the first reducing treatment confirmed the need for a pre-treatment step for Cr removal. Most of the Co-60 removal occurred during the first 4 h of the second and third reducing treatments.

Hot Leg Water Chemistry Results

Analysis of the water chemistry data (radioactivity and dissolved metal concentrations) provides similar insight into the corrosion and decontamination characteristics of the hot leg chemical decontamination processes. Figure 6-21 shows the Fe, Cr, Ni, Mn, and Co-60 concentrations in the decontamination reagent as functions of time. As discussed below, the water chemistry data complements the corrosometer data and indicates that Inconel 600 corrosion occurred during both the NP and NP/Citrox treatments. Inconel 600 decontamination probably occurred during the NP/Citrox treatment, while the stainless steel was decontaminated during both the LOMI and NP/Citrox treatments.

Cr and Ni were the primary species dissolved during the NP treatment, with two times more Ni removed than Cr (Fe dissolution is not expected due to the low solubility of Fe(III) oxides). The dissolved Cr and Ni may reflect oxidation of Inconel surfaces in the channel head since 1) the Cr:Ni stoichiometry is closer to Inconel than to the oxide on the stainless steel surfaces and 2) the corrosometer data indicated that Inconel was corroding during this treatment. In addition, the small levels of Co-60 present in the decontamination solution during the first NP stage suggest that the oxide on the stainless steel surfaces was not being dissolved.

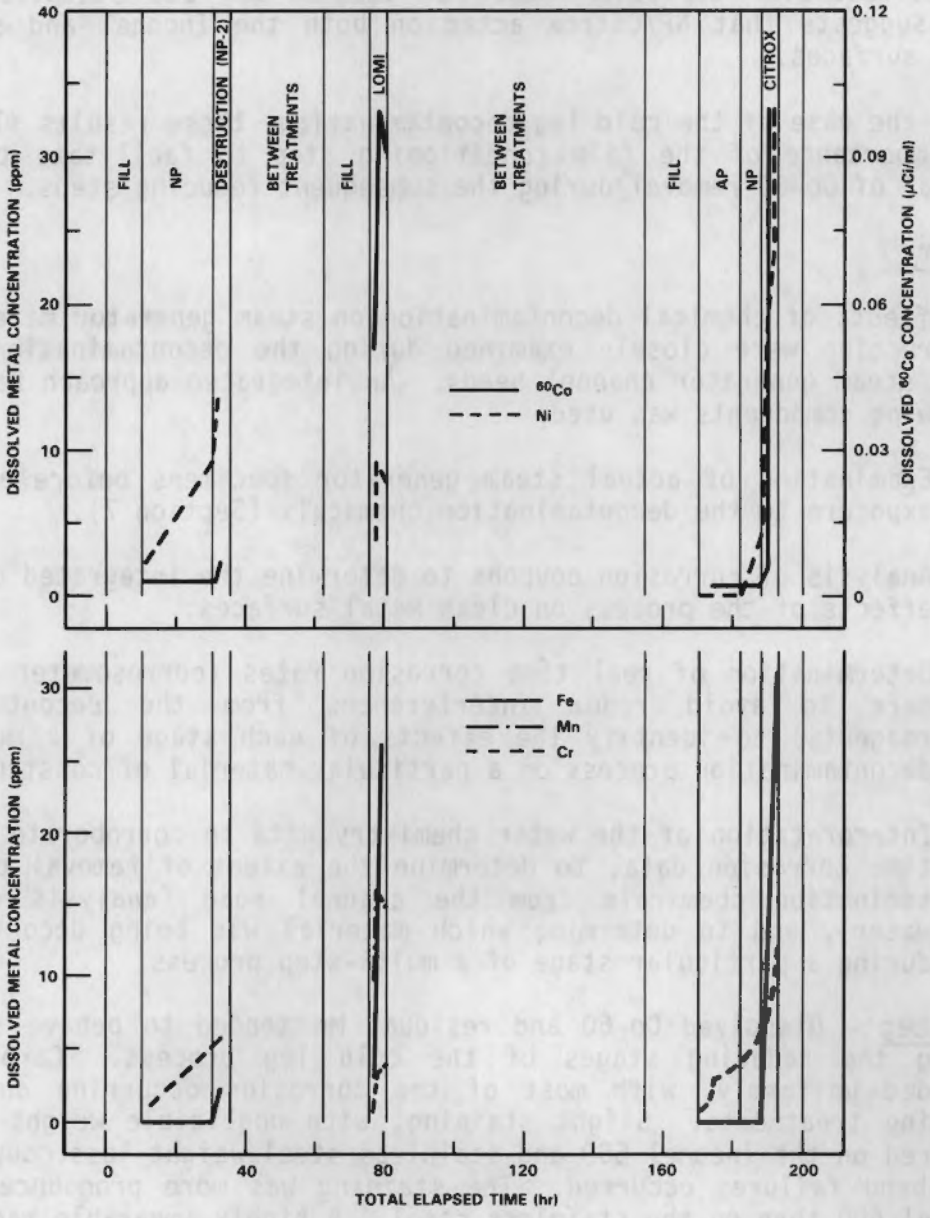

FIGURE 6-21. Fe, Cr, Ni, Mn, and Co-60 Concentrations in the Reagent During the Hot Leg Decontamination

The rapid increase in Fe and Co-60 during the LOMI step, coupled with a low corrosometer corrosion rate for Inconel, suggests that oxide on the stainless steel surfaces was being removed. Cr was the only significant species present during the AP step. This suggests that the AP step oxidized Cr in oxides on stainless steel surfaces, since the corrosometer data indicated low corrosion rates on Inconel surfaces and moderate corrosion rates on stainless steel. Concentrations of all species increased dramatically during the final NP/Citrox stage, as did the corrosometer corrosion rate for Inconel 600 and stainless steel. This suggests that NP/Citrox acted on both the Inconel and stainless steel surfaces.

As in the case of the cold leg decontamination, these results illustrate the importance of the film conditioning step to facilitate the rapid removal of Co-60 removal during the subsequent reducing steps.

Summary

The effects of chemical decontamination on steam generator materials of construction were closely examined during the decontamination of the Surry steam generator channel heads. An integrated approach having the following components was used:

- Examination of actual steam generator specimens before and after exposure to the decontamination chemicals (Section 7).
- Analysis of corrosion coupons to determine the integrated corrosion effects of the process on clean metal surfaces.
- Determination of real time corrosion rates (corrosometer was used here to avoid redox interferences from the decontamination reagents) to identify the effects of each stage of a multi-step decontamination process on a particular material of construction.
- Interpretation of the water chemistry data to corroborate the real time corrosion data, to determine the extent of removal of decontamination chemicals from the channel head (analysis of rinse water), and to determine which material was being decontaminated during a particular stage of a multi-step process.

Cold Leg - Dissolved Co-60 and residual Mn tended to behave similarly during the reducing stages of the cold leg process. Carbon steel corroded uniformly, with most of the corrosion occurring during the reducing treatments. Slight staining, with negligible weight changes, occurred on the Inconel 600 and stainless steel weight loss coupons, and no U-bend failures occurred. The staining was more pronounced on the Inconel 600 than on the stainless steel. A highly smearable radioactive deposit was present on the corrosion coupons following decontamination.

Hot Leg - The overall results for the hot leg decontamination indicated superficial pitting on Inconel 600 corrosion coupons (probably due to the NP and NP/Citrox steps), uniform corrosion on carbon steel (as expected), and negligible corrosion on the stainless steel specimens. However, galvanic coupling between carbon steel and stainless steel coupons enhanced stainless steel corrosion (as it did with the process for the cold leg decontamination). No U-bend failures were observed in the stainless steel, carbon steel, or Inconel 600 specimens. The hot leg corrosion coupons were relatively free of smearable radioactive decontamination when removed from the channel head (as compared with the cold leg coupons). However examination of the coupons at low magnification found traces of a white crystalline material, suggesting incomplete rinsing after the last step in the hot leg process. Variations between the post-decontamination deposits in the hot leg and cold leg may have been due, in large part, to differences in the flow characteristics of the two decontamination processes.

Overview - In general, the cold leg process was less corrosive than the hot leg process, which included the relatively corrosive NP/Citrox step. In particular, stainless steel corrosion was slight for both hot and cold leg decontaminations, while Inconel corrosion occurred during the NP and NP/Citrox steps of the hot leg decontamination. However, actual penetration of the Inconel base metal was relatively minor. Residual Mn deposits were found on smears from the channel head bowl after both decontaminations, and trace white crystals were found on the corrosion coupons after the hot leg process. This suggests that particular attention needs to be paid to the problem of adequate rinsing in future decontaminations for both processes. Although the hot leg decontamination achieved higher stainless steel DFs, comparison of the effectiveness of the cold leg and hot leg processes is difficult because of differences in the composition and morphology of deposits on the hot leg and cold leg surfaces, discussed in Section 7.

7. CHARACTERIZATION OF CHANNEL HEAD SURFACES BEFORE AND AFTER DECONTAMINATION

Introduction

The decontamination of the Surry steam generator channel head provided a unique opportunity to characterize the corrosion films on channel head surfaces. To date, the majority of the published data deals only with the characterization of films on Inconel steam generator tubes and not films on stainless steel. Specimens from the 304 stainless steel manway cover inserts, 309 stainless steel channel head bowl cladding, and Inconel 600 tube sheet cladding were studied before and after both the hot and cold leg decontaminations. Characterization of these surfaces was important for the following reasons:

- To determine the extent of corrosion during reactor operation.
- To document the pre-decontamination corrosion films on stainless steel and Inconel surfaces.
- To evaluate both the corrosion behavior and effectiveness of the decontamination processes.
- To assess the presence or absence of residual reagent which might affect corrosion.
- To provide information for future decontamination reagent development efforts.

Table 7-1 summarizes the specimens that were studied.

Cold Leg Channel Head Core Specimen (Before Decontamination)

A core drill was used to remove a specimen from the cold leg channel head wall for analysis. Figure 7-1 shows that the crud/oxide on the 309 stainless steel specimen appeared to be fairly thick, and had a dull black color. The surface of the specimen was characterized using SEM/XRF and low-angle XRD. A burr on the edge of the sample was removed and polished metallographically to study the crud/oxide in cross section.

Figure 7-2 shows a magnification series of SEM micrographs taken at the center of the cold leg core specimen. The micrographs suggest a duplex crud/oxide film, with a cracked outer layer over a uniform epitaxial inner film. Stereopair micrographs (not shown) of negatives #26893 and #26895 in Figure 7-2 suggested that the outer layer was 1 μm to 2 μm thick; however, metallographic cross sections (Figure 7-3) indicated that the actual thickness was ~4 μm. Figure 7-2 also shows that spherical particles are uniformly distributed over the specimen surface. EDX was used to analyze the composition of the features shown in Figure 7-2. Table 7-2 summarizes the analyses. The results show that the superficial spherical particles have more Cr than the compact oxide, and that

TABLE 7-1. Characterization Specimens

Specimen	Characterization	Comments
COLD LEG		
Cold leg manway cover coupons	XRD of in-situ primary side film	Pre-decontamination
	SEM analysis of primary side surface and metallographic cross section	Pre- and post-decontamination
Channel head core specimen	SEM and XRD analysis of primary side surface	Pre-decontamination
	SEM analysis of metallographic cross section of a burr removed from the original core specimen	Pre-decontamination
	SEM analysis of primary side surface	Post-decontamination
Channel head bowl smears	XRF analysis	Post-decontamination
Weight loss coupons	20X to 120X magnification inspection	Post-decontamination
	SEM examinations of metallographic cross sections	Post-decontamination
U-bend specimens	Dye penetrant treatment followed by 120X examination	Post-decontamination
Channel head divider plate and tube sheet	Visual inspection using a low power telescope (Questar)	Post-decontamination
Steam generator tube rings	SEM examination of primary side surface, metallographic cross section, and 20X to 120X magnification inspection of ID and OD surfaces	Pre- and post-decontamination

TABLE 7-1. (Continued)

Specimen	Characterization	Comments
HOT LEG		
Hot leg manway cover coupons	XRD of in-situ primary side film	Pre-decontamination
	SEM analyses of primary side surface and metallographic cross section	Pre- and post-decontamination
Channel head core specimen	SEM analyses of primary side surface	Pre- and post-decontamination
Channel head bowl smears	XRF analysis	Post-decontamination
Protected and unprotected tube sheet specimens	SEM analyses of primary side surface	Post-decontamination
Weight loss coupons	Visual inspection at 20X magnification	Post-decontamination
U-bend specimens	Dye penetrant treatment followed by visual examination at 20X magnification	Post-decontamination
Channel head divider plate and tube sheet	Visual inspection using a low power telescope (Questar)	Post-decontamination
Steam generator tube rings	SEM examination of primary side surface, metallographic cross section, and 20X to 120X magnification inspection of ID and OD surfaces	1) See cold leg section for pre-decontamination characterization 2) Includes specimens common to both hot leg and cold leg decontaminations

NEG. 8205283-7

NEG. 8205283-1

NEG. 8205283-9

FIGURE 7-1. Core Specimen Removed From the Cold Leg Channel Head Wall Before Decontamination

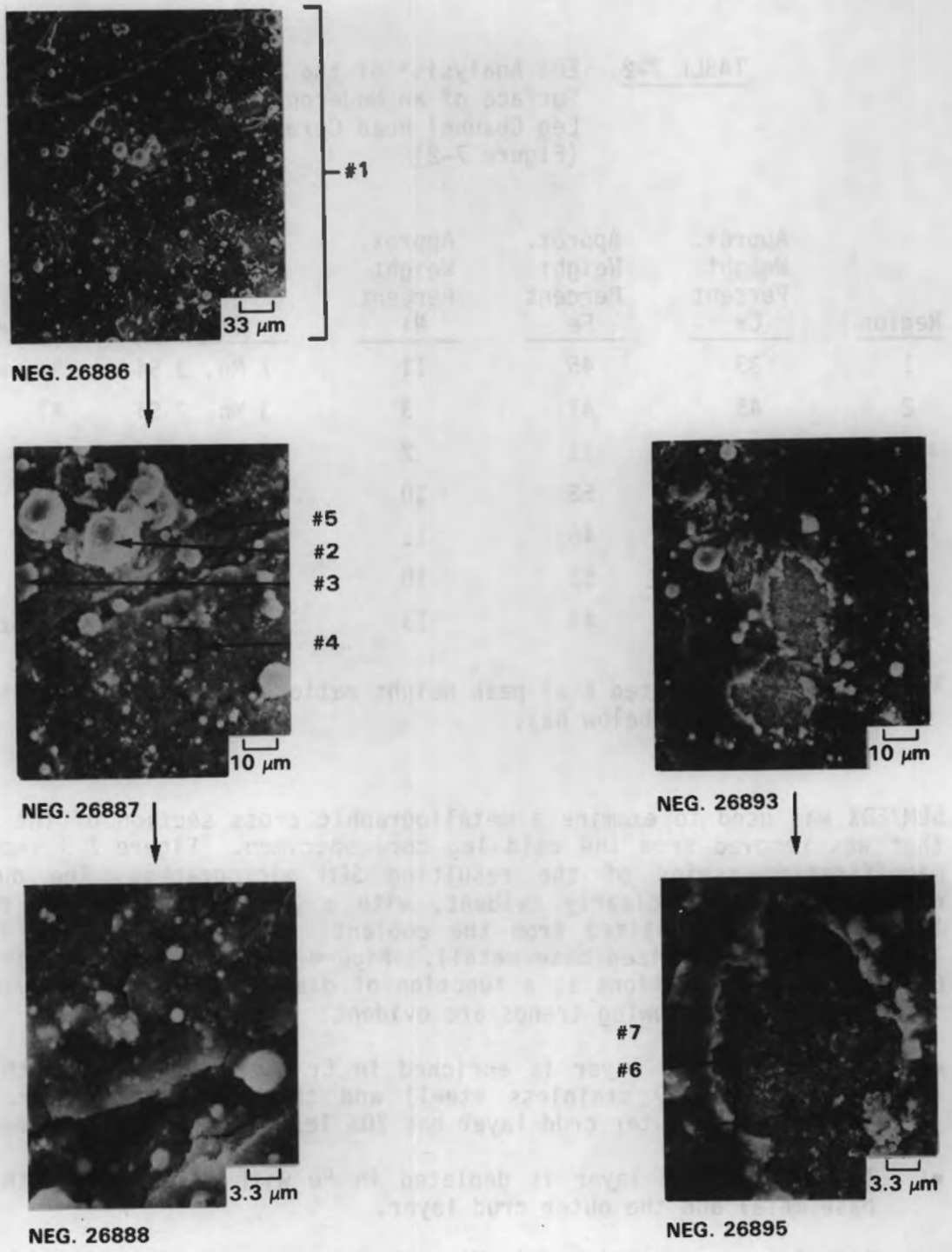

FIGURE 7-2. SEM Examination of the Primary Side Surface of the Pre-Decontamination Core Specimen From the Cold Leg Channel Head Wall

the faceted superficial particles (Figure 7-2, #3) are primarily Cr. The inner oxide appeared to be enriched in manganese and Si with respect to the outer oxide.

TABLE 7-2. EDX Analysis* of the Primary Side Surface of an Undecontaminated Cold Leg Channel Head Core Specimen (Figure 7-2)

Region	Approx. Weight Percent Cr	Approx. Weight Percent Fe	Approx. Weight Percent Ni	Approx. Weight Percent Other	Trace
1	33	45	11	7 Mn, 3 Si	Al, K, Ca
2	45	47	3	3 Mn, 2 Si	Al
3	75	11	2	10 Mn, 2 Si	
4	31	53	10	9 Mn, 3 Si	
5	35	46	11	13 Mn, 2 Si	Al
6	33	52	10	4 Mn, 1 Si	
7	34	41	13	10 Mn, 3 Si	K, Ca

*From baseline corrected K(α) peak height ratios (excluding elements with atomic numbers below Na).

SEM/EDX was used to examine a metallographic cross section of the burr that was removed from the cold leg core specimen. Figure 7-3 shows a magnification series of the resulting SEM micrographs. The duplex crud/oxide film is clearly evident, with a 3 μm to 5 μm thick outer layer (probably deposited from the coolant) and a 1.5 μm thick inner layer (probably oxidized base metal). Figure 7-4 plots approximate Fe, Cr, and Ni concentrations as a function of distance from the crud/oxide interface. The following trends are evident:

- The inner oxide layer is enriched in Cr with respect to both the base metal (309 stainless steel) and the outer crud layer. In addition, the outer crud layer has 70% less Cr than the base metal.
- The inner oxide layer is depleted in Fe with respect to both the base metal and the outer crud layer.
- Both layers are enriched in Ni with respect to the base metal.

In addition, cracking up to 70 μm deep into the base metal was found (Figure 7-5). The presence of corrosion products in the cracks indicates that a substantial subsurface crack network existed prior to specimen removal. The sub-surface cracking probably facilitates

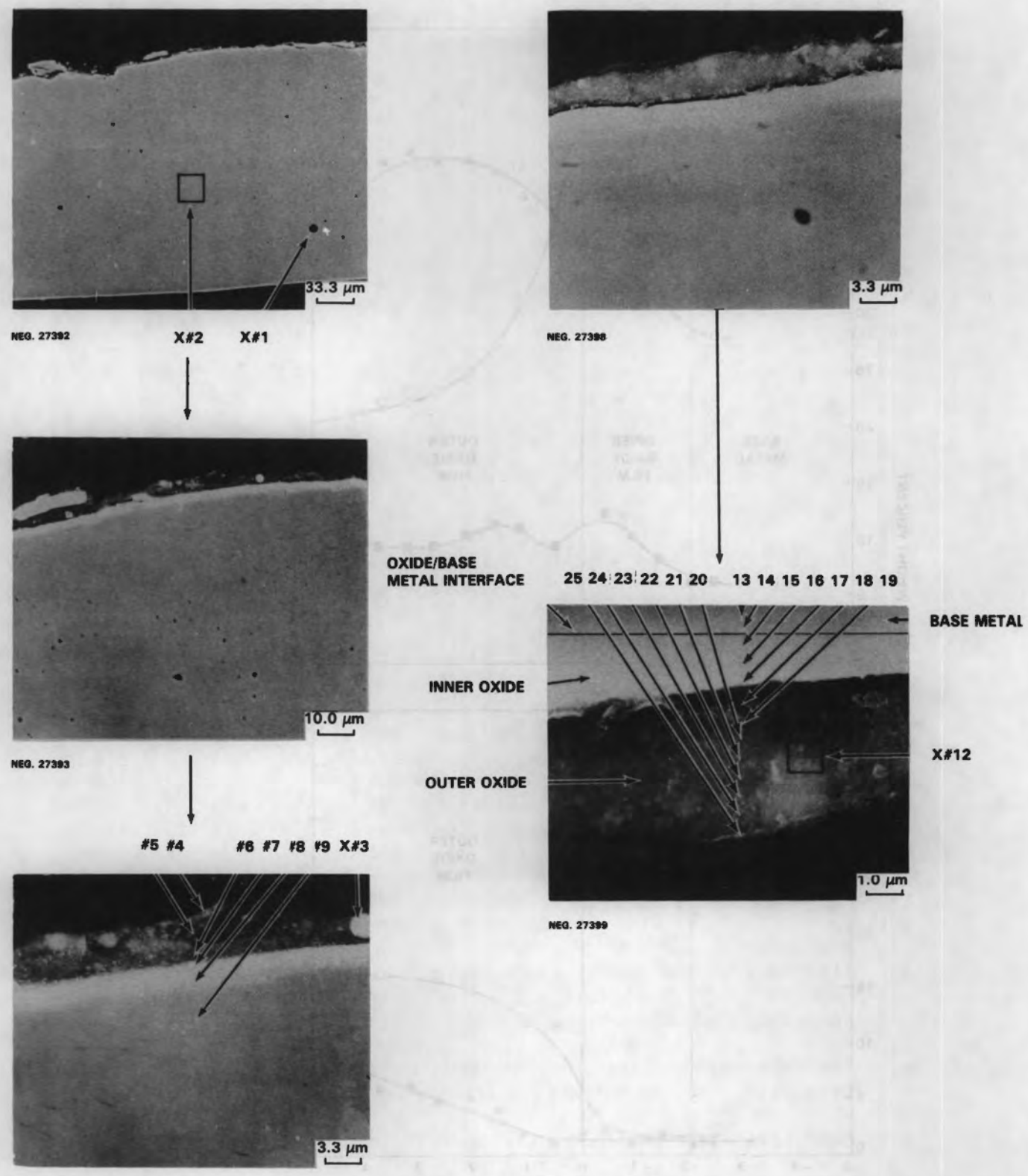

FIGURE 7-3. SEM Examination of a Metallographic Cross Section of a Burr Removed From the Pre-Decontamination Core Specimen Taken From the Cold Leg Channel Head Wall

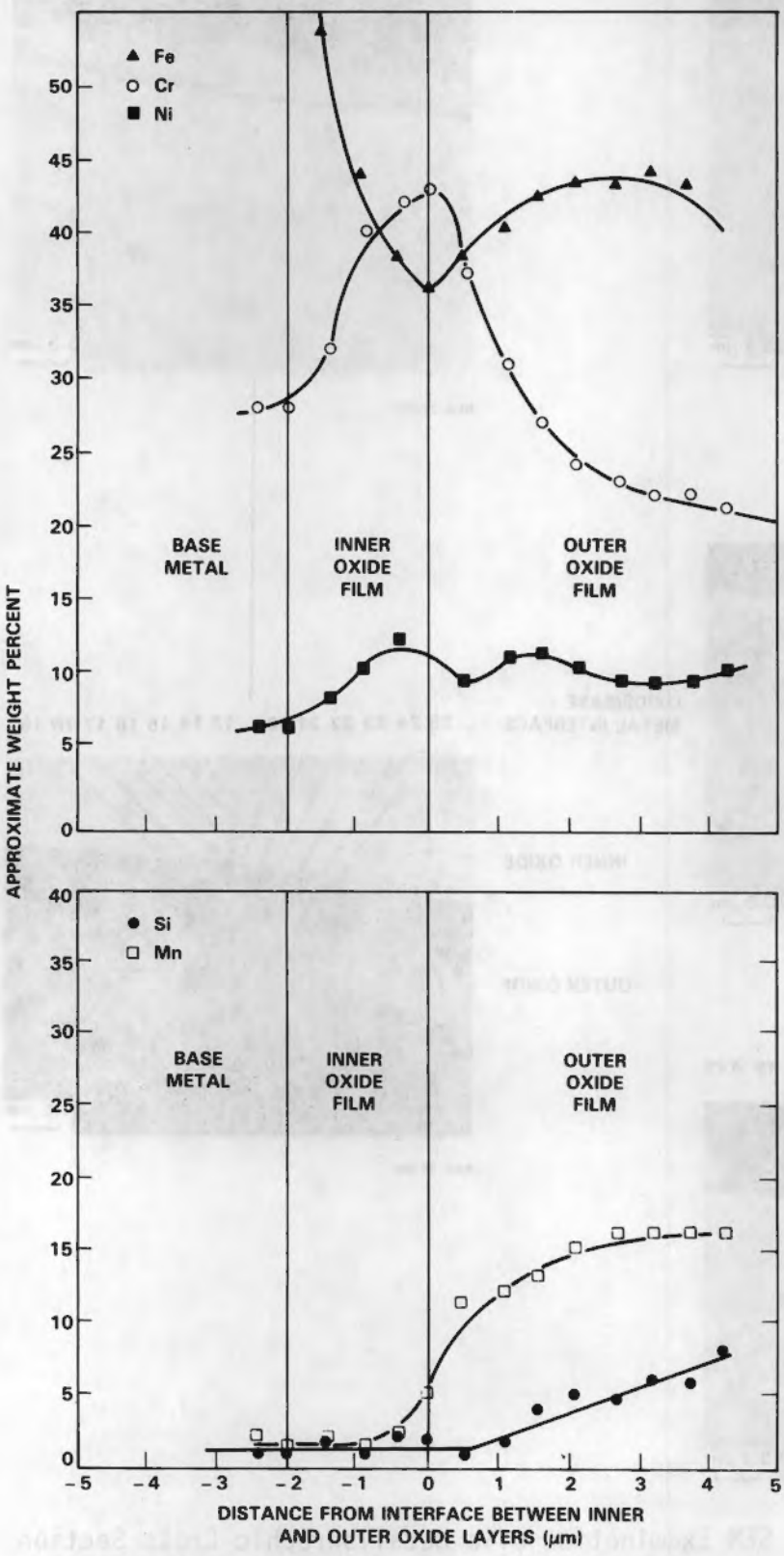

FIGURE 7-4. Composition Variations as a Function of Distance From the Base Metal/ Oxide Interface for the Core Specimen Removed From the Channel Head Wall

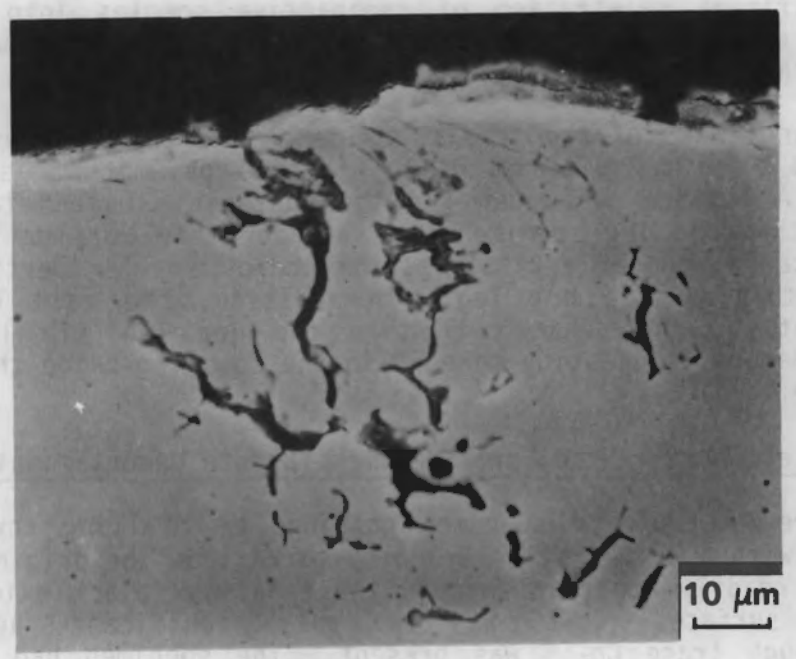

NEG. 27395

X#10

X#11

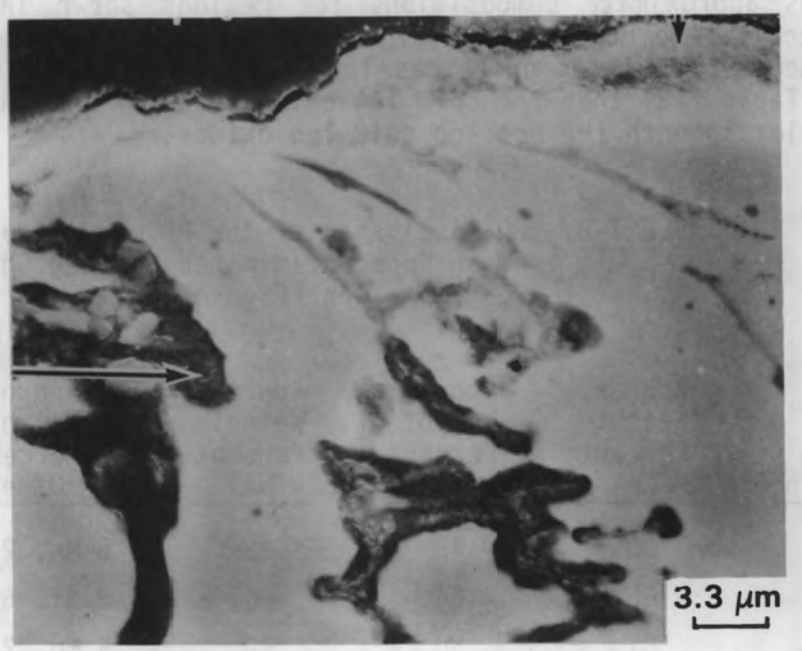

NEG. 27396

FIGURE 7-5. SEM Examination of a Metallographic Cross Section of a Burr Removed From the Pre-Decontamination Core Specimen Taken From the Cold Leg Channel Head Wall

significant penetration of radioactive species into the base metal. This correlates with the bleeding that was observed during the electropolishing decontamination as discussed in Section 4.

Low-angle XRD of the in situ oxide on the cold leg core specimen indicated a spinel with an 8.32 Å lattice parameter, as compared with a 3.58 Å lattice parameter for the austenitic base metal. Spinel lines for the cold leg specimen were broader than for the hot leg specimen, indicating poorer crystallization and/or smaller particles in the cold leg than in the hot leg. In addition, the cold leg spinel had a slightly larger unit cell than the hot leg spinel (8.29 Å lattice parameter), suggesting more Fe in the cold leg oxide than in the hot leg oxide.

Hot Leg Channel Head Core Specimen (Before Decontamination)

Figure 7-6 shows a specimen obtained by drilling through the channel head with a core drill. Grinding marks from the original surface finish were readily apparent through the tenacious black oxide on the primary side surface. Co-60 was the only significant radionuclide found, although trace Co-58 was present. The specimen had a specific Co-60 activity of 3 $\mu Ci/cm^2$, as compared with 5 $\mu Ci/cm^2$ for the cold leg core specimen.

SEM micrographs of the center area of the core specimen are shown in Figure 7-7. The oxide film on the 309 stainless steel hot leg specimen appears thinner and more uniform than the highly cracked film apparent on the cold leg specimen (Figure 7-2). Fewer superficial particles are present on the hot leg surface than on the cold leg surface. Table 7-3 gives approximate compositions for regions shown in Figure 7-7. The superficial particles have significantly higher Cr content than did the oxide. The hot leg oxide has lower Cr, higher Fe, higher Ni, and lower Mn (Table 7-3) than the cold leg oxide (Table 7-2). Silicon levels were similar in both the hot and cold leg oxides.

TABLE 7-3. EDX Analysis* of the Primary Side Surface of an Undecontaminated Hot Leg Channel Head Specimen (Figure 7-7)

Region	Approx. Weight Percent Cr	Approx. Weight Percent Fe	Approx. Weight Percent Ni	Approx. Weight Percent Other	Trace
1	30	48	12	5 Mn, 2 Si	S, Cl, K
2	62	24	1	8 Si, 5 Mn	
3	31	50	12	5 Mn, 2 Si	S, K
4	28	49	14	5 Mn, 2 Si	S, K, Ti

*From baseline corrected K(α) peak height ratios (excluding elements with atomic numbers below Na).

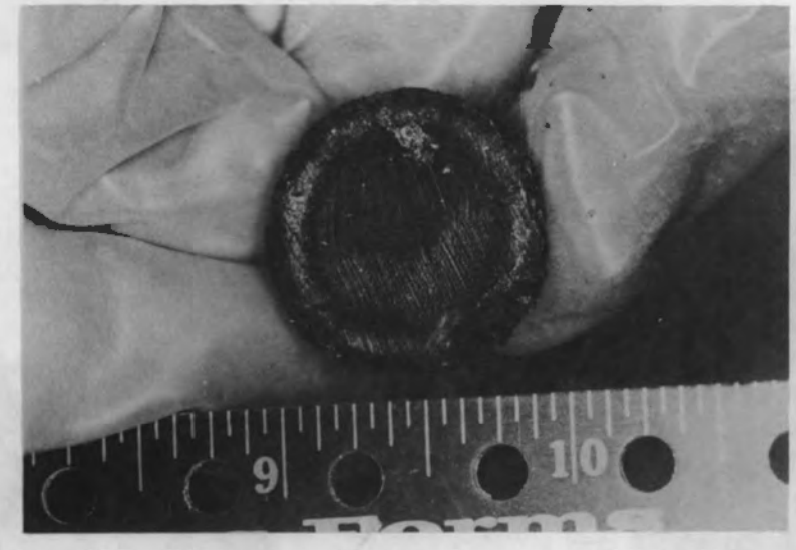

NEG. 8205283-23

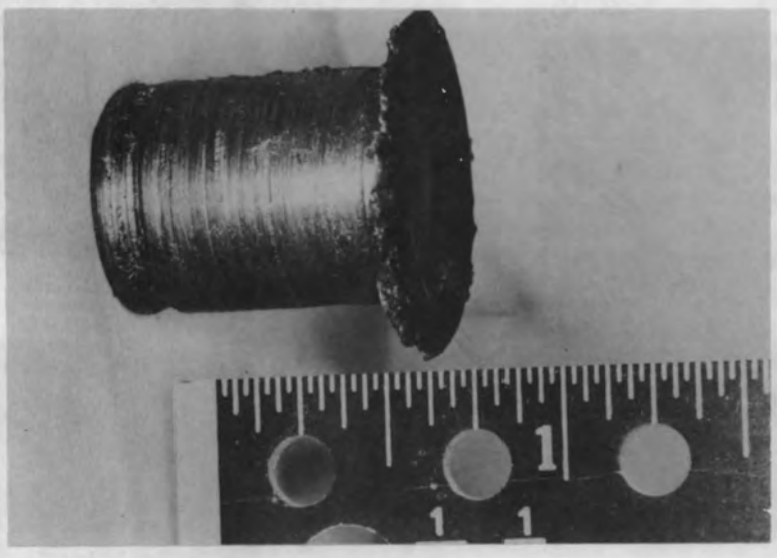

NEG. 8205283-13

NEG. 8205283-19

FIGURE 7-6. Core Specimen Removed From the Hot Leg Channel Head Wall Before Decontamination

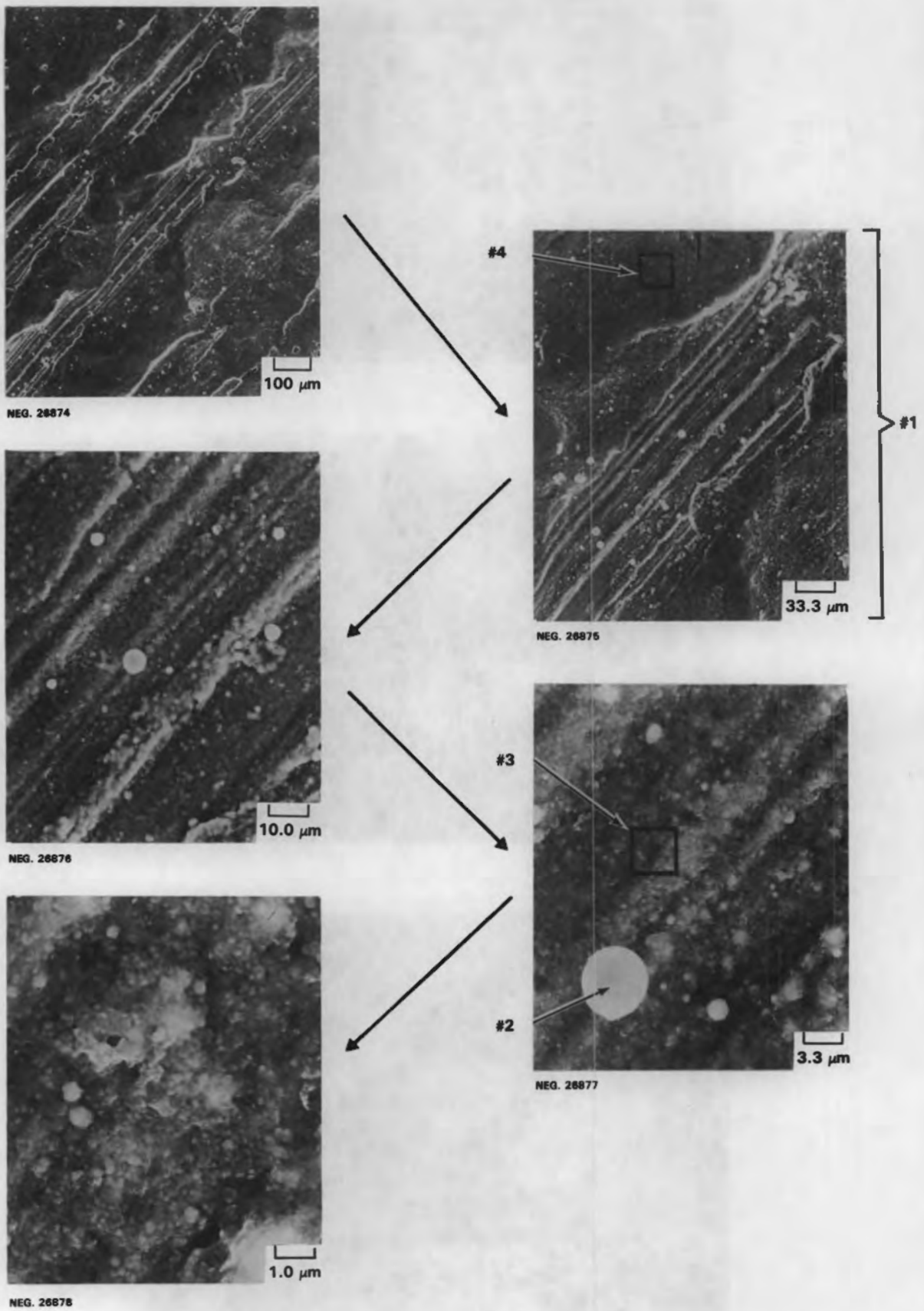

FIGURE 7-7. SEM Examination of the Primary Side Surface of the Pre-Decontamination Core Specimen From the Hot Leg Channel Head Wall

TABLE 7-4. EDX Analysis* of the Primary Side Surface of an Undecontaminated Cold Leg Manway Cover Insert Coupon (Figure 7-9)

Region	Approx. Weight Percent Cr	Approx. Weight Percent Fe	Approx. Weight Percent Ni	Approx. Weight Percent Other	Trace
1	30	48	13	4 Mn, 3 Si	Ti, Al, Zn
2	39	43	11	3 Mn, 2 Si	Al
3	13	50	29	4 Mn, 2 Si	Ti
4	13	75	9	1 Mn, 1 Si	
5	41	38	5	9 Mn, 4 Si	Ti
6	27	51	6	9 Mn, 5 Si	Ti, Cu
7	43	40	10	5 Mn, 1 Si	Zn
8	25	51	7	11 Mn, 4 Si	Ti
9	40	42	12	4 Mn, 2 Si	Ti, Zn

*From baseline corrected K(α) peak height ratios (excluding elements with atomic numbers below Na).

The primary side surface of the core specimen from the hot leg of the channel head was also characterized using low-angle XRD. The oxide is a spinel with a lattice parameter of 8.29 Å (8.32 Å on the cold leg). The base metal, as on the cold leg side, is austenitic with a lattice parameter of 3.58 Å. The spinel lines for the hot leg were sharper than those for the cold leg, which suggests that the hot leg oxide is better crystallized and/or has a larger grain size than the cold leg oxide.

Cold Leg Manway Cover Insert Coupon (Before Decontamination)

Figure 7-8 shows the appearance of typical coupons that were cut from the 304 stainless steel cold leg manway cover insert. The primary side crud/oxide had a similar (dull black) appearance to that on the 309 stainless steel core specimen. The primary side surface of the coupon was analyzed using SEM/EDX and low-angle XRD.

A magnification series of SEM micrographs of the cold leg manway cover coupon surface is given in Figure 7-9. Machining grooves in the base metal can be seen in the micrographs and the valley portions contain most of the superficial particulate. The deposit consists of superficial particles on a compact oxide, with some microcracking in the oxide base. More particulate was found on the manway cover insert than on the channel head core. Spires coming out of the crud/oxide (Figure 7-9, #6) may be due to superficial particulate that was incorporated into the deposit. EDX analyses of selected features are given in Table 7-4. In general, the compact substrate had similar amounts of Fe and Cr, while the particles were higher in Fe.

Based on low-angle XRD of the in situ oxide, the deposit is a spinel with a lattice parameter of 8.333 Å over an austenitic stainless steel face-centered-cubic (FCC) substrate with a 3.56 Å lattice parameter. Significantly, the lattice parameter for the crud on the cold leg manway insert coupon was almost identical to that for crud/oxide on the cold leg core specimen. Since the compositions are also similar (by microprobe analysis), chemical decontamination studies based on manway cover insert specimens may extrapolate well to other stainless steel PWR surfaces.

Hot Leg Manway Cover Insert Coupon (Before Decontamination)

Figure 7-10 shows the appearance of coupons cut from the insert for the hot leg manway cover. The primary side surface of the hot leg coupons appeared similar to that of the cold leg manway cover insert (Figure 7-8). The hot leg coupon surface has a rougher texture than the surface of the hot leg channel head core specimen. Undecontaminated hot leg coupons had a specific Co-60 surface activity of 3.6 $\mu Ci/cm^2$ as compared with 6 $\mu Ci/cm^2$ for cold leg coupons.

SEM micrographs of the center of a hot leg coupon are shown in Figure 7-11. Fewer superficial particles were found on the hot leg manway insert specimen than on the cold leg manway specimen. The substrate oxide showed little evidence of microcracking, unlike the base

CA-3 PRIMARY SIDE

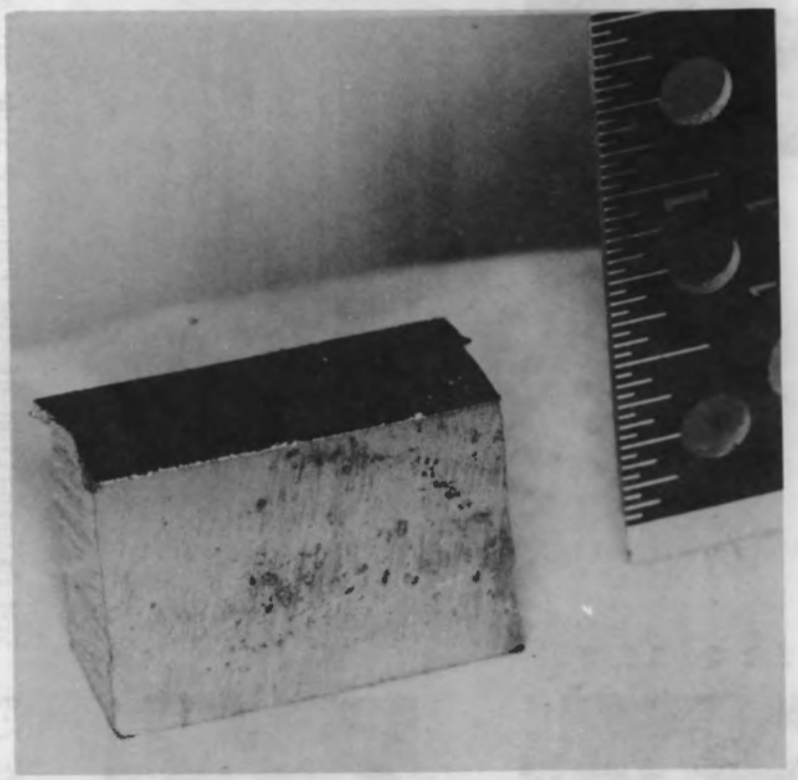

NEG. 8205283-31

CA-4 BACKING PLATE SIDE

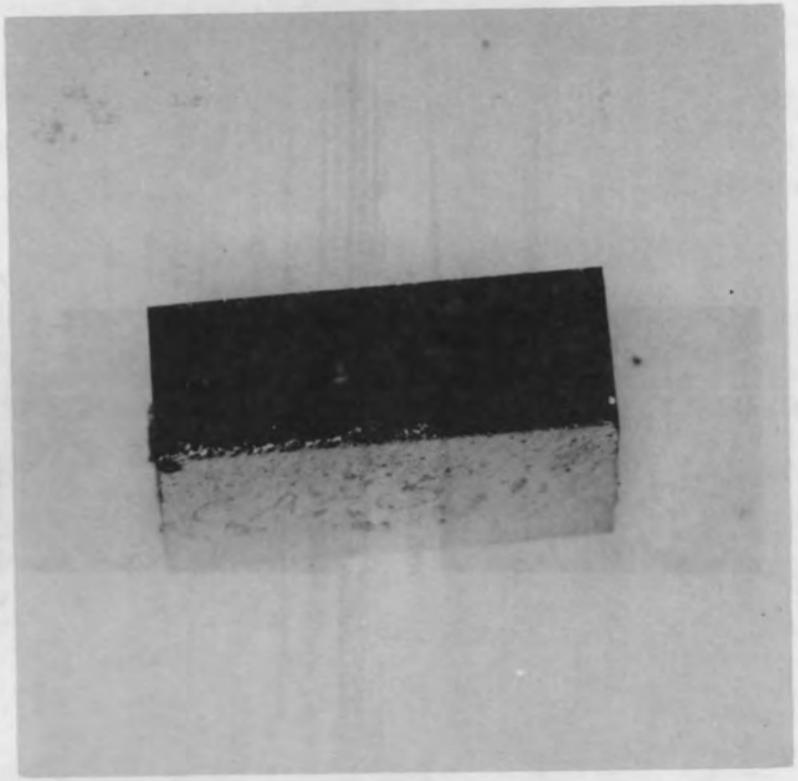

NEG. 8205283-40

FIGURE 7-8. Coupons From the Stainless Steel Cold Leg Manway Cover Insert

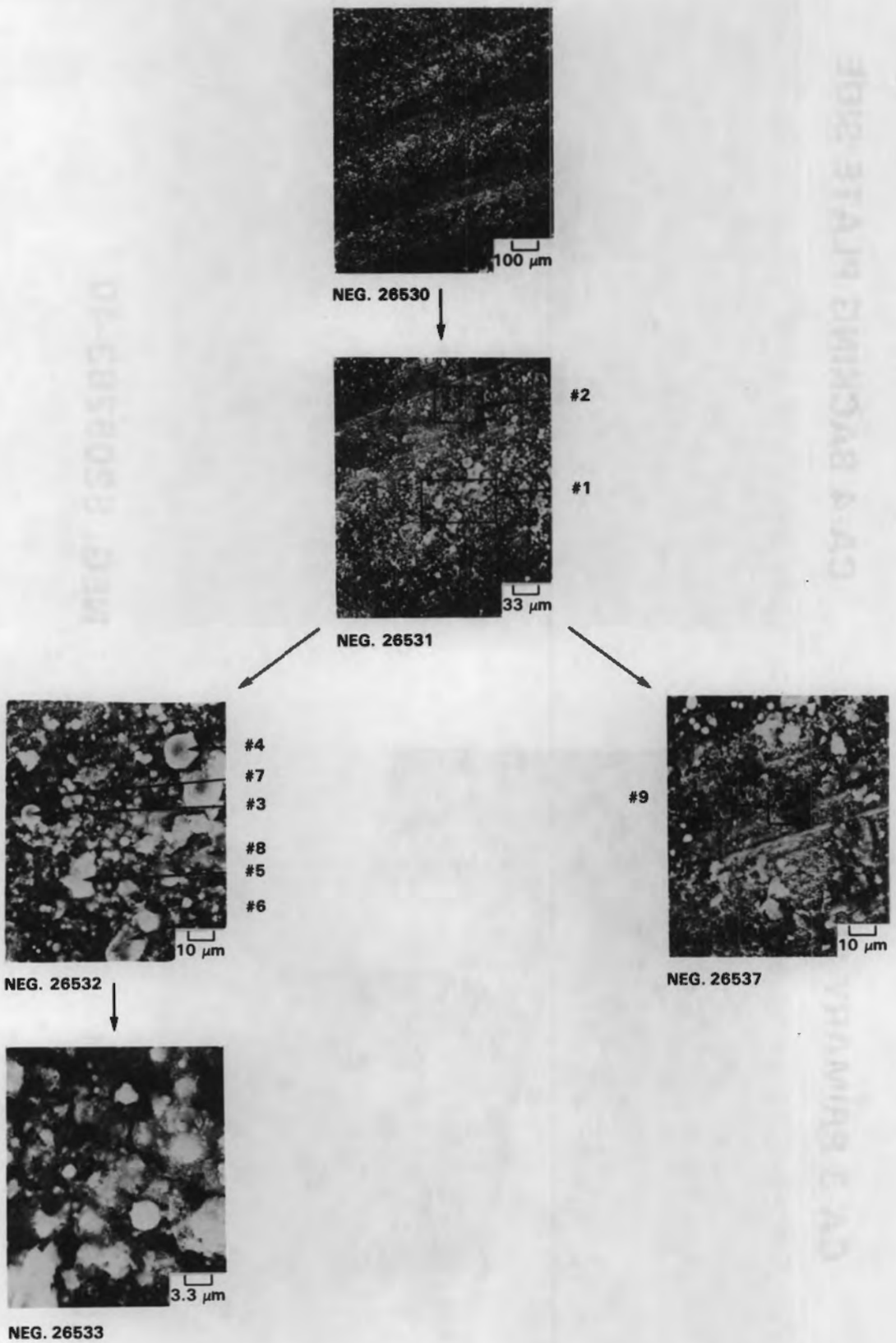

FIGURE 7-9. SEM Examination of the Primary Side Surface of the Cold Leg Manway Coupon

PRIMARY SIDE SURFACE

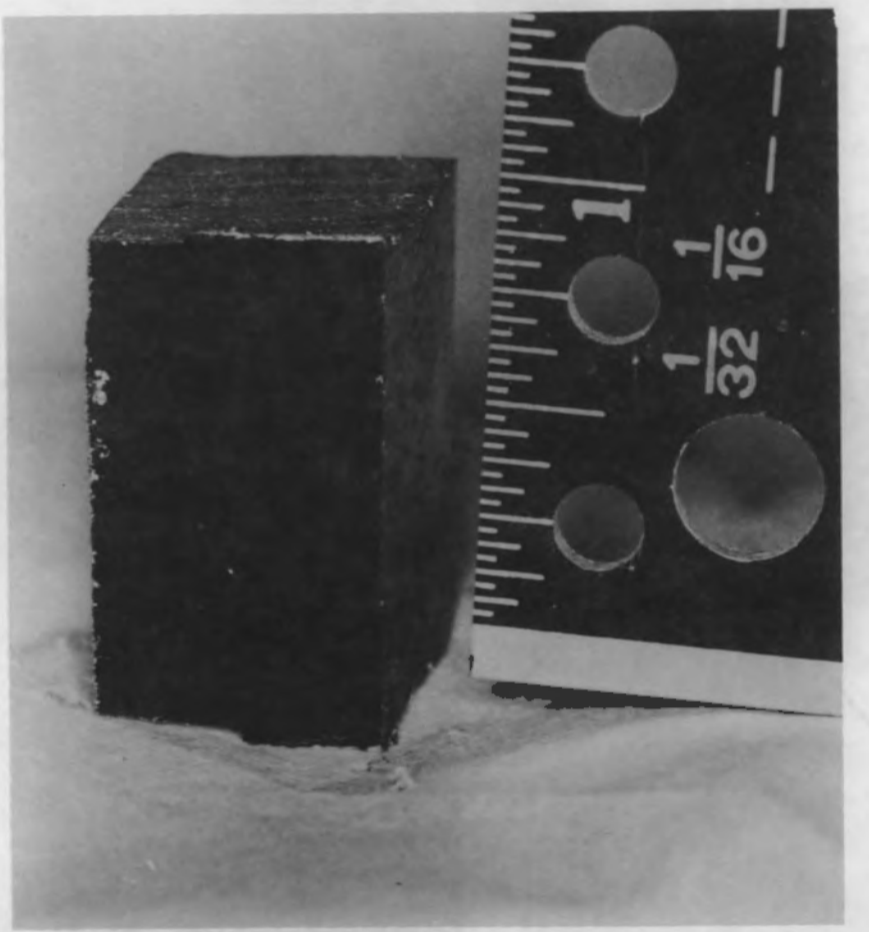

NEG. 8205283-54

BACKING PLATE SURFACE

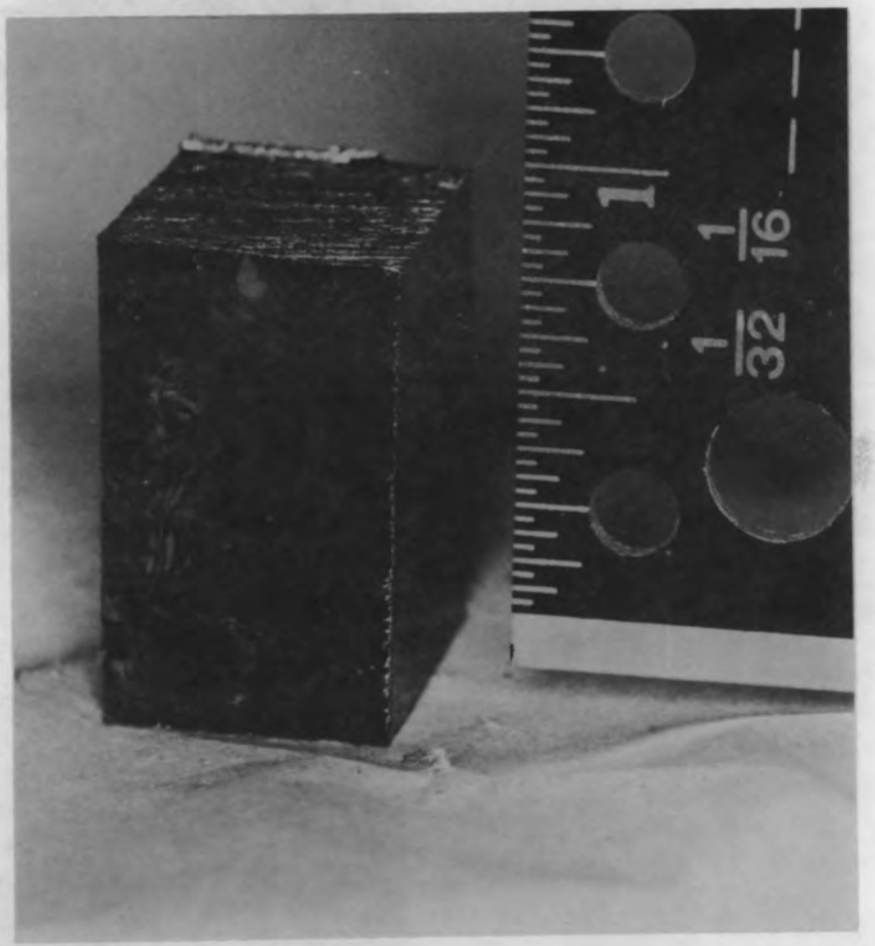

NEG. 8205283-55

FIGURE 7-10. Coupons From the Stainless Steel Hot Leg Manway Cover Insert

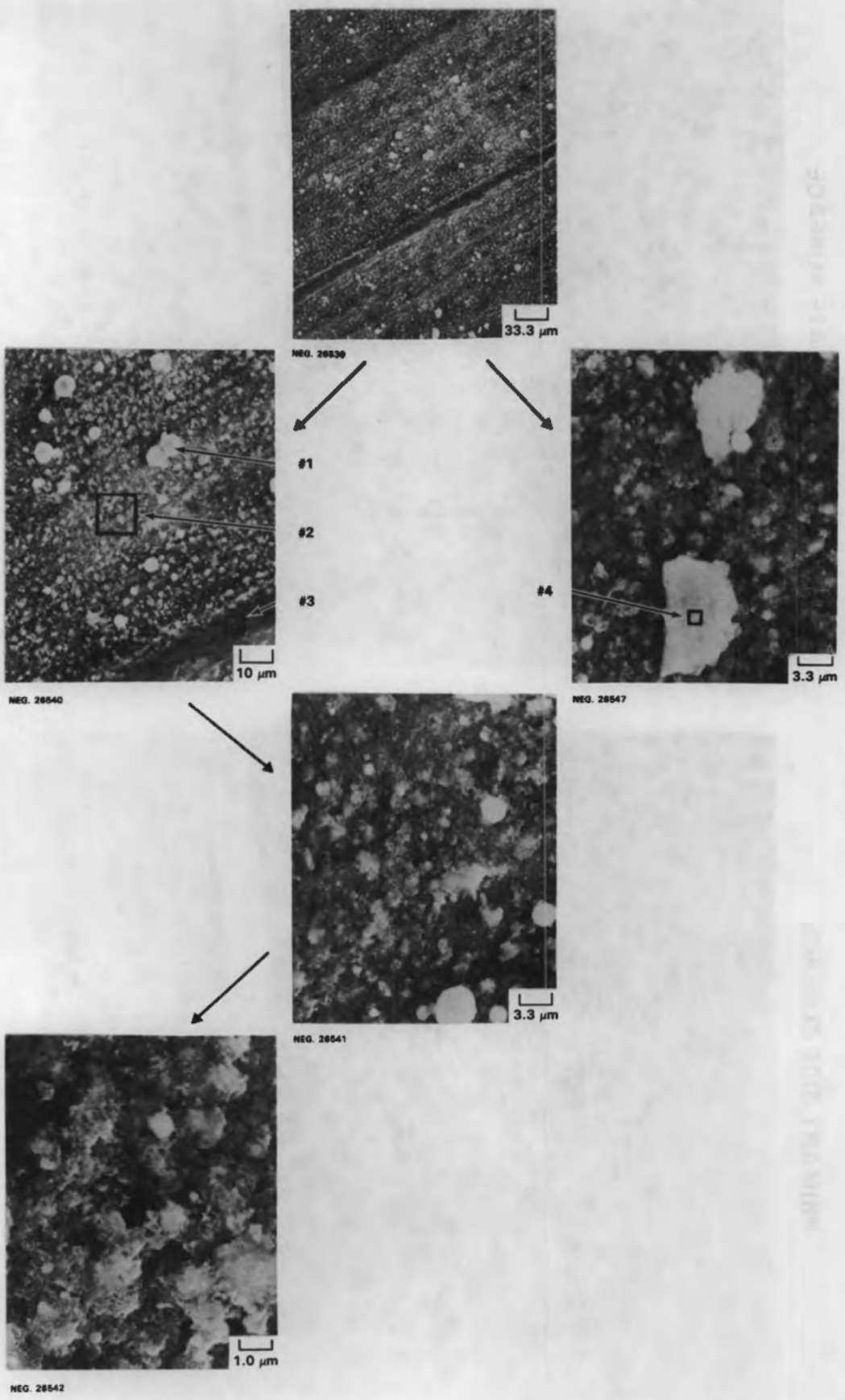

FIGURE 7-11. SEM Examination of the Primary Side Surface of the Hot Leg Manway Coupon

oxide on the cold leg specimen. In addition, the superficial particles on the hot leg specimen were not incorporated into the base oxide, in contrast to the cold leg surface. Table 7-5 gives approximate compositions, based on EDX analyses, of selected regions in Figure 7-11.

TABLE 7-5. EDX Analysis* of the Primary Side Surface of an Undecontaminated Hot Leg Manway Cover Insert Coupon (Figure 7-11)

Region	Approx. Weight Percent Cr	Approx. Weight Percent Fe	Approx. Weight Percent Ni	Approx. Weight Percent Other	Trace
1	27	62	6	3 Si, 2 Mn	Al, Mo
2	37	49	10	3 Mn, 1 Si	Al
3	36	51	10	2 Mn, 1 Si	Al
4	44	38	5	8 Mn, 6 Si	Ti

*From baseline corrected K(α) peak height ratios (excluding elements with atomic numbers below Na).

The Ni to Cr ratio for the base oxide on the hot leg manway insert coupon was lower than that for the corresponding core specimen from the channel head. Comparison of the oxide composition on the hot leg coupon (regions 2 and 3 in Figure 7-11) with the composition of the cold leg oxide (regions 2 and 9 in Figure 7-9) shows trends similar to those for the channel head specimens: higher Fe, and lower Cr, Ni, Mn and Si in the hot leg than in the cold leg. The Ni to Cr ratio is lower for the hot leg oxide than for the cold leg oxide. As with the cold leg surface (regions 3 and 4 in Figure 7-9), the superficial round particulate is lower in Cr and Ni and higher in Fe than the base oxide. An irregularly shaped superficial particle on the hot leg (region 4 in Figure 7-11) has a similar composition to the irregularly shaped particulate on the cold leg (region 5 in Figure 7-9).

A metallographic cross section was prepared from a hot leg manway cover insert coupon and examined using SEM. Figure 7-12 shows SEM photographs of the primary side/base metal interface. The photographs suggest a duplex corrosion film composed of deposited crud on top of oxidized base metal. The outer layer appears thinner for this specimen than for the cold leg specimen from the manway cover insert, while the inner layer has a similar thickness. An X-ray fluorescence map for Si (Figure 7-12, neg. 27409) shows Si segregation at the metal surface. Composition variations as a function of distance from the base metal/oxide interface are plotted in Figure 7-13, which shows the following trends:

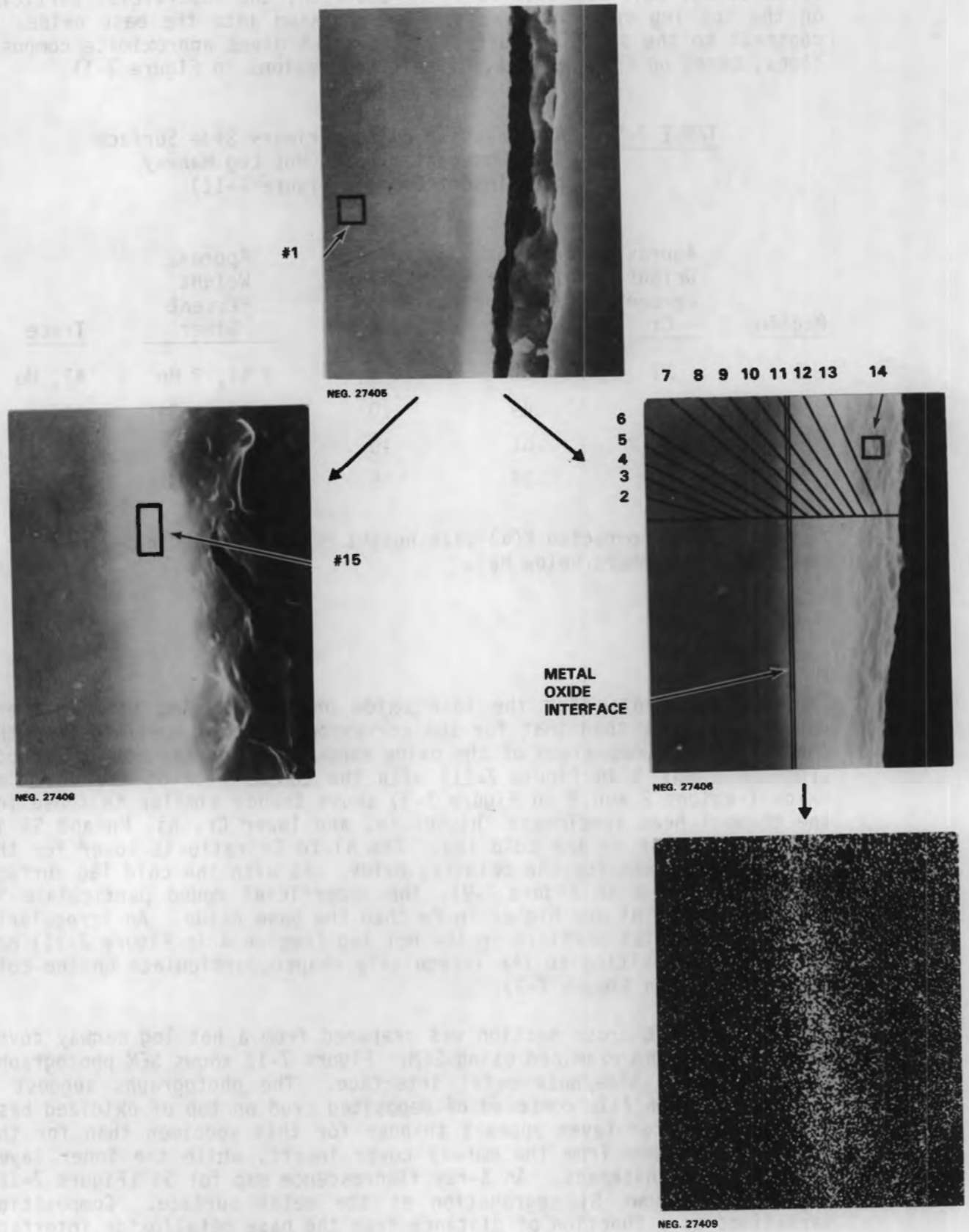

FIGURE 7-12. SEM Examination of a Metallographic Cross Section of a Hot Leg Manway Coupon

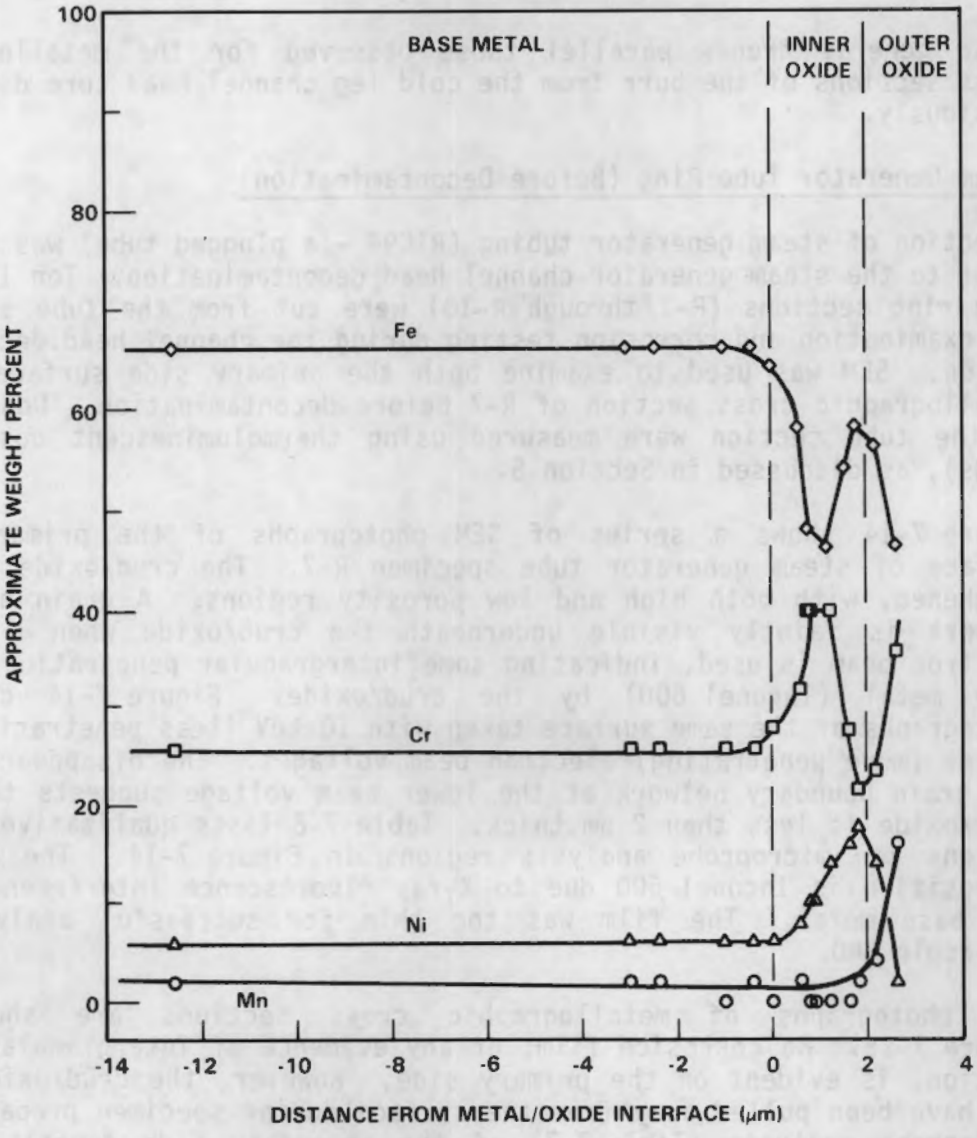

FIGURE 7-13. Composition Variations as a Function of Distance From the Metal/Oxide Interface for a Hot Leg Manway Coupon

- Cr concentration in the inner oxide layer increases and then decreases from the base metal value; Cr levels increase again in the outer layer.

- Fe trends are opposite to those of Cr.

- Ni increases steadily with distance from the base metal interface throughout the inner layer, and decreases in the outer layer.

- Mn remains constant in the base metal and inner oxide layer, but increases in the outer layer.

These general trends parallel those observed for the metallographic cross sections of the burr from the cold leg channel head core discussed previously.

Steam Generator Tube Ring (Before Decontamination)

A section of steam generator tubing (R1C94 - a plugged tube) was removed prior to the steam generator channel head decontamination. Ten 1.25-cm-long ring sections (R-1 through R-10) were cut from the tube specimen for examination and corrosion testing during the channel head decontamination. SEM was used to examine both the primary side surface and a metallographic cross section of R-7 before decontamination. Dose rates in the tube section were measured using thermoluminescent dosimeters (TLDs), as discussed in Section 5.

Figure 7-14 shows a series of SEM photographs of the primary side surface of steam generator tube specimen R-7. The crud/oxide appears roughened, with both high and low porosity regions. A grain boundary network is faintly visible underneath the crud/oxide when a 25 keV electron beam is used, indicating some intergranular penetration of the base metal (Inconel 600) by the crud/oxide. Figure 7-14 compares photographs of the same surface taken with 10 keV (less penetrating) and 25 keV (more penetrating) electron beam voltages. The disappearance of the grain boundary network at the lower beam voltage suggests that the crud/oxide is less than 2 μm thick. Table 7-6 lists qualitative compositions for microprobe analysis regions in Figure 7-14. The average composition is Inconel 600 due to X-ray fluorescence interference from the base metal. The film was too thin for successful analysis by low-angle XRD.

SEM photographs of metallographic cross sections are shown in Figure 7-15. No corrosion film, or any evidence of intergranular penetration, is evident on the primary side. However, the crud/oxide film may have been pulled away from the surface during specimen preparation. Microprobe analysis (Table 7-7) of the secondary side deposit showed large particles (10 μm) of almost pure Cu* and microcrystallites (0.5 μm) that were primarily Fe*.

*Excluding elements with atomic numbers below Na.

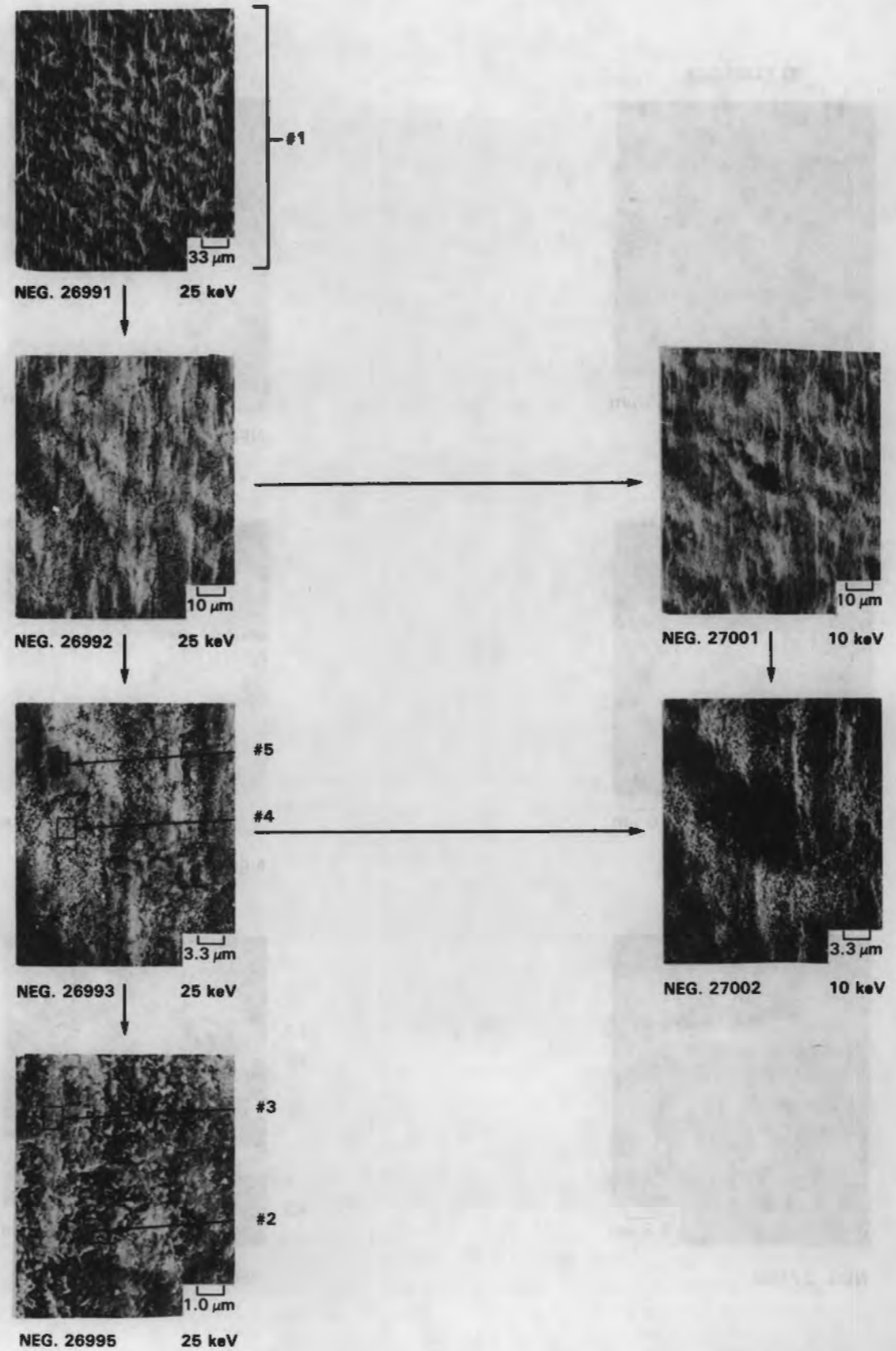

FIGURE 7-14. SEM Examination of the Primary Side Surface of Specimen R-7 From Steam Generator Tube R1C94 Before Decontamination

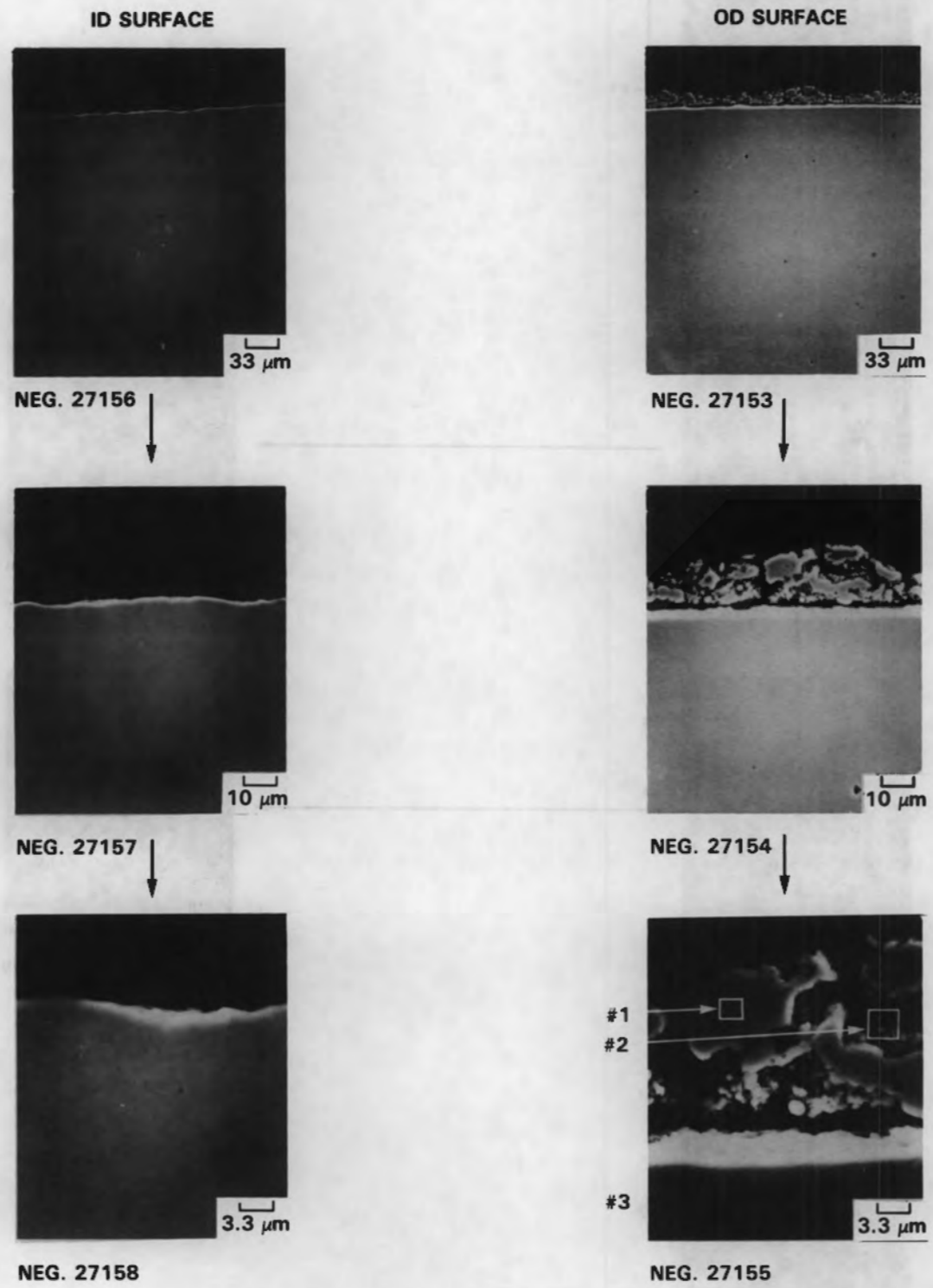

FIGURE 7-15. SEM Examination of Primary and Secondary Sides of a Metallographic Cross Section of the Undecontaminated Steam Generator Tube Specimen R-7

TABLE 7-6. EDX Analysis* of the Primary Side Surface of an Undecontaminated Steam Generator Tube Specimen (Figure 7-14)

Region	Approx. Weight Percent Cr	Approx. Weight Percent Fe	Approx. Weight Percent Ni	Trace
1	29	13	57	Al, Si, Ti
2	27	14	59	Al, Si, Ti
3	28	13	58	Si, Ti
4	29	15	55	Si, Ti
5	27	11	60	Si

*From baseline corrected K(α) peak height ratios (excluding elements with atomic numbers below Na).

TABLE 7-7. EDX Analysis* of the Secondary Side (Metallographic Cross Section) of an Undecontaminated Steam Generator Tube Specimen (Figure 7-15)

Region	Approx. Weight Percent Cr	Approx. Weight Percent Fe	Approx. Weight Percent Ni	Approx. Weight Percent Cu	Approx. Weight Percent Other	Trace
1	1	4	2	92		Al, Si
2	1	67	10	12	6 Zn	Al, Si, Mn
3	25	11	62	--		Al, Si

*From baseline corrected K(α) peak height ratios (excluding elements with atomic numbers below Na).

Specimen DFs After Cold Leg Decontamination

Figure 7-16 shows radioactive coupons from the cold leg manway cover insert that were included in the coupon racks to determine decontamination effectiveness. Specimen decontamination factors (DF = ratio of initial activity to final activity) ranged from 5.7 to 8.5 for the stainless steel manway cover specimens (Table 7-8). Differences in the

MANWAY COUPONS

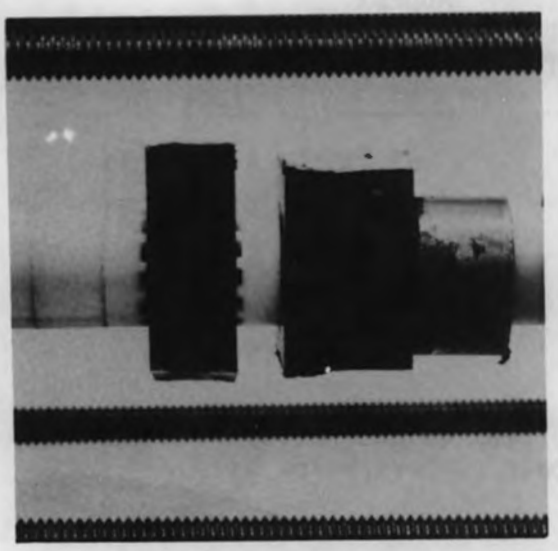

NEG. 8206771-13

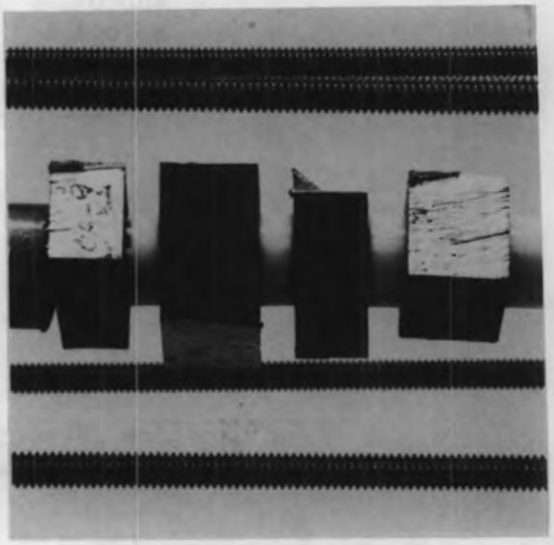

NEG. 8206771-17

STEAM GENERATOR TUBE RINGS

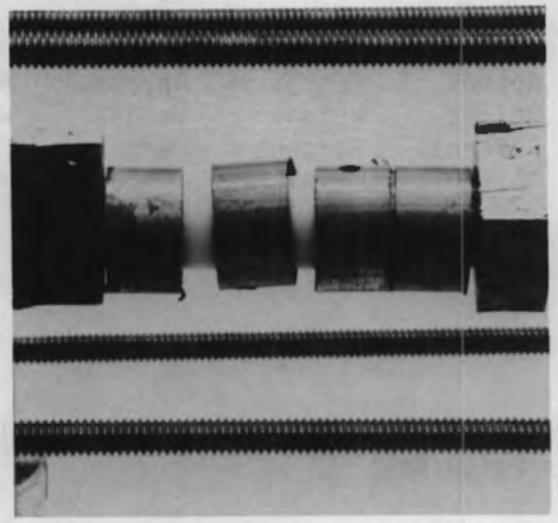

NEG. 8206771-15

FIGURE 7-16. Radioactive Steam Generator Specimens After the Cold Leg Decontamination

surface finish delineation between decontaminated and undecontaminated coupons indicate the degree of film removal (Figure 7-17). DFs for the Inconel 600 steam generator tube specimens ranged from 4.1 to 4.5 (Table 7-8). The cold leg process effectively removed the secondary side deposits from the steam generator tube specimens, with little or no penetration into the Inconel 600 base metal. Significant residual crud/oxide remained on the primary side (but not the secondary side) of the steam generator tube specimens after the decontamination, as shown in Figure 7-18. Since the specimens were loosely mounted, flow effects probably do not account for lower DFs on the steam generator tube specimens than on the manway coupons, especially considering differences in the Inconel 600 and stainless steel corrosion films.

TABLE 7-8. Decontamination Factors for Cold Leg Steam Generator Specimens

Specimen	Percent Co-60 Remaining	Decontamination Factor
Manway Coupon		
CA-8	16	6
CA-9	13	8
CA-10	12	8
CB-8	14	7
CB-9	18	6
CB-10	17	6
Steam Generator Tube Ring		
R-2	24	4
R-3	23	4
R-4	24	4
R-5	22	4
Channel Head Cores		
CL1	16	6
CL2	12	8
Tube Sheet	7	14

Specimen DFs After Hot Leg Decontamination

Specimens from the hot leg manway cover insert and steam generator tube R1C94 were included in the hot leg coupon racks to obtain specimen decontamination factors for stainless steel and Inconel 600 respectively. In addition, selected specimens from the cold leg decontamination were recycled to determine the effects of repeated decontamination (Figure 7-19). The post-decontamination appearance of the coupons is shown in Figure 7-20, with the twice decontaminated specimens appearing slightly brighter than those only exposed to the hot leg process. Table 7-9 summarizes the decontamination results for the steam generator

NO DECONTAMINATION

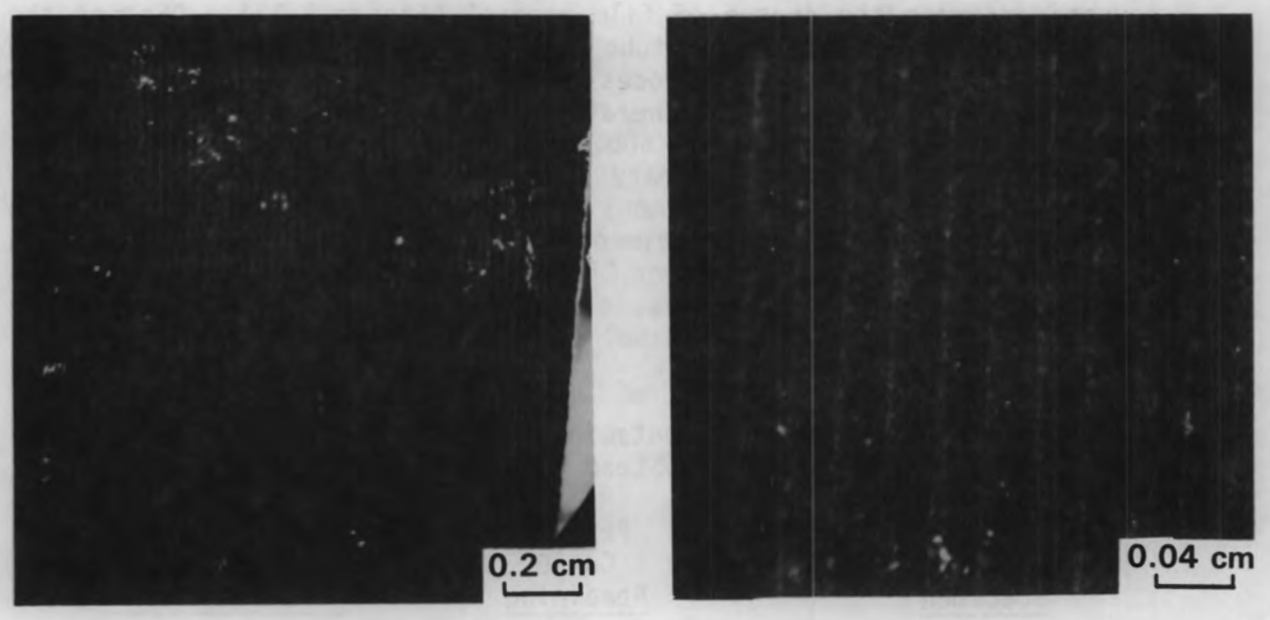

CC CENTER

CC CENTER

COLD LEG DECONTAMINATION

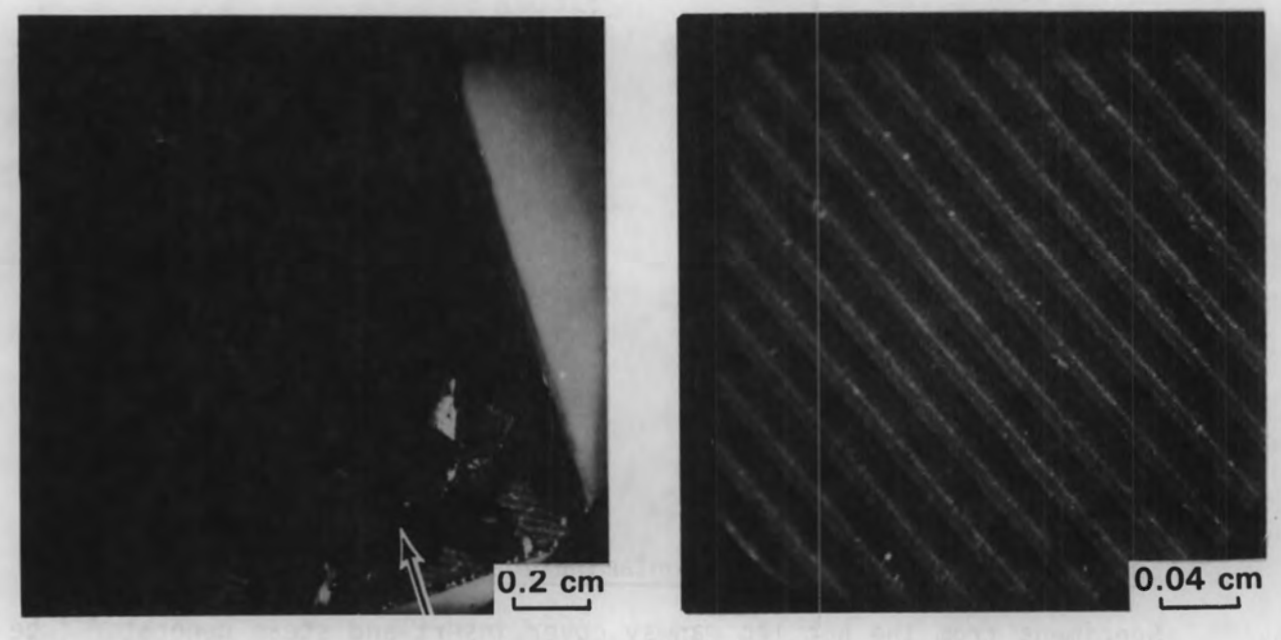

CB 8

RESIDUAL TAPE

CB 8

FIGURE 7-17. Appearance of Undecontaminated and Decontaminated Cold Leg Manway Coupons

NO DECONTAMINATION

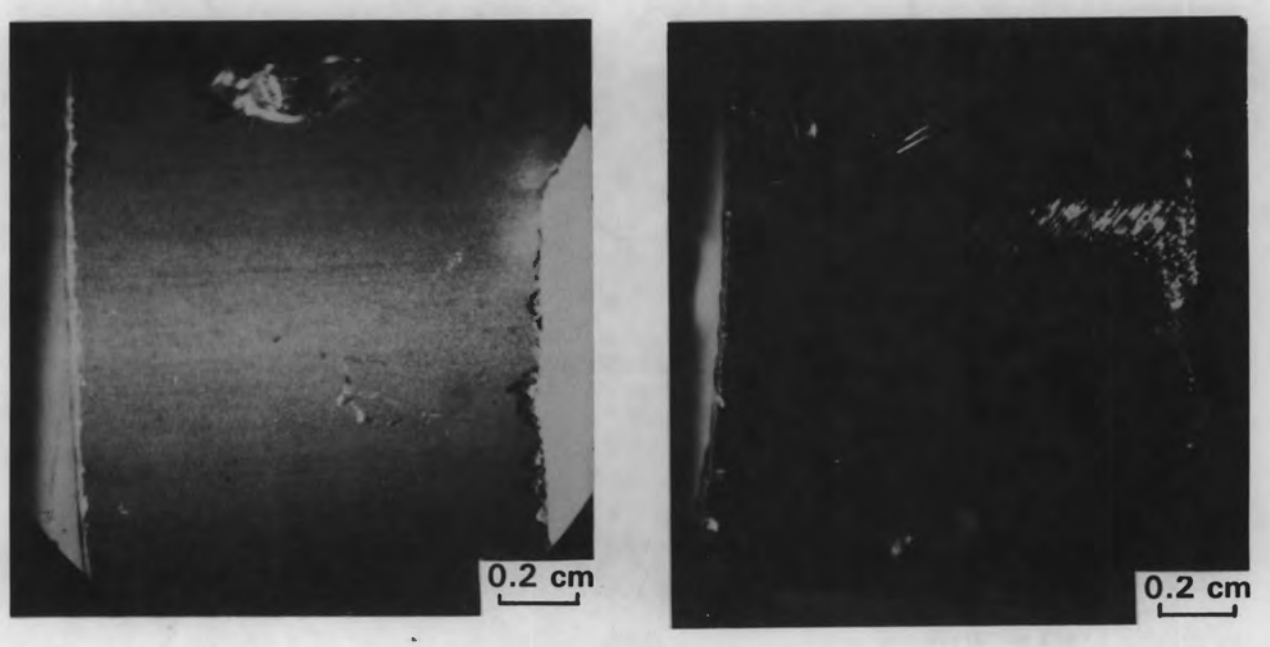

R9 ID

R9 OD

AFTER COLD LEG DECONTAMINATION

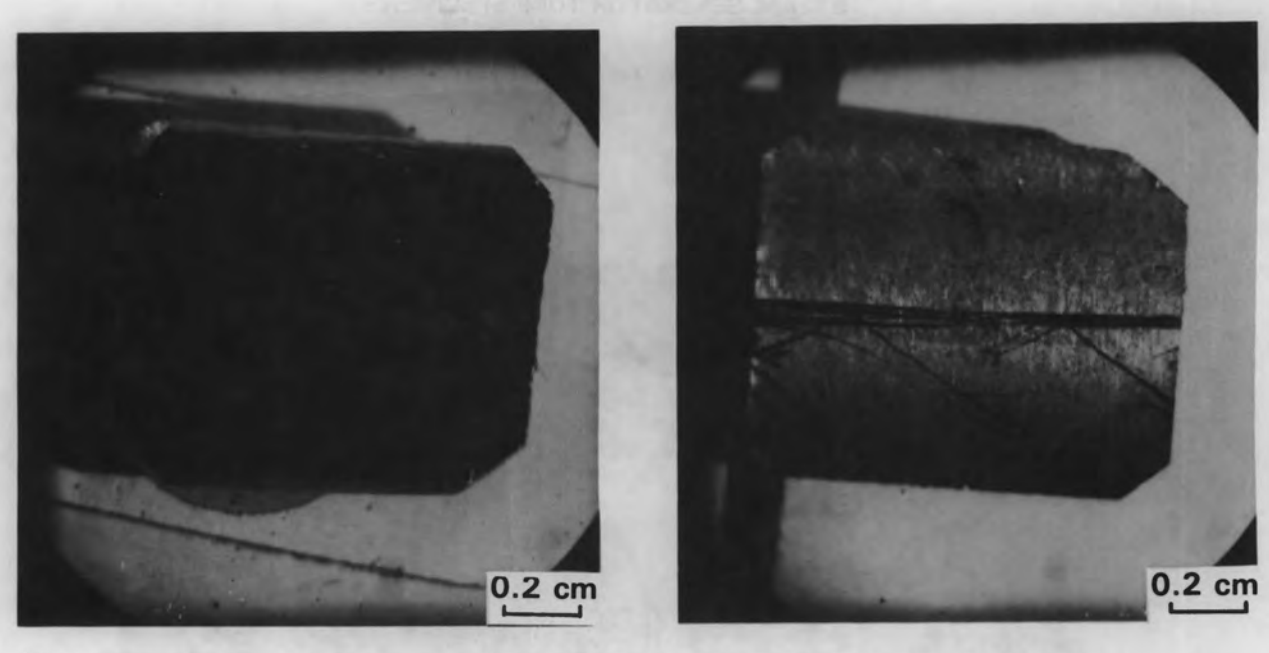

R5 ID

R5 OD

FIGURE 7-18. Appearance of the Primary and Secondary Side Surfaces of Steam Generator Tube Specimens Before and After the Cold Leg Decontamination

MANWAY COUPONS

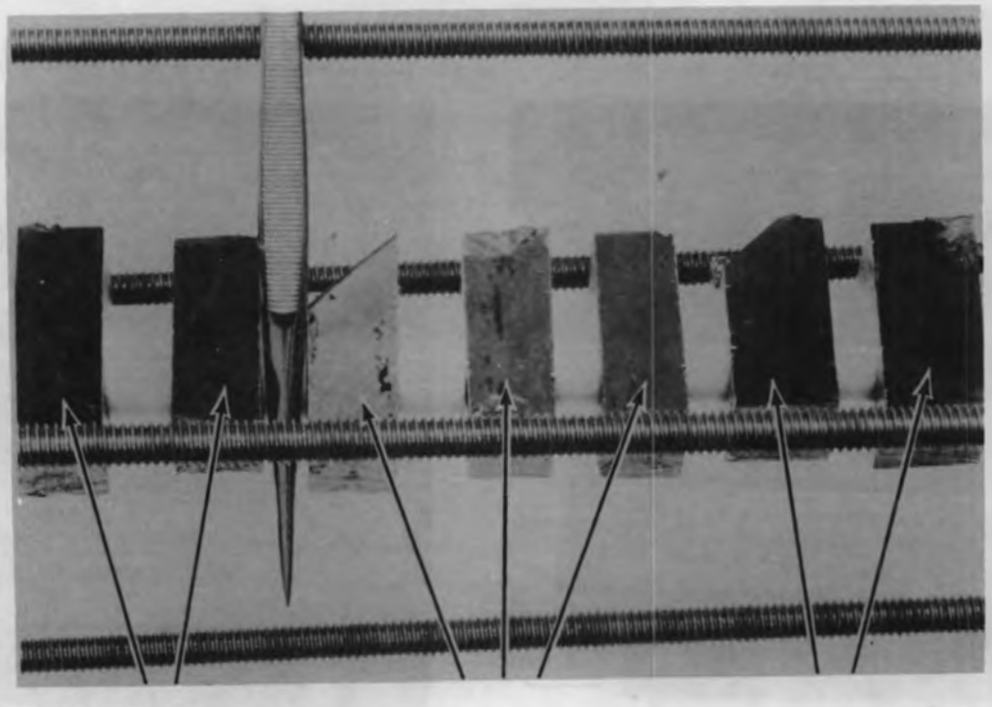

NEG. 8207279-79

NO DECONTAMINATION | AFTER COLD LEG DECONTAMINATION | NO DECONTAMINATION

STEAM GENERATOR TUBE SPECIMENS

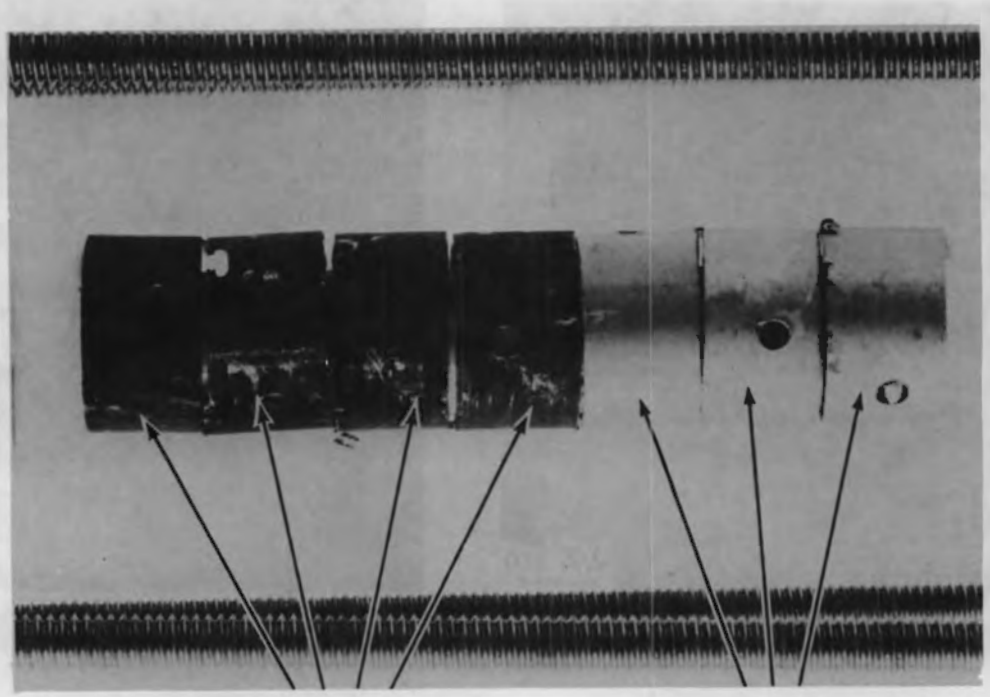

NEG. 8207279-70

NO DECONTAMINATION | AFTER COLD LEG DECONTAMINATION

FIGURE 7-19. Radioactive Steam Generator Specimens Before the Hot Leg Decontamination

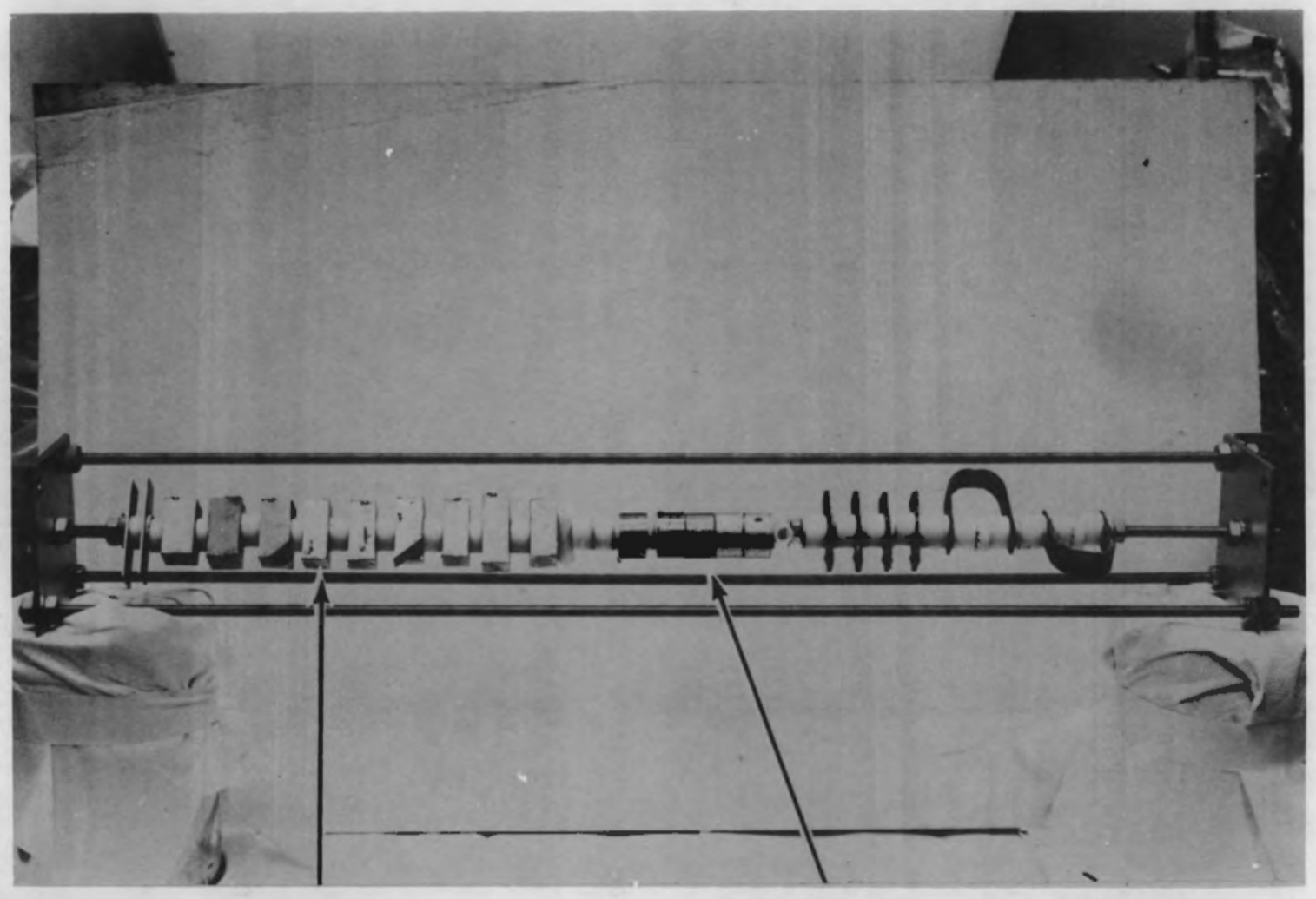

NEG. 8207985-2

FIGURE 7-20. Radioactive Steam Generator Specimens After the Hot Leg Decontamination

TABLE 7-9. Decontamination Factors for Hot Leg Steam Generator Specimens

Specimen	Percent Co-60 Remaining After Decontamination		Decontamination Factor	
	Post-LOMI	Post-Citrox	Post-LOMI	Post-Citrox
Manway Coupon				
HA-8	4	0.2	25	500
HA-9	4	0.03	25	333
HA-10	3	0.2	33	500
HB-8	5	0.3	20	333
HB-9	4	0.1	25	1000
HB-10	3	0.2	33	500
CA-8(1)	18(2)	1	6	100
CA-9(1)	25(2)	1	4	100
CA-10(1)	13(2)	2	8	50
Steam Generator Tube Ring				
R-1	71	25	1	4
R-6	68	21	2	5
R-8	63	20	2	5
R-10	63	18	2	6
R-2(1)	37(2)	4	3	25
R-3(1)	23(2)	4	4	25
R-4(1)	24(2)	4	4	25
Channel Head Core				
HL1		1.3		75
HL2		0.7		150
Tube Sheet		20		5

(1) Previously decontaminated in the cold leg channel head.

(2) 100% taken as the activity level following the cold leg decontamination.

specimens. The hot leg application, up through LOMI, removed ∿95% of the activity from the stainless steel specimens and ∿35% of the activity from the Inconel 600 primary side surfaces. The subsequent AP/NP/Citrox treatment removed an additional 3.6% of the activity from the stainless steel and an additional 45% of the activity from the Inconel 600. Final activity levels were similar for manway cover coupons decontaminated either by the hot leg process or by the cold leg and hot leg processes, while steam generator tube specimens decontaminated by both processes had activity levels that were twenty times lower than specimens decontaminated by a single process.

Cold Leg Channel Head Core Specimens (After Decontamination)

Two stainless steel specimens were removed from the cold leg channel head wall by core drilling after completion of the cold leg decontamination. Visual (Figure 7-21) and SEM (Figure 7-22) examination found only trace surface deposits. Comparison of the Co-60 activities for the decontaminated and undecontaminated specimens suggests that a DF of ∿7 was obtained (Table 7-8). Cracking was found in the center of the one of the decontaminated core specimens, as shown in Figure 7-22. While this may have occurred during specimen removal, indications of subsurface cracking on the undecontaminated burr specimen (Figure 7-5) suggest that the crack existed prior to decontamination. Once exposed, such cracks could trap decontamination chemicals. However, the potential for corrosion in these cracks may be low since the coupon crevice regions were resistant to corrosion.

Hot Leg Channel Head Core Specimens (After Decontamination)

Two specimens were removed from the hot leg of the channel head after decontamination and examined using SEM. The post-decontamination appearance of the primary side surface of the stainless steel core specimens was similar to that found on the cold leg specimens after decontamination. Figures 7-23 and 7-24 show SEM photographs of the hot leg specimens, and Table 7-10 summarizes EDX analyses of the surface features. The main features are summarized as follows:

- No residual oxide was found;
- No evidence of corrosion due to the chemical decontamination process was found. Surface roughness apparent in Figures 7-23 and 7-24 probably existed under the crud/oxide layer prior to decontamination;
- Fractures in the outer stainless steel cladding were uncovered by the decontamination;
- EDX analysis indicated that the two hot leg specimens had similar compositions and that the superficial particulate was probably sand.

NO DECONTAMINATION

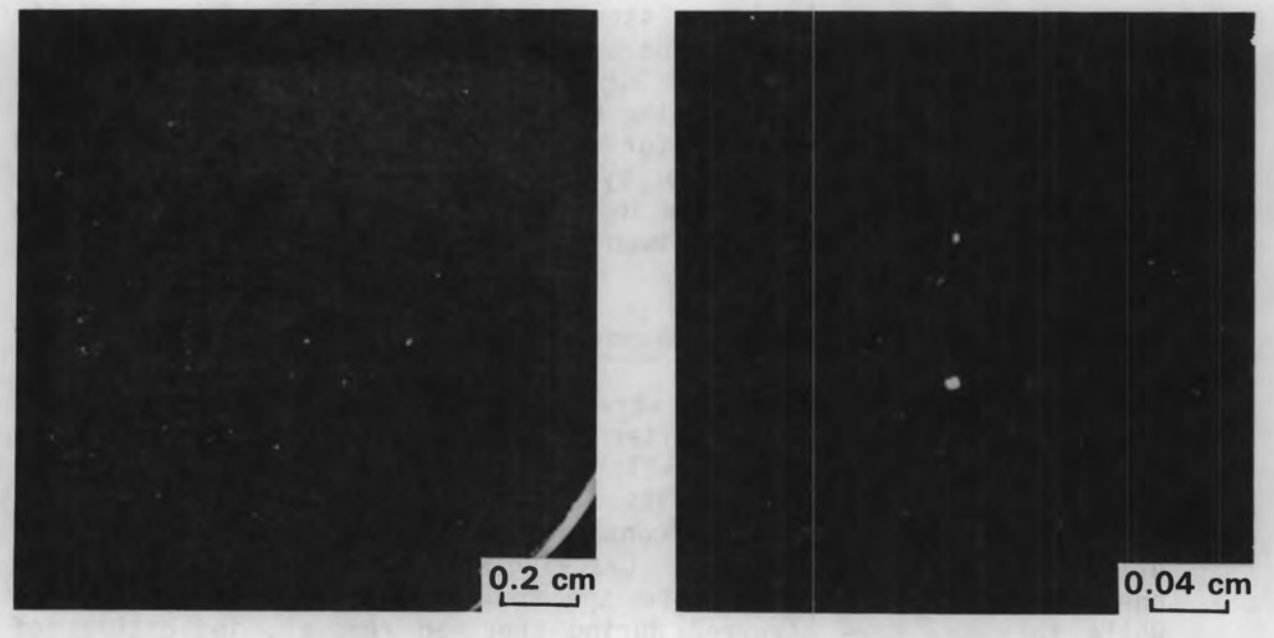

CL 0 CL 0

AFTER COLD LEG DECONTAMINATION

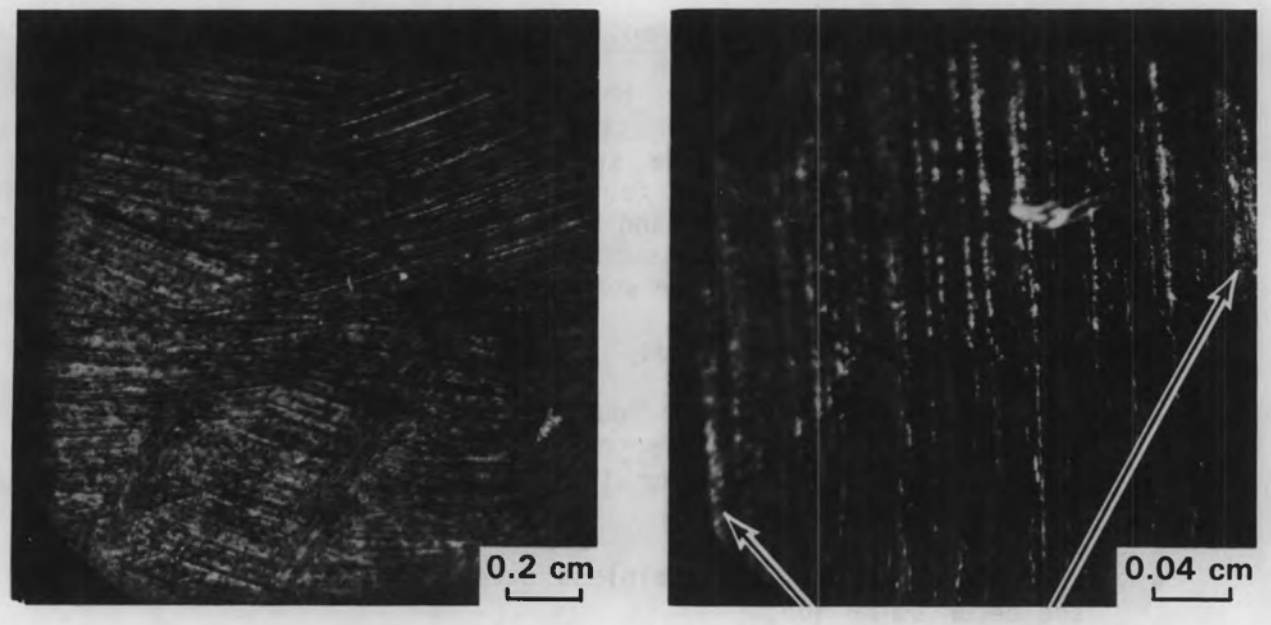

CL 1 CL 2 SURFACE CRACK

FIGURE 7-21. Comparison of Cold Leg Channel Head Wall Surfaces Before and After Decontamination

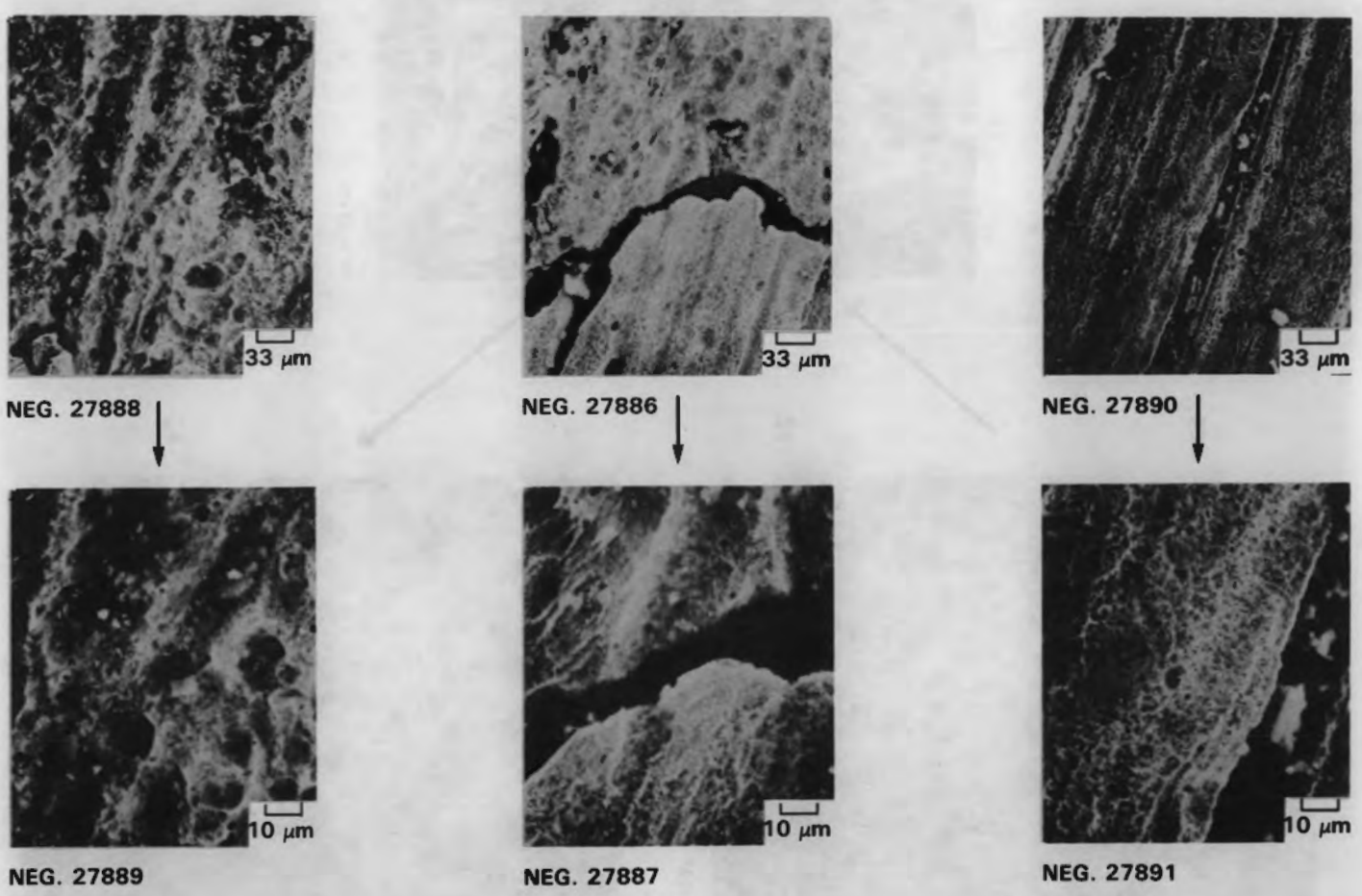

FIGURE 7-22. SEM Examination of the Primary Side Surface of Core Specimens From the Cold Leg Channel Head Wall After Decontamination

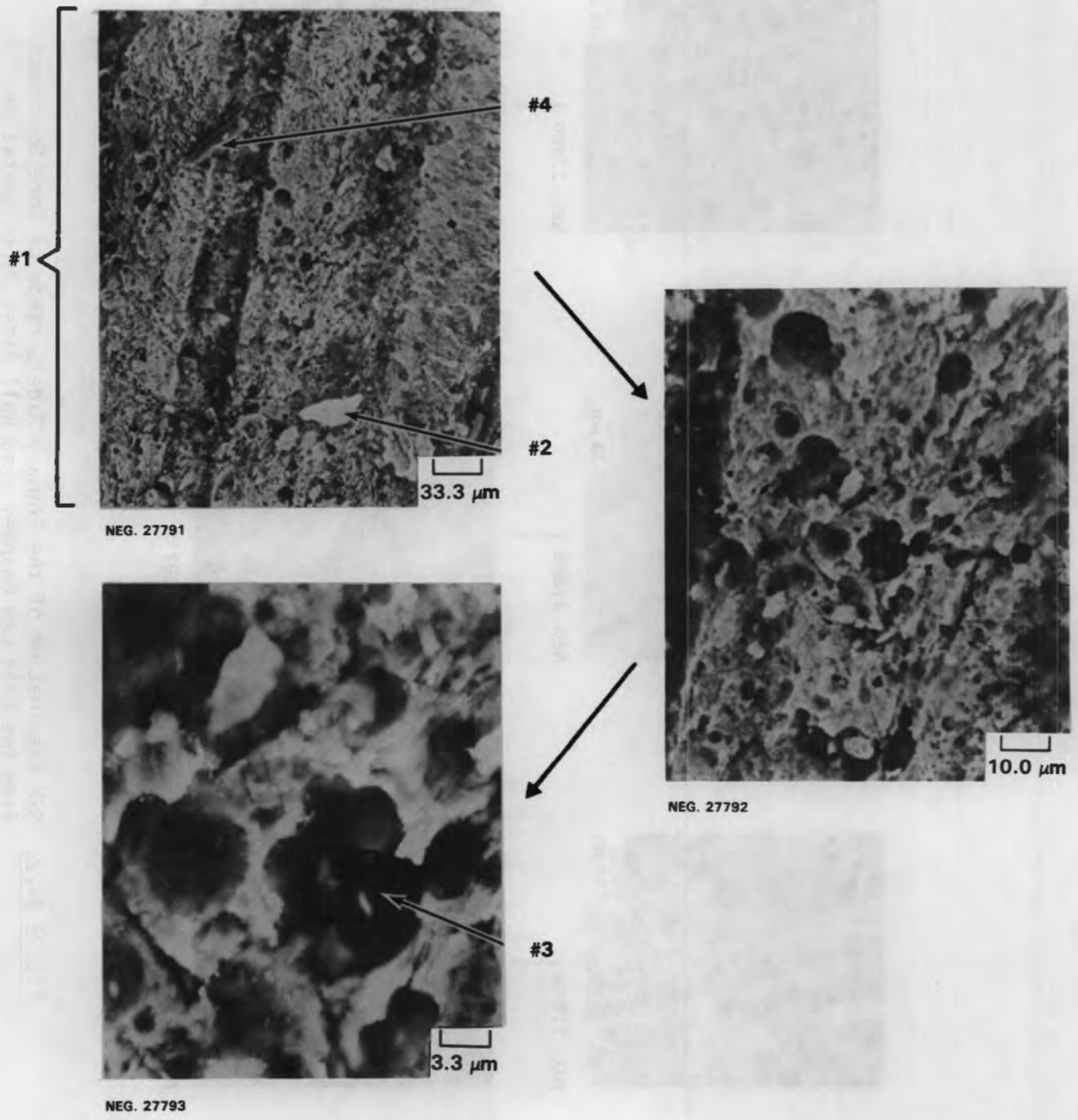

FIGURE 7-23. SEM Examination of the Primary Side Surface of Core Specimen HL-1 Removed From the Hot Leg Channel Head Wall After Decontamination

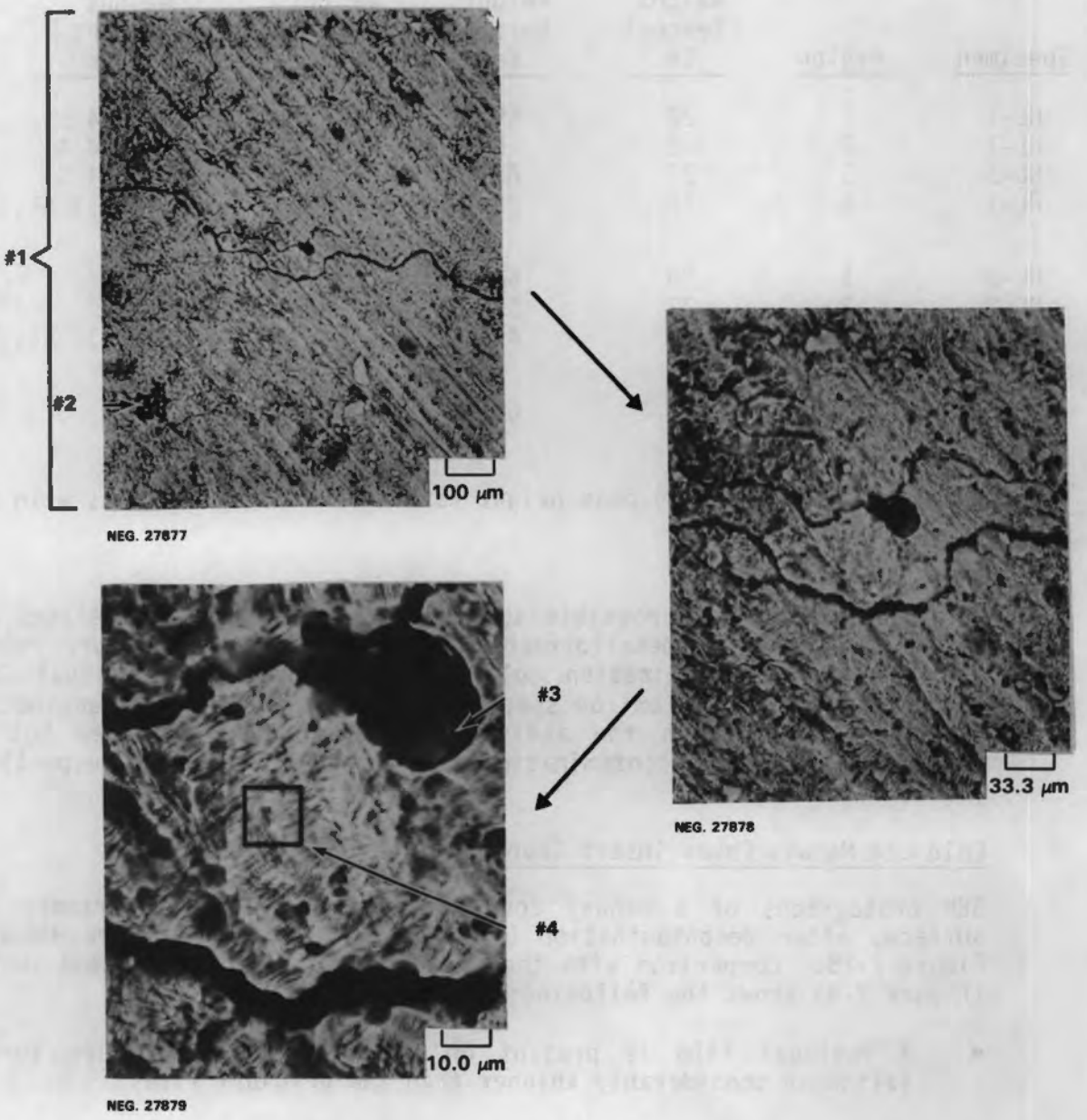

FIGURE 7-24. SEM Examination of Core Specimen HL-2 Removed From the Hot Leg Channel Head Wall After Decontamination

TABLE 7-10. EDX Analysis* of Post-Decontamination Hot Leg Channel Head Core Specimens HL-1 and HL-2 (Figures 7-23 & 7-24)

Specimen	Region	Approx. Weight Percent Cr	Approx. Weight Percent Fe	Approx. Weight Percent Ni	Approx. Weight Percent Other	Trace
HL-1	1	28	59	5	2 Mn, 4 Si	Mg, Al
HL-1	2	2	4	1	90 Si, 4 Al	
HL-1	3	27	62	3	4 Mn, 1 Si	Al, Mg, S
HL-1	4	10	28	1	18 Mg, 11 Al, 29 Si	Mn
HL-2	1	29	64	5	2 Si	Al
HL-2	2	37	52	9	2 Si	
HL-2	3	17	45	4	17 Si, 10 Al, 5 K	Cl, Mg
HL-2	4	27	66	5		Al, Si

*From baseline corrected K(α) peak height ratios (excluding elements with atomic numbers below Na).

Surface cracking with possible subsurface contamination correlates with observations on the metallographic cross section of the burr removed from the pre-decontamination cold leg core specimen. Residual Co-60 activity was 0.02 μCi/cm² on specimen HL-1 and 0.04 μCi/cm² on specimen HL-2; comparison with the activity on the undecontaminated hot leg specimens suggests decontamination factors of 75 and 150 respectively (Table 7-9).

Cold Leg Manway Cover Insert Coupons (After Decontamination)

SEM photographs of a manway cover insert coupon (CB-9) primary side surface, after decontamination by the cold leg process, are shown in Figure 7-25. Comparison with the undecontaminated primary side surface (Figure 7-9) shows the following:

- A residual film is present on the post-decontamination surface (although considerably thinner than the original film).
- Flakes of film appear to have come off (perhaps due to undercutting).
- Round particles were deposited on the surface.

Table 7-11 lists qualitative compositions for regions shown in Figure 7-25: the round particles have slightly higher Cr, Si, and Mn than the residual film, and lower Fe and Ni. Counting data indicated that 82% of the original Co-60 was removed from the surface during the

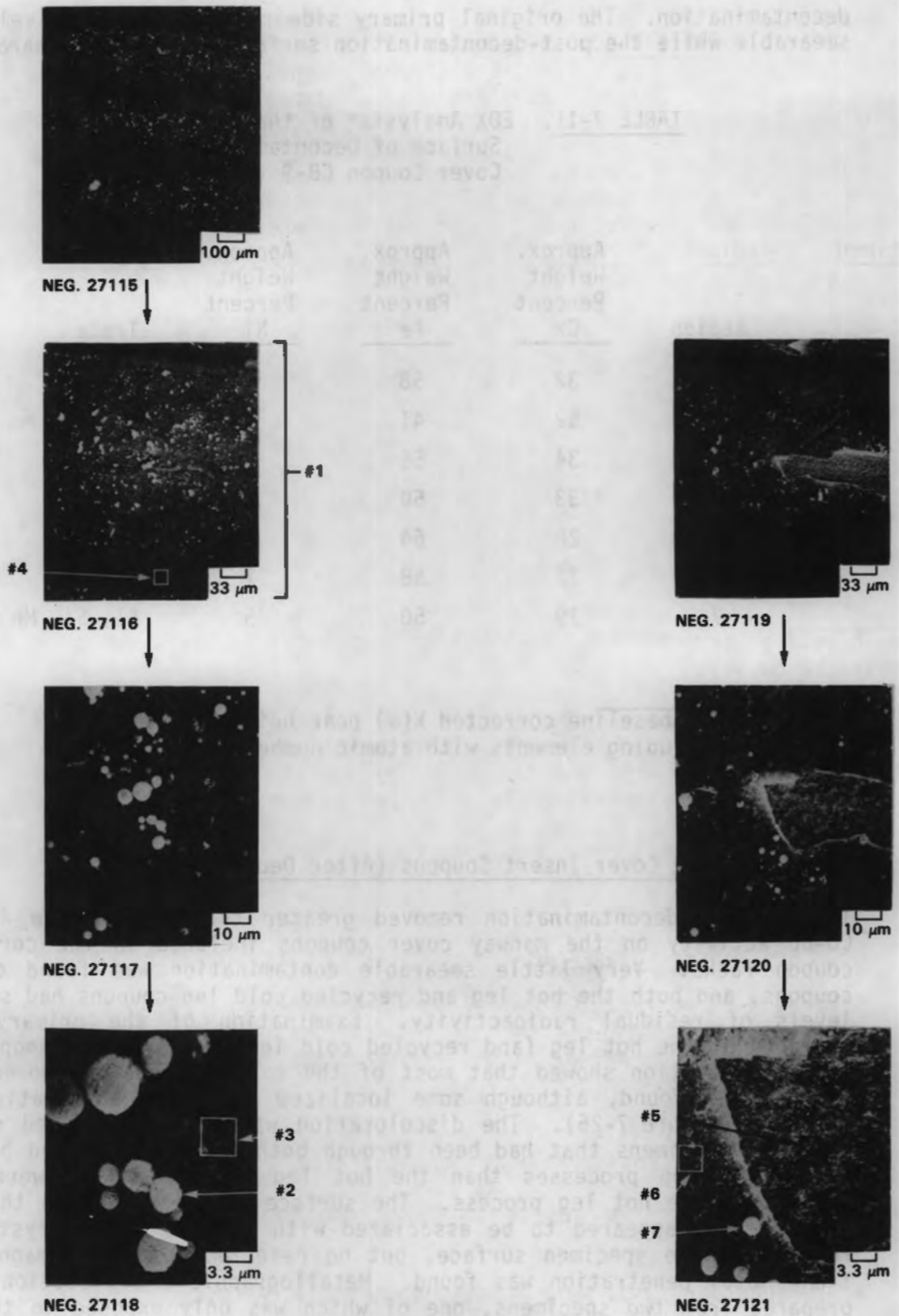

FIGURE 7-25. SEM Examination of the Primary Side Surface of Manway Coupon CB-9 After the Cold Leg Decontamination

decontamination. The original primary side surface was relatively non-smearable while the post-decontamination surface was highly smearable.

TABLE 7-11. EDX Analysis* of the Primary Side Surface of Decontaminated Manway Cover Coupon CB-9 (Figure 7-25)

Region	Approx. Weight Percent Cr	Approx. Weight Percent Fe	Approx. Weight Percent Ni	Trace
1	32	58	6	Mn, Si
2	52	41	2	Al, Si, Mn
3	34	56	7	Si, Mn
4	33	58	7	Si, Mn
5	28	64	4	Si, Mn
6	32	58	7	Si, Mn
7	39	50	5	Al, Si, Mn

*From baseline corrected K(α) peak height ratios (excluding elements with atomic numbers below Na).

Hot Leg Manway Cover Insert Coupons (After Decontamination)

The hot leg decontamination removed greater than 99% of the initial Co-60 activity on the manway cover coupons included in the corrosion coupon racks. Very little smearable contamination was found on the coupons, and both the hot leg and recycled cold leg coupons had similar levels of residual radioactivity. Examination of the primary side surfaces of the hot leg (and recycled cold leg) manway cover coupons at 70X magnification showed that most of the oxide had been removed. No pitting was found, although some localized surface discoloration was observed (Figure 7-26). The discoloration was more pronounced on the cold leg specimens that had been through both the cold leg and hot leg decontamination processes than the hot leg specimens that were only exposed to the hot leg process. The surface discoloration on the cold leg specimen appeared to be associated with a trace white crystalline residue on the specimen surface, but no detectable (at 70X magnification) metal penetration was found. Metallographic cross sections were prepared from two specimens, one of which was only exposed to the hot leg process while the other was exposed to both the cold leg and hot leg processes. SEM examination of these specimens (Figure 7-27) showed no evidence of metal penetration. Table 7-12 gives approximate base metal compositions for these specimens.

HOT LEG COUPON HB-9

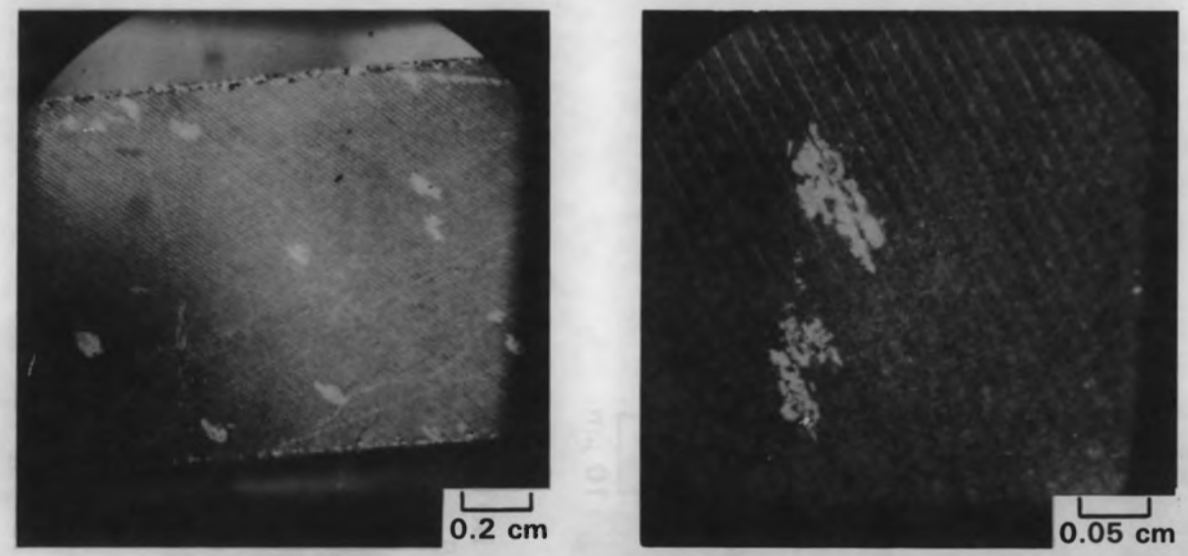

RECYCLED COLD LEG COUPON CA-9

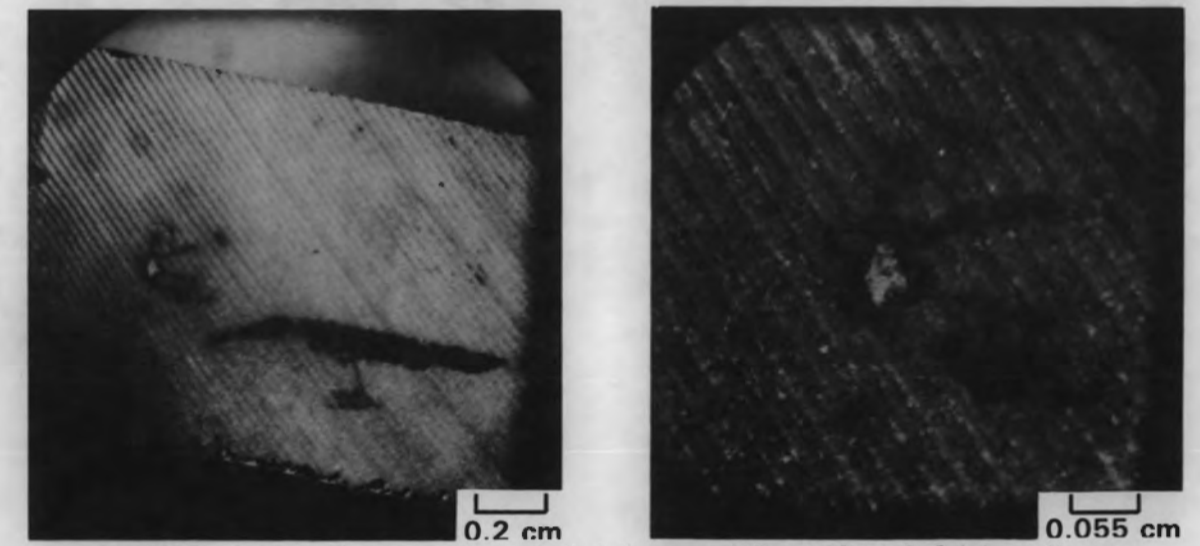

FIGURE 7-26. Appearance of Hot Leg and Recycled Cold Leg Manway Coupons After the Hot Leg Decontamination

AFTER HOT LEG DECONTAMINATION

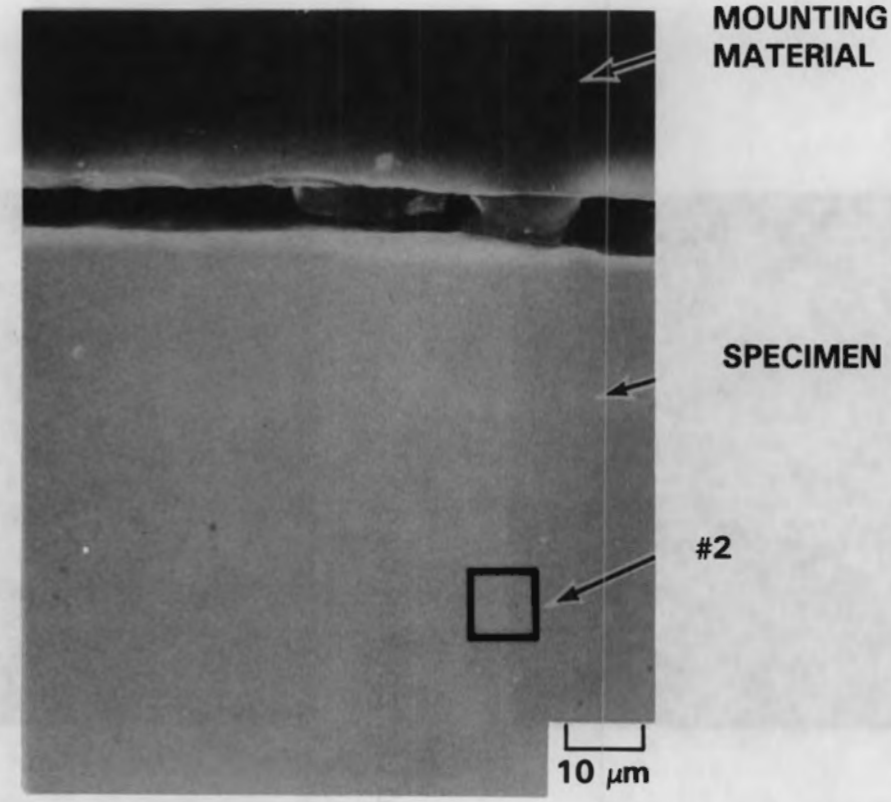

AFTER DECONTAMINATION IN BOTH THE COLD AND HOT LEGS

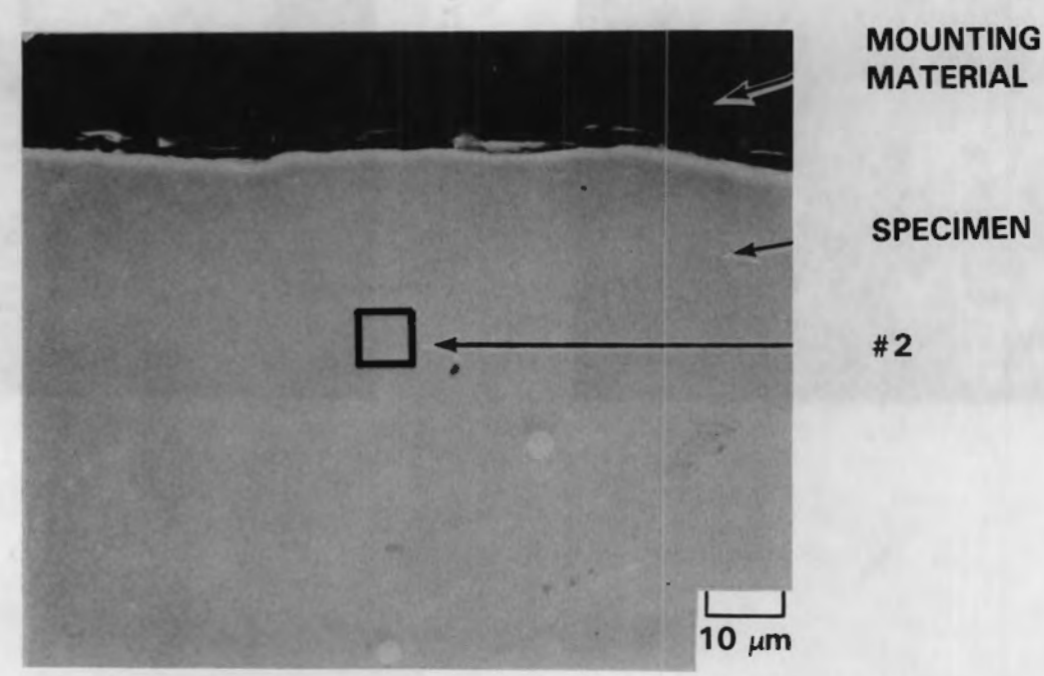

FIGURE 7-27. SEM Examination of Metallographic Cross Sections of Manway Coupons After the Hot Leg Decontamination

TABLE 7-12. EDX Analysis* of Base Metal Composition (Figure 7-27)

Specimen	Approx. Weight Percent Cr	Approx. Weight Percent Fe	Approx. Weight Percent Ni	Trace
HA-8	27	65	6	Al, Si
CA-8	28	65	5	Al, Si

*From baseline corrected K(α) peak height ratios (excluding elements with atomic numbers below Na).

Steam Generator Tube Specimen (After Cold Leg Decontamination)

Metallographic studies showing a greater tube surface grain boundary delineation after cold leg decontamination (Figure 7-28 vs. Figure 7-14) indicate that the decontamination process caused thinning of the primary side surface crud/oxide. Approximately 80% of the Co-60 activity was removed from the test specimen during the cold leg decontamination.

A metallographic cross section was prepared from a piece of tube specimen to determine the extent of penetration into the Inconel 600 base metal. Figure 7-29 shows the primary side and secondary side surfaces. No penetrations into the base metal of any sort, and complete removal of all deposits, were found on the secondary side surface. Minor intergranular penetration (up to 2 μm) was observed on the primary side surface, probably due to dissolution of crud/oxide that had penetrated into the base metal during service. Residual crud/oxide was not found on the primary side, possibly due to removal during preparation of the metallographic cross section.

Steam Generator Tube Specimen (After Hot Leg Decontamination)

Undecontaminated steam generator tube specimens and specimens that had been partially decontaminated by the cold leg process were incorporated into the corrosion coupon racks for the hot leg decontamination. As shown in Figure 7-30, an oxide film remained on the ID of a tube specimen that was only exposed to the hot leg process, but not on a specimen that was exposed to both decontamination processes. About 20% and 3%, respectively, of the initial Co-60 activity remained on the specimens. Like the cold leg process, the hot leg process removed essentially all of the secondary side deposits on the steam generator tubing. Figure 7-30 also shows surface roughness on the OD of the tube specimens decontaminated by both processes, indicating shallow corrosion of the Inconel 600 base metal. More surface roughness was present on the specimens that had been decontaminated by both processes than on the specimens that had been decontaminated by only the hot leg process. Figure 7-31 shows typical SEM photographs of metallographic cross sections of the two steam generator tube specimens (hot leg) and (cold leg + hot leg). Metal penetration was less than 6 μm and was not intergranular.

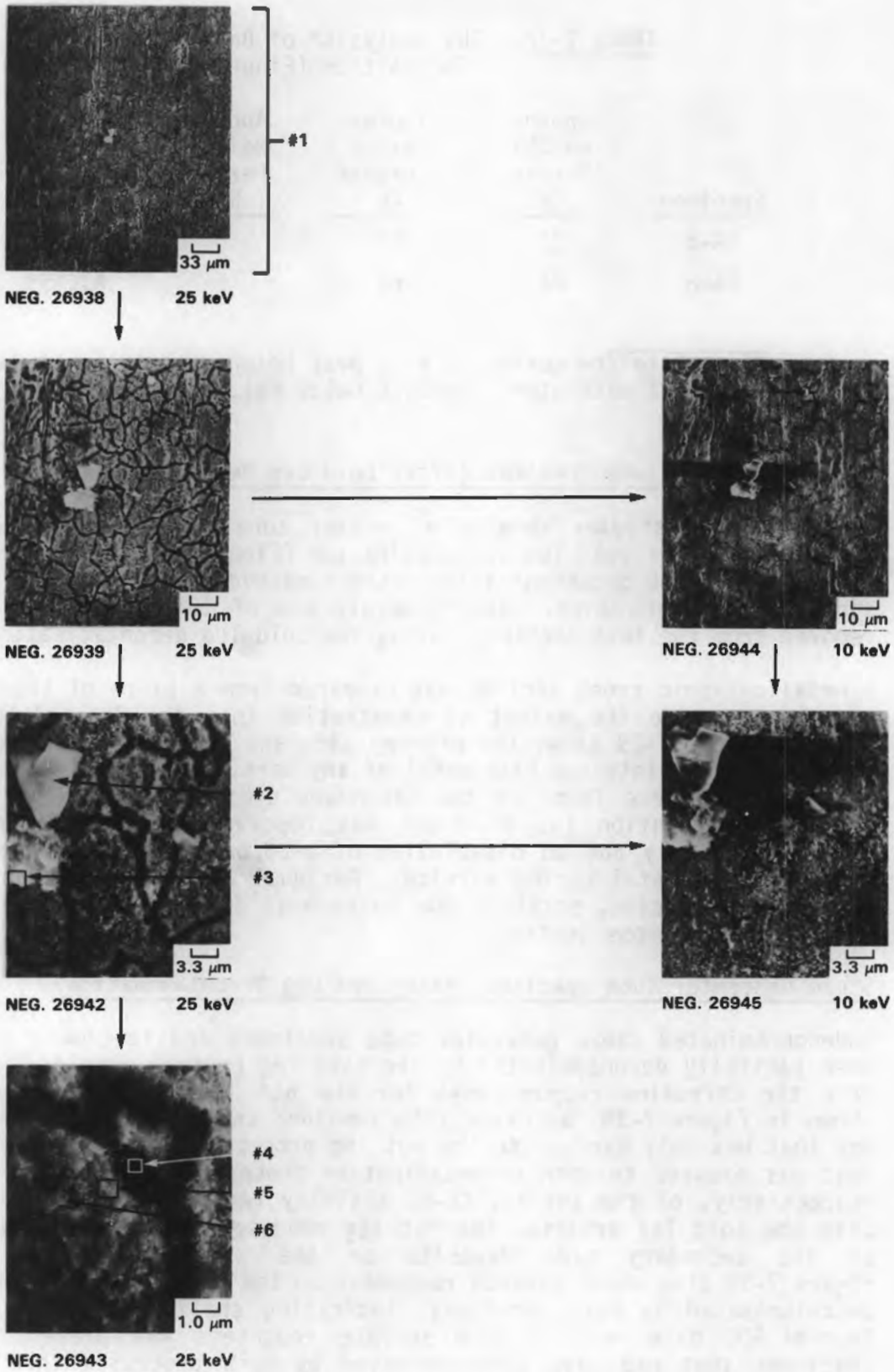

FIGURE 7-28. SEM Examination of the Primary Side Surface of Steam Generator Tube Specimen R-5 After the Cold Leg Decontamination

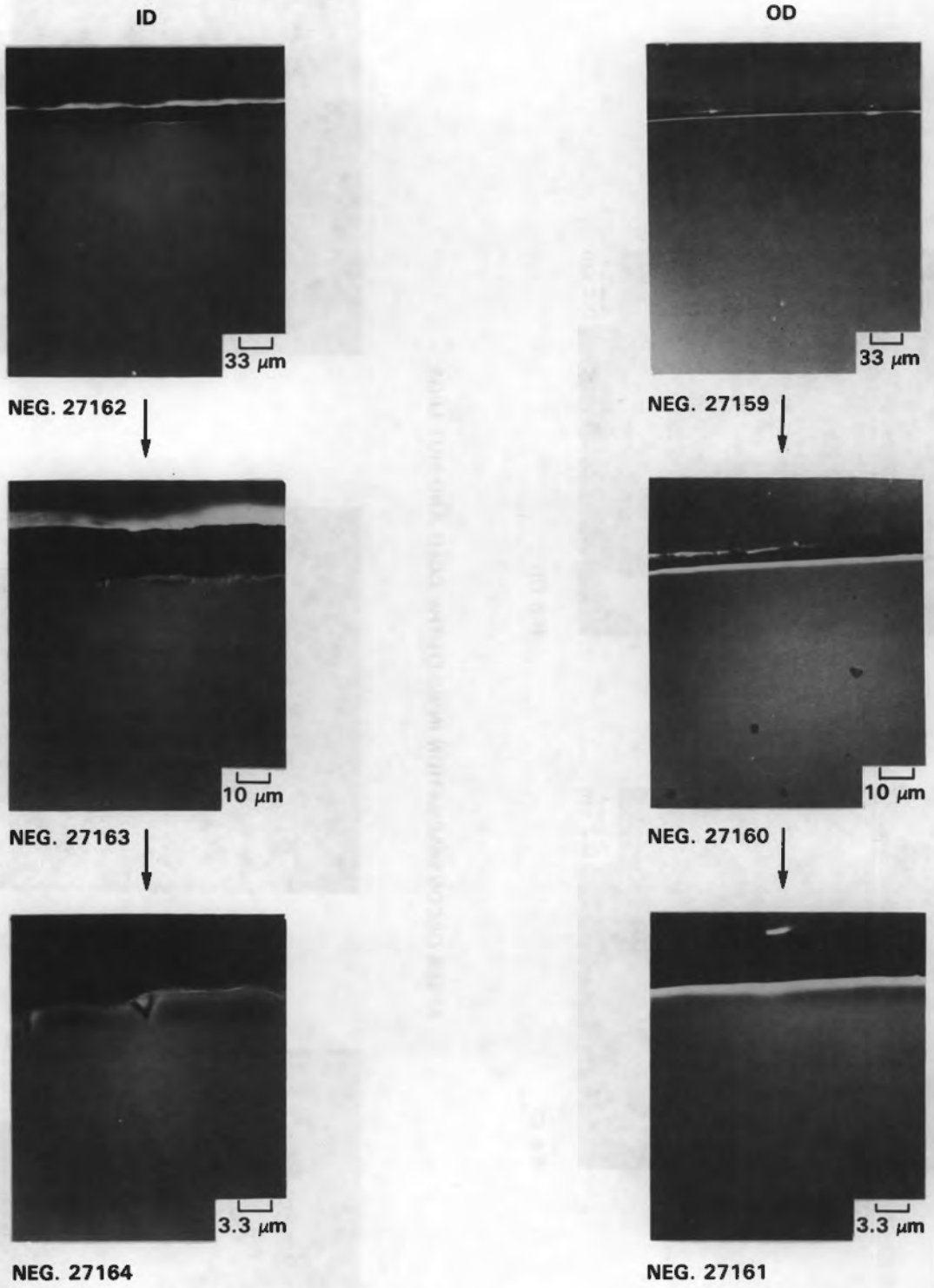

FIGURE 7-29. SEM Examination of a Metallographic Cross Section of Steam Generator Tube Specimen R-4 After the Cold Leg Decontamination

AFTER HOT LEG DECONTAMINATION

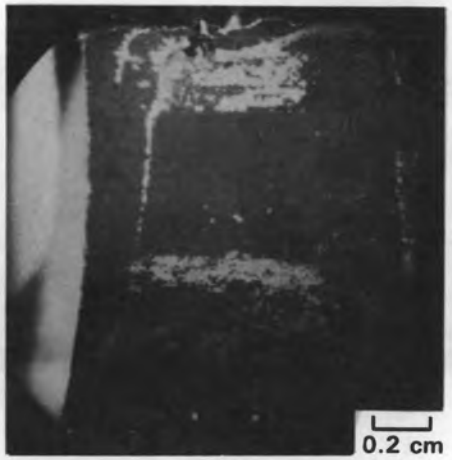

R-6 ID

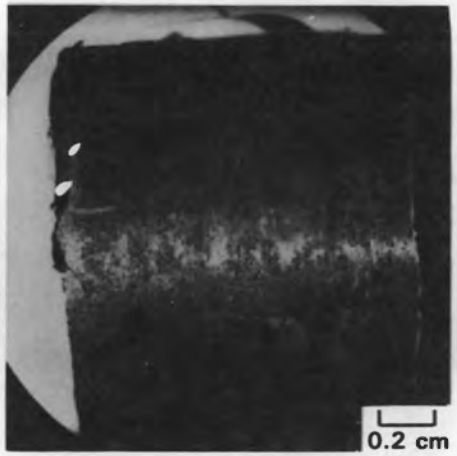

R-6 OD

AFTER DECONTAMINATION IN BOTH THE COLD AND HOT LEGS

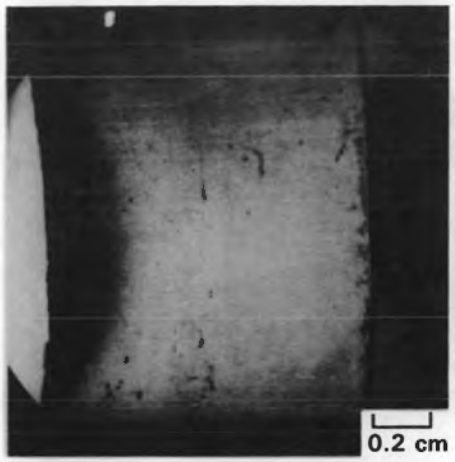

R-4 ID

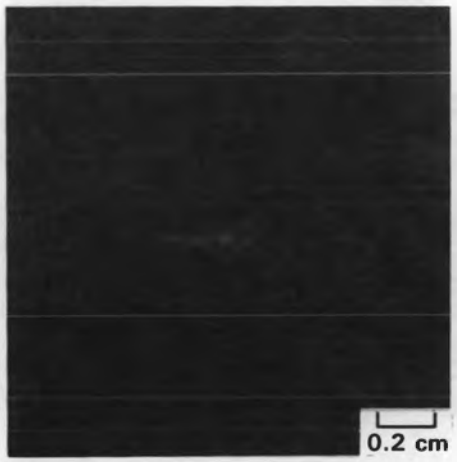

R-4 OD

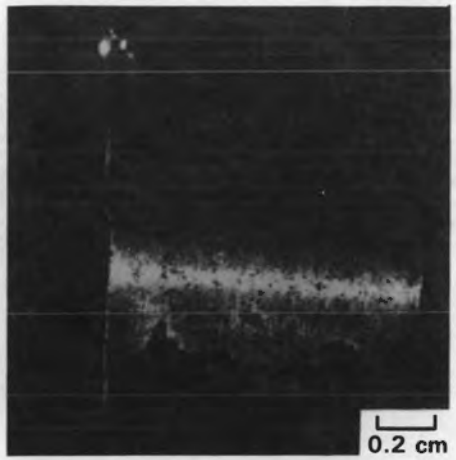

R-1 OD

FIGURE 7-30. Appearance of Steam Generator Tube Specimens After the Hot Leg Decontamination

AFTER HOT LEG DECONTAMINATION

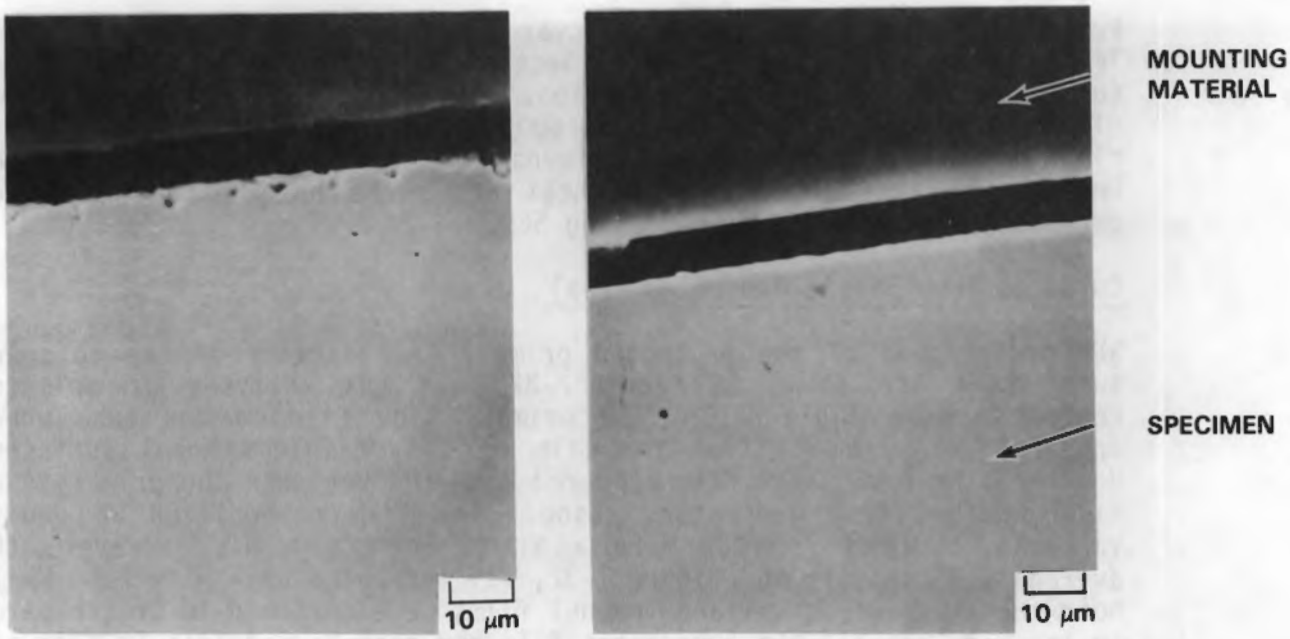

NEG. 27175 R-6 ID SURFACE NEG. 27172 R-6 OD SURFACE

AFTER DECONTAMINATION IN BOTH THE COLD AND HOT LEGS

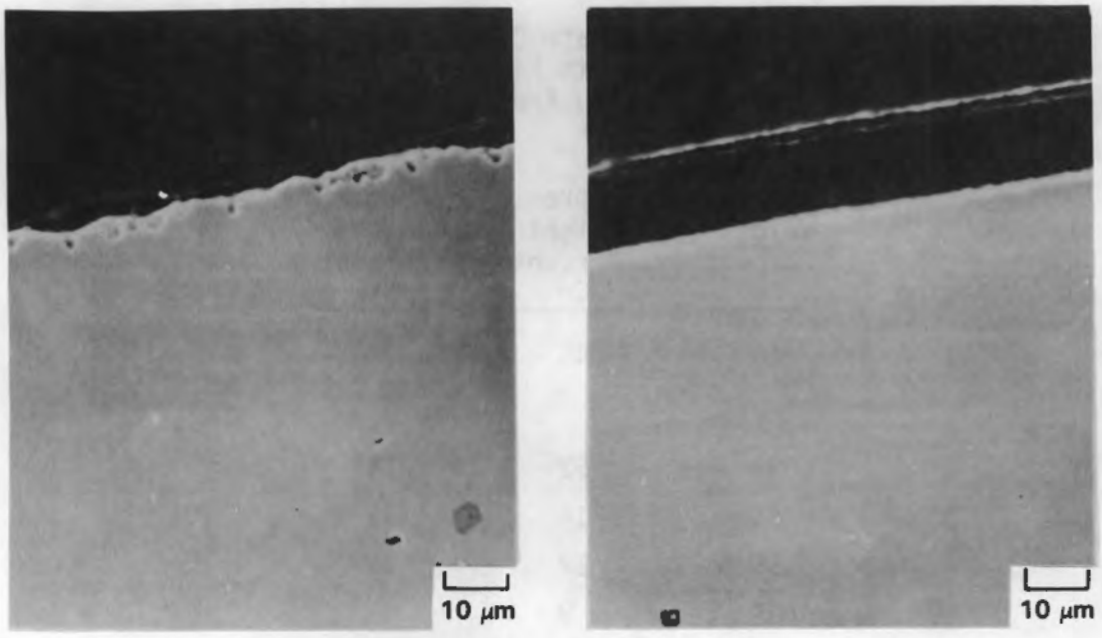

NEG. 27169 R-4 ID SURFACE NEG. 27166 R-4 OD SURFACE

FIGURE 7-31. SEM Examination of Metallographic Cross Sections of Steam Generator Tube Specimens After the Hot Leg Decontamination

Tube Sheet Specimens

Protective plates were installed over portions of the hot leg and cold leg tube sheets, as described in Section 2, to provide reference areas for comparison after decontamination. The tube sheet and channel head divider plate surfaces are Inconel 600, while the channel head walls are clad with stainless steel. Specimens were removed from protected and unprotected areas of the tube sheet after the hot leg and cold leg decontaminations and examined using SEM.

Cold Leg Tube Sheet (Protected Area)

SEM photographs of the protected primary side surface of the cold leg tube sheet are shown in Figure 7-32, and EDX analyses of selected regions are in Table 7-13. The primary side film on the tube sheet appeared more compact than the film on the stainless steel surfaces. However, the tube sheet film appeared much thicker than the primary side film on the steam generator tubing. The film composition was quite variable, ranging from Cr > Fe > Ni to Fe > Cr > Ni. However, the average EDX composition (Figure 7-32, #1) indicated Cr > Ni > Fe. While both the stainless steel and Inconel films were enriched in Cr (compared to the base metal), the tube sheet film had more Ni and less Fe than the film on the channel head wall (as expected). This reflects the influence of the base metal composition on the primary side film, and suggests that stainless steel films should have different decontamination characteristics than Inconel films. The specific surface activity of the tube sheet film from the protected area was 6.8 $\mu Ci/cm^2$.

TABLE 7-13. Approximate Compositions of Selected Regions in Figure 7-32 - Cold Leg Protected Area - Based on SEM/EDX Analysis*

Region	Approx. Weight Percent Fe	Approx. Weight Percent Cr	Approx. Weight Percent Ni	Trace
1	18	45	30	Al, Si, Nb, Ti, Zn
2	29	52	14	"
3	45	14	35	"
4	55	22	15	"
5	39	9	45	"
6	55	20	12	"

*From baseline corrected K(α) peak height ratios (excluding elements with atomic numbers below Na).

NEG. 28657

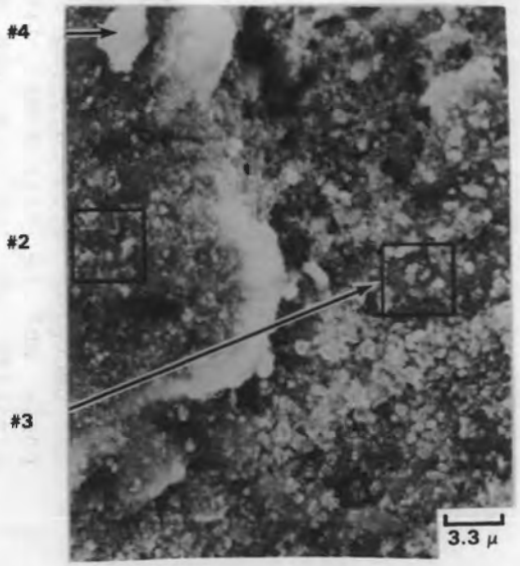

NEG. 28659

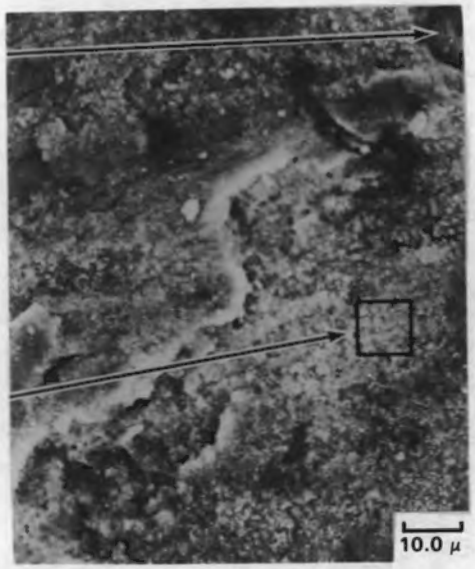

NEG. 28658

FIGURE 7-32. SEM Examination of a Specimen From the Protected Area of the Cold Leg Tube Sheet

Hot Leg Tube Sheet (Protected Area)

The gasket under the protective plate failed during the hot leg decontamination. Figure 7-33 shows the different primary side surfaces available for analysis with this specimen. SEM analysis of regions 4-A and 4-B found extensive Mn deposits. However, Figure 7-34 shows an area that was relatively free of Mn contamination. Both decontaminated areas (#2, indicated by intergranular etching of the base metal) and regions with residual film (#1) are evident. The intergranular etching probably occurred during service (primary side film formation) rather than during the decontamination. Table 7-14 gives approximate compositions for the base metal and residual oxide, based on EDX analyses. The specific activities were 5.1 $\mu Ci/cm^2$ for area 4-A, 3.0 $\mu Ci/cm^2$ for area 4-B, and 1.1 $\mu Ci/cm^2$ for area 4-C. These results suggest that areas 4-A and 4-B were relatively undecontaminated, and that area 4-C was significantly decontaminated. A round particle, similar to those found on the corrosion coupons after the cold leg decontamination (see below), was found in one of the areas (not shown) examined by SEM. No pitting, such as that observed on the corrosion coupons, was found during visual inspection (20X to 120X magnification). However, regions of possible pit initiation were found on area 4-C.

TABLE 7-14. Approximate Compositions of Selected Regions in Figure 7-34 - Hot Leg Protected Area - Based on SEM/EDX Analysis*

Region	Approx. Weight Percent Cr	Approx. Weight Percent Fe	Approx. Weight Percent Ni	Approx. Weight Percent Mn	Trace
1	37	35	21	3	Al, Si, Mo, K, Ca, Ti, Zn
2	27	11	57	--	Al, Si, Mo, Ca, Ti
3	39	51	5	3	Al, Si

*From baseline corrected K(α) peak height ratios (excluding elements with atomic numbers below Na).

Cold Leg Tube Sheet (Unprotected Area)

Figure 7-35 shows photographs from an SEM examination of a specimen from the decontaminated cold leg tube sheet. The extent of any residual film could not be determined from these photographs; however, the Co-60 activity on the specimen was only 0.45 $\mu Ci/cm^2$ as compared with 6.8 $\mu Ci/cm^2$ on the protected cold leg specimen. EDX analyses of selected regions in Figure 7-35 are given in Table 7-15, and show significantly lower Fe than in the exposed base metal regions on the protected hot leg specimen (Table 7-14 above). This suggests that a low

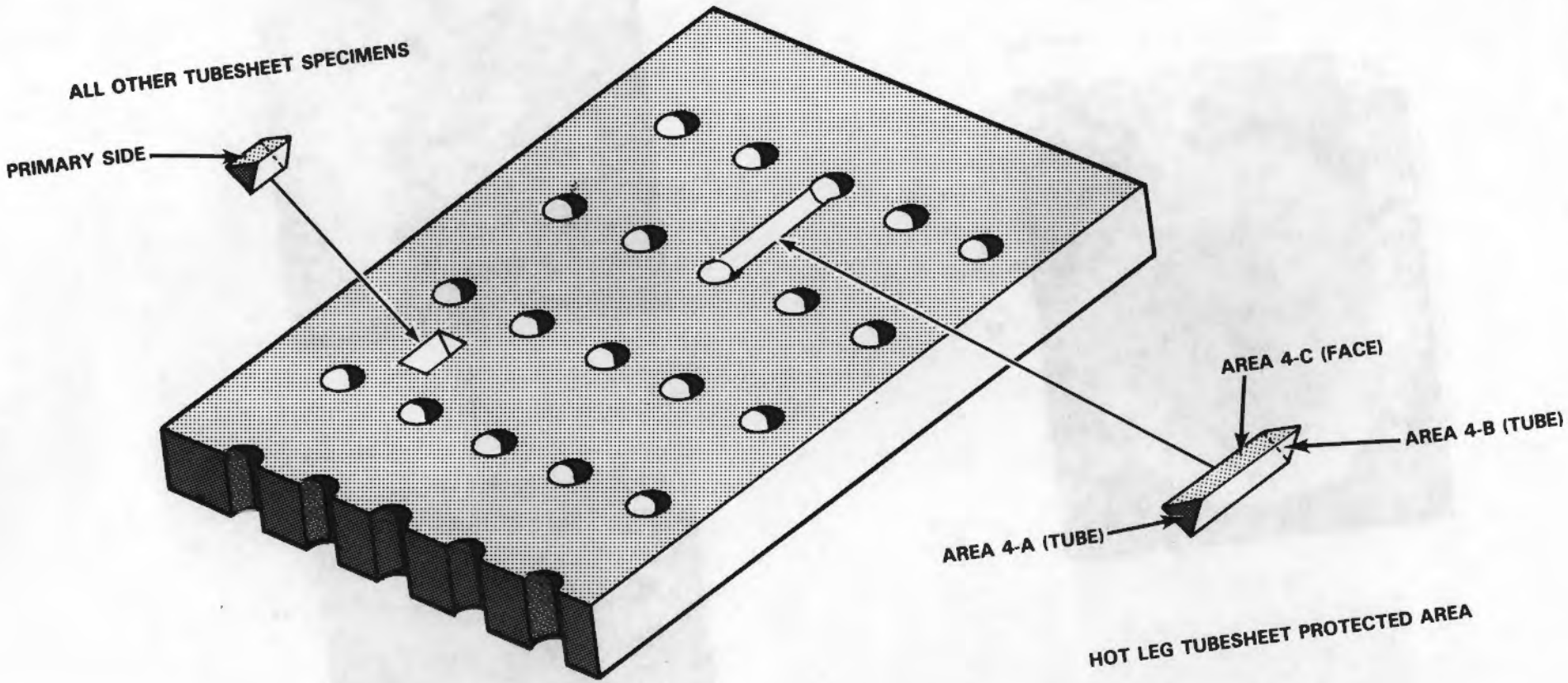

FIGURE 7-33. Tube Sheet Specimen Origins

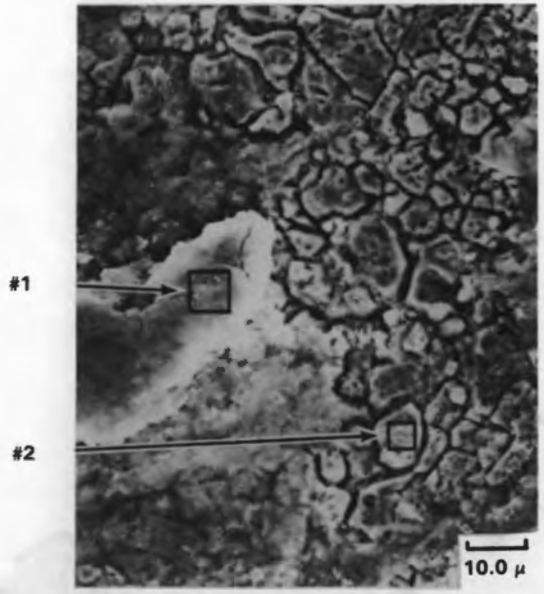

NEG. 2841

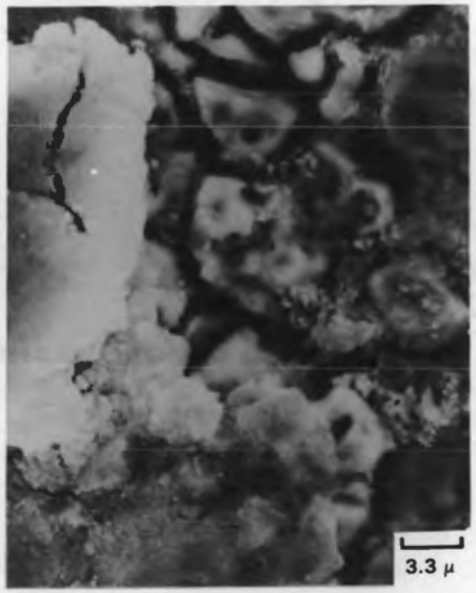

NEG. 2843

NEG. 28640

FIGURE 7-34. SEM Examination of a Specimen From the Protected Area of the Hot Leg Tube Sheet

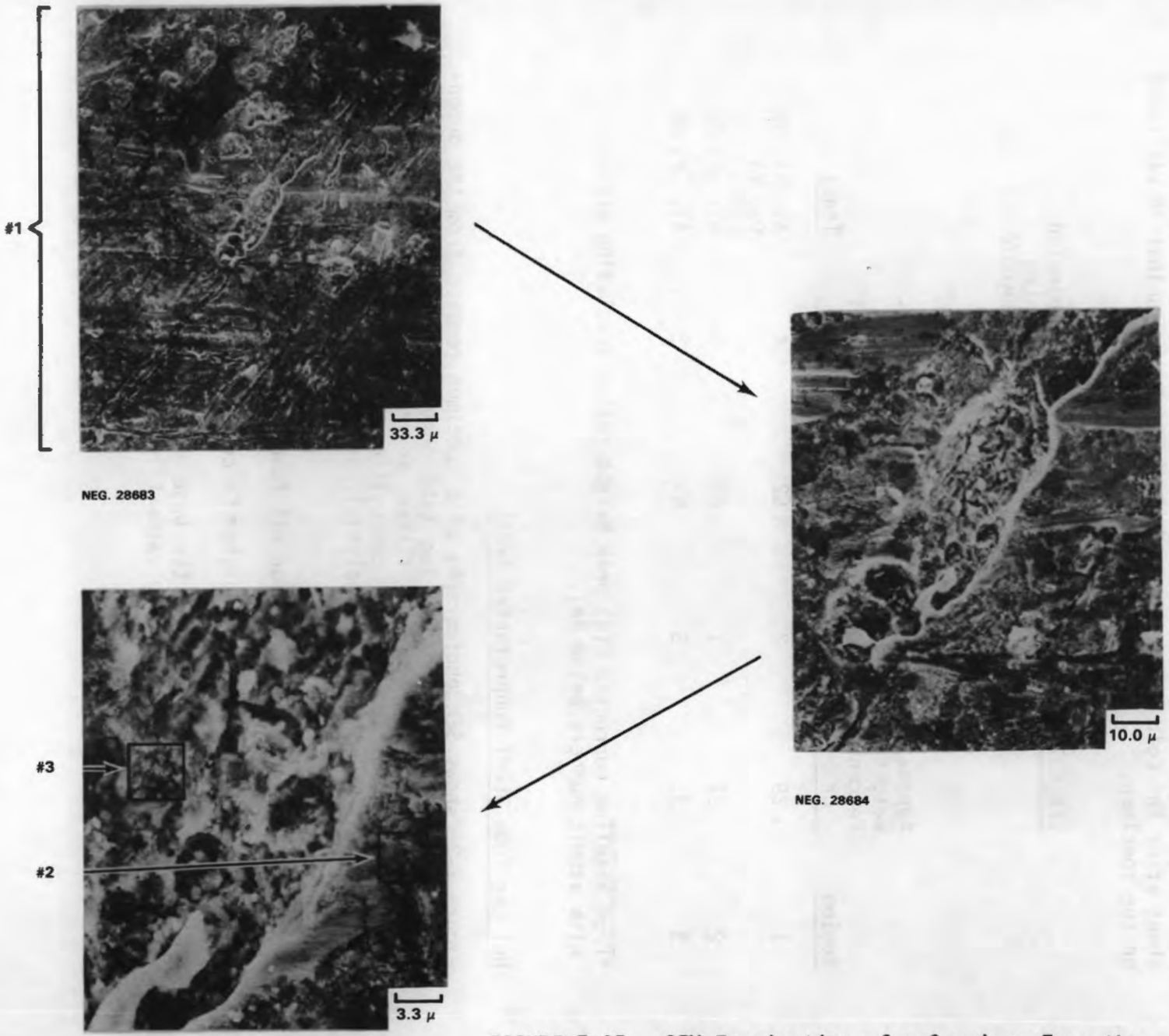

FIGURE 7-35. SEM Examination of a Specimen From the Unprotected Area of the Cold Leg Tube Sheet

Fe - high Cr, Ni corrosion film was present on the Inconel 600 tube sheet after the cold leg decontamination. No Mn contamination was found on the specimen.

TABLE 7-15. Approximate Compositions of Selected Regions in Figure 7-35 - Cold Leg Unprotected Area - Based on SEM/EDX Analysis*

Region	Approx. Weight Percent Cr	Approx. Weight Percent Fe	Approx. Weight Percent Ni	Approx. Weight Percent Mn	Trace
1	29	2	62	4	Al, Si, Mo, Ca, Ti
2	31	1	61	3	Al, Si, Mo
3	31	3	60	3	Al, Ca, Mo

*From baseline corrected K(α) peak height ratios (excluding elements with atomic numbers below Na).

Hot Leg Tube Sheet (Unprotected Area)

Figure 7-36 shows SEM photographs of a specimen removed from the decontaminated portion of the hot leg tube sheet. More than half of the surface was bare metal, but flakes of residual oxide were found. Table 7-16 gives approximate compositions of selected features in Figure 7-36 (based on EDX analysis). The overall results were as follows:

- Very little Mn contamination was found.
- The residual oxide has a higher Fe content than the base metal.
- Intergranular etching of the base metal was present; the etching may have existed under the oxide film prior to decontamination.

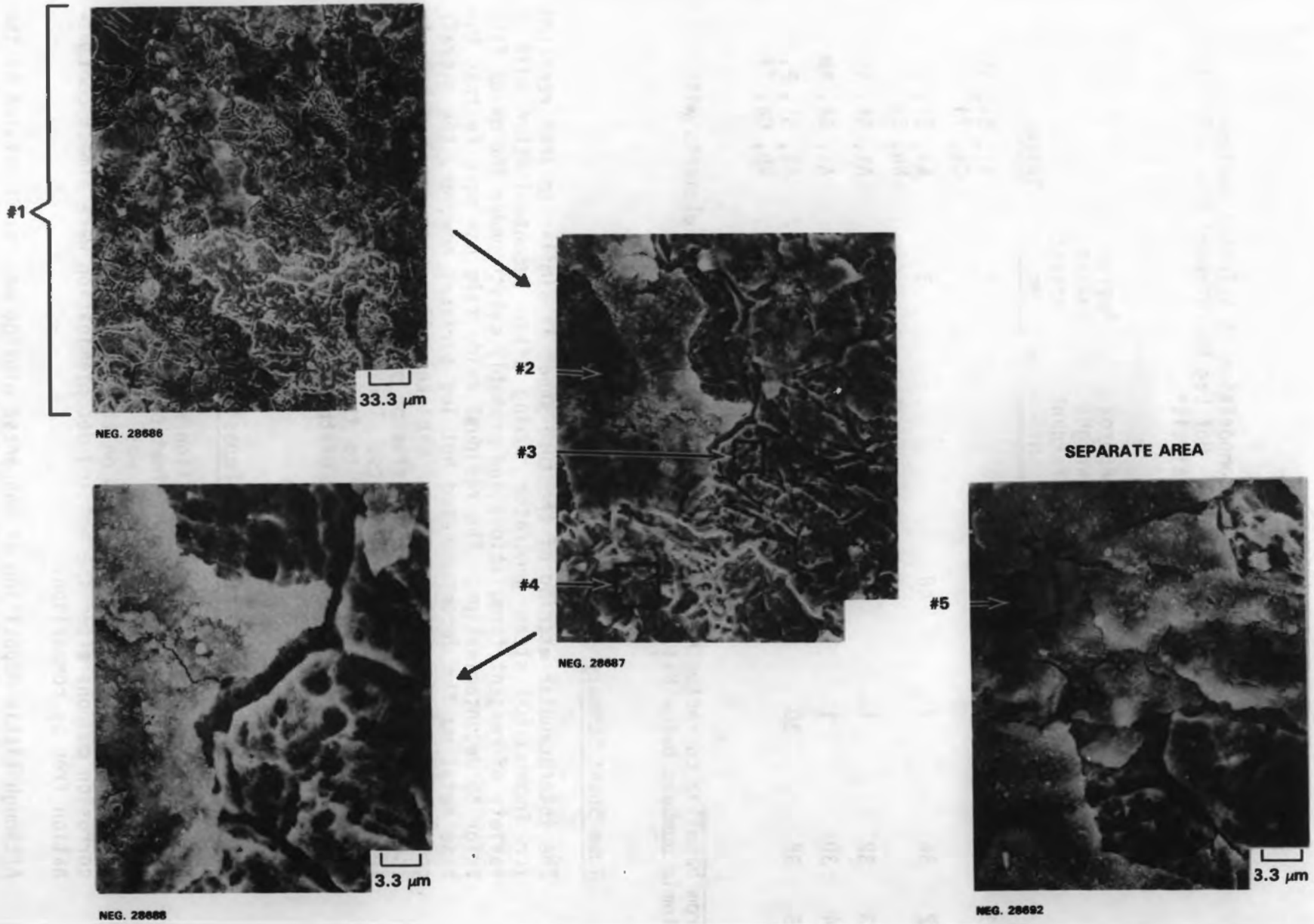

FIGURE 7-36. SEM Examination of a Specimen From the Unprotected Area of the Hot Leg Tube Sheet

TABLE 7-16. Approximate Composition of Selected Regions in Figure 7-36 - Hot Leg Unprotected Area - Based on SEM/EDX Analysis*

	Region	Approx. Weight Percent Cr	Approx. Weight Percent Fe	Approx. Weight Percent Ni	Approx. Weight Percent Mn	Trace
1	33	3	53		3	Al, Si, Nb Ca, Ti
2	36	7	48		3	Al, Si, P, Nb, Ca
3	32	1	60		3	Al, Si, Nb
4	30	1	65		1	Al, Si, Nb
5	38	10	40		5	Al, Si, P, Nb, Ca, Ti

*From baseline corrected K(α) peak height ratios (excluding elements with atomic numbers below Na).

Tube Sheet Summary

The intergranular etching of the tube sheet is similar to that reported for Inconel 600 steam generator tubing after decontamination with a variety of reagent formulations and probably exists under the oxide film prior to decontamination. The residual oxide film has more Fe than the base metal on the decontaminated hot leg surface; however, the overall composition of the film reflects a nickel alloy base metal origin in contrast to pre-decontamination films on stainless steel specimens where Fe and Cr are the major components. The absence of pitting on the hot leg specimens may have been due to the primary side film, which protected the base metal during most of the decontamination (similar to the steam generator tube specimens).

Cold Leg Channel Head Smears and Deposits (After Decontamination)

Significant radioactive contamination was found on the corrosion coupons following the cold leg decontamination. This was traced to a highly smearable, powdery deposit that was partially composed of inclusions from the pre-decontamination film on the stainless steel specimens. The corrosion coupons after the hot leg decontamination were almost contamination free by comparison.

Although little deposition of manganese dioxide was found outside of the crevice regions for coupons from both the hot and cold leg decontaminations, significant manganese contamination was found on smears taken

from the cold leg coupon rack. Bulk X-ray fluorescence was used to determine approximate compositions for deposits on the smears. The deposits collected on the smears had the following characteristics:

Smear 1: Cu > Fe, Mn, Cr > Ni (after 1st decontamination cycle)
Smear 2: Mn > Fe, Cr, Ni > Cu (after 2nd decontamination cycle)
Smear 3: Mn > Fe, Cr, Ni, Cu (after 2nd decontamination cycle)

Deposits from the cold leg decontamination made the corrosion coupon racks highly smearable (>100,000 cpm radioactivity at contact with a gas-filled micro window detector, or P-11 probe). Double-stick carbon tape was used to remove some of the deposit from a coupon rack endplate for SEM analysis, and rubber cement was used to collect some of the deposit for XRD. The first XRD sample indicated a spinel with a lattice parameter of 8.374 Å; the second specimen was also a spinel, but with a lattice parameter of 8.357 Å and weak lines at 4.5 Å, 3.34 Å, and 1.999 Å. The average lattice parameter of the deposit (3.365 Å) was higher than the lattice parameter of the in situ crud/oxide on either the manway cover insert (8.333 Å) or the channel head core specimens (8.32 Å). Since magnetite has a lattice parameter of 8.396 Å, the corrosion rack deposits may have lower Cr and Ni than the in situ crud/oxides.

SEM photographs of the deposited particulate are shown in Figures 7-37 and 7-38, and the corresponding microprobe compositions are in Tables 7-17 and 7-18. As shown in the figures, several different types of particles are evident:

- textured round particles,
- smooth round particles,
- rectangular and some flat particles,
- filamentous particles,
- sharp flakes,
- large flakes.

Approximate chemical compositions suggest origins for some of the particles. The very large Cu/Zn flake (#1; Figure 7-37) probably came from a damaged brass bushing in the pump used for the cold leg decontamination. The Si/Mg particles (#3, #7; Figure 7-37) are probably feldspar, indicating that some sand or dirt had been in the system. Since no filamentous features (#6; Figure 7-37) were observed on any of the in situ crud/oxide films, the filamentous particles probably precipitated from solution during some portion of the decontamination. If so, a significant fraction of the Co-60 activity in the particulate deposit may be associated with the filamentous particles, which are high in Cr and Fe but low in Ni. Both the textured and smooth round particles (#4, #9; Figure 7-37 and #3, #7; Figure 7-38) may have been inclusions in the crud/oxide film that were released to the system as the crud/oxide matrix dissolved during the decontamination. In contrast to the smears, little Mn was found during the SEM examination of the particulate. This suggests a non-uniform deposit since the smears and SEM specimens were from different locations.

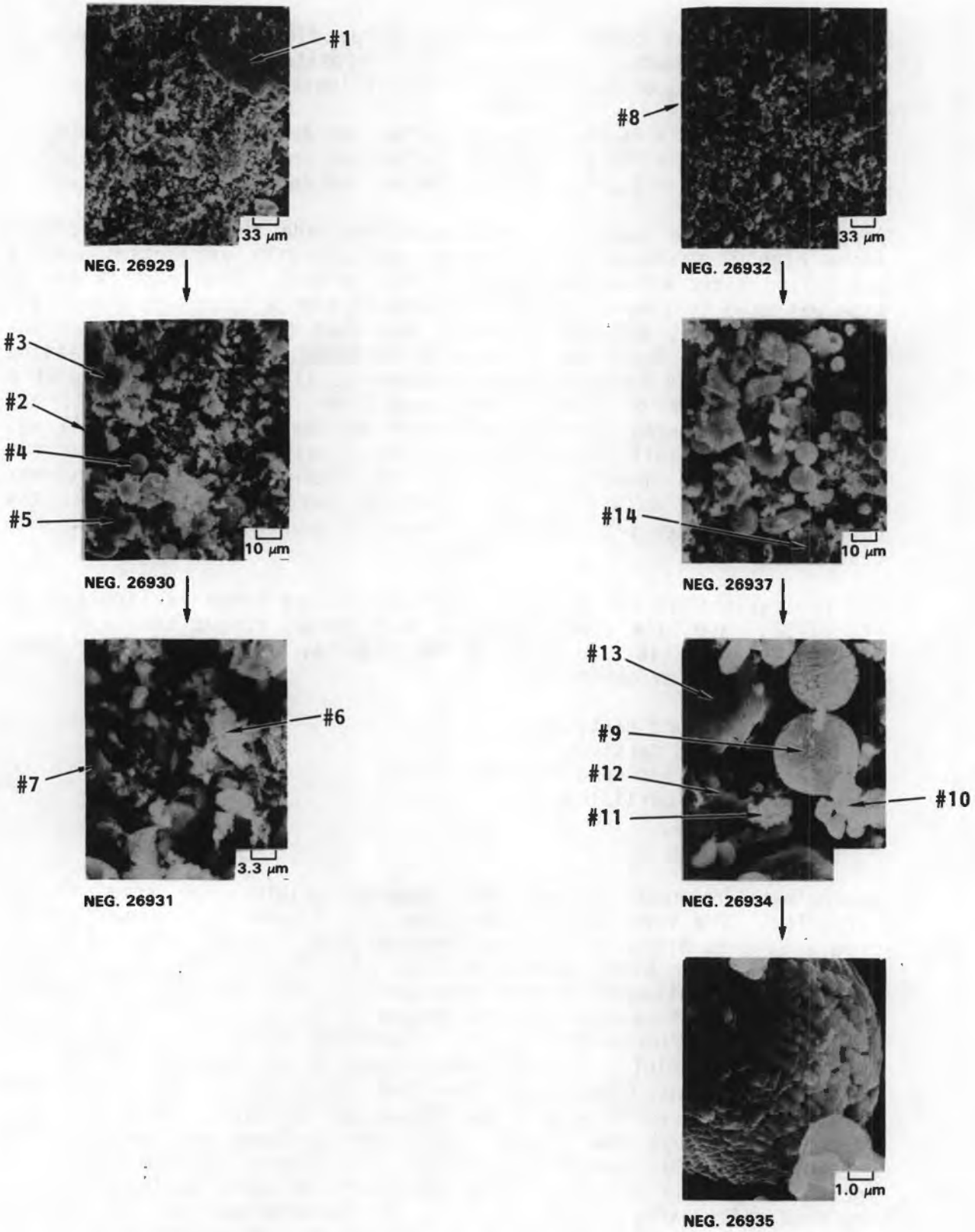

FIGURE 7-37. SEM Examination of Coupon Rack Deposits From the Cold Leg Decontamination

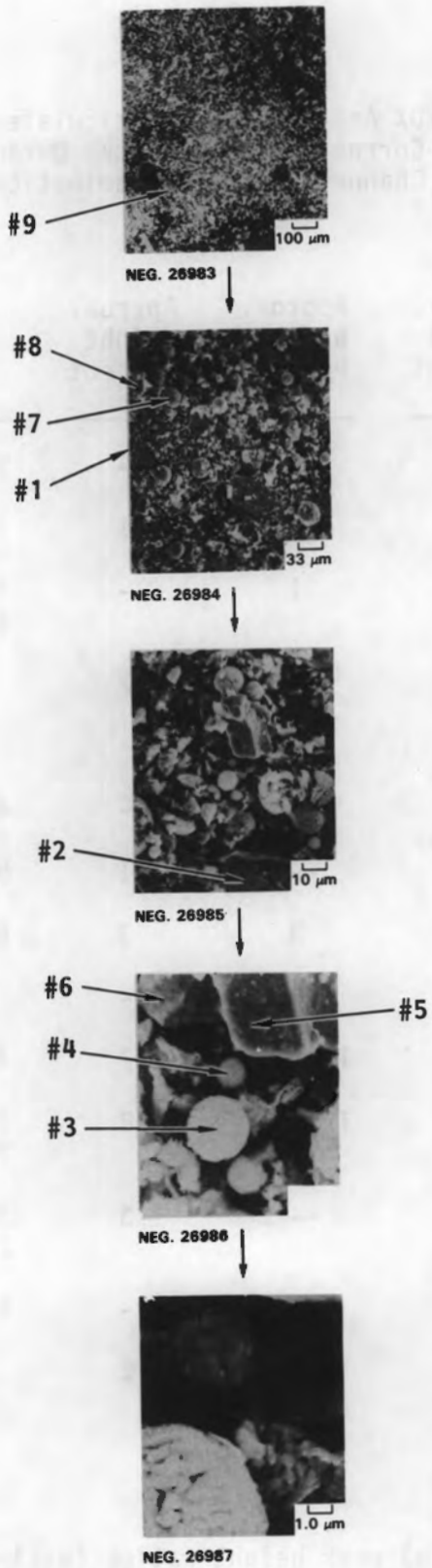

FIGURE 7-38. SEM Examination of Coupon Rack Deposits From the Cold Leg Decontamination

TABLE 7-17. EDX Analysis* of Particulate Deposited on Corrosion Coupon Racks During Cold Leg Channel Head Decontamination (Figure 7-37)

Region	Approx. Weight Percent Cr	Approx. Weight Percent Fe	Approx. Weight Percent Ni	Approx. Weight Percent Mn	Approx. Weight Percent Other	Trace
1	2	2	--	--	74 Cu, 20 Zn	Si
2	43	41	4	1	7 Si	Al, Cu
3	4	7	1	--	17 Mg, 5 Al, 62 Si	K, Ni, Cu
4	51	41	4	2		Al, Si, Cu
5	28	64	6	--		Al, Si
6	39	49	5	--	4 Si	Al, Cu
7	5	30	--	1	9 Mg, 54 Si	Cu
8	41	41	3	3	8 Si	Al, K, Ca, Ti
9	42	49	6	--		Al, Si, Cu
10	67	20	Trace	7	4 Si	Al, Ti
11	59	12	Trace	8	7 Si, 7 Ca, 7 Ti	Mg, Al
12	4	7	--	3	37 Ca, 46 Ti, 2 Si	Al
13	2	1	--	--	96 Si	Ti
14	79	17	--	2		Al, Si

*From baseline corrected K(α) peak height ratios (excluding elements with atomic numbers below Na).

TABLE 7-18. EDX Analysis* of Particulate Deposited on Corrosion Coupon Racks During Cold Leg Channel Head Decontamination (Figure 7-38)

Region	Approx. Weight Percent Cr	Approx. Weight Percent Fe	Approx. Weight Percent Ni	Approx. Weight Percent Other	Trace
1	42	40	4	4 Al, 7 Si	Mg, P, S, K, Ti, Cu
2	27	65	5		Al, Si, Mn, Cu
3	37	52	7	3 Si	Al
4	66	27	1	4 Mn	Al, Si
5	31	63	3		Al, Si, Mn
6	8	12	--	70 Zr	Al, Si, Cu, Zn
7	50	43	5	2 Si	Al
8	1	28	--	11 Mg, 53 Si, 4 Cu	Ti, Mn
9	1	94	--	2 Mn	Si, Cu

*From baseline corrected K(α) peak height ratios (excluding elements with atomic numbers below Na).

Smears of channel head surfaces after the cold leg decontamination found significant Mn contamination. Smears from the stainless steel surfaces (channel head walls) were 200 mrad/h to 300 mrad/h, while smears from the Inconel 600 divider plate and tube sheet were less than 15 mrad/h.

Hot Leg Channel Head Smears (After Decontamination)

Except for crevice regions, the corrosion coupons and coupon racks were practically free of any radioactive deposits or Mn concentration. Smears from the channel head surfaces after the hot leg decontamination were 5 mrad/h to 35 mrad/h, significantly lower than comparable smears from the cold leg. Some Mn contamination was found on the smears by bulk XRF, but the levels were significantly lower than on the cold leg smears.

Summary

- Decontamination factors for stainless steel specimens in the coupon racks and removed from the channel head bowl ranged from 6 to 8 for the cold leg decontamination and 300 to 1000 for the hot leg decontamination. Decontamination factors for Inconel 600 steam generator tubing in the coupon racks and specimens removed from the Inconel 600 clad tube sheet ranged from 4 (tubes) to 15 (tube sheet) for the cold leg decontamination and 4 to 6 for the hot leg decontamination.

- The decontamination characteristics and surface characterizations of coupons cut from the manway cover coupons agreed well with the results for the core specimens from the channel head. This suggests that decontamination testing on manway cover inserts should be a valid method for predicting the decontamination behavior of other PWR stainless steel surfaces.

- Trace Mn was found on smears of both the hot and cold leg channel head surfaces after decontamination.

- Metallographic cross sections indicated that the corrosion film on the undecontaminated cold leg core specimens was $\sim$4 μm thick and that the film on the hot leg manway cover insert was $\sim$3 μm thick.

- The activity of the undecontaminated cold leg core specimens was 5 $\mu Ci/cm^2$ as compared with 3 $\mu Ci/cm^2$ for the hot leg core specimen. In addition, activities for the undecontaminated cold and hot leg manway cover inserts were 6 $\mu m/cm^2$ and 3.6 $\mu m/cm^2$, respectively.

- The pre-decontamination corrosion film on the cold leg stainless steel surfaces appeared thick and had more cracking than the hot leg film. The cold leg film also appeared to have many more inclusions and superficial particles than the hot leg film. The smearable deposit found on the cold leg corrosion coupons after decontamination may have been due to inclusions that were released

from the bulk film, but not dissolved, during the decontamination. In addition, the extensive microcracking in the cold leg film may reflect different adherence properties than the hot leg film; e.g., spallation may have been more significant for the cold leg decontamination than for the hot leg decontamination.

- No significant intergranular corrosion was found on the decontaminated stainless steel or Inconel 600 specimens, although some cracks in the stainless steel channel head cladding existed prior to decontamination.

- The pre-decontamination corrosion ID films on Inconel 600 steam generator tubing were very thin, and appeared similar to the film on tubes from other steam generators.

- SEM/EDX examination of the stainless steel films in cross sections found a duplex film, with highest Cr concentration occurring at the interface between the inner and outer films.

REFERENCES

Bradbury, D., et al., 1982. "Decontamination Systems of BWRs and PWRs Based on LOMI Reagents." Paper presented at the 1982 International Joint ANS-CNA Topical Meeting on the Decontamination of Nuclear Facilities, September 19-22, 1982, Niagara Falls, Canada.

Pick, M. E., 1982. "Development of Nitric Acid Permanganate Pre-Oxidation and Its Application in the POD Process for PWR Decontamination." Paper presented at the 1982 International Joint ANS-CNA Topical Meeting on the Decontamination of Nuclear Facilities, September 19-22, 1982, Niagara Falls, Canada.

Reece, W. D., and G. R. Hoenes, 1983. Interim Topical Report, Steam Generator Group Project, Health Physics - Task 3, NUREG/CR-3578.

Smee, J. L., 1982. "Introduction to Chemical Decontamination." Paper presented at the ANS-CNA Tutorial on Decontamination, September 19, 1982, Niagara Falls, Canada.

APPENDIX A

Task 6 Pictures

Task 6 Pictures

Date	Number	Topic
4/06/82	8202467	Cold Leg Surfaces - Before Decontamination
4/16/82	8202573	Initial Radiation Level Measurements
5/04/82	8203096	Manway Cover Removal
7/19/82	8204823	Core Removal and SGEF Basement
8/26/82	8205627	Protective Plate and Installation System
8/27/82	8205654	Unpackaging of LNS Decontamination Equipment
8/31/82	8205697	LNS Equipment and Installation
9/03/82	8205988	Equipment Installation Details
9/07/82	8205997	Resin Slurry Operation
10/05/82	8206491	Cold Leg Surfaces - After Decontamination
10/05/82	8206784	Completion of Slurry Operation
10/15/82	8206957	Hot Leg Surfaces - Before Decontamination
10/20/82	8207037	Liquid Waste Transfer Operation
10/27/82	8207341	Cold Leg Surfaces - After Water Rinse
10/29/82	8207424	Hold-Down and Quadrex Nozzle
11/02/82	8207468	Laboratory Operations and Quadrex Equipment
11/04/82	8207739	Hot Leg Surfaces - After LOMI Process
11/11/82	8207891	Hot Leg Surfaces - After POD Process
11/15/82	8207925	Hot Leg Surfaces - After Water Rinse
11/23/82	8208035	In Situ Electropolishing Operations

APPENDIX B

Dissolved Metals and Co-60 Data for the Cold and Hot Leg Decontamination Operations

Dissolved Metals and Co-60 Data - Cold Leg Decontamination

Date	Time	Co-60 (ρCi/ml)	Fe(ppm)	Ni(ppm)	Cr(ppm)	Cu(ppm)	Mn(ppm)	Zn(ppm)
9/5/82	0145		0.3	0.8	<0.1	0.2	0.14	0.33
	0230	6.7	12.6	1.6	0.35	<0.1	0.57	0.79
	AIX*	1.4	4.5	0.3				
	0245	3.3	8.2	0.85	<0.2	<0.1	0.30	0.50
	AIX	0.7	5.7					
	0300	3.3	13.5	0.85	<0.2	<0.1	0.45	0.63
	AIX	1.9	11.2					
	0315	2.8	14.1	0.65	<0.2	<0.1	0.40	0.64
	AIX		5.2					
	0330		7.1	0.20	<0.2	<0.1	0.32	0.64
	AIX		5.9					
	0400	1.5	12.8	0.60	<0.2	<0.1	0.20	0.63
	AIX		9.9					
	0430	1.5	12.6	0.85	<0.2	<0.1	0.20	0.68
	AIX		11.4					
	0435	1.1	15.8	1.0	<0.2	<0.1	0.20	0.67
	AIX	0.0	5.5					
	0500	1.0	18.7	1.36	<0.2	<0.1	0.20	0.67
	AIX	0.1	5.7					
	0600	1.0	17.1	1.76	0.4	<0.1	0.16	0.67
	AIX		5.0		0.45			
	0700		14.5					
	AIX		5.0					
	0946	3.5	12.5					
	AIX		2.9					
	1100	1.4	14.7					
	AIX		4.5					
	1240	1.2	14.0					
	AIX		4.3					
	1335	2.7	15.0					
	AIX		4.0					
	1430	3.8	15.0					

*After Ion Exchange

Cold Leg Data (Cont)

Date	Time	Co-60 (ρCi/ml)	Fe(ppm)	Ni(ppm)	Cr(ppm)	Cu(ppm)	Mn(ppm)	Zn(ppm)
9/5/82	1500	4.2	14.5					
	1540		15.1					
	AIX		≈0.2					
	1630	1.3	6.0					
	AIX		<0.1					
	1700	0.5	5.0					
	AIX		<0.1					
	1915	2.7	3.6	<0.5	0.5			
	1950	1.4	4.3	1.0	1.0			
	2035	1.2	4.0	1.0	2.5			
	2130	1.0	3.5	1.0	2.5			
	2230	0.6	4.0	1.0	3.0			
	2330	1.3	4.0	1.0	4.0			
9/6/82	0030	1.2	4.3	1.0	4.2			
	0130	1.2	4.2	1.1	5.0			
	0230	1.1	3.8	1.0	5.5			
	0330	1.1	3.8	1.1	5.5			
	0430	1.1	3.8	1.1	5.9			
	0520	1.1	3.0	1.0	5.7			
	0845	1.3	4.0		5.8			
	0900	0.4	2.0		6.0			
	0930	1.0	4.0		3.0			
	AIX	1.8	6.5		≈0.1			
	1000	1.2	4.0		1.5			
	AIX	1.9	≈5.0		<0.1			
	1100	1.5	5.5		0.5			
	AIX	1.9	5.0		<0.1			
	1200	1.7	≈5.0		0.2			

Cold Leg Data (Cont)

Date	Time	Co-60 (ρCi/ml)	Fe(ppm)	Ni(ppm)	Cr(ppm)	Cu(ppm)	Mn(ppm)	Zn(ppm)
9/6/82	1655	1.2	<0.1		<0.1		0.2	
	1715	140	17.3		0.4		100	
	1730	110	17.5		0.4		75	
	AIX	1.2	1.5		0.2		0.6	
	1745	78	17.0	3.5	0.4		48	
	AIX	0.5	0.6	1.8			≈0.1	
	1800	59	17.0	4.1	0.4		34	
	AIX		6.3	4.7			14.2	
	1815	43	16.0	4.5			25.0	
	AIX	0.5	0.7	1.8			<0.1	
	1830	44	17.0	4.7	0.4		21.0	
	AIX	0.4	0.8	2.0	0.2		<0.1	
	1900	34	10.4	4.9			12.0	
	AIX		0.8	1.7			<0.1	
	1930	16	10.0	4.8			6.0	
	AIX		0.8	1.7			<0.1	
	2000	8.2	6.2	2.9	0.4		3.0	
	AIX		0.9	1.8	0.25		<0.1	
	2030	6.0	5.3	2.5	<0.3		2.0	
	AIX	1.1	1.4	1.9	<0.3		≈0.1	
	2130	9.5	6.3	3.3	0.6		1.3	
	AIX	0.0	1.2	2.3	0.4		<0.1	
	2230	3.9	9.4	4.8	1.5		0.8	
	AIX	0.0	2.4	6.0	1.3		<0.1	
	2330	3.5	13.3	6.6	2.9		0.5	
	AIX		2.4	7.2	2.3		<0.1	
9/7/82	0030	0.2	16.1	8.0	4.3			
	AIX		1.5	8.0	3.2			
	0240		47.9	10.8	9.2	<0.1	3.2	
	0330		17.5	4.2	3.5			
	0430	0.6	4.8	0.7	0.6			
	0530	2.3	2.2	0.2	0.1		0.1	
	0600		1.1	0.1	0.1		0.1	

Cold Leg Data (Cont)

Date	Time	Co-60 (μCi/ml)	Fe(ppm)	Ni(ppm)	Cr(ppm)	Cu(ppm)	Mn(ppm)	Zn(ppm)
9/8/82	2050	3.6	9.2		0.4			
9/9/82	0045	4.1	0.3		0.3			
	0200	1.2	1.0		1.8			
	0300	2.9	1.3		2.1			
	0400		1.3		2.2			
	0500		0.8		2.6			
	0600		1.1		2.7			
	0740	1.8	0.7		4.1			
	0815	0.0	0.6		3.5			
	0900	0.9	1.0		2.5			
	AIX	0.0	0.9		<0.1			
	0930	0.7	1.1		1.5			
	1000	0.6	0.6		0.45			
	1030	0.0	0.4		0.2			
	1100		0.2				11.2	
	1145	8.9	5.8				≈55	
	AIX	0.0	1.2				≈0.1	
	1200	14	9.4				≈40	
	AIX	0.0	1.3				<0.1	
	1215	0.2	10.2				≈25	
	AIX	0.0	1.5				<0.1	
	1230	18	11.5				13.3	
	AIX		1.7				<0.1	
	1245	0.2	12.0				8.7	
	AIX		1.8				<0.1	
	1315	8.9	12.5				4.7	
	AIX		1.7				<0.1	
	1345	4.7	12.3				3.7	
	AIX		2.0				<0.1	
	1430		15.6	5.0	0.6		9.7	
	AIX		3.9					

Cold Leg Data (Cont)

Date	Time	Co-60 (ρCi/ml)	Fe(ppm)	Ni(ppm)	Cr(ppm)	Cu(ppm)	Mn(ppm)	Zn(ppm)
9/9/82	1515	1.4	20.0	5.0	0.75		12.0	
	AIX		6.6					
	1530	1.4	20.6	5.0	0.8		7.6	
	1545	1.5	14.7	3.5	0.45		11.4	
	1650	0.0	1.5	0.2	<0.1	<0.1	0.7	0.13

Dissolved Metals and Co-60 Data - Hot Leg Decontamination

11/2/82	1925	2.2	<0.25	1.65	0.60
	1940	1.7	<0.25	1.83	0.81
	2010	2.3	<0.25	2.14	1.00
	2040	1.8	<0.25	2.40	1.20
	2110	1.7	<0.25	2.70	1.35
	2140	1.6	<0.25	3.20	1.90
	2210	2.0	<0.25	3.50	1.72
	2240	1.6	<0.25	3.70	2.14
	2310	1.2	<0.25	3.94	1.90
	2340	1.5	<0.25	4.25	2.10
11/3/82	0010	1.7	<0.25	4.00	2.15
	0040	2.0	<0.25	4.25	2.30
	0110	2.4	<0.25	4.45	2.35
	0210	2.6	<0.25	5.00	2.60
	0310	1.6	<0.25	5.60	2.85
	0410		<0.25	5.90	2.90
	0510	2.3	<0.25	6.20	3.25
	0610	1.5	<0.25	6.70	3.35
	0710	1.9	<0.25	6.95	3.50
	0810	8.2	<0.25	7.30	3.80

Hot Leg Data (Cont)

Date	Time	Co-60 (ρCi/ml)	Fe(ppm)	Ni(ppm)	Cr(ppm)	Cu(ppm)	Mn(ppm)	Zn(ppm)
11/3/82	0910	1.5	0.25	7.80	3.90			
	1015	0.8	0.25	8.20	4.25			
	1120	0.9	0.25	8.30	4.50			
	1220	1.1	0.25	8.45	4.60			
	1310	1.2	0.25	8.75	4.70			
	1450	0.8	0.25	9.10	4.80			
	1515	1.1	0.25	9.40	4.95			
	1535		2.00	10.60	5.05		325	
	1550	0.1	2.00	12.00	5.10		340	
	1556	2.0	1.65	12.30	5.10		275	
	1605	2.2	1.50	12.10	5.30		260	
	1620	5.7	1.0	13.10	5.70		260	
11/5/82	1320	50	3.0	4.3	0.85		12.0	
	1335	87	10.0	5.8	1.55		17.5	
	1350	91	10.6	6.0	1.86		17.4	
	1405	96	12.4	6.4	2.06		17.8	
	1420	94	14.7	6.9	2.26		18.3	
	1435	87	15.6	7.4	2.29		17.9	
	1450	100	18.7	8.3	2.66		19.1	
	1505	99	20.6	8.7	2.96		18.4	
	1520	99	22.2	8.4	3.56		18.4	
	1545	89	26.1	8.4	3.91		18.4	
11/9/82	1251	1.4	<0.25	<0.25	1.30		359	
	1312	3.1	<0.25	<0.25	2.00		359	
	1336	2.6	<0.25	<0.25	2.40		359	
	1406	1.7	<0.25	<0.25	2.55		355	

Hot Leg Data (Cont)

Date	Time	(μCi/ml)	Fe(ppm)	Ni(ppm)	Cr(ppm)	Cu(ppm)	Mn(ppm)	Zn(ppm)
11/9/82	1436	2.2	<0.25	<0.25	2.80		355	
	1506	1.5	<0.25	<0.25	2.90		355	
	1536	1.6	<0.25	<0.25	3.00		355	
	1636	1.4	<0.25	<0.25	3.15		354	
	1736	1.8	<0.25	<0.25	3.35		333	
	1836	1.7	<0.25	<0.25	3.47		321	
	1936	1.7	<0.25	<0.25	3.68		333	
	2036		<0.25	<0.25	3.65		330	
	2136	1.3	<0.25	<0.25	3.63		330	
	2236	1.3	<0.25	<0.25	3.58		330	
11/10/82	0036	1.7	<0.25	<0.45	3.52			
	0106	1.4	<0.25	1.13	3.84			
	0136	1.8	<0.25	1.8	4.1			
	0236	2.8	<0.25	2.5	4.5			
	0336	1.2	<0.25	3.0	4.8			
	0436	1.7	<0.25	3.5	5.8			
	0609	7.1	1.3	15.7	6.9		345	
	0640	100	10.4	19.4	7.4		320	
	0710	100	21.9	23.3	9.6		320	
	0740	100	31.3	32.7	11.8		320	

DISTRIBUTION

No. of Copies

OFFSITE

U.S. Nuclear Regulatory Commission
Division of Technical Information & Document Control
7920 Norfolk Avenue
Bethesda, MD 20014

3 Dr. Joseph Muscara
Materials Engineering Branch
Division of Engineering Technology
Nuclear Regulatory Commission
M/S 1130 SS
Washington, DC 20555

Dr. B. D. Liaw
Materials Engineering Branch
Division of Engineering Technology
Nuclear Regulatory Commission
M/S 1130 SS
Washington, DC 20555

Dr. C. McCracken
Nuclear Regulatory Commission
M/S P-302
Phillips Bldg.
Washington, DC 20555

3 Mr. Terry Oldberg
Electric Power Research Institute
3412 Hillview Avenue
P.O. Box 10412
Palo Alto, CA 94303

5 Mr. H. S. McKay
Virginia Electric Power Co.
The Electric Bldg.
P.O. Box 564
Richmond, VA 23204

No. of Copies

Foreign

3 Dr. J. L. Campan
Department Manager
Water Reactor Service
C.E.A./Caderache B.P.N.^{0}1
13115 Saint-Paul-Lez-Durance
FRANCE

3 Mr. M. Oishi, Manager
Steam Generator Project NUPEC
No. 2 Akiyama Bldg., 6-2, 3-Chome
Toranomon, Minatoku, Tokyo 105
JAPAN

4 Dr. R. De Santis
R&D Manager
Ansaldo DBGV
Viale Sarca 336
Milano, ITALY 20126

ONSITE

50 Pacific Northwest Laboratory

R. A. Clark (43)
Publishing Coordination (2)
Technical Information (5)

☆U.S. GOVERNMENT PRINTING OFFICE : 1984 O - 452-584 : QL3

NRC FORM 335 (2-84) NRCM 1102, 3201, 3202

U.S. NUCLEAR REGULATORY COMMISSION

BIBLIOGRAPHIC DATA SHEET

SEE INSTRUCTIONS ON THE REVERSE

1 REPORT NUMBER (Assigned by TIDC, add Vol. No., if any)

NUREG/CR-3841
PNL-4712

2 TITLE AND SUBTITLE

Steam Generator Group Project
Task 6 - Channel Head Decontamination

3 LEAVE BLANK

4 DATE REPORT COMPLETED

MONTH	YEAR
March	1983

5 AUTHOR(S)

R.P. Allen, R.L. Clark, W.D. Reece

6 DATE REPORT ISSUED

MONTH	YEAR
August	1984

7 PERFORMING ORGANIZATION NAME AND MAILING ADDRESS (Include Zip Code)

Pacific Northwest Laboratory
P. O. Box 999
Richland, WA 99352

8 PROJECT/TASK/WORK UNIT NUMBER

9 FIN OR GRANT NUMBER

B2097

10 SPONSORING ORGANIZATION NAME AND MAILING ADDRESS (Include Zip Code)

Division of Engineering Technology
Office of Nuclear Regulatory Research
U.S. Nuclear Regulatory Commission
Washington, D.C. 20555

11a TYPE OF REPORT

b PERIOD COVERED (Inclusive dates)

12 SUPPLEMENTARY NOTES

13 ABSTRACT (200 words or less)

The Steam Generator Group Project utilizes a retired from service pressurized water reactor steam generator as a test bed and source of specimens for research. Program objectives emphasize validation of the ability to nondestructively characterize the condition of steam generator tubing in service. Remaining integrity of tubing with service induced defects is studied through burst and leak rate tests. Other program objectives seek to characterize overall generator condition, including secondary side structure, and provide realistic samples for development of primary side decontamination, secondary side cleaning, and nondestructive examination technology. An important preparatory step to primary side research activities was reduction of the radiation field in the steam generator channel head. This task report describes the channel head decontamination activities. Though not a programmatic research objective, it was judged beneficial to explore the use of dilute reagent chemical decontamination techniques. These techniques presented potential for reduced personnel exposure and reduced secondary radwaste generation, over currently used abrasive blasting techniques. Two techniques with extensive laboratory research and vendors prepared to offer commercial application were tested, one on either side of the channel head. As indicated in the report, both techniques accomplished similar decontamination objectives. Neither technique damaged the generator channel head or tubing materials, as applied. This report provides details of the decontamination operations. Application system and operating conditions are described. Areas of improvement are suggested.

14 DOCUMENT ANALYSIS - a KEYWORDS/DESCRIPTORS

steam generator
channel head decontamination

b IDENTIFIERS/OPEN ENDED TERMS

15 AVAILABILITY STATEMENT

Unlimited

16 SECURITY CLASSIFICATION

(This page)
Unclassified
(This report)
Unclassified

17 NUMBER OF PAGES

18 PRICE